UNIVERSIDADE FEDERAL DE PERNAMBUCO
CENTRO DE TECNOLOGIA E GEOCIÊNCIAS
DEPARTAMENTO DE GEOLOGIA
PROGRAMA DE PÓS-GRADUAÇÃO EM GEOCIÊNCIAS

THYEGO ROBERTO DA SILVA

GRANITOS DA PORÇÃO SUDESTE DO BATÓLITO ÁGUAS BELAS–CANINDÉ, DOMÍNIO PERNAMBUCO–ALAGOAS: GEOQUÍMICA, PETROLOGIA, GEOCRONOLOGIA E CARACTERIZAÇÃO GEOTECTÔNICA

RECIFE

2017

THYEGO ROBERTO DA SILVA

GRANITOS DA PORÇÃO SUDESTE DO BATÓLITO ÁGUAS BELAS–CANINDÉ, DOMÍNIO PERNAMBUCO–ALAGOAS: GEOQUÍMICA, PETROLOGIA, GEOCRONOLOGIA E CARACTERIZAÇÃO GEOTECTÔNICA

Tese apresentada ao Programa de Pós-Graduação em Geociências do Centro de Tecnologia e Geociências da Universidade Federal de Pernambuco, como parte dos requisitos necessários à obtenção do grau de Doutor em Geociências.

Área de concentração: Geoquímica, Geofísica e Evolução Crustal.

Orientadora: Profª. Drª. Valderez Pinto Ferreira.

RECIFE

2017

Catalogação na fonte
Bibliotecária Valdicèa Alves, CRB-4 / 1260

S586g Silva, Thyego Roberto da.
Granitos da porção sudeste do batólito Águas Belas–Canindé, domínio Pernambuco–Alagoas: geoquímica, petrologia, geocronologia e caracterização geotectônica / Thyego Roberto da Silva. - 2017.
190folhas, Il. e Tabs.

Orientadora: Profª. Drª. Valderez Pinto Ferreira.

Tese (Doutorado) – Universidade Federal de Pernambuco. CTG. Programa de Pós-Graduação Geociências, 2017.
Inclui Referências, e Apêndices.

1. Geociências. 2. Granitos. 3. Geoquímica. 4. Isótopos de Sr–Nd–O–PB. 5. Condições de cristalização. 6. Domínio Pernambuco–Alagoas. 7. Orogênese Brasiliana. I.Ferreira, Valderez Pinto (Orientadora) II. Título.

UFPE

551 CDD (22. ed.) BCTG/2018-268

THYEGO ROBERTO DA SILVA

GRANITOS DA PORÇÃO SUDESTE DO BATÓLITO ÁGUAS BELAS–CANINDÉ, DOMÍNIO PERNAMBUCO–ALAGOAS: GEOQUÍMICA, PETROLOGIA, GEOCRONOLOGIA E CARACTERIZAÇÃO GEOTECTÔNICA

Tese apresentada ao Programa de Pós-Graduação em Geociências da Universidade Federal de Pernambuco, como parte dos requisitos necessários à obtenção do grau de Doutor em Geociências.

Área de concentração: Geoquímica, Geofísica e Evolução Crustal

Aprovado em: 02/08/2017

_____
Profª. Drª. Valderez Pinto Ferreira – Orientadora UFPE
Universidade Federal de Pernambuco

_____
Prof. Dr. Adejardo Francisco da Silva Filho
Universidade Federal de Pernambuco

_____
Profª. Drª. Maria de Lourdes da Silva Rosa
Universidade Federal de Sergipe

_____
Prof. Dr. Julio Cesar Mendes
Universidade Federal do Rio de Janeiro

_____
Profª. Drª. Anelise Losangela Bertotti
Universidade Federal de Pernambuco

Dedico esta obra a minha mãe Nadja Nascimento, a minha avó Helena Domingos, a meu pai Gener Roberto, a minha esposa e a todos os meus familiares... Amo vocês!

AGRADECIMENTOS

A Deus por tudo que tem me concedido ao longo da minha vida! Por mais esta conquista que Ele tem me dado, pois sem o meu Deus eu jamais teria conseguido sequer começar. Agradeço por cada dificuldade que foi posta diante de mim, todavia agradeço muito mais a solução concedida.

Aos projetos PRONEX/FACEPE APQ-0479-1.07/06, APQ-0844-1.07/08, APQ-0727-1.07/08 e APQ-1738-1.07/12, e CNPq Universal 478554/2009-5, 472842/2010-2, 471034/2012-6 e 404472/2016-8 coordenados pelos orientadores, com o apoio do Departamento de Geologia do Centro de Tecnologia e Geociências (DGEO-CTG/UFPE) do qual culminou com a produção da presente tese.

A minha professora orientadora Valderez Pinto Ferreira pela amizade e dedicação ao longo do desenvolvimento do trabalho, pelas sugestões e correções e pela tão grande paciência e compreensão na produção do trabalho, semelhantemente agradeço ao meu co-orientador Alcides Nobrega Sial pelo ensino (não apenas em geociências), dedicação, correções e sugestões ao longo desta caminhada.

Aos professores Sérgio Pacheco Neves (UFPE) e José Maurício Rangel da Silva (UFPE) pela disposição em ajudar e pela participação de trabalho de campo. Ao professor Adejardo Francisco da Silva Filho (UFPE) e a professora Ignês Guimarães (UFPE) pelos trabalhos e dados fornecidos. A Kei Sato (USP) e Ivone Keiko (USP) pelas análises e discussões.

Aos professores Maria de Lourdes da Silva Rosa (UFS), Julio Cezar Mendes (UFRJ), Anelise Losangela Bertotti (UFPE), Ignez de Pinho Guimarães, Adejardo da Silva Filho, Marcio Martins Pimentel (UNB) e Elson Paiva de Oliveira (UNICAMP) que aceitaram participar da qualificação e da banca do doutorado.

A todos os professores do curso de geologia da UFPE que contribuíram de maneira direta ou indireta para a realização deste trabalho e de forma direta na minha formação acadêmica. A todos os funcionários do DGEO que se tornaram grandes amigos ao longo dos anos.

Um agradecimento especial é feito aos professores Gorki Mariano e Lucila Ester que tanto me incentivaram e me apoiaram para que eu seguisse firme no curso e me formasse como um geólogo de rocha! A estes meus mais sinceros agradecimentos.

Aos amigos do curso de geologia Bruna Borba, Fernando Caetano, Marcos Felipe e Paulo (feldspato) pela ajuda, principalmente nos trabalhos de campo. Agradeço

enormemente a Aldine Maria que ajudou grandemente pegando no pesado!!! Agradeço a Deus por todos os amigos que conquistei ao longo dos anos e a cada um desses amigos que me ajudaram de forma direta ou indireta.

Áos amigos Charles Henrique, Renan Siqueira, Raphael Pereira e Natan Pereira que compõem o grupo de pesquisa NEG-LABISE, e aos técnicos Gilsa Santana, Vilma Bezerra, Severina Paulina e Anderson de Abreu da Silva por assistência com análises químicas e isotópicas e Deysi Araújo pelo suporte e solicitude, e a toda equipe pela amizade ao longo dos anos.

A Agência Pernambucana de Águas e Clima (APAC) pelo suporte a minha capacitação e aos gerentes e diretores Crystianne Rosal, Clenio Torres, Sergio Torres e Marconi Azevedo pela liberação para assistir as aulas e participar nas demais atividades na UFPE relacionadas ao doutorado.

À minha mãe Nadja Nascimento, meu pai Gener Roberto, minha avó Helena Domingos, minha irmã Tatiane Karine, minhas tias em especial Veroneide, ao meu avô Eloi (in memoriam), e a todos os meus familiares pelo imensurável amor, compreensão, suporte e incentivo.

Agradeço ao amor da minha vida e esposa Mariucha Maria Correia de Lima por ter confiado e me incentivado incansavelmente (contribuindo diretamente na realização desta obra) por me amar de uma maneira maravilhosa e por ter cuidado de mim e me acompanhado ao longo de todos os anos. Enfim por existir (a todos os seus familiares!). Amo você por tudo que és em minha vida!

E a todos aqueles que porventura aqui não mencionei. A todos só tenho a agradecer!

I press toward the mark for the prize of the high calling of God in Christ Jesus.

(Hole bible in King James Version, Philippians 3.14)

RESUMO

O Domínio Pernambuco–Alagoas representa um dos domínios crustais da Província Borborema e constituísse uma área chave para o entendimento da evolução tectônica da Província durante a orogênese Brasiliana. Este domínio é composto por diversos batólitos graníticos, entre eles o batólito Águas Belas–Canindé, que intrudiram rochas gnáissico-migmatiticas do embasamento. Este batólito foi pouco estudado; tendo sido selecionado por estar localizado no limite com o Domínio Sergipano e por ter um grande potencial para fornecer importantes pistas a fim de revelar a evolução tectônica do domínio Pernambuco–Alagoas durante a orogênese Brasiliana. Esta tese combina novos dados de química de elementos maiores e traços, química mineral, isótopos de Sr–Nd–O e idades U–Pb em zircão de alguns plutons a sudeste do batólito composto Águas Belas–Canindé, Domínio Pernambuco–Alagoas, NE do Brasil. Os resultados obtidos foram reunidos em quatro artigos. O artigo I concentra-se no aspecto geotectônico e trata do pluton Major Isidoro (627 Ma) derivado de uma crosta continental retrabalhada ($^{87}Sr/^{86}Sr(i)$ = 0,7069 a 0,7086; εNd = -2,12 a -1,09 e t_{DM} = 1,1 a 1,4; e $\delta^{18}O_{(magma)}$ = 8,74 a 8,76‰), e provavelmente associado à construção de um arco continental durante a orogênese Brasiliana. O artigo II trata do pluton Monteirópolis (626 Ma) com idade t_{DM} 1,0 Ga, dados isotópicos deste sugerem que material do manto foi adicionado à crosta ($^{87}Sr/^{86}Sr$ (i) = 0,7050 a 0,7052; εNd = -0,78 a +1,06; e $\delta^{18}O_{(zircão)}$ = 5,0 a 5,94‰) provavelmente durante o evento de rifteamento Cariris Velhos. Rochas Tonianas derivadas do manto possivelmente fundiram parcialmente devido a *underplating* de magma máfico derivado do manto no início da orogênese Brasiliana. O artigo III investiga os plutons Santo Antonio (636 Ma; $^{87}Sr/^{86}Sr$ (i) = 0,7050 a 0,7052; εNd = -0,67 a +1,17; e $\delta^{18}O_{(zircão)}$ médio de 5,45‰) e Jacaré dos Homens (642 Ma; εNd = −1,58; $^{87}Sr/^{86}Sr$ (i) de 0,7068; e $\delta^{18}O_{(zircão)}$ = 7‰) alojados ao longo da Zona de cisalhamento Jacaré dos Homens que foram formados por hibridização de rochas basálticas de médio-alto potássio derivados do manto (*Tonian mantle-derived basalts*) com rochas félsicas crustais. O artigo IV discute detalhadamente a assembleia mineral dos plutons Major Isidoro e Monteirópolis e investiga através de química mineral e de rocha total as condições de cristalização destes. Os dados de todos os plutons estudados evidenciaram que material do manto foi adicionado a crosta continental no Toniano provavelmente durante o evento Cariris Velhos. Estes plutons foram derivados por refusão parcial, de rochas basálticas de

médio a alto-K adicionadas à crosta no Toniano, durante o inicio da orogênese Brasiliana entre 642 e 626 Ma possivelmente devido à underplating de magma máfico. As fases minerais presentes nestes granitos sugerem cristalização a pressões típicas da crosta continental média-inferior (5,3 a 7,7 kbar) sob alta fO_2, e que o transporte deve ter sido rápido (taxas de ascensão maiores que 700 $m.ano^{-1}$) através de uma crosta continental quente durante a orogênese Brasiliana que permitiu preservação de epidoto magmático.

Palavras-chave: Granitos. Geoquímica. Isótopos de Sr–Nd–O–Pb. Condições de cristalização. Domínio Pernambuco–Alagoas. Orogênese Brasiliana.

ABSTRACT

The Pernambuco–Alagoas Domain represents one of the crustal domains of the Borborema Province and constitutes a key-area to the understanding of the tectonic evolution from the Province during the Brasiliano orogeny. This domain is composed of many granitic batholiths, between them the Águas Belas–Canindé batholith, which intruded migmatitic gneisses rocks from basement. This batholith was poorly studied; having been selected because it is located on the boundary of the Sergipano Domain, and because it has a huge potential to provide important clues to revealing the tectonic evolution of the Pernambuco–Alagoas Domain during the Brasiliano orogeny. This thesis combines new whole-rock major-trace elements, mineral chemistry, Sr–Nd–O isotopes, and U–Pb zircon ages of some plutons from the southeast Águas Belas–Canindé composite batholith, Pernambuco–Alagoas Domain, northeastern Brazil. The obtained results are presented in four articles. The article I focus on the tectonic aspects and deals with the Major Isidoro pluton (627 Ma) that was derived from a reworked continental crust ($^{87}Sr/^{86}Sr$ (i) = 0.7069 to 0.7086; εNd = -2.12 to -1.09 e t_{DM} = 1.1 to 1.4; and $\delta^{18}O_{(magma)}$ = 8.74 to 8.76‰), and probably associated to the continental arc build during the Brasiliano orogeny. The article II investigates the Monteirópolis batholith (626 Ma) that presents a t_{DM} model age of 1.0 Ga suggesting that mantle material was added to the continental crust ($^{87}Sr/^{86}Sr$ (i) = 0.7050–0.7052; εNd = -0.78 to +1.06; and $\delta^{18}O_{(zircão)}$ = 5.0 a 5.94‰), probably during to the extensional Cariris Velhos event. Tonian mantle-derived rocks possibly partially melted due to underplating of mantle-derived mafic magmas during the onset of the Brasiliano orogeny. The article III focus the Santo Antonio (636 Ma; $^{87}Sr/^{86}Sr$ (i) = 0.7050 to 0.7052; εNd = -0.67 a +1.17; and an average $\delta^{18}O_{(zircão)}$ of 5.45‰) and Jacaré dos Homens (642 Ma; εNd = −1.58; $^{87}Sr/^{86}Sr$ (i) of 0.7068; and $\delta^{18}O_{(zircão)}$ = 7‰) plutons, emplaced along the Jacaré dos Homens shear zone, that were formed for medium-to-high K basaltic rocks derived by hybridization of an enriched Tonian mantle source with more felsic crustal rocks. The article IV discusses detailed the mineral assemblage of the Major Isidoro and Monteirópolis plutons and investigates through mineral and whole-rock chemistries the crystallization conditions of them. The data from all studied plutons evidenced that mantle-derived material was added to the continental crust in the Tonian probably during the Cariris Velhos event. These plutons were derived from partial remelting of mantle-derived medium-to high-K basaltic rocks during the onset of

the Brasiliano orogeny between 642 and 626 Ma probably due to underplating of mafic magma. The mineral phases of these granites suggest crystallization at pressures of the lower-medium continental crust (5.3 a 7.7 kbar) under high oxygen fugacity, and that the ascension must have been fast (ascension rates higher than 700 $m.year^{-1}$) through a hot continental crust during the Brasiliano orogeny, which allowed magmatic epidote preservation.

Keywords: Granites. Geochemistry. Sr–Nd–O–Pb isotopes. Crystallization conditions. Pernambuco–Alagoas Domain. Brasiliano orogeny.

LISTA DE FIGURAS

1 INTRODUÇÃO

2 GEOLOGIA REGIONAL

7 DISCUSSÃO E CONCLUSÕES

LISTA DE TABELAS

7 DISCUSSÃO E CONCLUSÕES

SUMÁRIO

1 INTRODUÇÃO

Rochas graníticas têm um papel fundamental na diferenciação magmática e crustal, e o estudo isotópico e geocronológico destas constituem ferramentas para o conhecimento da evolução magmática e datação dos eventos tectônicos (P. ex. HAWKESWORTH & KEMP 2006; KEMP et al., 2007). Plutonismo granítico é o principal agente de diferenciação da crosta continental; granitos podem ser extraídos da crosta continental inferior para níveis crustais mais rasos (P. ex. DEPAOLO 1980, 1981; KEMP et al., 2007; entre outros). Os granitos representam um meio para a investigação indireta da constituição da própria crosta e das fontes das quais se originaram podendo prover informações a respeito de seus níveis mais profundos (P ex. SIAL 1986; FERREIRA et al., 1998). Estas rochas, ao ascender a níveis mais rasos da crosta continental, podem amostra-la através de xenólitos aprisionados pelo magma ou podem guardar as assinaturas geoquímicas e isotópicas das rochas fonte.

As fontes das quais podem ser derivadas as rochas graníticas são até certo ponto consensuais, podendo estas rochas se originar de material exclusivamente crustal, de material do manto ou de fontes mistas com proporções variadas entre os primeiros (P. ex. CHAPPELL & WHITE 1992, 2001; DEPAOLO 1980a, 1980b, 1981a, 1981b, 1981c, 1985, 1988; DEPAOLO et al., 1992; DEPAOLO & WASSERBURG 1979; FARMER & DEPAOLO 1983; LIU et al., 2014; NELSON & DEPAOLO 1985; MCCULLOCH & CHAPPELL 1982; PERRY et al., 1987; entre muitos outros), no entanto existem várias ideias competindo para explicar as variações químicas das series graníticas, dentre as quais podemos destacar: cristalização fracionada, mistura de magmas, fusão parcial, imiscibilidade de liquidus, assembleia peritetica (PAE) e "*restite unmixing*" (P ex. MCCULLOCH & CHAPPELL 1982; CHAPPELL et al., 1987; FERREIRA et al., 1994; BARBARIN 1999; CHAPPELL 1999; SISSON et al., 2005; BUCHOLZ et al., 2014; CHAPPELL et al., 2012; CLEMENS & STEVENS 2012; NANDEDKAR et al., 2014; KELLER et al., 2015; CLEMENS et al., 2016). Magmatismo granítico é frequentemente associado em tempo e espaço a eventos orogenéticos, podendo estas rochas ocorrer em uma diversidade de ambientes geotectônicos: margem continental, colisão continental ou rifte continental (P. ex. PEARCE et al., 1984; BARBARIN 1999). O alojamento de granitos pode ser controlado tectonicamente (sin-tectônico) por zonas de cisalhamento (P. ex. VAUCHEZ et al., 1995; BROW & SOLAR 1998; WEINBERG et al., 2004) ou pela pressão do magma (pós-tectônico).

Na Província Borborema (ALMEIDA et al., 1981) um grande número de intrusões graníticas que marcam o final do Neoproterozóico (orogênese Brasiliana–Pan-Africana), estão intimamente relacionadas a zonas de cisalhamento de baixo ou de alto ângulo (VAUCHEZ et al., 1995; NEVES & VAUCHEZ 1995, NEVES et al., 1996; FERREIRA et al., 1998; GUIMARÃES et al., 2004; NEVES et al., 2006; 2012, 2015). Algumas destas zonas de cisalhamentos são interpretadas como falhas litosféricas enraizadas no manto superior (P. ex. VAUCHEZ et al., 1995), que podem ter servido como condutos para a ascensão de magmas graníticos.

A Província Borborema tem sido tradicionalmente subdividida em domínios (BRITO NEVES et al., 2000; VAN SCHMUS et al., 2008; Fig. 2) dentre os quais pode se destacar na porção sul; o Domínio Pernambuco–Alagoas que inclui as maiores ocorrências de *stocks* e batólitos graníticos de idade Brasiliana. Alguns destes corpos foram estudados inicialmente através da sistemática Sm–Nd por SILVA FILHO et al. (2002) e VAN SCHMUS et al. (2008) que obtiveram valores de idades t_{DM} que se estendem de Neoproterozóicas a Arqueanas, sugerindo contribuições de fontes de diversas idades neste domínio. O Domínio Pernambuco–Alagoas tem sido alvo de investigações (ver: NEVES et al., 2008, 2012, 2016; SILVA FILHO et al., 2013, 2014, 2016), pois constituísse numa área chave para o entendimento do crescimento e da evolução tectônica da Província Borborema e por consequência da orogênese Brasiliana.

Apesar de ser foco de investições desde a década de 80 (BRITO NEVES et al., 1982) o estudo sistemático desse domínio começou a menos de duas décadas o que explica existirem algumas questões ainda não resolvidas. Algumas questões são: Quando precisamente aconteceu o inicio (*onset*) da orogênese Brasiliana no Domínio Pernambuco–Alagoas? Qual a fonte de calor (*heat source*) para a produção de centenas de km³ de rochas graníticas neste domínio? Qual a natureza geoquímica dos protólitos/Quais as fontes de magmas para a geração dos granitos? Quais as condições de pressão e temperatura que estas rochas experimentaram? Material juvenil foi adicionado a crosta no Brasiliano? Crescimento de crosta continental aconteceu neste domínio? Qual o cenário tectônico que foi mais favorável para a geração destes plutons? Com o desenvolvimento desta tese foi possível a elaboração de respostas plausíveis (mas não únicas) para estes questionamentos pontuados acima.

Neste trabalho são apresentados e discutidos dados de campo, petrográficos, geoquímicos de elementos maiores, menores e traços, química mineral, isotópicos (Sr–

Nd–O) e geocronológicos U–Pb SHRIMP em zircão de algumas intrusões graníticas cálcio-alkalinas de alto-K do batólito composto Águas Belas-Canindé, Domínio Pernambuco–Alagoas, alojadas ao longo da Zona de Cisalhamento Jacaré dos Homens, no limite com o Domínio Sergipano, que são convencionalmente tidos como distintos domínios crustais (VAN SCHMUS et al., 2008). Estes dados foram comparados sempre que possível com dados publicados na literatura dos domínios Pernambuco–Alagoas, Tectônico Central, Sergipano e com dados do Continente Africano. A integração destes dados adiciona um melhor conhecimento a evolução crustal do Domínio Pernambuco–Alagoas durante a orogênese Brasiliana–Pan Africana e lança luz no conhecimento da assembleia do Gondwana oeste.

1.1 OBJETIVOS

As principais metas desta tese foram:

(i) A caracterização petrológica das diversas intrusões graníticas do batólito composto Águas Belas–Canindé (porção sudeste) com a aquisição de informações sobre as rochas fontes.

(ii) a determinação das idades de cristalização e alojamento das rochas estudadas com o reconhecimento de todos os eventos ocorridos na área e a consequente delimitação da entrada (*onset*) da orogênese Brasiliana no Domínio Pernambuco–Alagoas.

(iii) a identificação dos períodos de possível crescimento e diferenciação da crosta continental com o reconhecimento se material juvenil foi ou não adicionado a crosta durante o orógeno Brasiliano.

(iv) a determinação das condições de pressão e temperatura em que estas rochas graníticas foram alojadas.

(v) a sugestão de um modelo tectônico para o Domínio Pernambuco–Alagoas e suas implicações para a evolução crustal desta parte da Província Borborema.

1.2 METODOLOGIA

A fim de alcançar os objetivos desta tese foram realizados trabalhos de escritório, campo e laboratório, com coleta de amostras para desenvolvimento de estudo sistemático com o intuito de decifrar as características geoquímicas, origem, evolução petrológica e o contexto tectônico do batólito composto Águas Belas–Canindé.

- Trabalhos de escritório e laboratório:

i. Pesquisa bibliográfica sobre a geologia da região além do acompanhamento e da leitura dos novos trabalhos publicados;

ii. Após cada etapa de campo, foram realizados estudos petrográficos para observação das fases minerais primárias e secundárias, suas relações texturais, e classificação mineralógica das rochas, usando a classificação de STRECKEISEN (1976). A porcentagem de ocorrência dos minerais foi obtida pelo método de contagem por visadas no microscópio petrográfico;

iii. Parte das amostras coletadas foi pulverizada, passante na peneira #200 ABNT (75 μm), para a realização de análises químicas de rocha total para elementos maiores e alguns menores (no laboratório de fluorescências de raios-X do DGEO) e de traços (em laboratório comercial - GEOSOL);

iv. Seleção de amostras e confecção de lâminas para análise da química das principais fases minerais por microssonda eletrônica (UNB);

v. Seleção de amostras e concentração de zircão para datação pelo método U–Pb (SHRIMP na USP) e para obtenção das razões isotópicas de $\delta^{18}O$;

vi. Aquisição de dados isotópicos Rb–Sr e Sm–Nd em rocha total (UnB e USP);

vii. Tratamento de dados geoquímicos e isotópicos: diagramas de correlação de multi-elementares usando planilhas de dados Microsoft Excel®; e o software Grapher®; diagramas de classificação química, e de discriminação de ambientes tectônicos; diagramas de correlação multi-elementares (elementos maiores e traços) usando o *software* GCDkit (JANOUŠEK et al., 2006).

viii. Integração dos dados obtidos na tese com os advindos da literatura e interpretação destes, culminando com o estabelecimento de hipóteses de evolução magmática e sugestão de um modelo de evolução geotectônica da região.

1.3 MÉTODOS

1.3.1 Fluorescência de Raios-X

As amostras para análise química foram pulverizadas em moinho de discos, passante na peneira 75 µm (ABNT nº 200). Uma porção de cada amostra foi colocada em estufa para secar a 110 ^{o}C e então levada a uma mufla, a 1000^{o}C, por 2 horas, para determinação de H_2O por perda ao fogo. Foram feitas pérolas fundidas usando tetraborato de lítio ($Li_2B_4O_7$) como fundente em cadinhos de liga especial (Pt com 5% de Au), usando uma relação amostra/fundente de 1:5 (MORI & MASHIDA 2005). As pérolas foram analisadas em Espectrômetro de Fluorescência de Raios-X (EFRX) Rigaku modelo RIX 3000 (Fig. 1) do NEG–LABISE, equipado com seis cristais analisadores e tubo de Rh, pelo método de curvas de calibração, as curvas foram construídas com materiais de referências internacionais. Todos os elementos maiores (SiO_2, TiO_2, Al_2O_3, CaO, Fe_2O_3, MnO, MgO, Na_2O, K_2O e P_2O_5) assim como alguns elementos menores (Rb, Ba, Sr, Nb, Zr, Y, Cr e Ni) foram dosados na Fluorescência de Raios-X (FRX).

Figura 1. Espectrômetro de Fluorescência de Raios-X Rigaku modelo RIX 3000 da Universidade Federal de Pernambuco.

1.3.2 U–Pb SHRIMP

A separação dos concentrados de zircão foi realizada reduzindo via britador e moinho, posteriormente extraindo a fração inferior a 500 µm. A partir do material recolhido foram concentrados os minerais pesados com uso da bateia. Os minerais pesados concentrados foram subsequentemente processados por separação magnética usando o separador isodinâmico Frantz do NEG–LABISE da Universidade Federal de

Pernambuco (UFPE). Após essa etapa, os concentrados foram levados a separação com bromofórmio que separa as fases por densidade. Esta etapa separou os cristais de zircão de minerais leves, como quartzo, feldspato e apatita, que se concentram na fração não magnética do separador Frantz. O concentrado foi então limpo de impurezas e de outros minerais com ácido fluorídrico. Para confecção dos *mounts*, grãos de zircão representativos foram selecionados a mão da fração não magnética em microscópio binocular e em seguida foram colocados em fita dupla face e montados em resina epóxi com material padrão e polidos a aproximadamente metade de sua espessura com pasta de diamante de 3 µm e 1 µm a fim de expor características da sua estrutura interna. Um revestimento de ouro condutor foi aplicado imediatamente antes da análise.

Os grãos foram fotografados em luzes refletidas e transmitidas no Centro de Pesquisas Geocronológicas (CPGeo) da Universidade de São Paulo (USP), e as imagens de catodo luminescência (CL) foram produzidas em um microscópio eletrônico de varredura, a fim de investigar as estruturas internas dos cristais de zircão, para caracterizar diferentes populações e assegurar que o ponto esteja totalmente dentro de um componente de idade único dentro dos grãos selecionados.

As análises isotópicas U–Pb foram realizadas utilizando a microssonda iônica SHRIMP IIe da Universidade de São Paulo, Brasil (Fig. 2), seguindo os procedimentos descritos em SATO et al. (2014), nas quais são determinadas as razões entre os isotópos de elementos: U–Th–Pb, Pb–Pb. A análise foi feita por bombardeamento de um feixe de O, que escava a superfície do mineral e ioniza partículas secundárias - essas são extraídas eletrostaticamente e aceleradas para dentro de um espectrômetro de dupla focalização. A medida foi feita in situ com elevada resolução especial e para datação de rochas por U–Pb em zircão através de SHRIMP é necessário apenas 2 ng de amostra. O feixe que colide com a amostra tem um diametro de ~20–25 µm e que provocam cratera de aproximadamente 2 µm de profundidade de escavação no cristal.

Abundancias de U foram calibradas usando o padrão SL 13 (U=238 ppm, WILLIAMS 1998). Correção de Pb comum foi feita usando ^{204}Pb medido. Os dados isotópicos U–Pb foram coletados em conjuntos de cinco varreduras ao longo das massas, e o zircão de referência TEMORA II (^{206} Pb/^{238}U 416,78 ± 0,33 Ma; BLACK et al., 2004) foi medido a cada três análises desconhecidas.

Erros nas razões isotópicas e idades foram cotados em nível de 1-sigma. Os dados brutos foram reduzidos utilizando o programa Squid (LUDWIG 2009). Idades Concordia e avaliações estatísticas foram realizadas usando o software geocronológico

ISOPLOT/Excel 4.0 (LUDWIG 2009) e os erros são dados em nível de 95% de confiança. As análises foram plotadas em diagramas concórdia U–Pb.

Figura 2. Equipamento de análise SHRIMP IIe (Sensitive High Resolution Ion Microprobe) da Universidade de São Paulo.

1.3.3 Rb–Sr e Sm–Nd

Análises isotópicas de Sr foram realizadas no Laboratório de Geocronologia da Universidade de Brasília (UnB) e no Centro de Pesquisas Geocronológicas (CPGeo) da Universidade de São Paulo (USP). Concentrações de Rb e Sr foram obtidas com um Rigaku RIX 3000 espectrômetro de FRX totalmente automatizado, na Universidade Federal de Pernambuco (UFPE). Aproximadamente 50 mg de amostras de rocha em pó foram dissolvidas em concentrado HF, HNO_3 e HCl. Alíquotas de Sr foram separadas das soluções utilizando técnicas de troca convencionais e foi depositado sobre filamentos de Re.

Análises isotópicas foram realizadas com um espectrômetro de massa Multicoletor Finnigan MAT-262 (Fig. 3) em modo estático. Correções para fracionamento de massa foram feitas usando $^{88}Sr/^{86}Sr$ de 8,3752. Erros 2σ são menores do que 0,01% para as razões $^{87}Sr/^{86}Sr$ e de cerca de 1% para a relação $^{87}Rb/^{86}Sr$.

Análises isotópicas Sm–Nd seguiram o método descrito por GIOIA & PIMENTEL (2000) e foram realizadas no Laboratório de Geocronologia da Universidade de Brasília (UnB) e no Centro de Pesquisas Geocronológicas (CPGeo) da Universidade de São Paulo (USP). Pós de rocha total (50 a 100 mg) foram misturadas com solução ^{149}Sm-

^{150}Nd e dissolvido em cápsulas Savillex . Extração de Sm e Nd de amostras de rocha total, seguido de técnicas de permuta iónica convencionais, basicamente como descrito em RICHARD et al. (1976) com a adição de alguns melhoramentos, usando colunas de teflon contendo resina comercial LN-Spec (ácido dietil hexil fosfórico - HDEHP embalado com politetrafluoretileno pó PTFE) .

Amostras de Sm e Nd foram carregados em assembleias de filamentos duplos de evaporação de Re e as medidas isotópicas foram realizadas em um espectrômetro de massa multicoletor Finnigan MAT-262 (Fig. 3) no modo estático .

Incertezas para os razões Sm/Nd e ^{143}Nd/^{144}Nd são melhores do que ± 0,4% (1σ) e ± 0,005 % (1σ), respectivamente, com base em análises repetidas de padrões de rochas internacionais BHVO - 1, BCR -1 (UnB), e JNdi-1 (USP). Razões ^{143}Nd/^{144}Nd foram normalizados para ^{146}Nd/^{144}Nd de 0,7219 e a constante de decaimento utilizada foi 6,54 × 10^{-12} a^{-1}.

Figura 3. Espectrômetro de massa multicoletor Finnigan MAT-262 da Universidade de Brasília.

1.3.4 Microssonda eletrônica

As lâminas petrográficas foram confeccionadas em espessura de aproximadamente 30 μm, tendo sido posteriormente polidas para possibilitar a análise na microssonda. As lâminas delgadas foram metalizadas com uma fina camada de carbono em câmara de vácuo (Fig. 4A), e analisadas com auxílio da microssonda elerônica JEOL modelo JXA-8230 do Laboratório de Microssonda Eletrônica da Universidade de Brasília (UnB), com cinco espectrômetros WDS e um EDS (Fig. 4B). As condições analíticas utilizadas foram de voltagem de aceleração de 15 kV, corrente de 10 ηA com um feixe eletrônico

de 5µ de diâmetro. Os cristais foram analisados utilizando os seguintes padrões: albita (Na), forsterita (Mg), topázio (F), microclina (Al, Si, K), andradita (Ca), vanadinita (V, Cl), $MnTiO_3$ (Ti, Mn), Cr_2O_3 (Cr), $SrSO_4$ (Sr), NiO (Ni), andradito (Fe), BaSO4 (Ba). Os tempos de contagem foram 10s no pico e 5s no *background* para todos os elementos.

Figura 4. A) Câmara metalizadora para recobrimento (metalização) com carbono.

Fgura 4. B) Microssonda elerônica JEOL modelo JXA-8230 da Universidade de Brasília.

1.3.5 Analise de $\delta^{18}O_{(zircão)}$

A separação dos concentrados de zircão foi realizada reduzindo via britador e moinho, posteriormente extraindo a fração inferior a 500 µm. A partir do material recolhido foram concentrados os minerais pesados com uso da bateia. Os minerais pesados concentrados foram subsequentemente processados por separação magnética usando o separador isodinâmico Frantz do NEG–LABISE. Após essa etapa, os concentrados foram levados a separação com bromofórmio que separa as fases por densidade. Esta etapa separou os cristais de zircão de minerais leves, como quartzo, feldspato e apatita, que se concentram na fração não magnética do separador Frantz. Em torno de 2 a 3 miligramas em peso de grãos de zircão foram usadas para análise.

As razões isotópicas dos grãos de zircão foram determinadas no laboratório NEG–LABISE usando um espectrômetro de massa Thermo Finnigan Delta V Advantage (Fig. 5A) que possui precisão ± 0,1‰. O oxigênio foi liberado em uma linha de extração a laser (Fig. 5B) por reação com BrF_5, reagido com um bastão de grafita a 750 ºC e convertido em CO_2 para análise no espectrômetro de massa seguindo os procedimentos descritos em VALLEY et al. (1995).

Figura 5. A) Espectrômetro de massa modelo Thermo Finnigan Delta V Advantage. B) linha de extração de oxigênio a laser de CO_2 do NEG–LABISE (UFPE).

1.3.6 Organização da tese

A presente tese esta estruturada com um capítulo introdutório, com os objetivos e os métodos de investigação utilizados no desenvolvimento desta; um capítulo do estado da arte com uma geologia regional; quatro capítulos com uma coletânea de quatro artigos onde Thyego Roberto da Silva é o primeiro autor de todos; e um capítulo de discussões e conclusões. Os artigos I e II não são passíveis de alterações, haja vista que já foram publicados nas revistas *Journal of South American Earth Sciences* e *Lithos*, no entanto sugestões são bem vindas, enquanto que o artigo III apesar de substanciamente revisado (submetido ao *International Journal of Earth Sciences*) e o artigo IV (em preparação para submissão), por serem manuscritos, podem ser alterados, sendo correções e sugestões muito bem vindas. O desenvolvimento deste projeto resultou, além destes artigos completos, em três resumos (SILVA et al., 2015b, 2016b, 2016c) apresentados no XXVI Simpósio de Geologia do Nordeste e 48º Congresso Brasileiro de Geologia.

No artigo I está apresentada a refêrencia: "Synkinematic emplacement of the magmatic epidote bearing Major Isidoro tonalite-granite batholith: Relicts of an Ediacaran continental arc in the Pernambuco–Alagoas Domain, Borborema Province, NE Brazil. *Journal of South American Earth Sciences* 64, 1–13." Neste trabalho são discutidas as relações estruturais de alojamento do pluton granítico Major Isidoro e sua cronologia. No mesmo trabalho, ainda são estabelecidas correlações com outros granitos da Provincia Borborema e as implicações tectônicas do conjunto dos dados.

No artigo II consta a referência: "Two stage mantle-derived granitic rocks and the onset of the Brasiliano orogeny: evidence from Sr, Nd, and O isotopes. *Lithos* 264, 189–200". Neste trabalho é determinada a idade de cristalização do batólito granítico Monteirópolis em conjunto com dados geocronológicos da literatura, e dados isotópicos, a fim de identificar as possíveis rochas fontes deste.

O manuscrito III contém a referência: "Isotope evidence for mantle connection in the source rock of high-K calc-alkaline granites, Pernambuco–Alagoas Domain, northeastern Brazil. Precambrian Research or Geoscience Frontiers (submitted to *International Journal of Earth Sciences*)". Neste trabalho são apresentadas as idades de colocação do ortognaisse granítico Jacaré dos Homens e do pluton granítico Santo Antonio, e são discutidos dados geoquímicos de elementos maiores, menores e traços, de química mineral e de isótopos.

O manuscrito IV contém a seguinte referência: “Mineralogy and mineral chemistry of the calc-alkaline epidote-bearing Major Isidoro and Monteirópolis plutons, Borborema Province, NE Brazil. (to submit)”. Neste manuscrito são apresentados dados petrográficos e de química mineral de dois plutons cálcio alcaninos, Major Isidoro e Monteirópolis, os quais contém epitoto magmático. Estes dados são integrados a fim de estabelecer as condições físico-químicas de cristalização, transporte e alojamento.

2 GEOLOGIA REGIONAL

2.1 PROVÍNCIA BORBOREMA

A Província Borborema, nordeste do Brasil, é parte da margem do Gondwana oeste (BRITO NEVES et al., 2000; NEVES 2011; VAN SCHMUS et al., 2011). Esta localizada entre os crátons oeste da África-São Luis a norte, Bacia Parnaíba a oeste e os crátons São Francisco-Congo a sul em uma reconstituição *pre-drift* (Fig. 1) (P. ex. DE WIT et al., 2008; TROMPETTE 1994, 1997; VAN SCHMUS et al., 1995, 2008, 2011; TOTEU et al., 2001; BRITO NEVES et al., 2002; SANTOS et al., 2009; GANADE DE ARAUJO et al., 2014a).

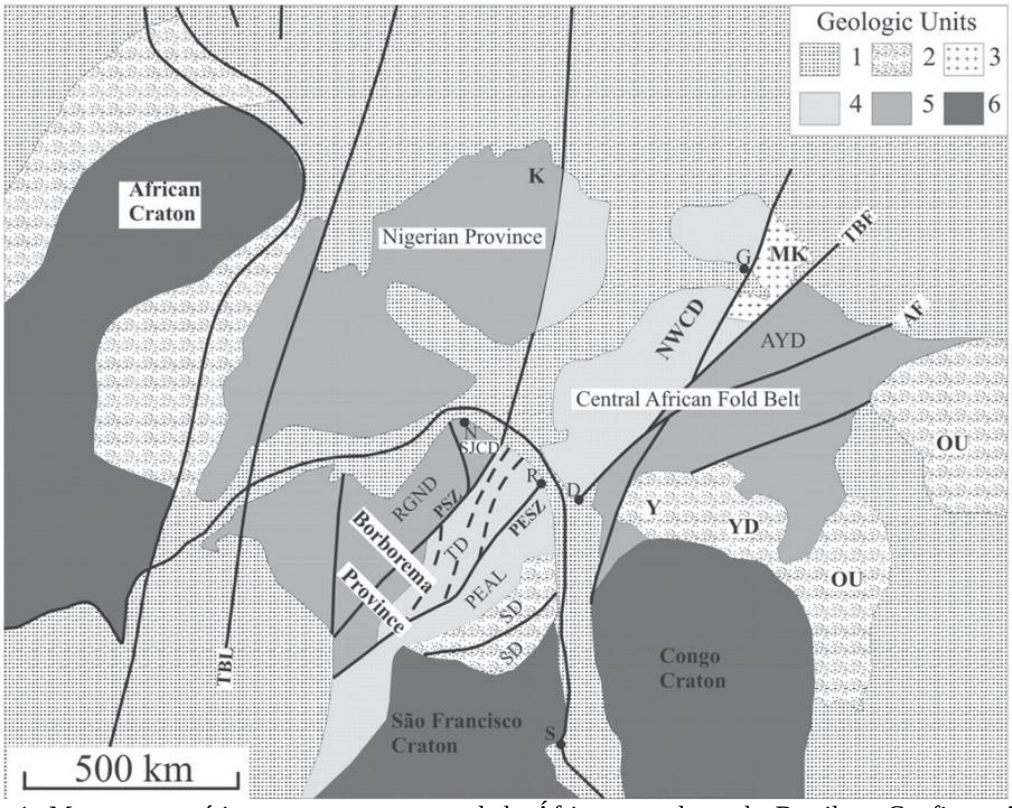

Figura 1. Mapa esquemático para o oeste central da África e nordeste do Brasil na Configuração do Gondwana (pre-drift) (500 Ma). Fonte VAN SCHMUS et al. (2008). 1: Cobertura Fanerozoica; 2: Cobertura Neoproterozoica; 3: Neoproterozoico (juvenil); 4: Embasamento Paleoproterozoico com domínios Brasiliano/Pan Africano; 5: Embasamento Paleoproterozoico abundante com domínios Brasiliano/Pan Africano; 6: Crosta Paleoproterozoica/Cratons Arqueano; AYD, Adamawa = Domínio Yadé; MK: Terreno Mayo Kebi; NWC: Domínio Cameroon NW; OU: Cinturão de dobramento Oubanguide; PEAL: Domínio Pernambuco–Alagoas; RGND: Domínio Rio Grande do Norte; SD: Domínio Sergipano; TD: Domínio Transversal; YD: Domínio Yaoundé. Falhas e zonas de cisalhamento: AF: Falha Adamawa; PSZ, Zona de cisalhamento Patos; PESZ: Zona de cisalhamento Pernambuco; SF: Falha Sanaga; TBF: Tcholliré–Banyo; TBL: Lineamento Transbrasiliano. Cidades: D: Douala; G: Garoua; K: Kaduna área da Nigeria; R: Recife; N: Natal; S: Salvador; Y: Yaoundé.

A Província Borborema consiste de gnaisses e complexos embasamentos migmatíticos, a maioria formados durante evento orogenético Paleoproterozóico (~2,2-2,0 Ga) (SANTOS 1995; VAN SCHMUS et al., 1995; BRITO NEVES et al., 2001; MELO et al., 2002; KOZUCH 2003; NEVES 2015; NEVES et al., 2015a; SANTOS et al., 2015) e dados Sm–Nd indicam a existência de protólitos arqueanos para alguns destes ortognaisse paleoproterozóicos (VAN SCHMUS et al., 1995; MELO et al., 2002). No entanto ortognaisses e meta-anortositos com idades entre 1,7 e 1,5 Ga foram encontrados e são interpretados como plutons anorogênicos deformados (ACCIOLY et al., 2000; SÁ et al., 2002). Um terceiro grupo de ortognaisses é derivado de granitóides com idades entre 1,0 e 0,87 Ga (VAN SCHMUS et al., 1995; KOZUCH, 2003; CARVALHO et al., 2005; SANTOS et al., 2008; SANTOS et al., 2010; OLIVEIRA et al., 2010, 2015, 2017; GUIMARÃES et al., 2012, 2016; CAXITO el al., 2014; NEVES et al., 2015b). Alguns autores interpretam esses como intrusões sintectônicas alojadas num evento orogênico cedo-Neoproterozoico denominado Cariris Velhos (SANTOS et al., 2010; CAXITO et al., 2014). No entanto, outros autores argumentam que este evento corresponde apenas a uma fase de rifteamento continental, e sendo assim o bandamento gnáissico teria sido desenvolvido apenas durante o evento Brasiliano (MARIANO et al., 2001; NEVES 2003; NEVES et al., 2006, 2008, 2015a; GUIMARÃES et al., 2012). Cobrindo parcialmente esse embasamento ocorrem rochas metassedimentares e metavulcânicas neoproterozoicas (P. Ex. VAN SCHMUS et al., 1995; DANTAS et al., 1998; BRITO NEVES et al., 2001; KOZUCH 2003; NEVES et al., 2008, 2009; OLIVEIRA et al., 2010; KALSBEEK et al., 2013; GANADE DE ARAUJO et al., 2014b; NEVES et al., 2017).

No final do Neoproterozoico (Brasiliano–Pan-Africano; 650–550 Ma) uma grande abundância de intrusões graníticas intrudiram a província, estando muitas destas associadas com zonas de cisalhamento (P ex. JARDIM DE SÁ 1994; NEVES & VAUCHEZ 1995; ARCHANJO et al., 1994, 2008; VAN SCHMUS et al., 2008; SIAL & FERREIRA 2015; SILVA et al., 2015, 2016). Esses granitos brasilianos compreendem uma porção significativa da Província Borborema (BRITO NEVES et al., 2000).

2.2 DOMÍNIO PERNAMBUCO–ALAGOAS

A denominação Domínio Pernambuco–Alagoas (PEAL) passou por modificações, dentre as quais se podem destacar; Maciço Pernambuco–Alagoas (BRITO NEVES 1975), Terreno Pernambuco–Alagoas (SANTOS 1995), Complexo Pernambuco–Alagoas (SILVA FILHO et al., 2002), sendo posteriormente designado de Domínio Pernambuco–Alagoas por VAN SCHMUS et al. (2008). O Domínio Pernambuco–Alagoas localiza-se entre a zona de cisalhamento Pernambuco e os domínios Sergipano e Riacho do Pontal (BRITO NEVES et al., 2000; VAN SCHMUS et al., 2008). Este possui uma forma triangular com aproximadamente 70.000 km^2 de área e está dividida em duas partes pelos sedimentos terrígenos fanerozóicos da Bacia de Jatobá (MARIANO et al., 2008). A geologia é dominada por ortognaisses e rochas metassedimentares de alto grau, frequentemente migmatizadas, e por grandes batólitos graníticos (Fig. 2) (BRITO NEVES et al., 2000; NEVES et al., 2008, 2012; SILVA FILHO et al., 2002, 2010, 2013, 2014, 2016; SILVA et al., 2015, 2016). As rochas supracrustais do Domínio Pernambuco–Alagoas freqüentemente são correlacionadas as rochas do Complexo Cabrobó (SANTOS 1995; MEDEIROS 1998; CARMONA 2000; SILVA FILHO et al., 2002), e as rochas ortoderivadas migmatizadas como Complexo Belém do São Francisco, utilizando como referência as descrições litológicas de SANTOS (1995) e MEDEIROS (1998). LEAL (1970) foi o primeiro a descrever o Complexo Cabrobó próximo à cidade homônima, localizada na região ocidental do Estado Pernambuco. Segundo este autor, o Complexo Cabrobó seria constituído por rochas supracrustais observadas na Faixa Pajeú–Paraíba na Zona Transversal da Província Borborema. O complexo Cabrobó divide-se em três suítes baseadas em seus litotipos: Sequências Venturosa, Inhapi e Palmares (VAN SCHMUS et al., 2008; SILVA FILHO et al., 2014).

Poucas idades estão disponíveis para o embasamento do Domínio Pernambuco–Alagoas (SILVA et al., 2002; NEVES et al., 2004; OSAKO 2005; SILVA FILHO et al., 2014). Este embasamento é assumido pertencer ao Complexo Belém do São Francisco, que é formado por biotita ortognaisse leucocrático de coloração cinza de composição tonalítica a granodiorítica comumente migmatizado. SILVA et al. (2002) obtiveram em um biotita-hornblenda granodiorito gnáisse com textura porfiroclástica, na localidade-tipo desse complexo, a idade de 2079 ± 34 Ma (U–Pb SHRIMP em zircão) que foi interpretada como a idade de cristalização magmática. VAN SCHMUS et al., 1995 estudaram os gnaisses com granada migmatizados localizados a oeste de Palmeira dos

Índios (AL) pelo método U–Pb em zircão e obtiveram um intercepto superior em 1577 ± 73 Ma e inferior em 538 ± 34 Ma. No entanto, estas idades representam errócronas não possuindo significado geológico (SILVA FILHO, 2017, comunicação verbal)

De acordo com SILVA FILHO et al. (2002, 2013), o plutonismo Neoproterozóico/Cambriano (Brasiliano), ocorre no domínio Pernambuco–Alagoas sob forma de vários batólitos graníticos. SILVA FILHO et al. (2014) agruparam os plútons graníticos do Domínio Pernambuco–Alagoas de SILVA FILHO et al. (2002) em três batólitos: Águas Belas–Canindé, Buíque–Paulo Afonso, Ipojuca–Atalaia e Garanhuns (Fig. 2). Baseado em dados de Sm–Nd SILVA FILHO et al. (2014) propuseram três subdomínios crustais: Garanhuns, Água Branca e Palmares. O subdomínio Garanhuns localizado na parte norte do terreno PE–AL, compreende rochas com idades modelos t_{DM} variando de 1,6 Ga a 2,6 Ga. Sugerindo que as rochas localizadas neste domínio não tiveram contribuições adicionais meso e neoproterozóicas significativas. Esse domínio crustal é constituído pelos corpos graníticos dos batólitos Garanhuns de SILVA FILHO et al. (2002), e ainda parte das rochas pertencentes aos complexos Cabrobó, Belém do São Francisco. Por outro lado, o subdomínio crustal Águas Branca abrange a parte sul do terreno PE–AL e engloba unidades litológicas com idades modelos t_{DM} entre 1,0 a 1,5 Ga (P. ex. SILVA FILHO et al., 2014, SILVA et al., 2016) sendo este domínio crustal constituído pelo batólito Águas Belas-Canindé e Sequência Inhapi. O subdomínio Palmares é constituído pelos batólitos Ipojuca–Atalaia e Buíque–Paulo Afonso. As idades U–Pb em zircão dos granitoides do Domínio Pernambuco–Alagoas estendem-se de 573 a 624 Ma (SILVA FILHO & GUIMARÃES, 2000; NEVES et al., 2008; SILVA FILHO et al., 2013, 2014, 2016). De acordo com SILVA FILHO et al. (2013) dois grupos de intrusões graníticas podem ser discriminados com base em idades U–Pb em zircão no Domínio Pernambuco–Alagoas: 1) granitoides com idades de cristalização mais velhas que 600 Ma e 2) granitoides com idades de cristalização de aproximadamente 590 Ma.

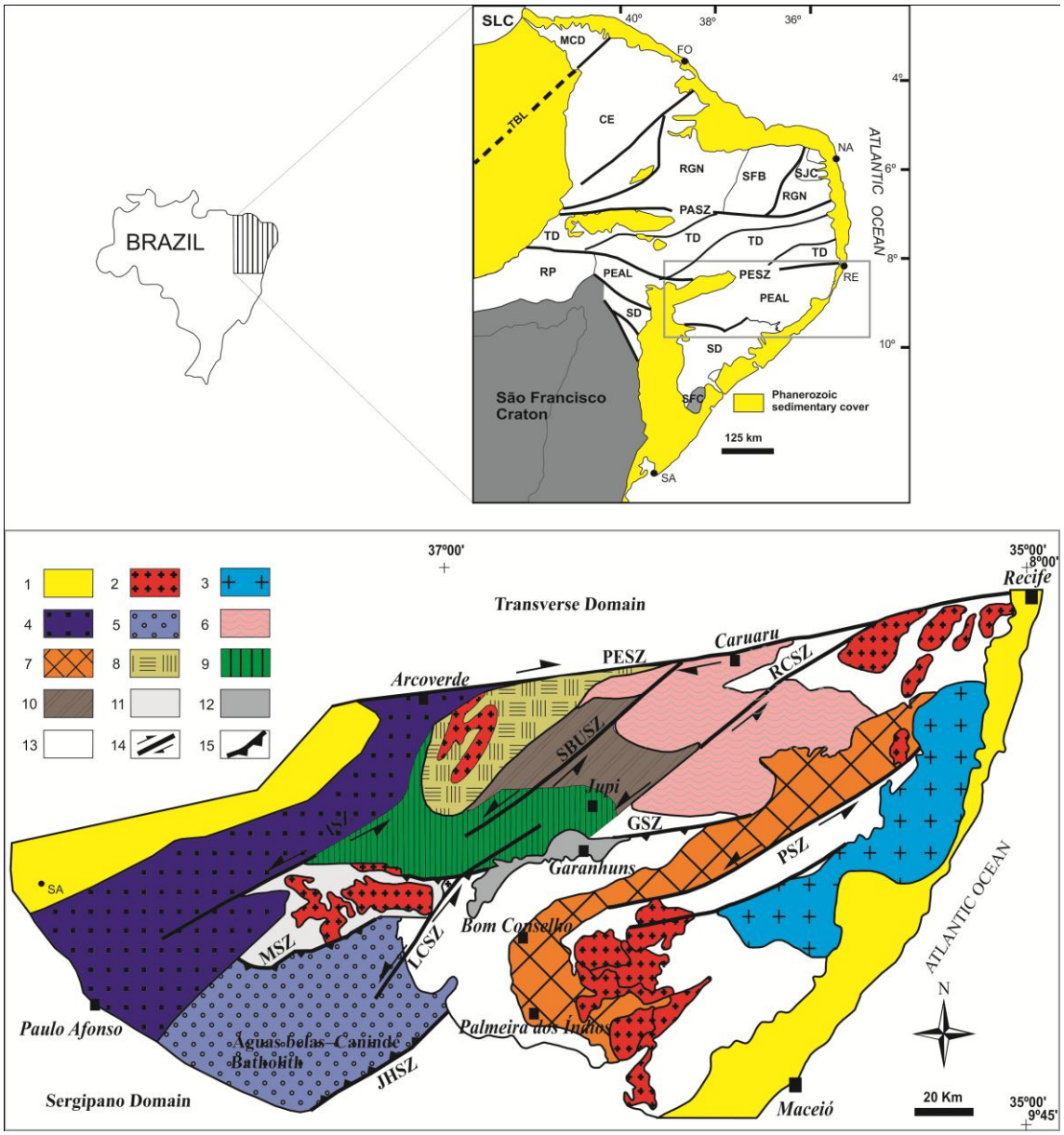

Figura 2. Província Borborema. Domínios: MCD - Médio Coreaú; CE - Ceará; RGN - Rio Grande do Norte (SFB - Faixa de Dobramentos Seridó; SJC - Núcleo Arqueano São José do Campestre); TD - Transversal; PEAL - Pernambuco–Alagoas; RP - Riacho do Pontal; SD - Sergipano; SFC - Craton São Francisco; SLC - Craton São Luís; Falhas e Zonas de Cisalhamento: PASZ - Zona de cisalhamento Patos; PESZ - Zona de cisalhamento Pernambuco; TBL - Lineamento Transbrasiliano. Cidades: Fo - Fortaleza; Na - Natal; Re - Recife; Sa - Salvador (VAN SCHMUS et al., 2008). Mapa Geológico do Domínio Pernambuco–Alagoas. 1 - Cobertura sedimentar Fanerozoica; 2 - Outros granitoides Brasilianos; 3 - Batólito Ipojuca–Atalaia; 4 - Batólito Buíque–Paulo Afonso; 5 - Batólito Águas Belas–Canindé; 6 - Granitoídes e ortognaisses; 7 - Sequência Palmares; 8 - Sequência Rio Una (Unidade 1); 9 - Sequência Rio Una (Unidade 2); 10 - Sequência Rio Una (Unidade 3); 11 - Sequência Inhapi; 12 - Quartzito Garanhuns; 13 - Embasamento Migmatítico; 14 - Zonas de Cisalhamento Transcorrente (PESZ - Pernambuco; RCSZ - Rio da Chata; PSZ - Palmares; LCSZ - Limitão-Caetés; ISZ - Itaíba; SBUSZ - São Bento do Una); 15 - Zonas de cisalhamento compressional (GSZ - Garanhuns; MSZ - Maravilha; ZCJH - Jacaré dos Homens) (modificado de SILVA FILHO et al., 2002, 2010, 2014).

Journal of South American Earth Sciences 64 (2015) 1–13

Contents lists available at ScienceDirect

Journal of South American Earth Sciences

journal homepage: www.elsevier.com/locate/jsames

Synkinematic emplacement of the magmatic epidote bearing Major Isidoro tonalite-granite batholith: Relicts of an Ediacaran continental arc in the Pernambuco–Alagoas domain, Borborema Province, NE Brazil

Thyego R. da Silva [a, *], Valderez P. Ferreira [a], Mariucha M. Correia de Lima [a], Alcides N. Sial [a], José Mauricio R. da Silva [b]

[a] NEG–LABISE, Department of Geology, Federal University of Pernambuco, Recife, PE, Brazil
[b] Department of Geology, Federal University of Pernambuco, Recife, PE, Brazil

ARTICLE INFO

Article history:
Received 22 May 2015
Received in revised form
28 August 2015
Accepted 4 September 2015
Available online 12 September 2015

Keywords:
Synkinematic granites
Calc-alkaline granites
U–Pb age
Sm and Nd isotopes
Oxygen isotopes
Pernambuco–Alagoas domain

ABSTRACT

The Neoproterozoic Major Isidoro batholith (~100 km^2), composed of metaluminous to slightly peraluminous magmatic epidote-bearing tonalite to granite, is part of the Águas Belas–Canindé composite batholith, which intruded the Pernambuco–Alagoas Domain of the Borborema Province, northeastern Brazil. These rocks contain biotite, amphibole, titanite and epidote that often shows an allanite core as key mafic mineral phases. K-diorite mafic enclaves are abundant in this pluton as well as are amphibole-rich clots. The plutonic rocks are medium-to high-K calc-alkaline, with SiO_2 varying from 59.1 to 71.6%, Fe# from 0.6 to 0.9 and total alkalis from 6.1 to 8.5%. Chondrite-normalized REE patterns are moderately fractionated, show $(La/Lu)_N$ ratios from 13.6 to 31.8 and discrete negative Eu anomalies (0.48–0.85). Incompatible-element spidergrams exhibit negative Nb–Ta and Ti anomalies.

This batholith was emplaced around 627 Ma (U–Pb SHRIMP zircon age) coevally with an amphibolite-facies metamorphic event in the region. It shows Nd-model age varying from 1.1 to 1.4 Ga, average $\varepsilon Nd_{(627Ma)}$ of −1.60 and back-calculated (627 Ma) initial $^{87}Sr/^{86}Sr$ ratios from 0.7069 to 0.7086. Inherited zircon cores that yielded $^{206}Pb/^{238}U$ ages from 800 to 1000 Ma are likely derived from rocks formed during the Cariris Velhos (1.1–0.9 Ga) orogenic event. These isotopic data coupled with calculated $\delta^{18}O$(w.r.) value of +8.75‰ VSMOW indicate an I-type source and suggest a reworked lower continental crust as source rock. A granodioritic orthogneiss next to the Major Isidoro pluton, emplaced along the Jacaré dos Homens transpressional shear zone, yielded a U–Pb SHRIMP zircon age of 642 Ma, recording early tectonic movements along this shear zone that separates the Pernambuco–Alagoas Domain to the north, from the Sergipano Domain to the south. The emplacement of the Major Isidoro pluton was synkinematic, coeval with the development of a regional flat-lying foliation, probably during the peak of metamorphism related to the convergence/contractional deformation of the São Francisco craton and Pernambuco–Alagoas block during the Brasiliano Orogeny.

1. Introduction

The evolution of the Borborema Province, northeastern Brazil was marked at the end of the Neoproterozoic by numerous granitic intrusions, many of them related to shear zones (Ferreira et al., 1998; Guimarães et al., 2004; Neves et al., 2008). The largest volume of intermediate to acidic plutons in this province occurs within the Pernambuco–Alagoas Domain in the southern portion of the province. These plutons exhibit T_{DM} ages ranging from the Archean to the Neoproterozoic and their study has shed light on the assembly of west Gondwana, allowing a better understanding of its tectonic evolution (e.g. Silva Filho et al., 2002; 2014).

The Borborema Province has a key position within western Gondwana, near the junction of northwestern-central Africa and northeastern Brazil, important for the reconstruction of western Gondwanaland. Igneous rocks play an important role in the crustal

* Corresponding author. NEG–LABISE, Dept. of Geology, Av. Acadêmico Hélio Ramos s/n, Cidade Universitária, Recife, PE, 50740-530, Brazil.
E-mail address: rthyego@yahoo.com (T.R. Silva).

http://dx.doi.org/10.1016/j.jsames.2015.09.002
0895-9811/

evolution and geochronological data of these rocks can constitute an important tool in dating of the tectonic events. Calc-alkaline granitic rocks are abundant in the Pernambuco–Alagoas Domain of the Borborema Province. According to Barbarin (1999) calc-alkaline granitic rocks are invariably emplaced above subduction zones, forming vast batholiths, elongated parallel to the trench in the active continental margins. Convergence between the PEAL (Pernambuco–Alagoas Domain) and the São Francisco Craton, to the south, resulted in the formation of the Sergipano belt (e.g. Oliveira et al., 2010 and references therein). The Major Isidoro pluton has a key position next to the boundary between the Pernambuco–Alagoas and Sergipano domains, preserving information on the timing and convergence of these two blocks. Unlike the Sergipano belt, granitic batholiths in the PEAL are not so well known as to their tectonic history. The Major Isidoro tonalite-granite batholith presents calc-alkaline nature that bears similar petrographical and geochemical characteristics to arc-related granites and its synkinematic emplacement can be related to a continental arc construction. In this report, we discuss field, petrographic, lithogeochemical and isotopic aspects of the Major Isidoro pluton that is part of the Águas Belas–Canindé composite batholith, the largest pluton within the Pernambuco–Alagoas Domain, and provide important clues to revealing the tectonic evolution of the Pernambuco–Alagoas Domain during the convergence with the São Francisco Craton.

2. Geologic setting

The Borborema Province is located in northeastern Brazil, to the north of the São Francisco Craton (Fig. 1a). It comprises a structural province formed as a result of the convergence of the Amazonian, West African-São Luis and São Francisco-Congo cratons during the assembly of west Gondwana at ~600 Ma (Trompette, 1997, 2000).

Six crustal segments are recognized in the Borborema Province. Among them is the Pernambuco–Alagoas segment (Fig. 1b) that is limited to the north by the Central Tectonic Domain, to the south by the Sergipano Domain, and to the west, by the Riacho do Pontal Domain (Brito Neves et al., 2000; Van Schmus et al., 2008 and references therein). The designation of this segment has undergone changes among which one can point out: Pernambuco–Alagoas Massif (Brito Neves et al., 1982), Pernambuco–Alagoas Terrane (Santos, 1995), Pernambuco–Alagoas Complex (Silva Filho et al., 2002) and Pernambuco–Alagoas Domain (Van Schmus et al., 2008).

The basement of this domain is dominated by orthogneisses and high-grade metasedimentary rocks, often migmatized, cut by large granitic batholiths (Brito Neves et al., 2000; Silva Filho et al., 2002, 2013). The supracrustal rocks of the Pernambuco–Alagoas Domain have been correlated to the Cabrobó Complex (e.g. Santos, 1995; Silva Filho et al., 2002), whereas migmatites, biotite-gneisses, tonalitic orthogneisses, and leuco-granodiorites to leuco-monzogranites are correlated to the infra-crustal Belém do São Francisco Complex (Santos, 1995).

Silva Filho et al. (2002) determined an age of 2079 ± 34 Ma (U–Pb SHRIMP zircon age) from a porphyroclastic biotite-hornblende granodiorite gneiss at the type locality of the Belém do São Francisco Complex (Santos, 1995), which is interpreted as the age of magmatic crystallization.

Neoproterozoic–Cambrian plutons occur in the Pernambuco–Alagoas Domain in the form of granitic batholiths, each batholith showing various intrusions (Brito Neves et al., 2000; Silva Filho et al., 2002, 2013). Based on petrography, geochemistry and geographical distribution within the Pernambuco–Alagoas Domain, Silva Filho et al. (2002) grouped the main granitic plutons into five major batholiths: Buíque–Paulo Afonso, Águas

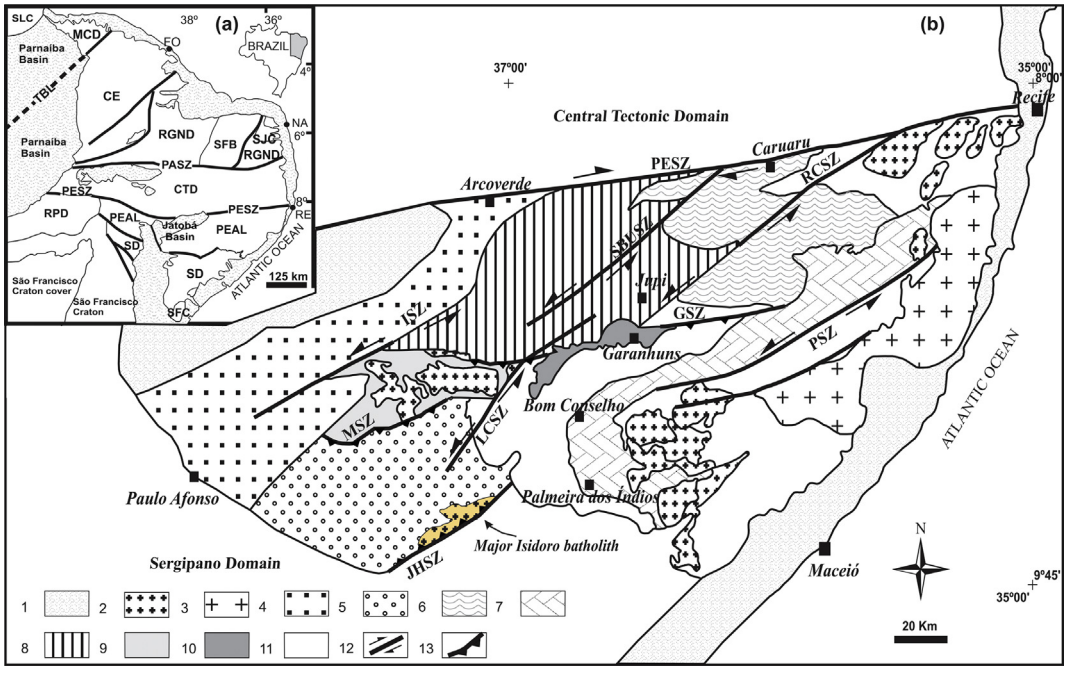

Fig. 1. (a) Borborema Province. Major domains, according to Van Schmus et al. (2008). Notes: CE–Ceará Domain; MCD–Médio Coreaú Domain; PEAL–Pernambuco–Alagoas Domain; RGND–Rio Grande do Norte Domain (SJC–São José do Campestre Archaean nucleus; SFB–Seridó Fold Belt); RPD–Riacho do Pontal Domain; SD–Sergipano Domain; SFC–São Francisco Craton; SLC–São Luís Craton; CTD–Central Tectonic Domain. Faults and shear zones: PASZ–Patos shear zone; PESZ–Pernambuco shear zone; TBL–Transbrasiliano Lineament. Cities and towns: Fo–Fortaleza; Na–Natal; Re–Recife. (b) Geological map of the Pernambuco Alagoas Domain, showing the location of the Major Isidoro batholith. 1–Palaeozoic sedimentary cover; 2–Brasiliano granitoids; 3–Ipojuca–Atalaia batholith; 4–Buique–Paulo Afonso batholith; 5–Águas Belas–Canindé composite batholith; 6–Garanhuns batholith; 7–Palmares Sequence; 8–Venturosa Sequence; 9–Inhapi Sequence; 10–Garanhuns quartzite; 11–Belém do São Francisco Complex; 12–Transcurrent Shear zones (PESZ–Pernambuco; RCSZ–Rio da Chata; PSZ–Palmares; LCSZ–Limitão–Caetés; ISZ–Itaíba; SBUSZ–São Bento do Una); 13–Transpressive shear zones (GSZ–Garanhuns; MSZ–Maravilha; ZCJH–Jacaré dos Homens) (modified from Silva Filho et al., 2010).

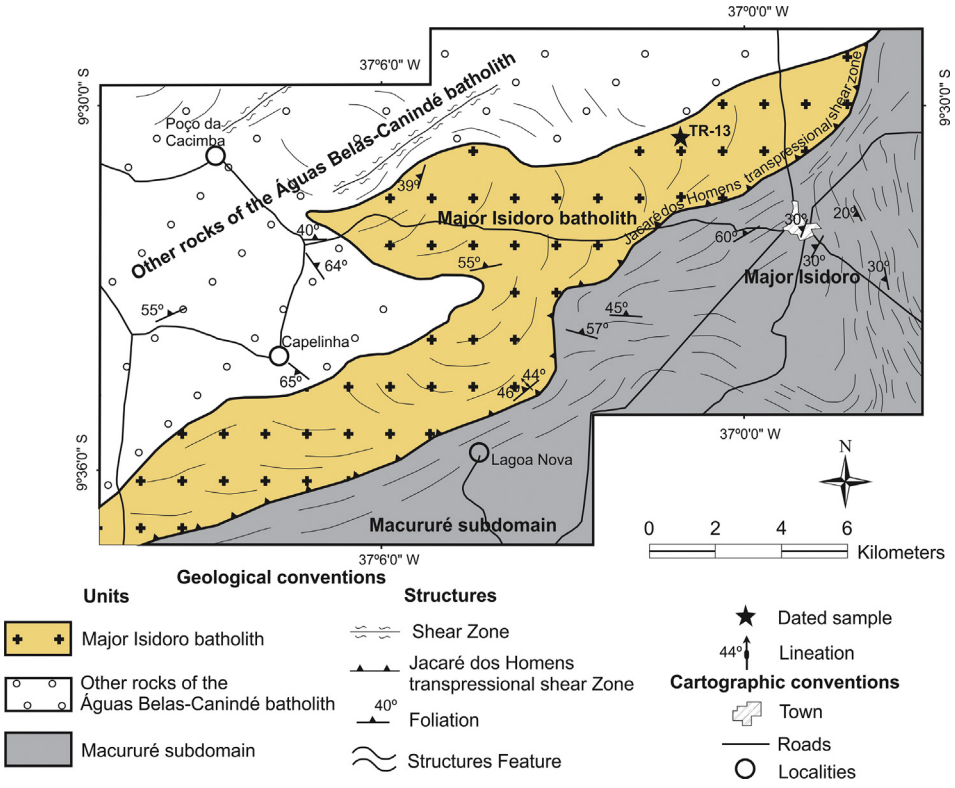

Fig. 2. Simplified geological map of the Major Isidoro batholith with the main geological units of the area and location of dated sample.

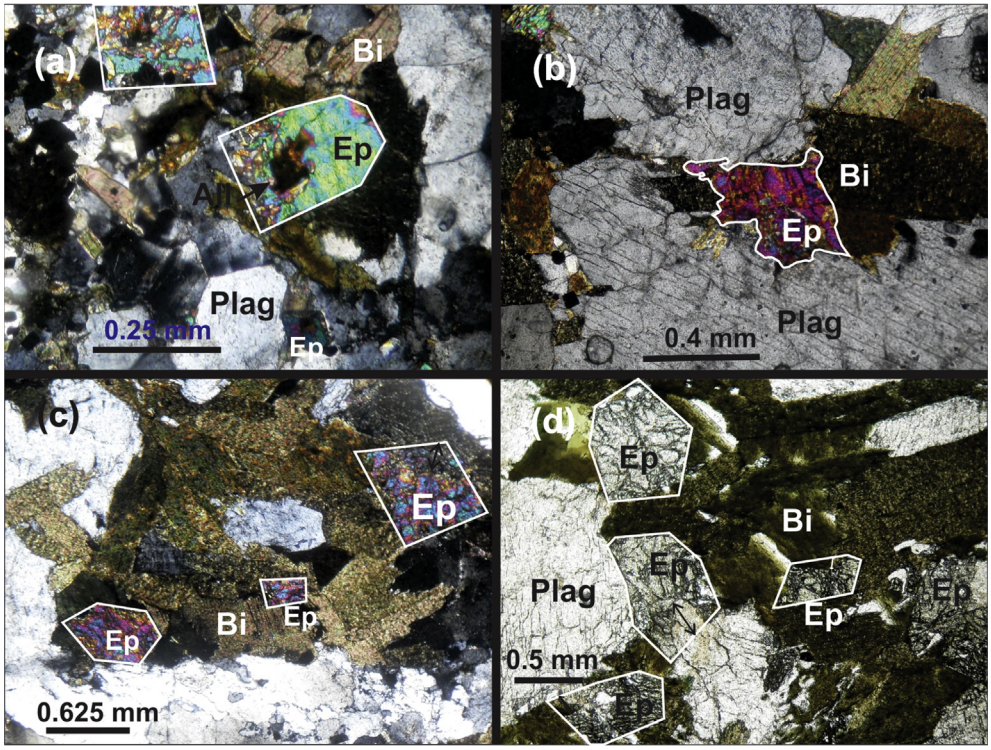

Fig. 3. Magmatic epidote textural relationships observed in Major Isidoro batholith: (a) epidote with allanite core, partially resorbed by the magma; (b) partially resorbed epidote included in biotite and plagioclase; (c) and (d) epidote partially or totally rimmed by biotite. Abbreviations are: All = allanite, Bi = biotite, Ep = epidote and Plag = plagioclase. Lines are an attempt to reconstruct original shape of epidote crystals, indicating how much some of them have been dissolved by host magma. Nicols crossed except for photo d. Field aspects of mafic enclaves in the Major Isidoro batholith: (e) Rounded to elliptical enclaves up to 50 cm long. Sledgehammer is 70 cm long; (f) Elliptical enclaves in the medium-grained tonalite; (g) Mafic enclaves in the medium-grained foliated granodiorite, showing lobate contacts. Hammer is 30 cm long.

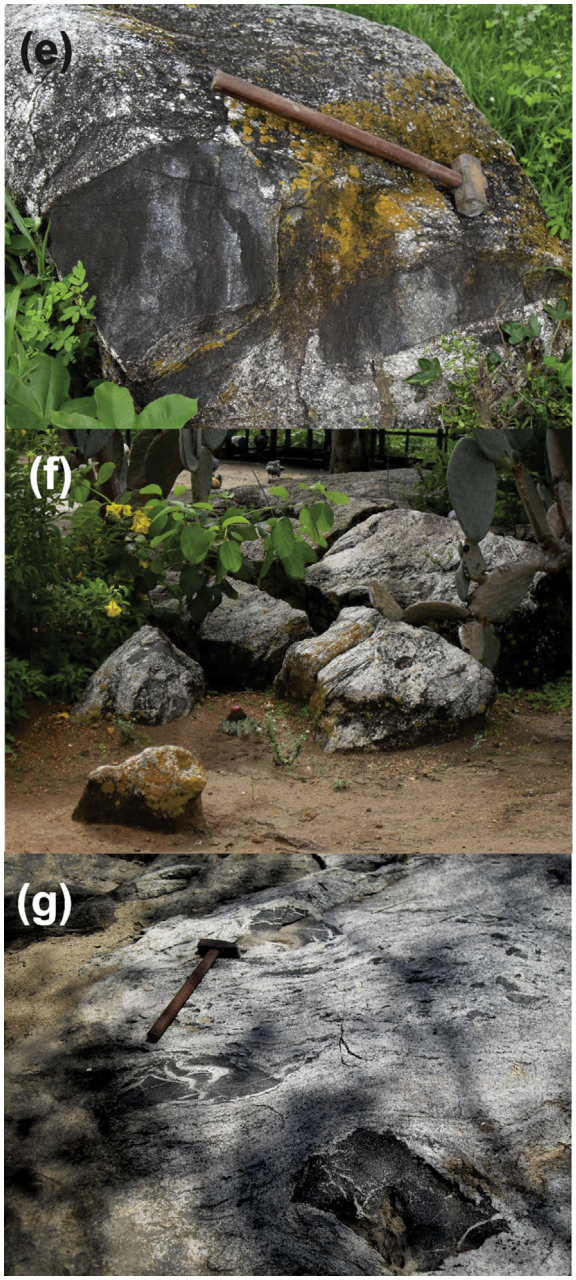

Fig. 3. (*continued*).

Belas–Canindé, Marimbondo–Correntes, Ipojuca–Atalaia, and Garanhuns. Later, based on new Sm–Nd isotopic data from granitoids, orthogneisses and supracrustal rocks, Silva Filho et al. (2014) proposed three crustal sub-domains for the Pernambuco–Alagoas Domain, namely Garanhuns, Água Branca and Palmares. Additionally five distinct model age subdivisions can be recognized in the Pernambuco–Alagoas Domain (Van Schmus et al., 2008). They are (a) T_{DM} older than 2.40 Ga, represented by several local occurrences of gneisses and migmatites, (b) T_{DM} between 2.00 and 2.20 Ga, represented by large areas in the northeastern half of the Pernambuco–Alagoas Domain, (c) T_{DM} between 1.70 and 2.00 Ga, represented by several plutons in the northeastern corner of the domain, (d) T_{DM} between 1.20 and 1.50 Ga, represented by large parts of the southwestern half of the Pernambuco–Alagoas Domain and (e) T_{DM} between 0.90 and 1.20 Ga, represented mainly by the Buique–Paulo Afonso batholith.

U–Pb zircon crystallization ages of granitoids of the Pernambuco–Alagoas Domain lie in the 572 Ma to 627 Ma time interval (Silva Filho and Guimaraes, 2000; Ferreira et al., 2015; Neves et al., 2008; Silva Filho et al., 2010, 2013, 2014; Silva et al., this study) and Nd T_{DM} model ages range from Archean to Neoproterozoic.

3. Field relationships and petrography

The Major Isidoro batholith has a NE–SW elongate shape, covering an area of about 100 km^2. The main axis of the batholith is approximately parallel to the trend of the regional foliation, roughly following the direction of the contact between the Pernambuco–Alagoas and Sergipano domains. This batholith is one of several intrusions that comprise the Águas Belas–Canindé composite batholith, part of the Água Branca crustal sub-domain (Silva Filho et al., 2002, 2013). It is located at the boundary of the Pernambuco–Alagoas Domain with the Sergipano Domain, limited to the south and east by the Jacaré dos Homens transpressional shear zone (Mendes et al., 2008), in contact with high-grade rocks of the Macururé sub-domain of the Sergipano Domain (Oliveira et al., 2006, 2010; Van Schmus et al., 2008; Lima et al., 2014) (Fig. 2). The Major Isidoro pluton has intruded, to the north and to the west, other Neoproterozoic granitic plutons of the Águas Belas–Canindé batholith.

The Major Isidoro batholith comprises leucocratic to mesocratic magmatic epidote-bearing biotite granite to tonalite with gray/pink color. Two main petrographic facies were recorded: Amphibole-biotite tonalite; epidote-biotite syenogranite. Rocks of the two facies are inequigranular, coarse-grained porphyritic, with alkali-feldspar megacrysts sometimes up to 5 cm in length; megacrysts of plagioclase and quartz also occur. Quartz chunks, up to 10 cm long, are also observed. The essential components are quartz, plagioclase and alkali feldspar (ca. of 70–80% of the mode), while biotite is the main mafic constituent and reaches up to 20%; amphibole, titanite, apatite, epidote, zircon and opaque minerals are the accessory minerals. Primary epidote is found as euhedral to subhedral crystals, sometimes it exhibits allanite cores and is partially included in biotite (Fig. 3a); less commonly it is seen within plagioclase (Fig 3b), or as subhedral grains partially or totally rimmed by biotite that were partially resorbed by the host magma (Fig. 3c, d). The textural relationships resemble those described by Zen and Hammarstrom (1984) and Sial, (1990), Sial et al. 1999, 2008) as typical of magmatic epidote.

High temperature solid-state deformation in the Major Isidoro pluton is expressed by chessboard extinction in quartz, development of myrmekitic intergrowths around alkali feldspar and static recrystallization of feldspar grains. Rounded to elliptical enclaves up to 50 cm long, sometimes with sharp contacts, are common (Fig. 3e, f). Coexistence of mafic and felsic magmas is suggested by the presence of felsic magma injections into mafic enclaves (Fig. 3g). Narrow aplitic dikes cut the granitic pluton.

Low-angle foliation, dipping northwest, is dominant in the pluton and country rocks suggesting that the emplacement of this batholith was coeval to the development of the flat-lying foliation. Partial melting was recorded in many areas within this pluton, suggesting high-strain synkinematic emplacement during the Brasiliano orogeny.

Based on partial melting, segregation and deformation recorded in rocks of this batholith, several people (e.g. Mendes et al., 2008) have regarded these rocks as part of the Belém do São Francisco complex (Paleoproterozoic in age, according to Silva Filho et al., 2002) due to the difficulty of distinguishing in the field these crustal rocks of the pre-to syn-tectonic Brasiliano plutons (Van Schmus et al., 2008).

Table 1
Representative geochemical data for granites from the Major Isidoro batholith. Sample TR-70M (enclave). Major elements in wt.%, trace elements in ppm.

Sample	TR-13	TR-18	TR-20	TR-21	TR-22	TR 24	TR-25	TR-26	TR-37	TR-38	TR-39	TR-70M
SiO_2	70.05	68.87	67.08	71.57	59.13	69.23	68.68	67.86	66.58	65.60	65.10	56.93
Al_2O_3	14.08	14.43	14.41	17.16	16.90	15.39	14.91	15.34	15.62	15.40	16.10	14.69
MgO	0.51	1.77	2.43	0.61	2.62	0.67	1.34	1.32	1.47	2.20	1.80	2.73
MnO	0.01	0.07	0.10	0.03	0.20	0.03	0.08	0.06	0.04	0.10	0.10	0.27
CaO	2.14	2.59	2.88	2.05	4.58	1.42	2.41	3.25	2.36	2.80	3.10	7.99
Na_2O	4.09	3.51	4.01	3.12	5.24	3.36	3.55	4.62	3.66	4.10	4.90	4.30
K_2O	4.20	3.58	2.12	4.54	2.07	5.10	4.95	1.59	4.60	2.20	2.00	0.55
TiO_2	0.40	0.85	0.68	0.24	1.28	0.45	0.57	0.58	0.63	0.90	0.80	1.67
P_2O_5	0.24	0.26	0.09	0.06	0.49	0.11	0.17	0.14	0.17	0.20	0.30	0.30
Fe_2O_{3T}	2.35	5.12	5.80	1.54	7.44	2.31	3.79	3.46	2.46	5.60	5.00	7.61
P.F	0.62	0.33	0.62	0.2	0.72	0.94	0.44	0.94	1.15	0.67	0.89	1.36
Total	98.74	101.38	100.29	101.32	100.67	99.01	100.92	99.16	98.74	99.90	99.80	98.39
Trace elements												
Cr	273.6	205.2	410.4	255	136.8	292	205.2	205.2	204	115	89	291
Ba	1172	1037	314	1223	279	1322	1627	371	2140	400	319	144
Rb	106.7	139.4	109.1	497	125.7	107	129.2	74.0	130	130	108	−5
Sr	440	402	389	166	436	464	555	522	1293	519	490	419
Zr	262	408	95	49	364	317	305	120	281	273	260	221
Y	33.0	58.36	17.53	166	92.00	35	47.88	10.0	44	29	47	37
Nb	17.64	24.94	12.22	6	49.88	9	21.47	7.57	22	6	19	27
Ni	11	25	40	23	7	21	17	12	91	20	12	31
La	26.2	131.9	34.3		34.0		44.7	29.3				
Ce	52.8	276.0	75.5		103.2		106.3	57.3				
Pr	7.98	27.36	7.33		17.41		11.54	8.12				
Nd	35.4	103.2	28.3		80.8		49.7	27.2				
Sm	7.5	16.1	4.1		19.8		10.2	3.1				
Eu	1.98	2.27	0.80		3.94		1.96	0.84				
Gd	6.71	12.86	3.55		18.08		8.86	13.11				
Tb	1.03	1.91	0.51		2.87		1.39	0.70				
Dy	6.12	9.74	3.02		16.80		7.52	86.49				
Ho	1.17	1.82	0.55		3.25		1.46	0.30				
Er	3.50	4.46	1.48		9.23		3.92	0.78				
Tm	0.44	0.62	0.17		1.33		0.56	0.08				
Yb	2.9	3.6	1.1		8.6		3.7	0.6				
Lu	0.20	0.43	0.13		0.99		0.48	0.05				
Hf	7.17	9.77	2.04		7.67		6.44	4.07				
Th	6.2	43.6	10.6		8.8		14.9	7.7				
U	1.94	2.25	0.34		3.96		1.68	0.65				
Ta	1.80	1.50	0.05		4.64		1.92	0.44				
Ga	18.2	21.1	23.3		28.9		18.9	20.5				
V	18	78	61		118		49	20				
Co	5.5	13.4	14.3		14.3		8.9	9.1				
Cs	2.08	5.63	6.44		23.29		2.76	3.04				
Cu	10	34	6		36		7	5				
Zn	27	99	144		136		86	39				
Sn	4.2	4.4	3.0		15.9		3.2	2.8				

4. Analytical procedures

4.1. SHRIMP methodology

U–Pb SHRIMP dating was used to determine the crystallization age of zircon grains from the studied granitoids. Zircon grains were separated from the whole-rock sample (sample TR–13) using standard crushing, washing and heavy liquid methods. The heavy mineral concentrates were subsequently processed by magnetic separation on a Frantz isodynamic separator at the Stable Isotope Laboratory (LABISE) at the Federal University of Pernambuco. Representative zircon grains were hand picked from the non-magnetic fraction under binocular microscope and were placed onto doublesided tape and mounted together with chips of reference zircon crystals in epoxy disks, ground to half thickness, and polished with 3 μm and 1 μm diamond paste in order to expose the internal structure. A conductive gold-coating was applied just prior to analysis.

The grains were photographed in reflected and transmitted lights, and cathodoluminescence (CL) images were produced in a scanning electron microscope in order to investigate the internal structures of the zircon crystals, to characterize different populations, and to ensure that the spot was wholly within a single age component within the sectioned grains. Analyses were performed on the SHRIMP IIe at the University of São Paulo (USP), São Paulo, Brazil.

The abundances of U, Th and Pb, as well as Pb isotope ratios, were normalized using the SL13 zircon standard (U = 238 ppm; Williams, 1998). Correction for common Pb was made using measured ^{204}Pb. The U–Pb isotope ratios were collected in sets of five scans throughout the masses, and the TEMORA 2 reference zircon ($^{206}Pb/^{238}U$ 416.8 ± 0.3 Ma; Black et al., 2004) was measured every third unknown analysis. Errors in the isotopic ratios and ages are quoted at 1 sigma level. Data reduction was performed using SQUID/Excel macro (Ludwig, 2009), and errors are given at 95%-confidence level. The analyses were plotted on a conventional Wetherill U–Pb concordia diagram.

4.2. Major and trace chemistry, and Sr, Nd and O isotope determinations

Whole-rock major and some trace element chemical analyses were performed by XRF at the Department of Geology, Federal University of Pernambuco. Rare-earth element analyses were done

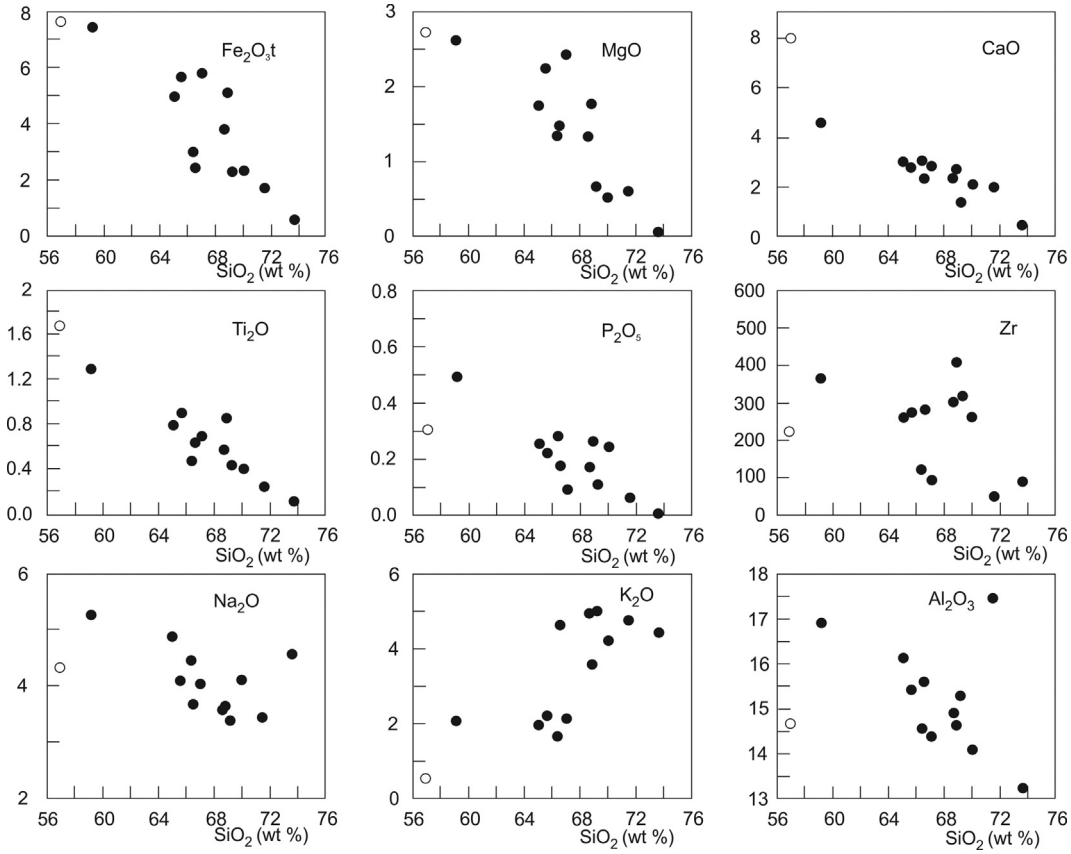

Fig. 4. Harker variation diagrams for samples from the Major Isidoro batholith. Filled dot–granites; unfilled dot–enclave. Same for Fig. 5a, b and c.

by ICP-OES at the SDS-Geosol Laboratory, Belo Horizonte, Brazil. Representative whole-rock chemical analyses for the Major Isidoro batholith are listed in Table 1.

Whole-rock Rb and Sr concentrations were obtained by X-ray fluorescence (XRF) with a fully automated Rigaku RIX-3000 XRF spectrometer at the NEG–LABISE, Department of Geology, Federal University of Pernambuco (UFPE), Recife, Brazil, by the calibration curves method prepared using certified reference standards. Sr isotopic analyses were performed at the Geochronology Laboratory of the University of Brasília, Brazil. Approximately 50 mg of powdered rock samples were dissolved in concentrated HF, HNO_3 and HCl. Sr aliquots were separated from the solutions using conventional ion exchange techniques and deposited on Re filaments. Isotopic analyses were carried out with a multicollector Finnigan MAT-262 mass spectrometer in static mode. Corrections for mass fractionation were done using $^{88}Sr/^{86}Sr$ of 8.3752. 2σ errors are smaller than 0.01% for the $^{87}Sr/^{86}Sr$ ratios and of ca. 1% for the $^{87}Rb/^{86}Sr$ ratio. Sm–Nd isotopic analyses followed the method described by Gioia and Pimentel (2000) and were carried out at the Geochronology Laboratory of the University of Brasília. Whole-rock powders (ca. 50 mg) were mixed with $^{149}Sm/^{150}Nd$ spike solution and dissolved in Savillex capsules. Sm and Nd extraction of whole-rock samples followed conventional cation exchange techniques, using Teflon columns containing LN-Spec resin (HDEHP–diethylhexil phosphoric acid supported on PTFE powder). Sm and Nd samples were loaded on Re evaporation filaments of double filament assemblies and the isotopic measurements were carried out on a multi-collector Finnigan MAT-262 mass spectrometer in static mode. Uncertainties for Sm/Nd and $^{143}Nd/^{144}Nd$ ratios are better than ±0.4% (1σ) and ±0.005% (1σ) respectively, based on repeated analyses of international rock standards BHVO-1 and BCR-1. $^{143}Nd/^{144}Nd$ ratios were normalized to $^{146}Nd/^{144}Nd$ of 0.7219 and the decay constant used was 6.54×10^{-12} a^{-1}. Oxygen isotope ratios of 2.5–3 mg of zircon were analyzed at the LABISE, Department of Geology, Federal University of Pernambuco, Recife, Brazil. Oxygen was liberated in a laser-based extraction line by reaction with BrF5, reacted with hot graphite, and converted into CO_2 for mass spectrometer analysis following the procedures described by Valley et al. (1995). Isotope ratios were determined in a Delta V Advantage Thermofinningan mass spectrometer. Results are reported in standard permil notation relative to Vienna Standard Mean Ocean Water (VSMOW). Precision is better than±0.1‰.

5. Geochemistry

The Major Isidoro batholith shows SiO_2 varying between 59.13 and 71.57%. The Al_2O_3 contents vary from 14.08 to 17.46%, K_2O ranges from 1.66 to 5.0%, Na_2O values are between 3.36 and 5.24% with an average of 4.07%. CaO ranges from 1.42 to 4.58%, the Fe_2O_3t ranges between 1.74 and 7.44%, MgO from 0.51 to 2.62%. The MnO contents vary from 0.01 to 0.20%, P_2O_5 from 0.06 to 0.49%, while TiO_2 values range from 0.24 to 1.28% with a mean of 0.7%.

In a SiO_2 versus all oxides diagram, the Major Isidoro batholith samples exhibit negative trends except for K_2O, suggesting crystal fractionation as the major controlling magmatic process (Fig. 4). Inverse correlations between P_2O_5 and TiO_2 with SiO_2 point to early saturation of apatite and an Fe–Ti oxide. On the other hand the decrease in Zr with increasing SiO_2 is consistent with saturation with zircon.

The total alkali contents are high, ranging from 6.09 to 8.50%, K_2O/Na_2O ratios ranging from 0.37 to 1.49 with an average of 0.89. In the total alkali versus silica (TAS) diagram (Fig. 5a), with fields of

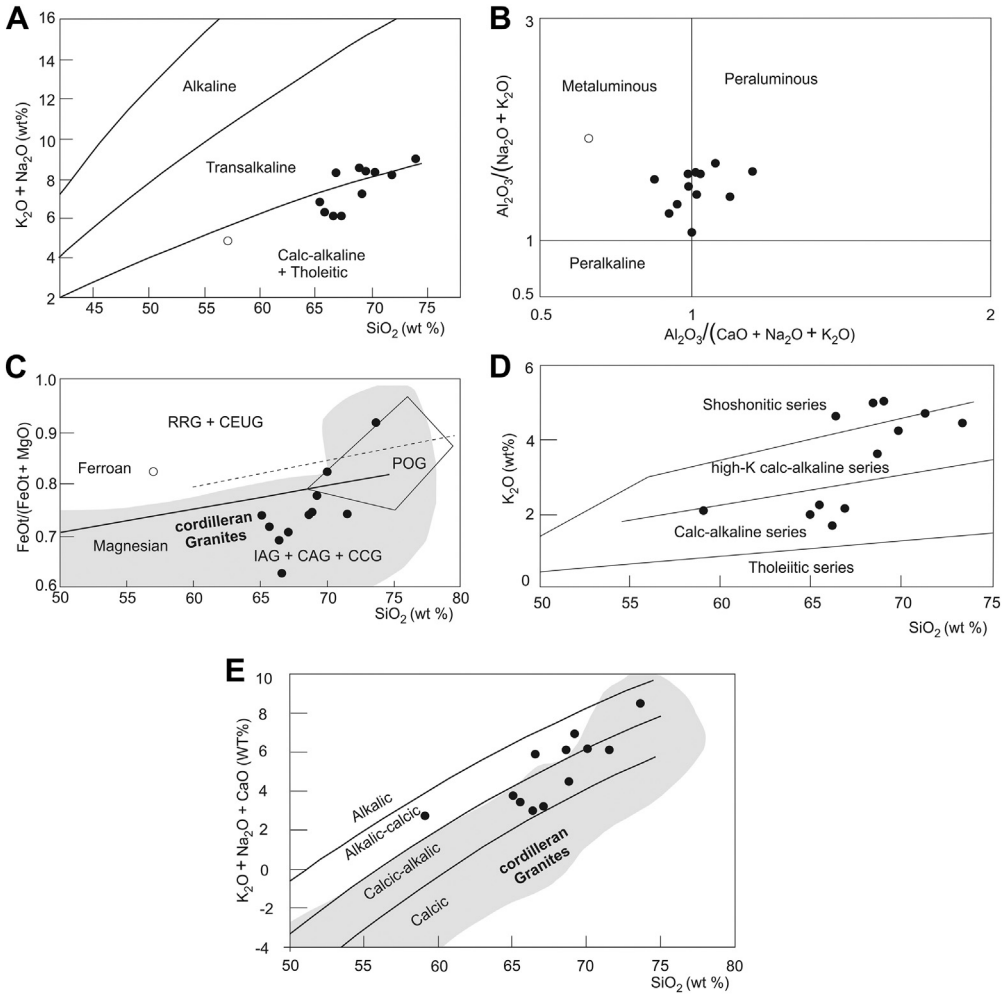

Fig. 5. (a) Total Alkalis/Silica (TAS) classification with fields after Middlemost (1997). (b) Aluminum saturation index (Shand, 1947; Maniar and Picolli, 1989). (c) The composition range of the studied granitoids in the $FeO^t/(FeO^t + MgO)$ versus SiO_2 diagram. Fields of ferroan and magnesian granitoids are from Frost et al. (2001). The fields of RRG + CEUG (anorogenic granitoids), POG (post-orogenic granitoids) and IAG + CAG + CCG (orogenic granitoids) after Pearce et al. (1984) (d) Studied granitoids plotted in the K_2O versus SiO_2 diagram with fields after Peccerillo and Taylor (1976). (e) Modified alkali-lime index (MALI)/$Na_2O + K_2O - CaO$ vs wt % SiO_2 diagram.

plutonic rocks after Middlemost (1997), the samples fall within the calc-alkaline to trans-alkaline series field. This batholith shows metaluminous to slightly peraluminous (molar $Al_2O_3/(CaO + Na_2O + K_2O) \leq 1.21$; average of 1.02) character, with a small variation in the alumina saturation index (ASI) that ranges from 0.88 to 1.21 (Fig. 5b). The coexistence of hornblende and biotite in the Major Isidoro batholith rocks indicates that they are metaluminous. It is known that granitoids of mixed or mantle origin can acquire peraluminous composition after amphibole fractionation, volatile interaction, or pelitic rock assimilation (Barbarin, 1999 and references therein).

The analyzed samples plot within the field of magnesian series of magmas in the $FeO_{tot}/(FeO_{tot} + MgO)$ versus SiO_2 diagram (0.62–0.92) (Fig. 5c), reflecting hydrous, oxidizing magmas (Frost and Lindsley, 1991; Frost et al., 2001). In the K_2O versus SiO_2 diagram (Fig. 5d) with fields after Peccerillo and Taylor (1976) the samples plot in a variety of fields: calc-alkaline, high K calc-alkaline and shoshonitic. In the ($Na_2O + K_2O$–CaO) *versus* SiO_2 discrimination diagram (Frost et al., 2001), the samples from the Major Isidoro batholith plot in the alkali-calcic to calc-alkalic series fields (Fig. 5e), most of them plotting within the field formed by Cordilleran-type granitoids.

In an attempt to infer the tectonic environment in which the Major Isidoro batholith was emplaced, we have used a number of trace-element discrimination diagrams. In the Nb–Y discriminant diagram of Pearce et al. (1984), most samples plot within or along the boundary of the volcanic arc granitoid field (Fig. 6a). In the Rb/30 x Hf x Ta*3 diagram of Harris et al. (1986), most samples plot within the volcanic arc field (Fig. 6b).

This batholith displays several characteristics of amphibole-bearing calc-alkaline granitoids (ACG) of Barbarin (1999), the most abundant granitoids in volcanic island arcs and active continental margins associated with K-rich calc-alkaline granitoids. The essential mineral assemblage (biotite + magnetite + amphibole), accessory minerals (titanite + allanite) and geochemical signatures (metaluminous to slightly peraluminous), together with moderate Na_2O and large variation of silica content (SiO_2 = 59.13–71.57%) are compatible with I-type granitoids of Chappell and White (1974, 1992, 2001), and White (1979). These types of granitoids form under high-oxygen fugacity conditions and correspond to the magnetite-series granitoids of Ishihara (1977), with a mineral assembly that encompasses magnetite + titanite + epidote.

Rare earth element (REE) patterns normalized to the chondrite values of Evensen et al. (1978) show slight enrichment of light rare earth elements (LREE) relative to the heavy rare earth elements (HREE) (Fig. 7a), with La_N/Lu_N = 13.6–31.8, relatively flat HREE patterns (Gd_N/Lu_N ranging from 2.3 to 4.2), and discrete negative Eu anomalies (Eu/Eu^* = 0.48–0.85). La_N/Sm_N ratios range from 1.1 to

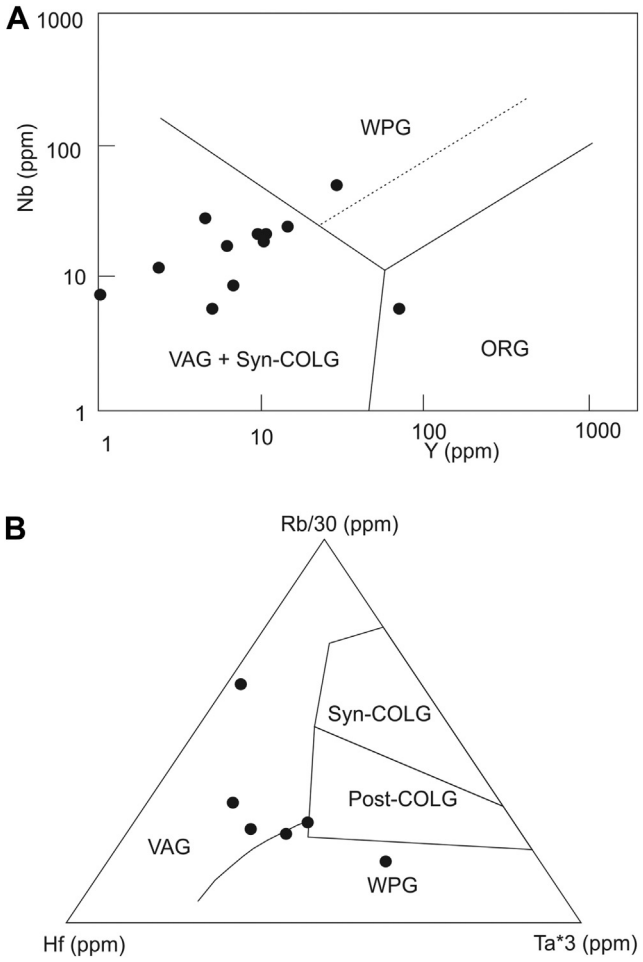

Fig. 6. (a) Nb vs. Y discrimination diagram (Pearce et al., 1984). (b) Diagram proposed by Harris et al. (1986) using trace elements Rb, Hf, and Ta. Syn-COLG, syncollision granite; VAG, volcanic arc granite; WPG, within-plate granite; ORG, ocean ridge granite; Post-COLG, post-collision granite.

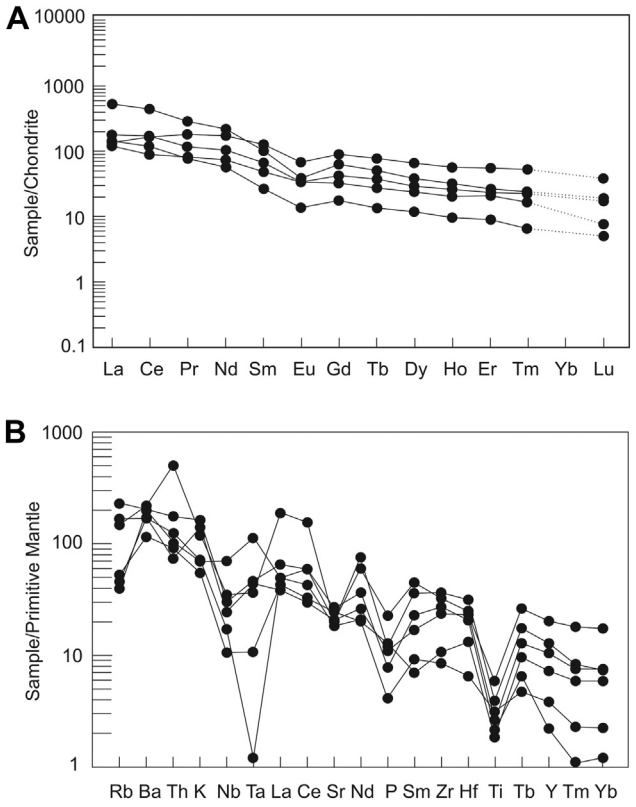

Fig. 7. (a) Rare earth elements are normalized against chondrite values of Evensen et al. (1978). (b) Variation diagram for whole-rock element abundances in the Major Isidoro batholith, normalized to abundances for primitive mantle compiled by Sun and McDonough (1989).

5.3. These rocks are also enriched in large ion lithophile elements (LILE) compared to high field strength elements (HFSE), a general characteristic of calc-alkaline granitoids. Incompatible-element variation diagrams normalized to primitive mantle are characterized by deep Ti troughs and small Sr, P and Nb troughs, with either negative or positive Ta anomalies (Fig. 7b).

6. Zircon description and U–Pb SHRIMP ages

The analyzed zircon population consists of pink and yellow crystals. The main grains are sub-euhedral to euhedral, some of them are corroded. Zircon grains are elongated and present bipyramidal terminations, typical of magmatic growth. Grains have lengths ranging from 315 to 175 μm (Fig. 8) and length-width ratios, from 3:1 to 3:2. Images from scanning electron microscope (SEM) and cathodoluminescence (CL) reveal the main grain features that include margins with oscillatory zoning and rounded inherited cores some of which also have oscillatory zonation. Some zircon cores are lighter in CL images than their margins and exhibit greater roundness and truncation of internal zoning. Core-rim contacts are sometimes irregular and sharp.

Eleven zircon grains were analyzed, totaling fourteen spots (Table 2). Eight grains cluster close to concordia and yield a weighted $^{206}Pb/^{238}U$ mean age of 626.6 ± 4.1 Ma, with MSDW of 2.1 (Fig. 9). These grains show high Th/U ratios ranging from 0.25 to 0.60, typical of magmatic zircon (Williams and Claesson, 1987). The euhedral shape and high Th/U ratio of the zircon grains suggest that this age should correspond to the zircon crystallization age and, thus, to the emplacement age of the Major Isidoro batholith.

Four zircon cores have been dated and exhibit $^{206}Pb/^{238}U$ ages that range from 797 to 1007 Ma (Fig. 9) and Th/U ratios from 0.37 to 0.72. Just one zircon core has showed a Th/U ratio above 0.6 and, therefore, the cores are mostly from igneous sources.

Two zircon grains (3.1 and 9.1) with ages younger than 600 Ma, one nearly concordant (% disc = 3), show Th/U ratios of 0.33 and 0.30, respectively. These ages may be young due to some undefined Pb loss.

7. Sm–Nd and Rb–Sr results

The Major Isidoro batholith shows Nd model ages ranging from 1.1 to 1.4 Ga, and negative εNd (627 Ma) that varies from −1.09 to −2.12 (Fig. 10a), with $^{143}Nd/^{144}Nd$ ranging from 0.512167 to 0.512249 (Table 3). Initial $^{87}Sr/^{86}Sr$ ratios, back-calculated to 627 Ma, vary from 0.7069 to 0.7086 and suggest presence of a continental-crust component in the source. The εSr (627 Ma) ranges from 44 to 69 (Fig. 10b).

8. Oxygen isotopes

Zircon oxygen isotope ratios tend to reflect the $\delta^{18}O$ of magmatic source rocks (Valley, 2003; Valley et al., 2005). Igneous zircon crystals in high temperature equilibrium with mantle magmas have average $\delta^{18}O = 5.3 \pm 0.3‰$ (Valley et al., 1998, 2005) and high- $\delta^{18}O$

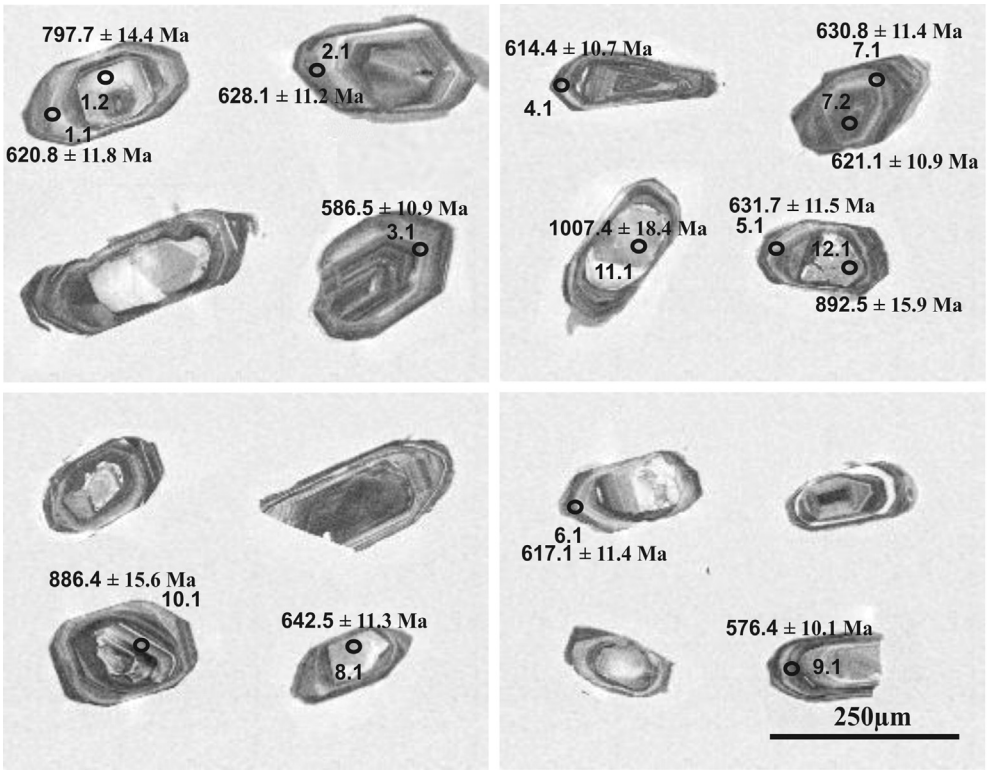

Fig. 8. Cathodoluminescence (CL) images of the zircon crystals. Circles indicate the position of the U–Pb analysis listed in Table 2.

zircon indicates a supracrustal, metasedimentary source, or a source that interacted with seawater at low temperature (Cavosie et al., 2011).

Valley et al. (1994) were the first to use the correlation of ^{18}O whole rock and zircon in four model rock compositions of varying SiO_2 content to derive an approximate relationship of ^{18}O (WR–Zrc) as a function of wt % SiO_2 of corresponding rock, and this empirical relationship among $\delta^{18}O$ (zircon), $\delta^{18}O$ (whole rock), and SiO_2 (whole-rock) is currently used (e.g. Valley et al., 2005; Lackey et al., 2008). Applying the empirical relationship for Major Isidoro batholith, $\delta^{18}O$ (zircon) values of 6.95‰ and 7.02‰ and whole-rock SiO_2 (70.05 and 69.23 wt.%) provide calculated magmatic whole-rock $\delta^{18}O$ values of +8.74‰ and +8.76‰. Values of $\delta^{18}O$ higher than ~6.3‰ in igneous zircon are not found in mantle-derived igneous rocks, and require a component of crust altered at low temperatures (Cavosie et al., 2009). Intra-pluton $\delta^{18}O$ variations typically are small, <0.3‰ (e.g. Lackey et al., 2008), and the $\delta^{18}O$ variation of Major Isidoro batholith is within this interval.

9. Discussion

A compressional deformation related to the Brasiliano/Pan-African Orogeny is roughly coeval through a large portion of the Borborema province, starting around 640–630 Ma (Neves et al., 2012, 2015). The resultant foliation is preserved in host rocks to the south of the Major Isidoro pluton, member of Águas Belas–Canindé composite batholith, in schists and gneisses of the Macururé sub-domain (Oliveira et al., 2006, 2010; Lima, 2013; Lima et al., 2014). The crystallization age of 627 Ma of Major Isidoro pluton is near the early time boundary of the deformation associated with the Brasiliano orogeny, and similar to that of the peak of high-temperature metamorphism, and development of low-angle foliation during the event associated with the collision between the São Francisco Craton and the Pernambuco–Alagoas Block (Oliveira et al., 2010). Lima (2013) obtained a U–Pb SHRIMP age of 642.4 ± 3.4 Ma for zircon in a granodiorite gneiss from the Jacaré dos Homens transpressional shear zone. Structural data coupled with geochronological data are suggestive that the Major Isidoro batholith has intruded approximately 15 M y. after earlier tectonic movements along the Jacaré dos Homens transpressional shear zone during development of the regional low-angle foliation. This foliation in the Pernambuco–Alagoas Domain is possibly related to continental arc construction in the Sergipano orogen. In this domain Oliveira et al. (2015) found granites of 630–618 Ma with penetrative low-angle foliation or containing microstructures indicative of solid-state deformation probably related to a continental arc. The Major Isidoro and Monteirópolis (to be published elsewhere) batholiths are probably remnants of the linear belt of juvenile plutons in the Pernambuco–Alagoas Domain.

In the Água Branca crustal sub-domain of the Pernambuco–Alagoas Domain (Silva Filho et al., 2002; Van Schmus et al., 2008), the emplacement of the Água Branca, Mata Grande, Serra da Caiçara and Serra do Catu plutons occurs as syn-to post-collisional intrusions (Silva Filho et al., 2013) and are coeval with the Major Isidoro intrusion. Its crystallization age lies in the time interval (630–615 Ma) common to intrusions of granitoids in various domains of the eastern Borborema Province, such as in the Central Tectonic Domain (e.g. Sial, 1993; Guimarães et al., 2004, 2011; Ferreira et al., 2004, 2011; Van Schmus et al., 2011; Cruz and Accioly, 2012) and in the Sergipano Domain (Bueno et al., 2009; Long et al., 2005; Oliveira et al., 2015).

Within the Pernambuco–Alagoas Domain, similar ages (or just slightly younger) have been reported as the crystallization age of the protolith of the Jupi orthogneiss (606 Ma) and of the protolith of the Caruaru orthogneiss (618 Ma), which were inferred to have been intruded and deformed during development of the regional flat-lying foliation (Neves et al., 2008, 2012).

In the Central Tectonic Domain, U–Pb (zircon) crystallization

Table 2
Summary of SHRIMP U–Pb zircon data. Sample TR–13.

Grain. Spot	%$^{206}Pb_c$	U ppm	Th ppm	$^{232}Th/^{238}U$	ppm $^{206}Pb^*$	(1)$^{206}Pb/^{238}U$age	(1)$^{207}Pb/^{206}Pb$ age	% Dis	(1)$^{207}Pb^*/^{206}Pb^*$	± %	(1)$^{207}Pb^*/^{235}Pb$	± %	(1)$^{206}Pb^*/^{238}Pb$	± %	Erro corr
1.1	−0.12	254	113	0.46	22.1	620.8 ± 11.8	699.1 ± 41	13	0.0627	1.9	0.8744	2.8	0.1011	2.0	0.7232
1.2	0.38	194	70	0.37	22.1	797.7 ± 14.4	783.0 ± 63	−2	0.0653	1.8	11.854	3.5	0.1317	1.9	0.5420
2.1	−0.24	230	118	0.53	20.2	628.1 ± 11.2	789.1 ± 35	26	0.0655	1.7	0.9237	2.5	0.1023	1.9	0.7440
3.1	0.13	355	113	0.33	29.1	586.5 ± 10.9	664.5 ± 36	13	0.0617	1.4	0.8106	2.6	0.0952	1.9	0.7589
4.1	−0.02	293	70	0.25	25.2	614.4 ± 10.7	636.3 ± 48	4	0.0609	2.2	0.8400	2.9	0.1000	1.8	0.6339
5.1	0.07	333	112	0.35	29.4	631.7 ± 11.5	622.6 ± 37	−1	0.0605	1.5	0.8593	2.6	0.1030	1.9	0.7405
6.1	0.17	185	91	0.51	16.0	617.1 ± 11.4	603.9 ± 46	−2	0.0600	1.9	0.8312	2.9	0.1005	1.9	0.6715
7.1	0.11	170	99	0.60	15.0	630.8 ± 11.4	640.0 ± 48	1	0.0610	1.9	0.8650	2.9	0.1028	1.9	0.6501
7.2	0.00	309	86	0.29	26.9	621.1 ± 10.9	614.0 ± 34	−1	0.0603	1.6	0.8408	2.4	0.1011	1.8	0.7564
8.1	−0.24	235	95	0.42	21.1	642.5 ± 11.3	718.0 ± 35	12	0.0633	1.6	0.9145	2.5	0.1048	1.8	0.7459
9.1	0.23	331	96	0.30	26.7	576.4 ± 10.1	593.7 ± 37	3	0.0597	1.4	0.7703	2.5	0.0935	1.8	0.7317
10.1	0.12	174	100	0.59	22.1	886.4 ± 15.6	895.3 ± 37	1	0.0689	1.5	14.001	2.6	0.1474	1.9	0.7200
11.1	0.00	124	87	0.72	18.1	1007.4 ± 18.4	973.1 ± 34	−3	0.0715	1.7	16.687	2.6	0.1691	2.0	0.7635
12.1	0.15	168	92	0.56	21.5	892.5 ± 15.9	853.1 ± 33	−4	0.0675	1.5	13.820	2.5	0.1485	1.9	0.7667

Errors are 1-sigma; Pb_c and Pb^* indicate the common and radiogenic portions, respectively. 1) Common Pb corrected using measured ^{204}Pb.

ages ranging from 920 to 1000 Ma have been recorded in a Cariris Velhos (1.1–0.9 Ga)-age orthogneisses (Brito Neves et al., 2001; Santos et al., 2010; Guimarães et al., 2012; Van Schmus et al., 2011). Igneous rocks with Tonian ages are scarce in the Pernambuco–Alagoas or Sergipano domains. In the Sergipano Domain, ages of ca. 1.0 Ga in detrital zircon grains from metasedimentary rocks (quartzites and mica schists) of the Macururé sub-domain have been determined (Oliveira et al., 2006, 2010), while in the Poço Redondo sub-domain, Van Schmus et al. (1995) reported U–Pb ages of 1007 Ma on zircon grains from a metarhyolite and 1045 Ma from a sub-volcanic granitic sheet. In this domain, ages of 980 and 961 Ma were found in migmatitic gneisses (Oliveira et al., 2010, and references therein). In this work we find nuclei of igneous zircon with ages in the interval 800 to 1000 Ma, indicating that the source of these rocks is related to the so-called Cariris Velhos event (widespread and first described in the Central Tectonic Domain). This is the first Cariris Velhos age found in igneous rocks in the Pernambuco–Alagoas Domain. Similar ages within this Domain have been reported from orthogneiss in the southeastern part of this domain (eastern Jatobá Basin) with an upper intercept of 972 Ma (Silva Filho et al., 2014) and western part of the Domain (western Jatobá Basin) in the Rocinha orthogneiss (956 Ma) (Cruz and Accioly, 2013).

The T_{DM} model ages for the Major Isidoro batholith ranging from 1.1 to 1.4 Ga are compatible with the full range of T_{DM} model ages of the oldest (650–620 Ma) granitoids (Ferreira et al., 2004) or stage I plutons (Van Schmus et al., 2011) of the Central Tectonic Domain. Many other plutons of the southeastern Pernambuco–Alagoas Domain are within this interval (1.4–1.1 Ga) of T_{DM} model ages of the Major Isidoro batholith (e.g. Silva Filho et al., 2002, 2014; Van Schmus et al., 2008). The Águas Belas–Canindé composite batholith shows a narrow envelope in the diagram εNd vs time, suggesting that the granitic plutons have originated from a unique and homogeneous source rock (Silva Filho et al., 2002).

The Major Isidoro batholith is calc-alkaline, shows a magmatic arc geochemical signature and is classified as a magnesian granitoid. The origin of magnesian granitoids according to Frost et al. (2001) is subduction related. Calc-alkaline granitic to dioritic batholiths are characteristic in subduction-zone environments (Bonin, 1990; Liégeois et al., 1998; Barbarin, 1999). Perhaps the most abundant granitoids on Earth are those that are in the exposed plutonic parts of magmatic arcs (Frost et al., 2001). This type is called volcanic arc granitoids (Pearce et al., 1984), island arc and continental arc granitoids (Maniar and Picolli, 1989), or amphibole-bearing calc-alkalic granitoids (Barbarin, 1999). The samples of the Major Isidoro batholith plot in the field for volcanic arc granitoids in tectonic discrimination diagrams, and thus probably formed in an arc setting (e.g. Bonin, 1990; Brown, 1977; Barbarin, 1990, 1999; Frost et al., 2001).

The average calculated $\delta^{18}O$ (whole rock) value of 8.75‰ for this batholith points to an I-type magma (values in the interval of +7.7 to +9.9‰ are regarded as typical of I-type granites according to O'Neil et al., 1977). An important continental crust component seems to be involved in the petrogenesis of Major Isidoro batholith. This contention is suggested by inherited zircon cores, high εSr (44–69), low εNd (−1.09 to −2.12), as well as high $\delta^{18}O$ (zircon) values. Absence of pronounced Eu anomalies in chondrite-normalized REE patterns in this pluton could be explained by magma crystallization under high-oxygen fugacity, which would inhibit the formation of Eu^{2+} and thus the entrance of Eu into the feldspar structure (Hanson, 1980). This idea finds support in the observed coexistence of titanite + quartz + magnetite (Wones, 1989). It may also indicate that partial melting took place at pressures above the stability field of plagioclase, consistent with partial melting in deep levels of a thickened crust. Epidote is stable only at

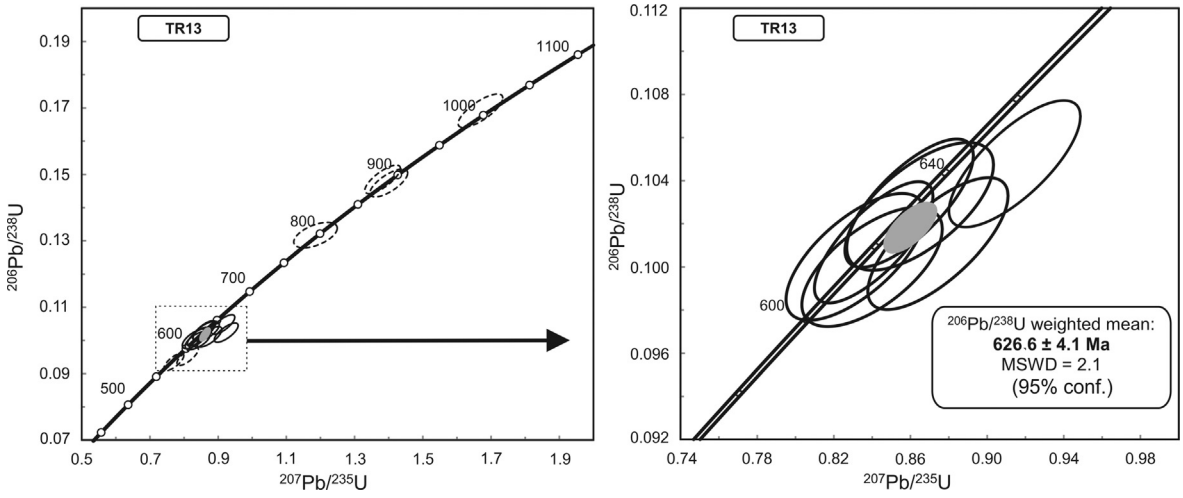

Fig. 9. Concordia plot for SHRIMP 204-corrected, zircon analyses from the Major Isidoro batholith sample (TR–13).

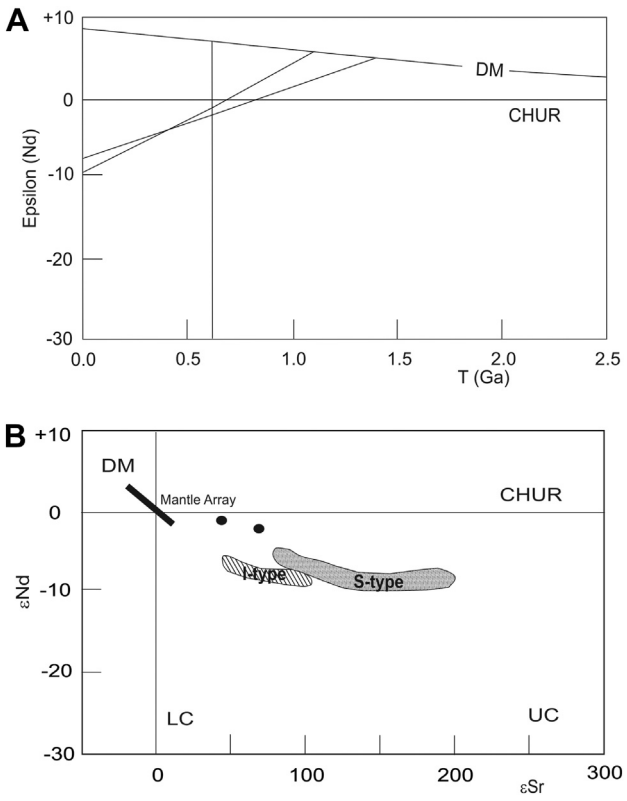

Fig. 10. (a) Nd isotopic composition of the Major Isidoro batholith. (b) εNd(t) versus εSr (t) diagram for granitoids from the Major Isidoro batholith. S-type and I-type granitoids (Australian), fields from Harmon et al. (1984).

high pressure in granitic magmas and survival of magmatic epidote is possible only when upward magma transport from the deep crust is rapid (Brandon et al., 1996). Schmidt and Thompson (1996) demonstrated experimentally that epidote and plagioclase can coexist around 10 kbar in tonalitic magmas.

The U–Pb crystallization age, Nd model age, εNd and $^{87}Sr/^{86}Sr(i)$ data for the Major Isidoro magmatic epidote-bearing calc-alkalic granite are similar to those for magmatic epidote-bearing calc-alkalic granitoids in the Cachoerinha–Salgueiro and Alto Pajeú belts (Central Tectonic Domain) and Sergipano Belt. In those three belts, magmatic epidote-bearing plutons crystallized from calc-alkalic magmas formed from partial fusion of amphibolite (meta-basaltic) sources that previously interacted with seawater at low temperature (e.g. Sial, 1993, 1999, 2008; Ferreira et al., 2003, 2011). The presence of amphibole-rich clots in the Major Isidoro pluton together with relatively high $\delta^{18}O$(magma) values similarly may reflect the presence of a metabasaltic component in the source as assumed for magmatic epidote-bearing granites elsewhere in the Borborema Province (e.g. Sial et al., 1998).

Oliveira et al. (2010) proposed a plate tectonic model for the tectonic evolution of the Neoproterozoic Sergipano Belt, located on the southwest margin of Borborema Province. According to Oliveira et al. (2010), convergence of the Pernambuco–Alagoas Domain and the São Francisco Craton led to build up of a continental arc between 630 Ma and 620 Ma in the Macururé, Poço Redondo–Marancó and Canindé sub-domains of the Sergipano Domain, coeval with the deposition of the sedimentary sequences of the Sergipano Belt and Yaoundé Belt, Cameroon (Oliveira et al., 2006). Brito Neves and Fuck (2013) argued that the Late Cryogenian accretionary interactions (660–630 Ma) are recorded in all sub-domains of the Borborema Province (Fig. 1a), and that the accretionary events were nearly coeval (650–620 Ma). However, evidence for Brasiliano subduction of oceanic lithosphere has not been found in the Central Tectonic and Pernambuco–Alagoas domains (Neves et al., 2009; Guimarães et al., 2011; Neves et al., 2012). Alternately Neves et al. (2012) proposed, for the emplacement of plutons associated with compressional deformation, an environment of immature magmatic arcs resulting from closing of small oceanic basins or during crustal thickening, given that evidence for long lasting oceanic subduction is lacking (extension prevailed until

Table 3
Summary of representative Sm–Nd and Rb–Sr isotopic results.

Sample	Nd ppm	Sm ppm	147Sm/143Nd	143Nd/144Nd	εNd (Today)	εNd (T)	TDM (Ga)	Rb ppm	Sr ppm	87Rb/86Sr	87Sr/86Sr	εSr (Today)	εSr (T)
1	77	16	0.1288	0.512249	−7.60	−2.12	1.4	130	413	0.9115	0.71677	174	69
2	25	4	0.0960	0.512167	−9.19	−1.09	1.1	86	714	0.3486	0.70996	78	44

642 Ma). Contrasting with this model Oliveira et al. (2010) proposed that continental deformation resulted from closing of large oceanic domains and that the Neoproterozoic Sergipano Belt was formed by the collision of the Pernambuco–Alagoas Block in the north with the São Francisco Craton in the south.

10. Conclusions

The Major Isidoro pluton preserves magmatic epidote which points to rapid magma transport through hot continental crust during the peak of metamorphism at 627 Ma in early stages of the Brasiliano orogeny (e.g. Ferreira et al., 2011).

Inherited zircon cores record Cariris Velhos orogeny ages (800–1000 Ma) and indicate that the source of the Major Isidoro pluton may be related to the so-called Cariris Velhos event.

The Major Isidoro granites present petrological, geochemical and isotopic characteristics that point to an I-type granite that has characteristics of both mantle- and crust-derived magmas. Its mineralogical characteristics, and the metaluminous nature together with intermediate $^{87}Sr/^{86}Sr$ initial ratio (0.7069–0.7086), low values of εNd (−1.09 to −2.12; close to 0) and inherited zircon cores suggest a reworked lower continental crust as source rock.

The age of 642 Ma for an orthogneiss next to the Jacaré dos Homens transpressional shear zone that limits the Sergipano and Pernambuco–Alagoas domains, a possible paleo suture, probably dates early movements along this transpressional shear zone. Moreover, the 627 Ma crystallization age of the Major Isidoro batholith implies emplacement during early stages of the Brasiliano orogeny, after the starting of movements along the Jacaré dos Homens shear zone. This pluton was intruded during a peak of high-grade metamorphism associated with the convergence of the São Francisco–Congo Craton and the Pernambuco–Alagoas Massif, around 630 Ma. U–Pb results from this study and from the literature date the beginning of the Brasiliano orogeny of this studied area in the interval 630–640 Ma.

Acknowledgments

We thank Emanuel F. Jardim de Sá and Edward W. Sawyer for discussions. TRS thanks the Brazilian agency Conselho Nacional de Desenvolvimento Científico e Tecnológico (CNPq) for a Master of Science scholarship (process 830099/1999–9). VPF and ANS acknowledge the continuous financial support from the CNPq and FACEPE through several grants (PRONEX/FACEPE APQ-0479-1.07/06, APQ 0844-1.07/08, APQ 0727-1.07/08, and CNPq 478554/2009–5, 472842/2010-2). We are grateful to Elson P. Oliveira, Michael Roden and Reinhardt Fuck for comments and suggestions that have improved considerably the original manuscript. This is the NEG–LABISE contribution n. 273.

References

Barbarin, B., 1990. Granitoids: main petrogenetic classifications in relation to origin and tectonic setting. Geol. J. 25, 227–238.
Barbarin, B., 1999. A review of the relationships between granitoid types, their origins and their geodynamic environments. Lithos 46, 605–626.
Bonin, B., 1990. From orogenic to anorogenic settings: evolution of granitoid suites after a major orogenesis. Geol. J. 25, 261–270.
Brown, G.C., 1977. Mantle origin of Cordilleran granites. Nature 265, 21–24.
Black, L.P., Kamo, S.L., Allen, C.M., Davis, D.W., Aleinikoff, J.N., Valley, J.W., Mundil, R., Campbell, I.H., Korsch, R.J., Williams, I.S., Foudoulis, C., 2004. Improved $^{206}Pb/^{238}U$ microprobe geochronology by the monitoring of a trace-element-related matrix effect; SHRIMP, ID-TIMS, ELA-ICP-MS and oxygen isotope documentation for a series of zircon standards. Chem. Geol. 205, 115–140.
Brandon, A.D., Creaser, R.A., Chacko, T., 1996. Constraints on rates of granitic magma transport from epidote dissolution kinetics. Science 271, 1845–1848.
Brito Neves, B.B., Campos Neto, M.C., Van Schmus, W.R., Santos, E.J., 2001. O Sistema Pajeú – Paraíba e o Maciço São José de Campestre no leste da Borborema. Rev. Bras. Geociências 31, 173–184.
Brito Neves, B.B., Sial, A.N., Rand, H.M., Manso, V.V., 1982. The Pernambuco-Alagoas massif, Northeastern Brazil. Rev. Bras. Geociências 12, 240–250.
Brito Neves, B.B., Santos, E.J., Van Schmus, W.R., 2000. Tectonic history of the Borborema Province, Northeastern Brazil. In: Cordani, U., Milani, E.J., Thomaz Filho, A., Campos, D.A. (Eds.), Tectonic evolution of South America. International Geological Congress, 31st, Rio de Janeiro, Brazil, pp. 151–182.
Brito Neves, B.B., Fuck, R.A., 2013. Neoproterozoic evolution of the basement of the South-American platform. J. S. Am. Earth Sci. 47, 72–89.
Bueno, J.F., Oliveira, E.P., McNaughton, N., Laux, J.H., 2009. U–Pb dating of granites in the Neoproterozoic Sergipano Belt, NE-Brazil, and implications for the timing and duration of continental collision. Gondwana Res. 15, 86–97.
Cavosie, A.J., Kita, N.T., Valley, J.W., 2009. Primitive oxygen-isotope ratio recorded in magmatic zircon from the Mid-Atlantic Ridge. Am. Mineral. 94, 926–934.
Cavosie, A.J., Valley, J.W., Kita, N.T., Spicuzza, M.J., Ushikubo, T., Wilde, S.A., 2011. The origin of high $\delta^{18}O$ zircons: marbles, megacrysts, and metamorphism. Contribut. Mineral. Petrol. 162, 961–974.
Chappell, B.W., White, A.J.R., 1974. Two contrasting granite types. Pac. Geol. 8, 173–174.
Chappell, B.W., White, A.J.R., 1992. I- and S-types granites in Lachlan Fold Belt. Trans. R. Soc. Edinb. Earth Sci. 83, 1–26.
Chappell, B.W., White, A.J.R., 2001. Two contrasting granite types: 25 years later. Aust. J. Earth Sci. 48, 489–499.
Cruz, R.F., Accioly, A.C.A., 2012. Idade e litogeoquímica do metagranitoide Caldeirão Vermelho (Parnamirim-PE), Zona Transversal, Província Borborema. Estud. Geol. 22, 129–148.
Cruz, R.F., Accioly, A.C.A., 2013. Petrografia, geoquímica e idade U/Pb do ortognaisse Rocinha, no Domínio Pernambuco-Alagoas W da Província Borborema. Estud. Geol. 23, 3–27.
Evensen, N.M., Hamilton, P.J., Onions, R.K., 1978. Rare-earth abundances in Chondritic Meteorites. Geoch. Cosmochim. Acta 42, 1, 199–1.212.
Ferreira, V.P., Sial, A.N., Jardim de Sá, E.F., 1998. Geochemical and isotopic signatures of the Proterozoic granitoids in terranes of the Borborema Province, northeastern Brazil. J. S. Am. Earth Sci. 11, 439–455.
Ferreira, V.P., Sial, A.N., Pimentel, M.M., Armstrong, R., Guimarães, I.P., Silva Filho, A.F., Lima, M.M.C., Silva, T.R., 2015. Reworked old crust-derived shoshonitic magma: the Guarany pluton, Northeastern Brazil. Lithos 232, 150–161.
Ferreira, V.P., Sial, A.N., Pimentel, M.M., Armstrong, R., Spicuzza, M., Guimarães, I.P., Silva Filho, A.F., 2011. Contrasting sources and P-T crystallization conditions of epidote-bearing granitic rocks, northeastern Brazil: O, Sr, and Nd Isotopes. Lithos 121, 189–201.
Ferreira, V.P., Sial, A.N., Pimentel, M.M., Moura, C.A.V., 2004. Acidic to intermediate magmatism and crustal evolution in the Transversal Zone, northeastern Brazil. In: Mantesso, Neto, Bartorelli, V., Carneiro, A., Dal Re, C., e Brito Neves, B.B. (Eds.), Geologia do Continente Sul-americano: a evolução da obra de Fernando Flávio Marques de Almeida. Editora, São Paulo, USP, pp. 189–201 chapter XII.
Ferreira, V.P., Valley, J.W., Sial, A.N., Spicuzza, M., 2003. Oxygen isotope compositions and magmatic epidote from two contrasting metaluminous granitoids, NE Brazil. Contribut. Mineral. Petrol. 145, 205–216.
Frost, B.R., Lindsley, D.H., 1991. The occurrence of Fe-Ti oxides in igneous rocks. Oxide minerals: petrologic and magnetic significance. Mineralogical Society of America. Rev. Mineral. 25, 433–486.
Frost, B.R., Arculus, R.J., Barnes, C.G., Collins, W.J., Ellis, D.J., Frost, C.D., 2001. A geochemical classification of granitic rocks. J. Petrol. 42, 2033–2048.
Gioia, S.M., Pimentel, M.M., 2000. A metodologia Sm–Nd no Laboratório de Geocronologia da Universidade de Brasília. An. Acad. Bras. Ciências 72, 219–245.
Guimarães, I.P., Silva Filho, A.F., Almeida, C.N., Van Schmus, W.R., Araújo, J.M.M., Melo, S.C., Melo, E.B., 2004. Brasiliano (Pan-African) granitic magmatism in the Pajeu–Paraiba belt, northeast Brazil: an isotopic and geochronological approach. Precambrian Res. 135, 23–53.
Guimarães, I.P., Silva Filho, A.F., Almeida, C.N., Macambira, M.J.B., Armstrong, R., 2011. U–Pb SHRIMP data constraints on calc-alkaline granitoids with 1.3–1.6 Ga Nd TDM model ages from the Central Domain of the Borborema Province, NE Brazil. J. S. Am. Earth Sci. 31, 383–396.
Guimarães, I.P., Van Schmus, W.R., Neves, Brito, Bittar, S.M.B., Silva Filho, A.F., Armstrong, R., 2012. U–Pb zircon ages of orthogneisses and supracrustal rocks of the Cariris Velhos belt: onset of Neoproterozoic rifting in the Borborema Province, NE Brazil. Precambrian Res. 192, 52–77.
Hanson, G.N., 1980. Rare earth elements in petrogenetic studies of igneous systems. Annu. Rev. Earth Planet. Sci. 8, 371–405.
Harmon, R.S., Halliday, A.N., Clayburn, J.A.P., Stephens, W.E., 1984. Chemical and isotopic systematics of the Caledonian intrusions of Scotland and northern England: a guide to magma source region and magma crust interaction. Philos. Trans. Geolological Soc. Lond. A310, 439–456.
Harris, N.B.W., Pearce, J.A., Tindle, A.G., 1986. Geochemical characteristics ofcollision-zone magmatism. In: Coward, M.P., Ries, A.C. (Eds.), vol. 19. Collision Tectonics, Geological Society, London, pp. 67–81. Special Publication.
Ishihara, S., 1977. The magnetite-series and ilmenite-series granitic rocks. Min. Geol. 27, 293–305.
Lackey, J.S., Valley, J.W., Chen, J.H., Stockli, D.F., 2008. Dynamic magma systems, crustal recycling, and alteration in the Central Sierra Nevada Batholith: the oxygen isotope record. J. Petrol. 49, 1397–1426.
Liégeois, J.P., Navez, J., Hertogen, J., Black, R., 1998. Contrasting origin of postcollisional high-K calc-alkalic and shoshonitic versus alkalic and peralkalic granitoids. The use of sliding normalization. Lithos 45, 1–28.
Lima, M.M.C., 2013. Caracterização geoquímica, isotópica e geotectônica dos

complexos Araticum e Arapiraca, faixa Sergipana-Alagoas. 2013. Unpublished MSc. dissertation. Federal University of Pernambuco, Recife, Brazil, p. 89 (in Portuguese).
Lima, M.M.C., Silva, T.R., Ferreira, V.P., Silva, J.M.R., 2014. Metasedimentary rocks of the northern part of the Macururé Domain, Sergipano Belt (northeastern Brazil): geochemical characterization of their protoliths and tectonic implications. Estud. Geol. 24, 89–107.
Long, L.E., Castellana, C.H., Sial, A.N., 2005. Age, origin and cooling history of the Coronel João Sá Pluton, Bahia, Brazil. J. Petrol. 46, 255–273.
Ludwig, K.R., 2009. User's Manual for Isoplot/Ex, Version 3.71: a Geochronological Tool Kit for Microsoft Excel, vol. 5. Berkeley Geochronology Center Special Publication.
Maniar, P.D., Picolli, P.M., 1989. Tectonic discrimination of granitoids. Geol. Soc. Am. Bull. 101, 635–643.
Mendes, V.A., Brito, M.F.L., Paiva, I.P., 2008. Folha Arapiraca (SC.24-X-D, escala 1: 250,000). Integration Geological (Geologic map). Brazilian Geological Survey (CPRM), Recife-PE, Brazil.
Middlemost, E., 1997. In: Magmas, Rocks and Planetary Development. A Survey of Magma/Igneous Rock Systems. Longman, Harlow, 1997.
Neves, S.P., Bruguier, O., Bosch, D., Silva, J.M.R., Mariano, G., 2008. U–Pb ages of plutonic and metaplutonic rocks in southern Borborema Province (NE Brazil): timing of Brasiliano deformation and magmatism. J. S. Am. Earth Sci. 25, 285–297.
Neves, S.P., Bruguier, O., Silva, J.M.R., Bosch, D., Alcantara, V.C., Lima, C.M., 2009. The age distributions of detrital zircons in metasedimentary sequences in eastern Borborema Province (NE Brazil): evidence for intracontinental sedimentation and orogenesis? Precambrian Res. 175, 187–205.
Neves, S.P., Monié, P., Bruguier, O., Silva, J.M.R., 2012. Geochronological, thermochronological and thermobarometric constraints on deformation, magmatism and thermal regimes in eastern Borborema Province (NE Brazil). J. S. Am. Earth Sci. 38, 129–146.
Neves, S.P., Bruguier, O., Bosch, D., Silva, J.M.R., Mariano, G., Silva Filho, A.F., Teixeira, C.M.L., 2015. From extension to shortening: dating the onset of the Brasiliano Orogeny in eastern Borborema Province (NE Brazil). J. S. Am. Earth Sci. 58, 238–256.
Oliveira, E.P., Bueno, J.F., McNaughton, N., Silva Filho, A.F., Nascimento, R.S., Donatti-Filho, J.P., 2015. Age, composition, and source of continental arc- and syn-collision granites of the Neoproterozoic Sergipano Belt, Southern Borborema Province, Brazil. J. S. Am. Earth Sci. 58, 257–280.
Oliveira, E.P., Toteu, S.F., Araújo, M.N.C., Carvalho, M.J., Nascimento, R.S., Bueno, J.F., McNaughton, N., Basilici, G., 2006. Geologic correlation between the Neoproterozoic Sergipano belt (NE Brazil) and the Yaoundé schist belt (Cameroon, Africa). J. Afr. Earth Sci. 44, 470–478.
Oliveira, E.P., Windley, B.F., Araújo, M.N.C., 2010. The Neoproterozoic Sergipano orogenic belt, NE Brazil: a complete plate tectonic cycle in western Gondwana. Precambrian Res. 181, 64–84.
O'Neil, J., Shaw, S.F., Flood, R.H., 1977. Oxygen and hydrogen isotope compositions of granite genesis in the New England batholith, Australia. Contribut. Mineral. Petrol. 62, 313–325.
Pearce, J., Harris, N.B.W., Tindle, A.D., 1984. Trace element discrimination diagrams for the tectonic interpretation of granitic rocks. J. Petrol. 25, 956–983.
Peccerilo, A., Taylor, S.R., 1976. Geochemistry of Eocene calc-alkaline basaltic volcanic rocks from the Kastamonu area, northern Turkey. Contribut. Mineral. Petrol 58, 63–81.
Santos, E.J., 1995. O complexo granítico de Lagoa das Pedras: Acresção e colisão na região de Floresta (PE), Província Borborema. Unpublished Doctoral Dissertation. University of São Paulo, São Paulo, Brazil, p. 219 (in Portuguese).
Schmidt, M.W., Thompson, A.B., 1996. Epidote in calc-alkaline magmas: an experimental study of stability, phase relationships, and the role of epidote in magmatic evolution. Am. Mineralogist 81, 424–474.
Santos, E.J., Van Schmus, W.R., Kozuch, M., Brito Neves, B.B., 2010. The Cariris Velhos tectonic event in Northeast Brazil. J. S. Am. Earth Sci. 29, 61–76.
Shand, S.J., 1947. Eruptive Rocks, third ed. Hafner Publishing Company, New York, p. 488.
Sial, A.N., 1990. Epidote-bearing calc-alkaline granitoids in Northeast Brazil. Rev. Bras. Geociências 20, 88–100.
Sial, A.N., 1993. Contrasting metaluminous magmatic epidote-bearing granitic suites from two Precambrian Foldbelts in Northeast Brazil. In: Sial, A.N., Ferreira, V.P. (Eds.), Anais Academia Brasileira Ciências, vol. 65 (Suppl.). Academia Brasileira de Ciências, Rio de Janeiro, pp. 141–162.
Sial, A.N., Ferreira, V.P., Fallick, E.A., Cruz, M.J., 1998. Amphibole-rich clots in calc-alkalic granitoids in the Borborema Province, Northeastern Brazil. J. S. Am. Earth Sci. 11, 457–472.
Sial, A.N., Toselli, A.J., Saavedra, J., Parada, M.A., Ferreira, V.P., 1999. Emplacement, petrological and magnetic susceptibility characteristics of diverse magmatic epidote-bearing granitoid rocks in Brazil, Argentina and Chile. Lithos 46, 367–392.
Sial, A.N., Vasconcelos, P.M., Ferreira, V.P., Pessoa, R.R., Brasilino, R.G., Morais Neto, J.M., 2008. Geochronological and mineralogical constraints on depth of emplacement and ascension rates of epidote-bearing magmas from northeastern Brazil. Lithos 105, 225–238.
Silva Filho, A.F., Guimaraes, I.P., 2000. Sm/Nd isotopic data and U/Pb geochronology of collisional to post-collisional high-K shoshonitic granitoids from the Pernambuco–Alagoas terrane, Borborema Province, NE. Brazil. In: International Geological Congress, vol. 31. International Union of Geological Sciences, Rio de Janeiro. Resumos... Rio de Janeiro. CD-ROM.
Silva Filho, A.F., Guimarães, I.P., Van Schmus, W.R., 2002. Crustal evolution of the Pernambuco-Alagoas complex, Borborema Province, NE Brazil: Nd isotopic data from neoproterozoic granitoids. Godwana Res. 5, 409–422.
Silva Filho, A.F., Guimarães, I.P., Ferreira, V.P., Armstrong, R.A., Sial, A.N., 2010. Ediacaran Águas Belas pluton, Northeastern Brazil: evidence on age, emplacement and magma sources during Gondwana amalgamation. Gondwana Res. 17, 676–687.
Silva Filho, A.F., Guimarães, I.P., Van Schmus, W.R., Dantas, E.L., Armstrong, R., Cocentino, L.M., Lima, D.R., 2013. Long-lived neoproterozoic high-K magmatism in the Pernambuco–Alagoas domain, Borborema Province, Northeast Brazil. Int. Geol. Rev. 55, 1280–1299.
Silva Filho, A.F., Guimarães, I.P., Van Schmus, W.R., Armstrong, R., Silva, J.M.R., Cocentino, L.M., Osako, L.S., 2014. SHRIMP U–Pb zircon geochronology and Nd signatures of supracrustal sequences and orthogneisses constrain the Neoproterozoic evolution of the Pernambuco–Alagoas Domain, southern part of Borborema Province, NE Brazil. Int. J. Earth Sci. (Geol Rundsch) 103, 2155–2190.
Silva, L.C., Armstrong, R., Pimentel, M.M., Scandolara, J., Ramgrab, G., Wildner, W., Angelim, L.A.A., Vasconcelos, A.M., Rizzoto, G., Quadros, M.L.E.S., Sander, A., Rosa, A.L.Z., 2002. Reavaliação da evolução geológica em terrenos pré-cambrianos brasileiros com base em novos dados U–Pb SHRIMP, Parte III: Províncias Borborema, Mantiqueira meridional e Rio Negro–Juruena. Rev. Bras. Geociências 32, 529–544.
Sun, S.-S., McDonough, W.F., 1989. Chemical and isotopic systematics of ocean basalts: implications for mantle composition and processes. In: Saunders, A.D., Norry, M.J. (Eds.), Magmatism in the Ocean Basins, vol. 42. Geological Society, London, pp. 313–345. Special Publications.
Trompette, R., 1997. Neoproterozoic (~600 Ma) aggregation of Western Gondwana: a tentative scenario. Precambrian Res. 82, 101–112.
Trompette, R., 2000. Gondwana evolution; its assembly at around 600 Ma. Acad Sci Paris, Sciences de la Terre et des planètes. Earth Planet. Sci. 330, 305–315.
Valley, J.W., 2003. Oxygen isotopes in zircon. In: Hanchar, J.M., Hoskin, P.W.O. (Eds.), Zircon. Mineralogical Society of America/Geochemical Society, Reviews in Mineralogy and Geochemistry, vol. 53, pp. 343–385.
Valley, J.W., Chiarenzelli, J.R., McLelland, J.M., 1994. Oxygen isotope geochemistry of zircon. Earth Planet. Sci. Lett. 126, 187–206.
Valley, J.W., Kitchen, N.E., Kohn, M.J., Niendorf, C.R., Spicuzza, M.J., 1995. UWG-2, a garnet standard for oxygen isotope ratio: strategies for high precision and accuracy with laser heating. Geochim. Cosmochim. Acta 59, 5223–5231.
Valley, J.W., Kinny, P.D., Schulze, D.J., Spicuzza, M.J., 1998. Zircon megacrysts from kimberlite: oxygen isotope variability among mantle melts. Contribut. Mineral. Petrol. 133, 1–11.
Valley, J.W., Lackey, J.S., Cavosie, A.J., Clechenko, A., Spicuzza, M.J., Basei, M.A.S., Bindeman, I.N., Ferreira, V.P., Sial, A.N., King, E.M., Peck, W.H., Sinha, A.K., Wei, C., 2005. 4.4 billion years of crustal maturation from oxygen isotope ratios of zircon. Contribut. Mineral. Petrol. 15, 561–580.
Van Schums, W.R., Brito Neves, B.B., Hackspacher, P.C., Babinsky, M., 1995. U/Pb and Sm/Nd geochronlogic studies of the eastern Borborema Province, NE Brazil. J. S. Am. Earth Sci. 8, 267–288.
Van Schmus, W.R., Oliveira, E.P., Silva Filho, A.F., Toteu, S.F., Penaye, J., Guimarães, I.P., 2008. Proterozoic Links between the Borborema Province, NE Brazil and the Central African Fold Belt, vol. 94. Geological Society, London, pp. 69–99. Special Publications.
Van Schmus, W.R., Kozuch, M., de Brito Neves, B.B., 2011. Precambrian history of the Zona Transversal of the Borborema Province, NE Brazil: insights from Sm–Nd and U–Pb geochronology. J. S. Am. Earth Sci. 31, 227–252.
White, A.J.R., 1979. Sources of Granite Magmas. Abstract with Programs. In: Geological Society of America, vol. 11, p. 539.
Wones, D.R., 1989. Significance of the assemblage titanite+magnetite+quartz in granitic rocks. Am. Mineralogist 74, 744–749.
Williams, I.S., 1998. U–Th–Pb geochronology by ion microprobe. In: McKibben, M.A., Shanks, W.C., Ridley, W.I. (Eds.), In Applications of Microanalytical Techniques to Understanding Mineralizing Processes: Reviews in Economic Geology, vol. 7, pp. 1–35.
Williams, I.S., Claesson, S., 1987. Isotopic evidence for the Precambrian provenance and Caledonian metamorphism of high grade paragneisses from the Seve Nappes, Scandinavian Caledonides II.Ion microprobe zircon U–Pb–Th. Contribution Mineralogy Petrology 97, 205–217.
Zen, E-an, Hammarstrom, J.M., 1984. Magmatic epidote and its petrologic significance. Geology 12, 515–518.

Lithos 264 (2016) 189–200

Contents lists available at ScienceDirect

Lithos

journal homepage: www.elsevier.com/locate/lithos

Two stage mantle-derived granitic rocks and the onset of the Brasiliano orogeny: Evidence from Sr, Nd, and O isotopes

Thyego R. Silva *, Valderez P. Ferreira, Mariucha Maria C. Lima, Alcides N. Sial

NEG–LABISE, Department of Geology, Federal University of Pernambuco, Recife, PE 50740-550, Brazil

ARTICLE INFO

Article history:
Received 25 March 2016
Accepted 19 August 2016
Available online 31 August 2016

Keywords:
Pernambuco–Alagoas Domain
Onset of the Brasiliano orogeny
Sr–Nd isotopes
O isotopes
U–Pb SHRIMP zircon dating

ABSTRACT

The elongate Monteirópolis batholith (270 km^2) is composed of alkali feldspar granite to granodiorite, it is part of the Águas Belas–Canindé composite batholith and it intruded rocks of the Pernambuco–Alagoas Domain, northeastern Brazil. This batholith is bounded by the NNE–SSW-trending Jacaré dos Homens transpressional shear zone on its southwestern margin, and displays low-angle foliation, coeval to the development of a regional flat-lying foliation. Microgranular dioritic enclaves and amphibole-rich clots are abundant. The mineralogy of this pluton comprises biotite and amphibole as major accessory phases, and titanite and magmatic epidote as trace minerals. Major and trace element chemistry shows high SiO_2, total alkalis, Ba and Sr, low Fe# and Nb contents, all of these conferring a high-K calc-alkaline character. The rocks are enriched in LREE and LILE and depleted in HFSE, and show fractionated chondrite-normalized REE patterns with Eu/Eu* = 0.67 to 1.25. Chondrite-normalized spidergrams show marked negative Nb–Ta and Ti anomalies, typical of subduction-related magmas. U–Pb SHRIMP zircon data yielded a crystallization age of 626 ± 4 Ma. Regional structures and U–Pb geochronological data for the Jacaré dos Homens transpressional shear zone suggest that shearing was initiated at ca. 640 Ma. Dilatational movements along this shear zone opened space for magma emplacement. The rocks in this batholith are characterized by slightly negative to slightly positive εNd values (−0.78 to +1.06), average Nd-model age of 1.0 Ga, low initial $^{87}Sr/^{86}Sr_{(626\ Ma)}$ values of 0.7050 to 0.7052, and low $\delta^{18}O$ values (zircon) of +5.00 to +5.94‰ V-SMOW. A possible protolith, Tonian mantle-derived rocks in the lower continental crust, could have been partially melted by underplating of mantle-derived mafic magma during collision of the São Francisco Craton and the Pernambuco–Alagoas Domain during onset of the Brasiliano orogeny.

1. Introduction

Lying to the north of the São Francisco Craton (Almeida et al., 1981), the Borborema Province is a structural province in northeastern Brazil. It formed by convergence of the Amazonian, West African-São Luis, and São Francisco-Congo cratons during the assembly of west Gondwana (~600 Ma) (Trompette, 1997; Van Schmus et al., 2008, and references therein). In pre-drift reconstructions, the southern parts of the Borborema Province are seen to belong to a large Brasiliano–Pan-African orogenic belt (Dada, 2008; De Wit et al., 2008; Neves, 2003; among others). Within the southern Borborema Province, the Pernambuco–Alagoas Domain contains voluminous occurrences of intermediate to acidic igneous rocks exposed as stocks and batholiths, with t_{DM} ages that vary from Archaean to Neoproterozoic (Silva Filho et al., 2002; Silva Filho et al., 2014).

Granites are of prime importance in studies of crustal development because they constitute one of the main components of continental areas and are related in space and time with orogenic belts. Knowledge of their genesis may provide information about deeper crustal levels (e.g., Ferreira et al., 1998; Sial, 1986). The Sm–Nd and Rb–Sr isotopic systems and oxygen isotope ratios constitute effective tools for regional studies on the evolution of the continental crust.

This paper discusses field relations, petrography, major and trace geochemistry, O and Nd isotope data, and U–Pb zircon data of the Monteirópolis granitoid, which is located in the southern Borborema Province, whose field relationships tie its emplacement to the onset of the Brasiliano orogeny. We present evidence for a two-stage derivation of Monteirópolis magma.

2. Geologic background

Brito Neves et al. (2000) recognized the major contiguous tectonic domains in the Borborema Province, later renamed by Van Schmus et al. (2008) (from south to north) the: (1) Sergipano, (2) Pernambuco–Alagoas, (3) Riacho do Pontal, (4) Transverse, (5) Rio Grande do Norte, (6) Ceará, and (7) Médio Coreaú domains (Fig. 1). Of interest here is the Pernambuco–Alagoas Domain consisting of granite-migmatite basement intruded by numerous Brasiliano plutons,

* Corresponding author at: NEG–LABISE, Dept. of Geology, Av. Acadêmico Hélio Ramos s/n, Cidade Universitária, Recife, PE 50740-530, Brazil.
E-mail address: rthyego@yahoo.com (T.R. Silva).

http://dx.doi.org/10.1016/j.lithos.2016.08.030
0024-4937/

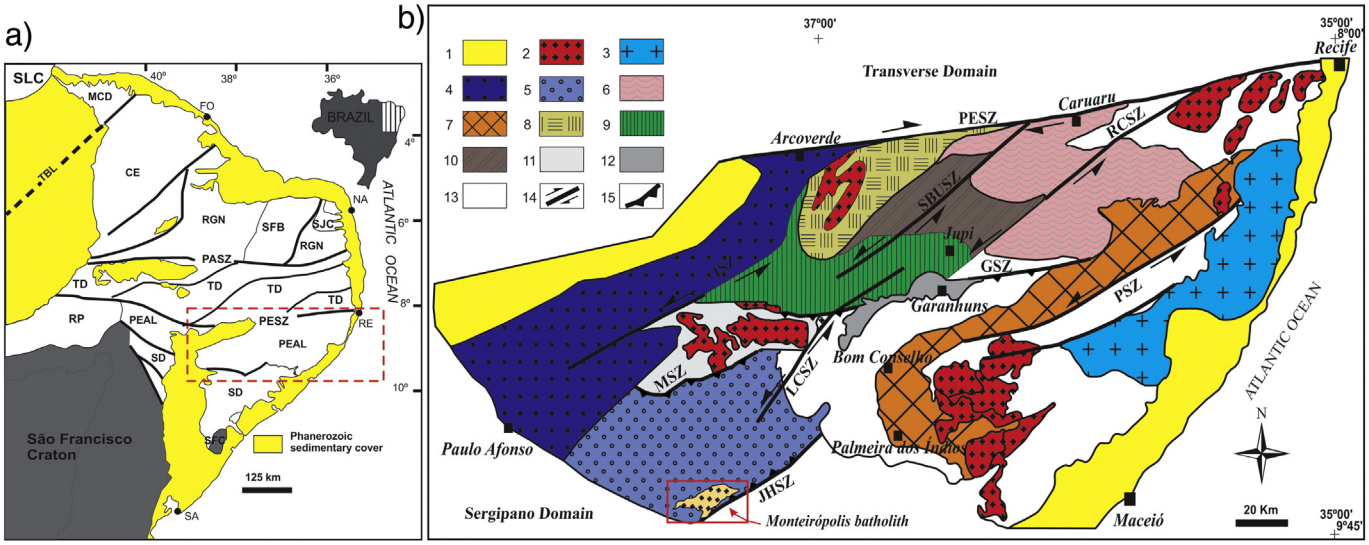

Fig. 1. (a) Borborema Province (after Van Schmus et al., 2008). Major domains: MCD-Médio Coreaú; CE-Ceará; RGN-Rio Grande do Norte (SFB-Seridó Fold Belt; SJC-São José do Campestre Archaean nucleus); TD-Transverse; PEAL-Pernambuco–Alagoas; RP-Riacho do Pontal; SD-Sergipano; SFC-São Francisco Craton; SLC-São Luís Craton; Faults and shear zones: PASZ-Patos shear zone; PESZ-Pernambuco shear zone; TBL-Transbrasiliano Lineament. Cities and towns: Fo-Fortaleza; Na-Natal; Re-Recife; Sa-Salvador. (b) Geologic map of the Pernambuco–Alagoas Domain, showing the location of the Monteirópolis batholith. 1-Phanerozoic sedimentary cover; 2-other Brasiliano granitoids; 3-Ipojuca–Atalaia batholith; 4-Buique–Paulo Afonso batholith; 5-Águas Belas–Canindé batholith; 6-Granitoids and orthogneisses; 7-Palmares Sequence; 8-Rio Una (Unit 1) Sequence; 9-Rio Una (Unit 2) Sequence; 10-Rio Una (Unit 3) Sequence; 11-Inhapi Sequence; 12-Garanhuns Quartzites; 13-basement-migmatites; 14-transcurrent shear zones (PESZ-Pernambuco; RCSZ-Rio da Chata; PSZ-Palmares; LCSZ-Limitão-Caetés; ISZ-Itaíba; SBUSZ-São Bento do Una); 15-compressive shear zones (GSZ-Garanhuns; MSZ-Maravilha; ZCJH-Jacaré dos Homens). (Modified from Silva Filho et al., 2002, 2010, 2014).

some of batholithic dimension (e.g. Brito Neves et al., 2000; Silva Filho et al., 2002; Silva Filho et al., 2013; Van Schmus et al., 2008). These ubiquitous plutons comprise about 30% of the exposed bedrock (Brito Neves et al., 2000 and references therein). Local basement, the Belém do São Francisco complex, consists of a metasedimentary-magmatic sequence, an infra-crustal segment composed of migmatites, biotite-gneisses,

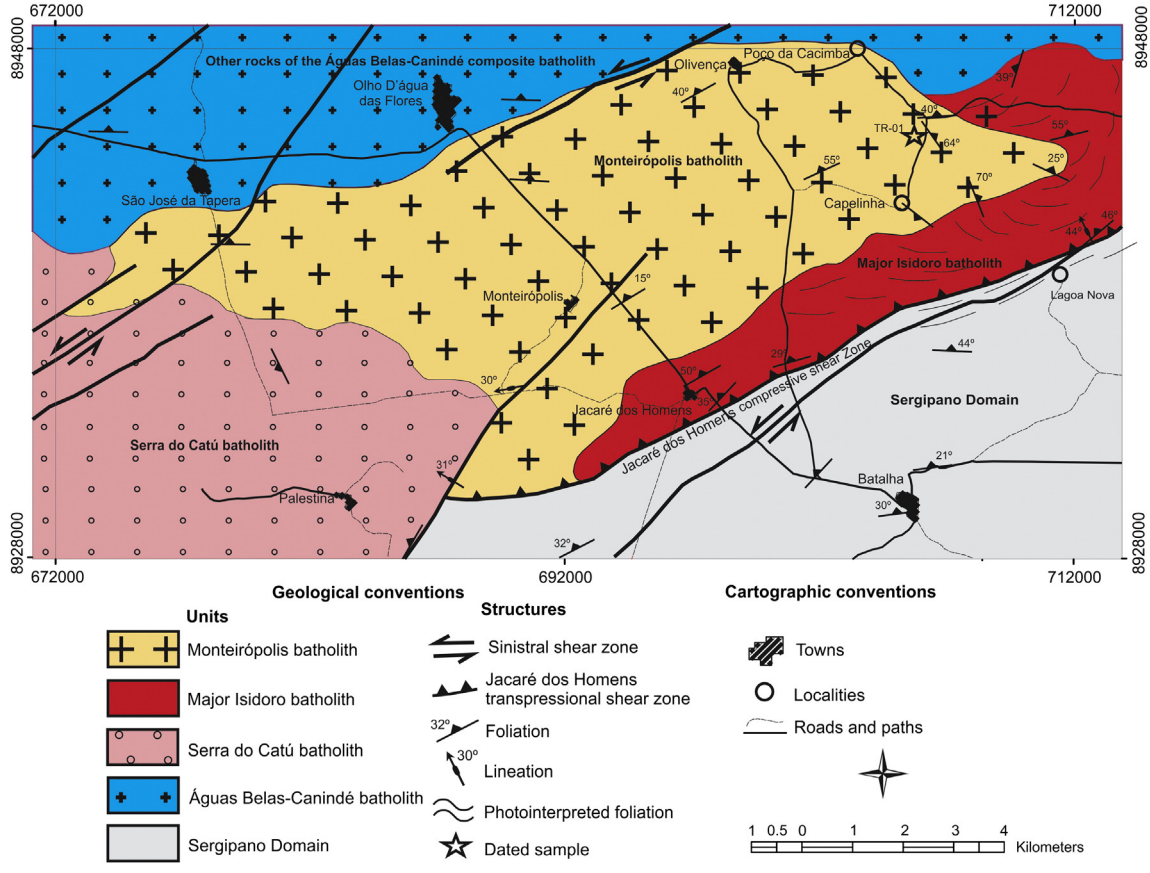

Fig. 2. Simplified geologic map of the Monteirópolis batholith.

tonalitic orthogneisses, and metagranodiorites to metamonzogranites (Santos, 1995). At the type locality of the Belém do São complex, Silva et al. (2002) obtained a U–Pb zircon magmatic crystallization SHRIMP age of 2,079 ± 34 Ma from a porphyroclastic biotite-hornblende granodiorite gneiss. Widespread Neoproterozoic granitic plutons within the Pernambuco–Alagoas Domain were dated by U–Pb zircon ages that range from to 573 to 635 Ma (e.g., Silva Filho et al., 2002; Neves et al., 2008; Van Schmus et al., 2008; Silva Filho et al., 2010, 2013, 2014, 2016; Ferreira et al., 2015; Silva et al., 2015; among others).

Silva Filho et al. (2002) used petrography and geochemistry as criteria to group the Pernambuco–Alagoas granitic plutons into the Buique-Paulo Afonso, Águas Belas–Canindé, Marimbondo-Correntes, Ipojuca-Atalaia, and Garanhuns major batholiths. In a later work, five distinct Nd model age subdivisions were recognized in the Pernambuco–Alagoas Domain (Van Schmus et al., 2008). They are (a) t_{DM} older than 2.40 Ga, represented by several local occurrences of gneisses and migmatites, (b) t_{DM} between 2.00 and 2.20 Ga, represented by large areas in the northeastern half of the Pernambuco–Alagoas Domain, (c) t_{DM} between 1.70 and 2.00 Ga, represented by several Brasiliano plutons in the NE corner of the domain, (d) t_{DM} between 1.20 and 1.50 Ga, represented by large parts of the southwestern half of the Pernambuco–Alagoas Domain and (e) t_{DM} between 0.90 and 1.20 Ga, represented mainly by the Buique-Paulo Afonso batholith.

Silva Filho et al. (2014) used Sm–Nd isotope data to propose three crustal subdomains within the Pernambuco–Alagoas Domain — a northern zone in which rocks are derived predominately from older crustal sources, the Garanhuns subdomain, and a southern zone where rocks are derived from substantially younger sources (Água Branca and Palmares subdomains). The Água Branca subdomain contains the Monteirópolis batholith, the subject of this paper.

3. Field relationships and petrography

The Monteirópolis comprises a ENE–WSW lobate intrusion occupying an area over 270 km^2 (Fig. 2). Its long axis, generally parallel to the regional foliation, roughly follows the direction of the boundary

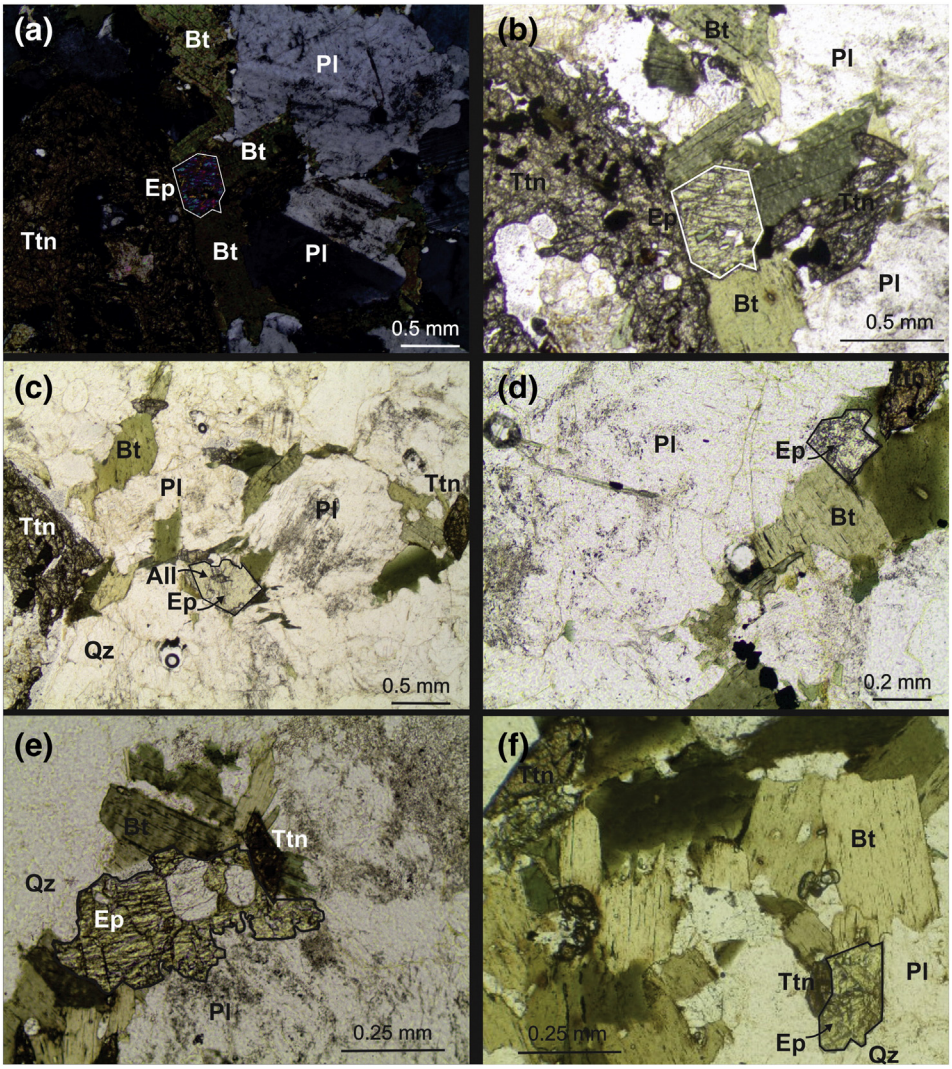

Fig. 3. Magmatic epidote textural relationships observed in Monteirópolis batholith: (a) and (b) euhedral epidote armored by biotite and titanite; (c) euhedral epidote with allanite core, partially resorbed by the magma; (d) subhedral epidote adjacent to biotite; (e) epidote partially rimmed by biotite and plagioclase, showing resorbed margins in contact with the melt; and (f) euhedral epidote rimmed by biotite and plagioclase, showing resorbed margins in contact with the melt. Parallel polarizers except for photo a. Mineral abbreviations after Whitney and Evans (2010) are: All = allanite; Bt = biotite; Ep = epidote; Pl = plagioclase; Ttn = titanite and Qz = quartz. Lines are an attempt to reconstruct original shape of epidote crystals, indicating how much some of them have been dissolved by host magma. Textural relationships and microstructural aspects of the Monteirópolis batholith. (g) and (h) Foliation defined by elongate K-feldspar grain and aggregates of biotite and green amphibole. (i) Microcline (K-feldspar) megacrystal of 4 mm length with cross-hatched twinning and myrmekitic intergrowths. j) Xenomorphic crystal of plagioclase of ca. 2 mm length with deformed polysynthetic twinning and chessboard extinction in recrystallized quartz. Polarizers crossed except for photo g.

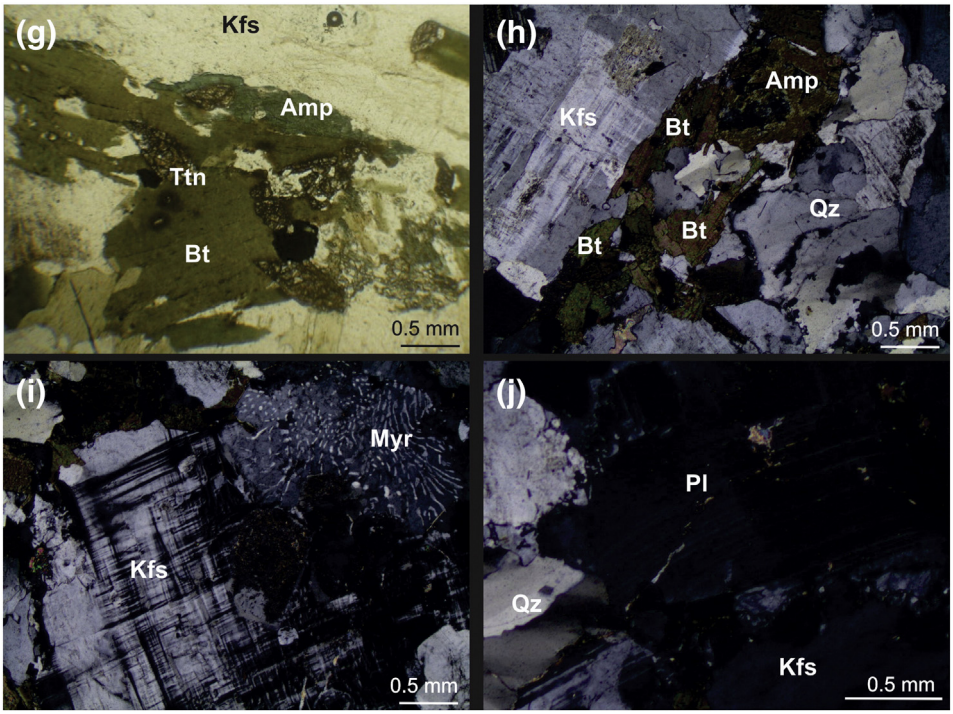

Fig. 3 (*continued*).

between the Pernambuco–Alagoas and the Sergipano domains. To the east, west and north, it is in sharp contact with other major batholiths of similar age. The Monteirópolis batholith cuts the adjoining Serra do Catú pluton and the contacts are sharp or made by faults with direction NE–SW. To the southwest lies the Jacaré dos Homens transpressional shear zone (Fig. 2) and high-grade metasedimentary rocks of the Sergipano Domain (Lima et al., 2014; Oliveira et al., 2006, 2010). The Monteirópolis batholith comprises medium-to coarse-grained leucocratic alkali feldspar granite to granodiorite. In decreasing order, the essential phases are K-feldspar which contains inclusions of biotite and titanite, quartz, and plagioclase. Biotite that may include titanite and apatite occurs as the dominant mafic mineral; other accessory phases are green amphibole, epidote, zircon, rare allanite, and opaque minerals. Epidote occurs as euhedral to subhedral crystals, partially or totally rimmed/included by biotite and plagioclase and, less commonly, epidote exhibits allanite cores (Fig. 3a–f), in a textural relationship similar to that described by Zen and Hammarstrom (1984) and by Sial and Ferreira (2015 and references therein).

Magmatic foliation in the Monteiropólis batholith is defined by the shape-preferred orientation of alkali feldspar and aggregates of biotite and amphibole (Fig. 3g and h), a texture that is evident in outcrop, and by mafic enclaves aligned parallel to the foliation that dominantly plunges and dips gently (15°–25°, sometimes up to 55°) to the northwest (Fig. 4c). Solid-state deformation that overprints the magmatic foliation is restricted to weak high-T deformation as shown by chessboard extinction in quartz, by deformed twinning, and by development of myrmekitic intergrowths around K-feldspar (Fig. 3i and j).

Diorite enclaves and amphibole-rich clots, typically a few centimeters to about 25 cm long (Fig. 4a–c), are present mainly in the eastern portion of the batholith. These enclaves have sharp contacts with the host granite and show regular, generally oval, but occasionally lobate or diffuse contours. Irregular shapes and crenulated contacts suggest interaction between dioritic (mafic) and host granitic (felsic) magma (Fig. 4d). Syn-plutonic dikes of diorite composition are also present, dipping 30–40° to the northwest.

4. Analytical procedures

Zircon grains were prepared for U–Pb SHRIMP dating by standard procedures (panning, magnetic separation, etc.) in the Stable Isotope Laboratory (NEG–LABISE), Department of Geology, Federal University of Pernambuco, Recife, Brazil. Representative grains, handpicked under a binocular microscope, were mounted in epoxy resin and polished to approximately half their thickness in order to expose internal structures, and then plated with conductive gold coating just prior to analysis.

Zircons fixed in the mount were studied by transmitted and reflected light microscopy and cathodoluminescence imaging before analysis. Spot areas of about 20–30 μm diameter were chosen on the igneous growth sectors in order to obtain zircon crystallization ages. Isotopic analyses were performed on a SHRIMP IIe at the University of São Paulo, São Paulo, Brazil. U–Pb isotope ratios were collected in sets of five scans throughout the mass range, and the TEMORA 2 reference zircon ($^{206}Pb/^{238}U$ age = 416.18 ± 0.33 Ma; Black et al., 2004) was measured after every third unknown analysis. Abundances of U, Th, and Pb, and Pb isotope ratios, were normalized using the SL13 zircon standard (U = 238 ppm; Williams, 1998). Correction for common Pb was made using measured ^{204}Pb. Errors in the isotope ratios and ages are quoted at 1 sigma level. Data reduction was performed using SQUID/Excel macro (Ludwig, 2009) (Table 2).

Oxygen isotope ratios of ~3 mg of zircon were also analyzed at NEG-LABISE. Oxygen was released in a CO_2 laser-based extraction line by reaction with BrF_5, reacted with hot graphite, and converted into CO_2 for mass spectrometer analysis following the procedures described by Valley et al. (1995). Isotope ratios were determined in a Delta V Advantage Thermofinningan mass spectrometer. Precision is better than ±0.1‰. Results are reported in standard permil notation relative to Vienna Standard Mean Ocean Water (VSMOW).

Whole-rock major and trace element concentrations were obtained by X-ray fluorescence (XRF) with a fully automated Rigaku RIX-3000 XRF spectrometer at NEG–LABISE by the method of calibration curves that were prepared using certified reference standards. Rare earth

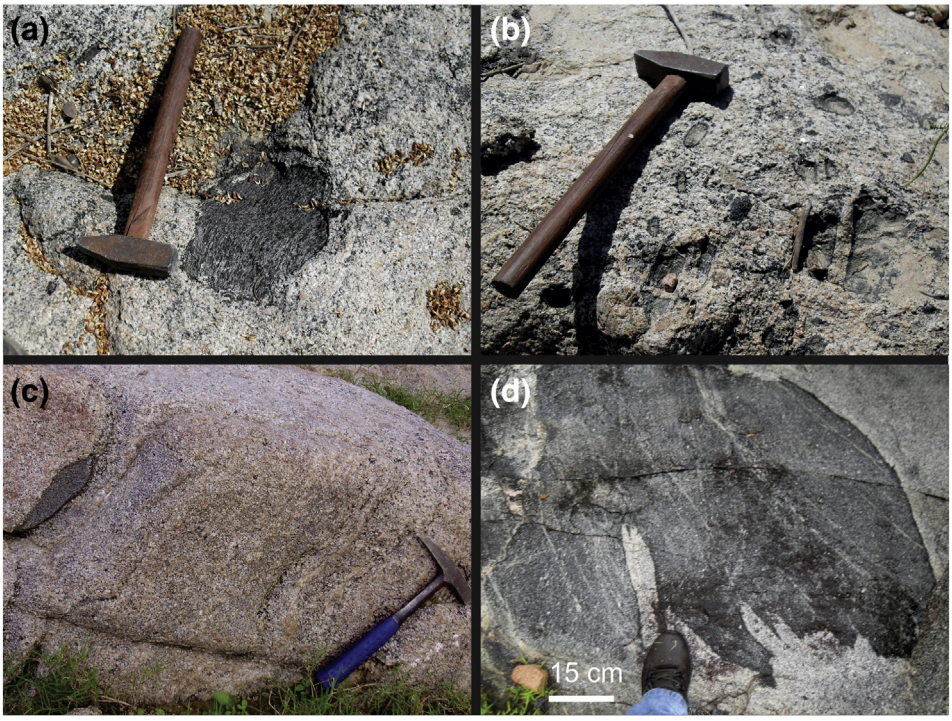

Fig. 4. Field aspects of the Monteirópolis batholith. (a) Medium-grained granite containing a large amphibole-rich clot. (b) Rounded to elliptical amphibole-rich clots armored by a narrow hornblende fringe in high-K calk-alkaline granite. (c) Granite with mafic enclave parallel to the subhorizontal magmatic foliation. Hammer is 30 cm long. (d) Felsic and mafic magmas, exhibiting crenulated contacts.

element analyses were done by ICP-OES at the SGS Geosol Laboratories, Belo Horizonte, Brazil (Table 1).

Sr isotopic analyses were performed at the Geochronological Research Center (CPGeo) of the University of São Paulo, Brazil following the method described by Kawashita (1972). Approximately 50 mg of powdered rock sample was dissolved in concentrated HF, HNO_3, and HCl. Sr aliquots were separated from the solutions using conventional ion exchange techniques and deposited on Re filaments. Isotopic analyses were performed with a multicollector VG-354 mass spectrometer in static mode. Sm–Nd isotopic analyses, also performed in the São Paulo lab, followed the method described by Sato et al. (1995). Whole-rock powders (approximately 50 mg) were mixed with $^{149}Sm/^{150}Nd$ spike solution and dissolved in Savillex capsules. Extraction of Sm and Nd from the samples followed conventional cation ion exchange techniques using a two-column technique. The isotope ratios were measured on a VG-354 multi-collector mass spectrometer, with analytical precision of 0.0014% (2σ). Laboratory blanks for the chemical procedure during the period of analyses yielded maximum values of 0.4 ng for Nd and 0.7 ng for Sm. Uncertainties for Sm/Nd and $^{143}Nd/^{144}Nd$ ratios are better than ±0.1% (1σ) and ±0.005% (1σ) respectively, based on repeated analyses of international rock standards La Jolla and BCR-1. The $^{143}Nd/^{144}Nd$ ratios were normalized against $^{146}Nd/^{144}Nd = 0.7219$. The calculations of the model ages were based on the depleted-mantle evolution model of DePaolo (1981) and DePaolo et al. (1991).

5. Geochemistry and geothermometry

5.1. Major and trace chemistry

In the Monteirópolis batholith, silica contents vary between 59.72 and 77.88 wt%. Plots of selected major- and trace-element concentrations versus SiO_2 (Harker diagrams, Fig. 5) exhibit negative trends except for K_2O and Na_2O. Inverse correlations between P_2O_5 with SiO_2 point to early saturation of apatite. This pattern indicates an I-type characteristic, as P_2O_5 increases during progressive fractional crystallization in S-type granites (Chappell and White, 2001). Negative correlation between Zr and SiO_2 points to early crystallization of zircon as indicated by inclusions of zircon in other phases.

The Monteirópolis pluton is metaluminous to slightly peraluminous (A/CNK ≤ 1.2), which is an I-type attribute (Chappell and White, 1992, 2001; Chappell et al., 2012). According to the geochemical classification proposed by Frost et al. (2001), the Monteirópolis granitoid is alkali-calcic and magnesian. Frost and Frost (2008) stated that magnesian rocks with alkali-calcic composition are formed in arc or post-collisional environments, such as the Cordilleran granites. However, magmas derived by partial melting of magnesian crustal rocks may inherit this magnesian character. Some of the studied rocks are of high-alumina-type trondhjemite affinity based on their chemical composition (Al_2O_3 more than 15 wt% at 70 wt% SiO_2; Barker, 1979) with peraluminous character (Shand indices greater than 1.0). K_2O (up to 6.79 wt%) contents in the studied rocks are higher than primitive trondhjemites (K_2O ca. 1.35 wt%; e.g. Barker, 1979). Trondhjemitic rock requires partial melting of basaltic rocks in equilibrium with garnet at high pressures (10–30 kb) (e.g. Rapp et al., 2003; Martin et al., 2005; Scaillet et al., 2016; among others). On the contrary, the peraluminous nature would indicate a crustal source.

REE data normalized to chondrite values (Fig. 6a) display closely parallel patterns. These rocks are also enriched in large ion lithophile elements (LILEs) compared to high field strength elements (HFSE), a general characteristic of fractionated calc-alkaline granitoids. Chondrite-normalized rare earth element patterns are fractionated for the Monteirópolis batholith (La_N/Lu_N = 27.6–125), with Eu anomalies negative to positive (0.67 to 1.25). The rocks show moderate enrichment of the HREE segment Gd_N/Lu_N 2.4–12.5 (Fig. 6a). The total rare earth element (ΣREE) of the Monteirópolis granitoids ranges from 209 to 500 ppm, possibly tied to allanite, epidote and titanite. Trace element distribution patterns are characterized by strong negative slopes and deep troughs at Nb, Ta and Ti and less pronounced Sr deep, interpreted as reflecting a subduction-related signature (e.g. Condie and Kröner, 2013) (Fig. 6b).

Table 1
Representative geochemical data for granitoids from the Monteirópolis batholith and temperature estimates from apatite (T_{Ap}) saturation thermometry. Sample TR–01 M (enclave). Major elements in wt%, trace elements in ppm.

Sample	TR-01	TR-43	TR-44	TR-45	TR-46	TR-47	TR-48	TR-49	TR-50	TR-51	TR-52	TR-53	TR-73	TR-74	TR-76	TR-77	TR-78	TR-79	TR-80	TR-83	TR-85	TR-88	TR-89	TR-01M
SiO_2	59.72	67.50	77.88	69.44	71.86	74.83	62.72	71.49	73.43	71.27	64.53	73.94	71.04	66.47	68.78	70.77	70.68	70.23	71.27	77.64	67.43	66.19	63.73	44.50
$Al2O_3$	17.50	13.81	12.39	14.41	14.45	15.08	15.18	15.82	14.56	15.19	17.14	13.84	14.78	15.74	16.19	13.92	14.94	15.31	15.27	13.78	15.10	19.56	14.51	15.48
MgO	1.71	1.05	0.18	0.60	0.45	0.44	2.48	0.45	0.41	0.77	1.73	0.43	0.77	1.01	0.75	0.77	1.03	0.30	0.62	0.38	1.71	1.62	1.85	5.65
MnO	0.07	0.06	0.01	0.05	0.01	0.01	0.09	0.01	0.01	0.03	0.10	0.01	0.03	0.03	0.04	0.02	0.03	0.02	0.03	0.01	0.09	0.06	0.07	0.40
CaO	3.70	2.09	0.30	1.55	1.31	0.70	2.52	1.18	0.74	1.06	2.43	0.31	1.53	1.89	2.08	1.38	1.21	0.20	1.56	1.27	2.19	1.55	2.65	4.31
Na_2O	5.78	3.14	3.47	3.39	4.04	4.31	3.07	4.20	3.87	4.42	5.12	4.76	3.66	4.22	4.54	4.19	4.73	5.73	3.71	3.81	4.11	4.27	4.84	2.15
K_2O	3.04	5.44	5.02	5.39	4.27	3.96	6.79	4.66	5.05	4.47	3.77	4.35	5.68	5.21	4.84	4.43	4.42	3.22	4.53	3.35	3.92	3.58	4.92	4.18
TiO_2	1.04	0.61	0.10	0.41	0.13	0.09	0.91	0.16	0.13	0.22	0.75	0.11	0.39	0.48	0.44	0.39	0.37	0.25	0.26	0.07	0.71	0.35	0.75	1.28
P_2O_5	0.40	0.18	0.01	0.11	0.05	0.01	0.52	0.09	0.03	0.13	0.45	0.04	0.18	0.22	0.18	0.17	0.15	0.04	0.08	0.06	0.24	0.11	0.34	0.10
Fe_2O_{3T}	5.92	2.80	0.91	3.41	1.15	0.29	5.14	0.86	0.68	1.36	4.31	0.54	2.51	3.02	2.43	2.06	1.87	2.01	1.96	0.59	4.20	2.55	3.81	19.34
P.F	0.47	1.08	0.27	1.08	0.93	0.63	0.38	0.50	0.69	1.22	0.36	0.70	0.42	1.08	0.22	0.59	0.57	1.47	0.50	0.37	0.46	1.13	1.31	1.22
Total	99.37	97.76	100.56	99.84	98.65	100.35	99.82	99.42	99.6	100.14	100.7	99.03	101.01	99.37	100.49	98.69	100.00	98.78	99.79	101.33	100.17	100.96	98.79	98.61
Trace elements in ppm																								
Cr	136.8	185	205.2	343	106	111	136.8	58	69	105	136.8	96	68.4	279	68.4	200	125	371	155	142	136.8	354	282	973
Ba	824	1267	1098	1501	1497	658	4607	1090	1107	865	908	1080	1624	1620	1550	1289	1072	572	1339	947	921	829	1549	910
Rb	126.7	210	130.8	142	108	119	180.3	103	138	205	213.3	128	136.2	129	114	148	193	104	120	83	170.1	162	256	211
Sr	541	428	421	421	683	540	1440	646	686	554	691	490	545	925	744	870	600	287	431	61	486	533	1068	292
Zr	455	221	83	267	158	85	515	128	112	121	388	76	323	294	280	220	164	159	210	44	176	146	295	53
Y	38	62	2.09	44	22	21	30.92	26	28	34	16	27	9.9	23	5.36	29	43	24	39	25	18.91	37	52	52
Nb	22.71	27	2.88	13	0	5	19.3	9	1	4	16.15	1	6.69	1	5.57	15	9	11	6	−4	14.84	9	18	13
Ni	10	29	9	29	15	18	42	13	15	21	20	15	10	29	9	30	121	27	14	14	16	42	44	66
La	63.9		2.1				111				60.2		57.4		53.3						68.90			
Ce	134		12.2				230.2				105.7		107.7		104.4						138.90			
Pr	15.19		1.15				24.07				12.22		9.79		9.38						13.82			
Nd	55.8		4				95.6				44.8		33.2		32.8						52			
Sm	10.1		0.50				14.9				7.2		4.2		3.7						7.4			
Eu	1.9		0.18				3.24				1.6		1.22		1.1						1.58			
Gd	7.52		0.37				9.49				5.02		2.33		1.96						4.81			
Tb	1.1		0.05				1.21				0.61		0.32		0.18						0.64			
Dy	6.47		0.32				5.24				3.03		1.49		0.85						3.08			
Ho	1.32		0.05				0.91				0.50		0.27		0.15						0.53			
Er	3.63		0.16				2.13				1.43		0.71		0.41						1.36			
Tm	0.52		0.05				0.30				0.19		0.09		0.05						0.18			
Yb	3.8		0.20				1.90				1.3		0.80		0.40						1.3			
Lu	0.24		0.05				0.25				0.05		0.12		0.05						0.18			
Hf	9.52		1.96				10.2				9.23		6.93		5.39						3.65			
Th	16.8		3.10				16.1				25.8		14.3		9.50						15.1			
U	1.22		0.59				2				3.98		2.1		0.90						3.86			
Ta	1.94		0.05				0.53				1.1		0.05		0.05						0.54			
Ga	24.1		14				22.5				31.7		17.7		21.5						25			
V	98		5				86				72		45		27						50			
Co	11.3		1.9				13.2				9.3		5.7		3.9						8.8			
Cs	2.12		1.77				3.45				8.67		2.34		1.21						10.67			
Cu	17		5				22				7		37		5						8			
Zn	135		18				133				83		55		69						125			
Sn	4.5		0.30				4				5.10		0.3		0.3						2.5			
T_{Ap}(°C)	951	940	785	907	857	757	1023	908	828	944	1023	857	977	954	954	965	953	814	895	927	974	872	976	548

Table 2
Summary of SHRIMP U–Pb zircon data of the Sample TR-01 from the Monteirópolis batholith.

Grain. spot	% $^{206}Pb_c$	U ppm	Th ppm	$^{232}Th/^{238}U$	$^{206}Pb^*$ ppm	(1) $^{206}Pb/^{238}Pb$ age		(1) $^{207}Pb/^{206}Pb$ age		% Dis	(1) $^{207}Pb^*/^{206}Pb^*$	±%	(1) $^{207}Pb^*/^{235}Pb$	±%	(1) $^{206}Pb^*/^{238}Pb$	±%	Erro corr
1.1	0.16	112	87	0.80	9.8	625.2	±11.8	621	±76	−1	0.0605	3.5	0.8492	4.0	0.1018	2.0	0.4905
2.1	0.24	477	171	0.37	37.2	558.6	±9.6	565	±32	1	0.0589	1.5	0.7356	2.3	0.0905	1.8	0.7741
3.1	0.08	227	60	0.27	20.5	643.0	±11.3	610	±40	−5	0.0602	1.8	0.8705	2.6	0.1049	1.9	0.7091
3.2	0.33	108	65	0.62	10.0	657.3	±12.5	662	±82	1	0.0616	3.8	0.9123	4.3	0.1073	2.0	0.4647
4.1	0.29	191	336	1.81	16.6	618.5	±12.2	599	±46	−3	0.0599	2.1	0.8315	2.9	0.1007	2.1	0.7004
5.1	0	233	271	1.20	20.3	624.2	±11.0	570	±54	−9	0.0591	2.5	0.8280	3.1	0.1017	1.9	0.6013
6.1	0	183	67	0.38	16.1	628.8	±11.4	599	±44	−5	0.0599	2.0	0.8459	2.8	0.1025	1.9	0.6827
7.1	0.21	231	249	1.11	20.3	625.2	±11.2	629	±39	1	0.0607	1.8	0.8524	2.6	0.1018	1.9	0.7199
8.1	0.12	404	127	0.32	34.9	616.4	±10.6	614	±35	0	0.0603	1.6	0.8343	2.4	0.1003	1.8	0.7388
9.1	0	107	157	1.52	9.9	657.4	±12.4	726	±50	10	0.0635	2.4	0.9406	3.1	0.1074	2.0	0.6445
10.1	0	202	172	0.88	17.8	629.7	±13.3	619	±39	−2	0.0604	1.8	0.8551	2.9	0.1026	2.2	0.7791
11.1	0.25	121	92	0.79	10.7	632.6	±11.9	636	±76	1	0.0609	3.5	0.8659	4.1	0.1031	2.0	0.4865

Errors are 1-sigma; Pb_c and Pb* indicate the common and radiogenic portions, respectively. 1) Common Pb corrected using measured ^{204}Pb.

5.2. Geothermometry

As applied to the less differentiated samples in this batholith, calculated apatite saturation temperatures exceed 950 °C (Harrison and Watson, 1984). Green and Watson (1982) demonstrated that there is a relationship, which is generally pressure-independent, between apatite saturation and the silica content of the host magma, establishing the levels of P_2O_5 as a function of the silica content at which apatite

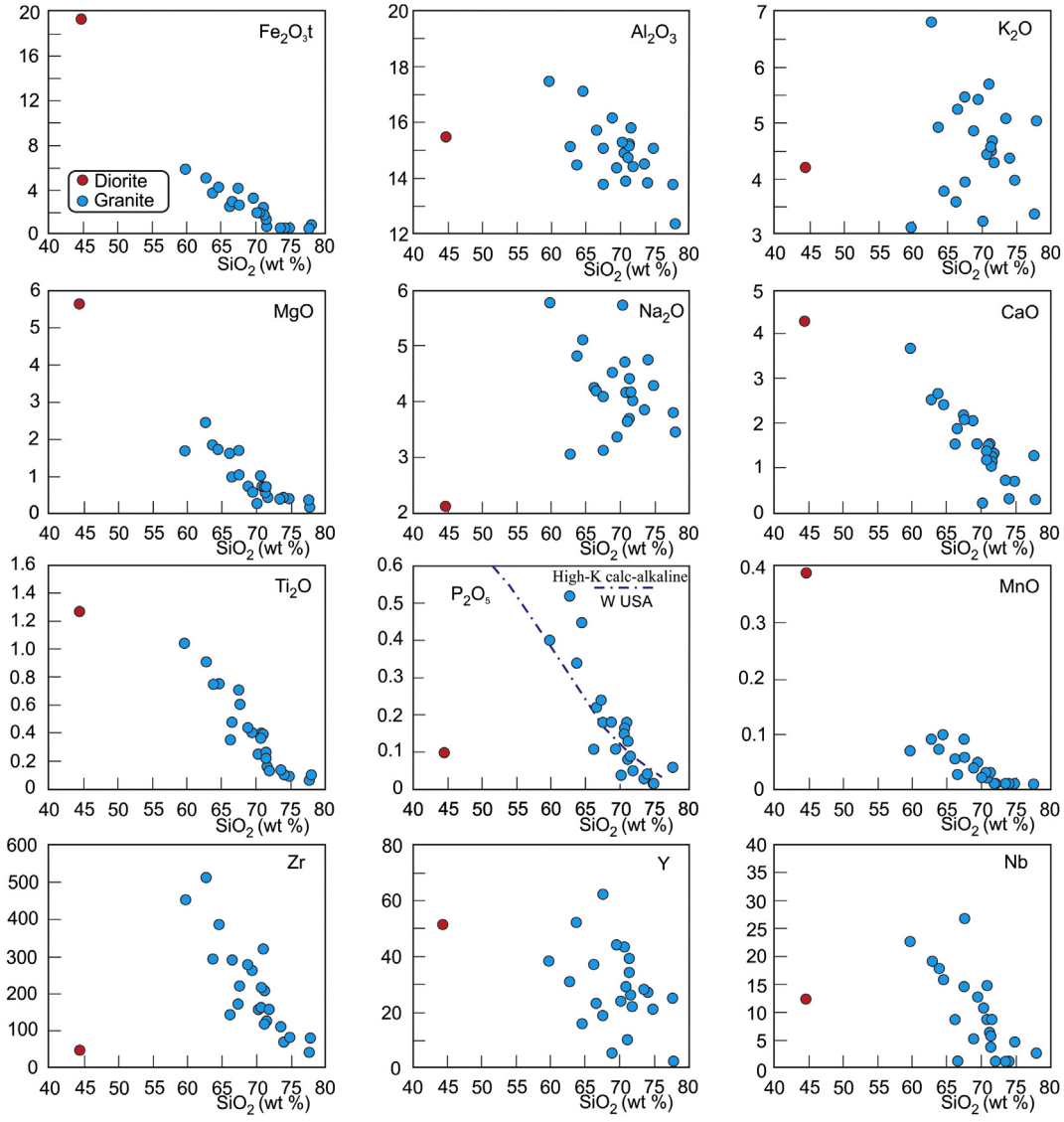

Fig. 5. Harker diagrams of samples from the Monteirópolis batholith. Dashed line in the P_2O_5 versus SiO_2 plot corresponds to average of high-K calk-alkaline rocks after Green and Watson (1982) (compilations of chemical data for 'orogenic' rock series (Western USA) presented by Ewart, 1979, 1981).

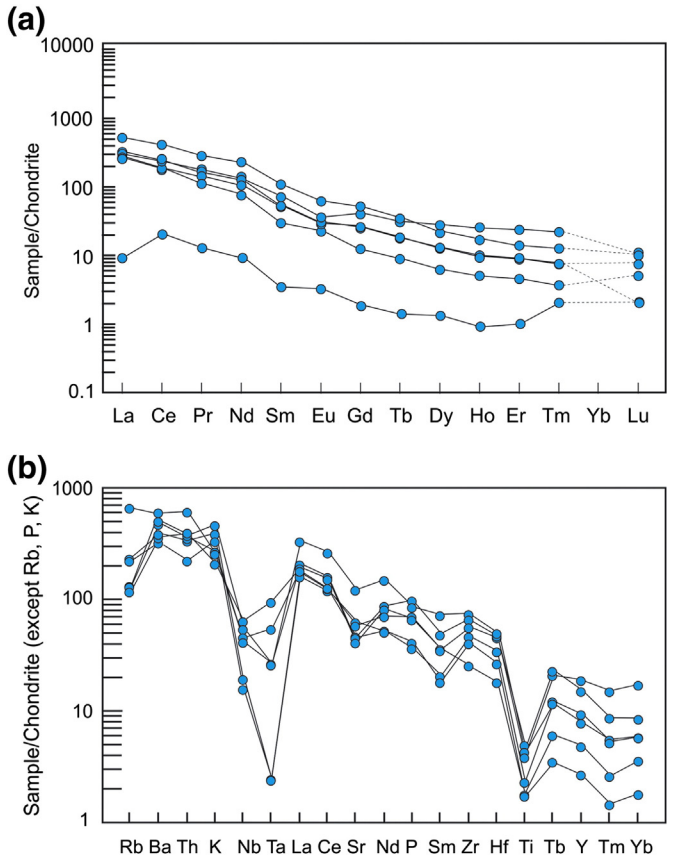

Fig. 6. (a) Chondrite-normalized rare earth element patterns. Chondrite values from Evensen et al. (1978). (b) Trace elements distribution (spidergrams) normalized to the chondrite values of Thompson (1982).

starts crystallizing. Plot of whole-rock SiO_2 vs. P_2O_5 generates a roughly defined trend between the 950 and 800 °C isotherms at P = 7.5 kb (not shown).

6. U–Pb geochronology of zircon

The analyzed zircon population consists of pink to yellow crystals, mostly euhedral but some corroded grains. They are short-to-elongated and they present bipyramidal terminations typical of magmatic growth. Lengths range from 140 to 245 μm, with length–width ratios ranging from 1:1 to >3:2. SEM and cathodoluminescence (CL) images reveal grain edges with oscillatory zoning, corresponding to magmatic growth (Fig. 7).

Table 2 displays sample TR-01 data, for which twelve points were analyzed in eleven zircon grains. A cluster of nine concordant data yields a mean weighted $^{206}Pb/^{238}U$ age of 625.8 ± 3.7 Ma with MSDW (Mean Square of Weighted Deviates) = 1.08 (Fig. 8). High Th/U, 0.32 to 1.81, is typical of magmatic zircons. (Generally, Th/U in igneous zircon is ≥0.25; e.g. Williams and Claesson, 1987; Hoskin and Black, 2000; Hoskin and Schaltegger, 2003). We interpret this as the age of crystallization and emplacement of the Monteirópolis batholith. Data for two other zircon grains (3.2 and 9.1) from the same sample plot concordantly at a $^{206}Pb/^{228}U$ age = 657 ± 12.5 Ma, attributed to inheritance from a previous magmatic pulse. The 558 ± 9.6 Ma age of another zircon grain (2.1) (disc = 1% and Th/U = 0.37) may reflect some undefined Pb loss in a damaged area.

7. Whole rock Rb–Sr and Sm–Nd and O isotope zircon data

For the Monteirópolis batholith, a Nd-model age is 1.0 Ga, at which $\varepsilon Nd_{0.626\ Ga}$ is slightly positive (+0.14) (Fig. 9a). Initial $^{87}Sr/^{86}Sr_{0.626\ Ga}$ varies over a narrow range from 0.7050 to 0.7052 (Table 3). In the εNd vs. εSr diagram (Fig. 9b), the data plot close to the mantle array.

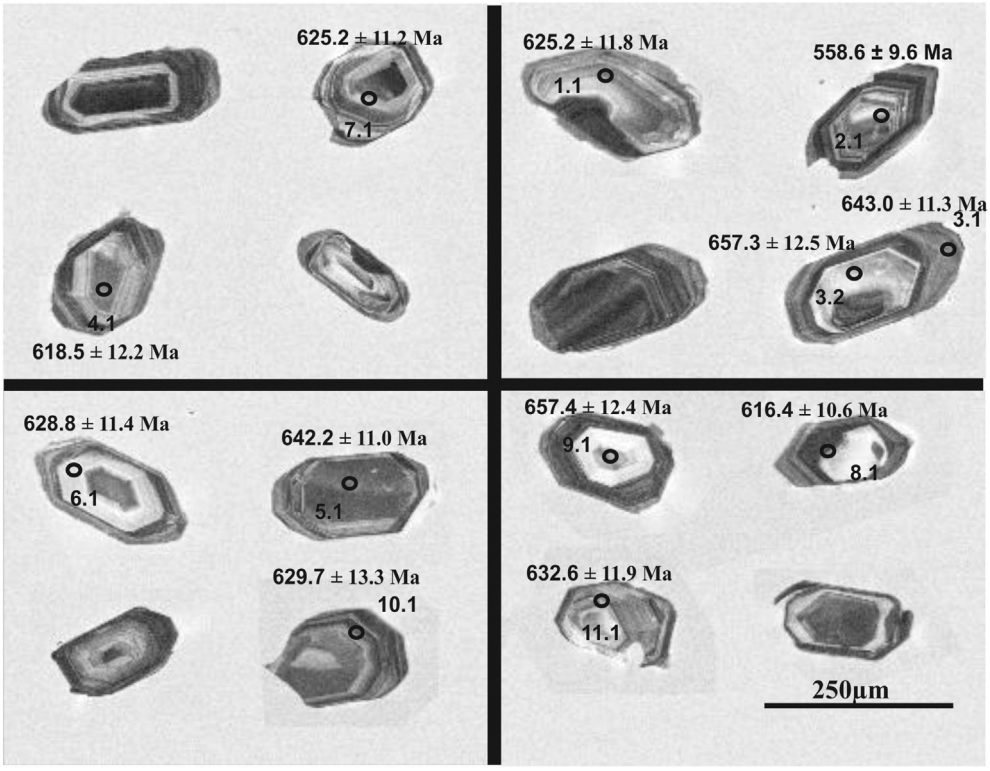

Fig. 7. Cathodoluminescence (CL) Images of selected dated zircon grains of the Monteirópolis batholith showing position of the SHRIMP spot listed in Table 2.

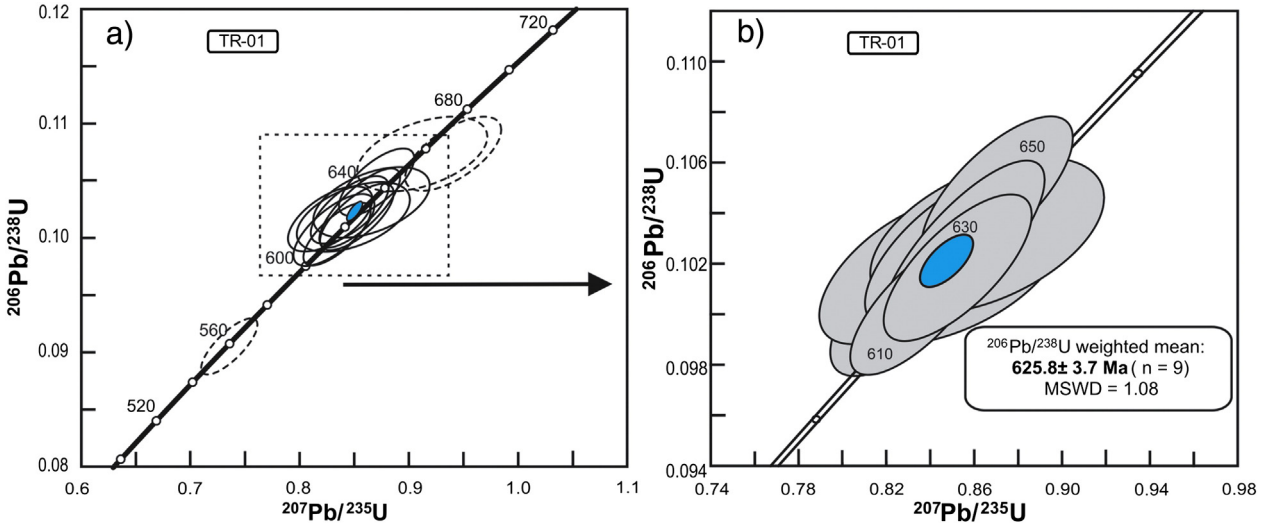

Fig. 8. (a) U–Pb concordia diagram for zircons from the Monteirópolis batholith. (b) Zoom showing the weighted mean age of zircon analyses.

With the assumption of equilibrium O isotope fractionation between zircon and silicate melt, Valley et al. (1994) and as refined by Lackey et al. (2008), used $\delta^{18}O$ in zircon to empirically estimate $\delta^{18}O$ in the magma. For the Monteirópolis batholith, $\delta^{18}O_{zircon}$ values of 5.00 to 5.94‰ and whole-rock SiO_2 (59.72 to 64.98 wt%) translate to $\delta^{18}O_{magma} = +6.92$ to 7.42‰. This oxygen isotope composition, the low initial $^{87}Sr/^{86}Sr$ ratios, and slightly positive εNd values are consistent with the granitic magma that had formed from a mantle-derived magma.

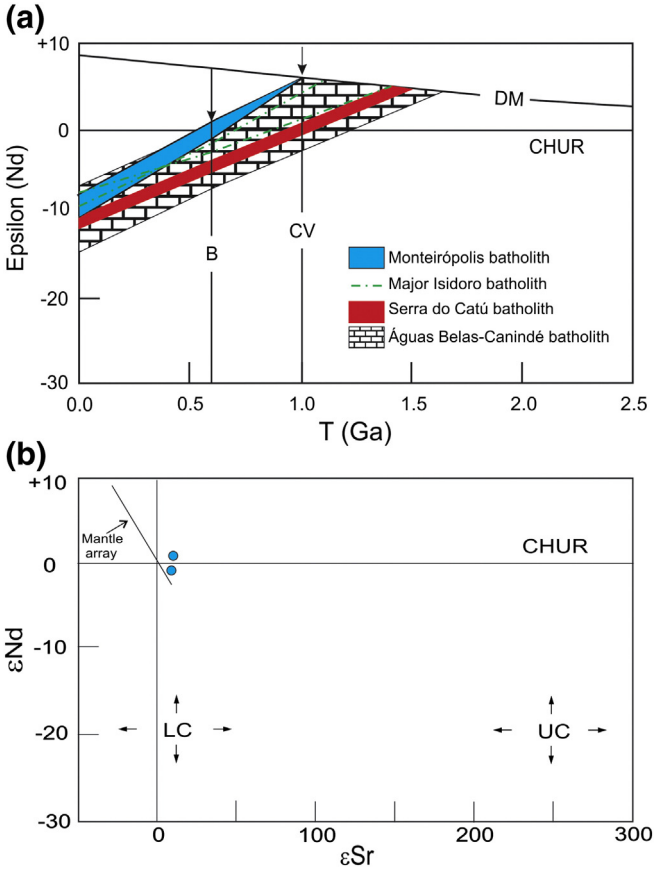

Fig. 9. (a) Nd isotopic compositions of the Monteirópolis, Major Isidoro, and Serra do Catú granitoids and of the Águas Belas–Canindé batholith. B = Brasiliano orogeny; CV = Cariris Velhos event. Águas Belas–Canindé batholith data from Silva Filho et al. (2014). (b) εNd(t) versus εSr (t) diagram for granitoids from the Monteirópolis batholith. LC (lower crust) and UC (upper crust), fields from Harmon et al. (1984).

8. Discussion

In the light of regional age data, Monteirópolis is a synkinematic (i.e., early) Brasiliano intrusion, probably emplaced in the early stages of convergence in an environment that was later subjected to transcurrent/transpressional deformation (Ganade de Araujo et al., 2014; Neves et al., 2006; Neves et al., 2012; Neves et al., 2015; Van Schmus et al., 2008). Its flat-lying foliation corresponds to the regional D_2 deformation, which produced recumbent folds in the Pernambuco–Alagoas Domain, and that constitutes the main foliation (Silva Filho et al., 2014). Other ages that can be more directly related to structural events include SHRIMP zircon U–Pb data of an orthogneiss in the Jacaré dos Homens transpressional shear zone (642 ± 3 Ma; Lima, 2013), and amphibole ^{40}Ar–^{39}Ar cooling ages of mylonitic rocks from the Belo Monte Jeremoabo and Macururé shear zones (637 ± 7 Ma to 623 ± 2 Ma; Araújo et al., 2004). Intrusion of the Monteirópolis batholith followed these initial events at 626 Ma, after approximately 15 m.y. during development of low-angle regional foliation.

Did magma emplacement trigger nucleation of shear zones (Neves et al., 1996) or did the shearing control ascent and emplacement of magma (Brown and Solar, 1998)? In the Borborema Province, the shape and distribution of most plutons are clear indicators of the latter interpretation: shear-zone control of the emplacement of synkinematic plutons (Weinberg et al., 2004, 2005), Monteirópolis among them.

The Monteirópolis batholith is composed of high-K calc-alkaline rocks that show a volcanic arc geochemical signature (Harris et al., 1986; Pearce, 1996; Pearce et al., 1984) and are classified as magnesian granites, which could be interpreted as subduction related (Frost et al., 2001). High-K calc-alkaline magmatism extensively occurs at post-collisional stages (e.g. Barbarin, 1999; Liégeois et al., 1998) but it also occurs at active continental margins (e.g. Barbarin, 1999; Condie, 1989; Wilson, 1989). It has long been recognized that there is a genetic relationship between high-K calc-alkaline magmatism and subduction zones (e.g. Barbarin, 1999; Peccerillo, 1985; Rogers et al., 1985). According to Barbarin (1999) calc-alkaline granitic rocks are invariably emplaced above subduction zones, forming vast batholiths, elongated parallel to the trench in the active continental margins.

In a plot of Na_2O and K_2O vs. silica, the samples have compositions similar to experimentally produced melts of medium- to high-K basaltic rocks (Fig. 10a, b). They show compositions that are distinct from those of melts produced by the partial melting of quartz amphibolites (Patiño

Table 3
Summary of representative Sm–Nd and Rb–Sr isotopic results. Initial compositions recalculated to crystallization age.

Sample	Nd ppm	Sm ppm	$^{147}Sm/^{143}Nd$	$^{143}Nd/^{144}Nd$	εNd (Today)	εNd (T)	TDM (Ga)	Rb ppm	Sr ppm	$^{87}Rb/^{86}Sr$	$^{87}Sr/^{86}Sr$	εSr (Today)	εSr (T)
Mont I	32	4	0.0756	0.512099	−10.51	−0.78	1.0	172	486	1.027	0.7142	137.6	17.93
Mont II	23	3	0.0845	0.512230	−7.96	+1.06	1.0	149	340	1.267	0.7166	171.3	21.11
*SC	31	6	0.1105	0.512105	−10.40	−3.80	1.4	129	1265	0.294	0.7098	75.2	48.98
*SC	60	11	0.1109	0.512037	−11.71	−5.15	1.5	228	1642	0.402	0.7107	88.0	48.33
*SC	76	14	0.1107	0.512042	−11.62	−5.04	1.5	240	1681	0.413	0.7106	86.6	45.63
#MI	77	16	0.1288	0.512249	−7.60	−2.12	1.4	130	413	0.911	0.7167	174	69
#MI	25	4	0.0960	0.512167	−9.19	−1.09	1.1	86	714	0.348	0.7099	78	44

Mont-Monteirópolis batholith; SC-Serra do Catú pluton; and MI-Major Isidoro batholith.
*Serra do Catú data from Brito et al. (2009) and #Major Isidoro data from Silva et al. (2015).

Douce and Beard, 1995), amphibolites (Beard and Lofgren, 1991) and metabasalts (Rapp and Watson, 1995), which have low K contents and variable Na_2O and CaO contents. Monteirópolis magma was plausibly derived from partial melting of medium-K basaltic rocks. Such rocks are common in subduction-related magmatic arcs, and granitic and rhyolitic magmas can be formed by advanced crystallization-differentiation or by low-degree partial remelting of mantle-derived basaltic sources (Sisson et al., 2005).

If a depleted mantle source had developed, followed promptly by partial melting, the εNd model age and emplacement age of the magma would agree. For the Monteirópolis batholith these two ages are respectively 1.0 Ga and 0.63 Ga. The t_{DM} age corresponds to the extensional Cariris Velhos event first identified in the Transverse Domain (e.g. Guimarães et al., 2012, 2015; Van Schmus et al., 1995, 2008) but which occurs elsewhere in the Borborema Province. Guimarães et al. (2015) proposed that mafic melts associated with crustal thinning comprised heat sources for Tonian granitic magmas (~1 Ga) elsewhere in the oriental Borborema Province. Inherited zircon cores occur in the Monteirópolis granitoid, which together with Tonian model age, εNd values and Ediacaran crystallization age, provide evidence for two stages magma derivation.

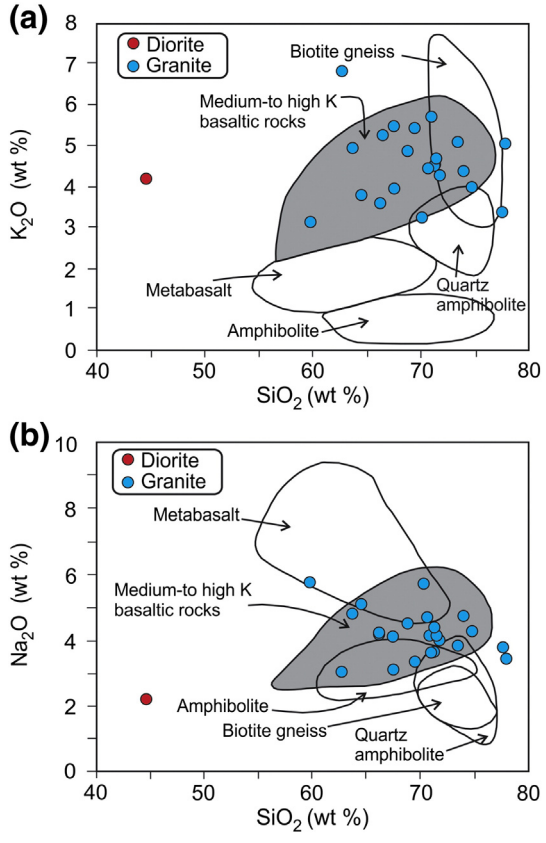

Fig. 10. (a) wt% SiO_2 vs. K_2O and (b) wt% SiO_2 vs. Na_2O diagrams with published data for experimental melts as compiled by Chen et al. (2013) from the literature: Beard and Lofgren (1991) (Amphibolites; 1, 3, 6, 9 kb; 800–1000 °C), Rapp and Watson (1995) (Metabasalt; 8–32 kb; 1000–1125 °C), Patiño Douce and Beard (1995) (Quartz amphibolites; 3–15 kb; 850–930 °C); Patiño Douce and Beard (1995) (Biotite gneiss; 3–15 kb; 850–930 °C) and Sisson et al. (2005) (Medium-to-high K basaltic rocks; 700 Mpa; 825–975 °C).

Eu anomalies are absent at the Monteirópolis (average $\delta_{Eu} = 0.93$), possibly because partial melting took place at pressures above the stability field of plagioclase. Another explanation is crystallization at high fO_2, which inhibits the formation of Eu^{2+} and entrance of Eu into feldspar (Hanson, 1980). Coexistence of titanite + quartz also suggests high oxygen fugacity (Wones, 1989). Preserved magmatic epidote corresponds to crystallization at moderately high pressures (lower crustal depths) under fairly oxidizing conditions (Sial et al., 2008; Zen and Hammarstrom, 1984). Upward magma transport from the deep crust must have been rapid (Brandon et al., 1996; Sial et al., 2008).

9. Concluding remarks

The back-calculated $^{87}Sr/^{86}Sr_I = 0.705$ suggests an I-type source (e.g., Barbarin, 1999; Chappell and White, 2001; among others). Likewise, calculated whole-rock $\delta^{18}O$ (+6.92 to +7.42‰) lies within the I-type range according O'Neil et al. (1977) and Eiler (2001), who recommend 6.0 to 10‰. Monteirópolis $\delta^{18}O$ values are slightly higher than normal mantle-derived magmas (mantle-derived magmas have $\delta^{18}O$ values of 5.7 ± 0.5‰; Eiler et al., 1998; Harmon and Hoefs, 1995; Hawkesworth and Kemp, 2006; Hoefs, 2009), and the $\delta^{18}O$ (zircon) values (+5.00 to 5.94‰) are near to values of zircon crystallized from mantle-derived magmas that has $\delta^{18}O = 5.3 \pm 0.3$‰ (Valley et al., 1998, 2003, 2005).

Depleted mantle Nd-model age of 1.0 Ga and slightly positive εNd(t), mantle-like back-calculated $^{87}Sr/^{86}Sr(i)$, and mantle-like $\delta^{18}O$ (zircon) values suggest that the investigated granites from the Monteirópolis batholith have been produced by partial melting of Tonian mantle-derived rocks. The Monteirópolis granites are high-K calc-alkaline, similar to granitoids in the Transverse, Sergipano and Pernambuco–Alagoas domains that constitute intrusions (630–611 Ma) whose ages are syn-orogenic (within errors). U–Pb zircon ages of the Monteirópolis batholith (625.8 ± 3.7 Ma) and of the orthogneiss from the Jacaré dos Homens transpressional shear zone (642 ± 3 Ma) could establish the onset of the Brasiliano orogeny at 626–642 Ma in this domain. The orogeny could have begun earlier but older plutons or shear zones have not been yet found.

Acknowledgments

We are thankful to Prof. Leon Long, an anonymous reviewer and the editor-in-Chief Prof. Nelson Eby for their comments and suggestions that significantly improved the original version of the manuscript. We thank Sergio P. Neves for discussions on an earlier version of this manuscript. TRS thanks CNPq for a scholarship (process 830099/1999-9). Thanks are also due to Gilsa M. Santana and Vilma Sobral Bezerra for the assistance with oxygen isotope analyses, and to Severina Paulina

for assistance with chemical analyses at the Stable Isotope Laboratory (LABISE) in the Federal University of Pernambuco, Brazil. VPF and ANS acknowledge the financial support of the Brazilian agencies FACEPE (PRONEX/FACEPE APQ-0479-1.07/06, APQ 0844-1.07/08, APQ-1738-1.07/12) and CNPq (Universal project 478554/2009-5, 471034/2012-6). This is the NEG–LABISE contribution n. 279.

References

Almeida, F.F.M., Hasui, Y., Brito Neves, B.B., Fuck, R.A., 1981. Brazilian structural provinces: an introduction. Earth-Science Reviews 17, 1–29.
Araújo, M.N., Oliveira, E.P., Onoe, A.T., 2004. Geocronologia Ar/Ar de Sucessivos episódios Deformacionais Em Limite de Terrenos Da Faixa Sergipana. XLII Congresso Brasileiro de Geologia, Araxá, Brazil, CD-ROM.
Barbarin, B., 1999. A review of the relationships between granitoid types, their origins and their geodynamic environments. Lithos 46, 605–626.
Barker, F., 1979. Trondhjemite: definition, environment, and hypothesis of origin. In: Barker, F. (Ed.), Trondhjemites, Dacites, and Related Rocks. Elsevier, Amsterdam, pp. 1–12.
Beard, J.S., Lofgren, G.E., 1991. Dehydration melting and water-saturated melting of basaltic and andesitic greenstones and amphibolites at 1.3 and 6.9 kb. Journal of Petrology 32, 365–401.
Black, L.P., Kamo, S.L., Allen, C.M., Davis, D.W., Aleinikoff, J.N., Valley, J.W., Mundil, R., Campbell, I.H., Korsch, R.J., Williams, I.S., Foudoulis, C., 2004. Improved $^{206}Pb/^{238}U$ microprobe geochronology by the monitoring of a trace-element-related matrix effect; SHRIMP, ID-TIMS, ELA-ICP-MS and oxygen isotope documentation for a series of zircon standards. Chemical Geology 205, 115–140.
Brandon, A.D., Creaser, R.A., Chacko, T., 1996. Constraints on rates of granitic magma transport from epidote dissolution kinetics. Science 271, 1845–1848.
Brito Neves, B.B., Santos, E.J., Van Schmus, W.R., 2000. Tectonic history of the Borborema Province, Northeastern Brazil. In: Cordani, U., Milani, E.J., Thomaz Filho, A., Campos, D.A. (Eds.), Tectonic Evolution of South America. International Geological Congress, 31st, Rio de Janeiro, Brazil, pp. 151–182.
Brito, M.F.L., Silva Filho, A.F., Guimarães, I.P., 2009. Geologia isotópica do batólito shoshonítico-ultrapotássico Neoproterozóico Serra do Catú e implicações na evolução da interface dos Domínios Canindé e Pernambuco–Alagoas. Revista Brasileira de Geociencias 39, 324–337.
Brown, M., Solar, G.S., 1998. Shear-zone systems and melts: feedback relations and self-organization in orogenic belts. Journal of Structural Geology 20, 211–227.
Chappell, B.W., White, A.J.R., 1992. I- and S-types granites in Lachlan Fold Belt. Transactions of the Royal Society of Edinburgh: Earth Sciences 83, 1–26.
Chappell, B.W., White, A.J.R., 2001. Two contrasting granite types: 25 years later. Australian Journal of Earth Sciences 48, 489–499.
Chappell, B.W., Bryanta, C.J., Wybornb, D., 2012. Peraluminous I-type granites. Lithos 153, 142–153.
Chen, J.-Y., Yang, J.-H., Zhang, J.-H., Sun, J.F., Wilde, S.A., 2013. Petrogenesis of the Cretaceous Zhangzhou batholith in southeastern China: zircon U–Pb age and Sr–Nd–Hf–O isotopic evidence. Lithos 162–163, 140–156.
Condie, K.C., 1989. Plate Tectonics and Crustal Evolution. 3rd. Edition. Pergamon Press (476 pp.).
Condie, K.C., Kröner, A., 2013. The building blocks of continental crust: evidence for a major change in the tectonic setting of continental growth at the end of the Archean. Gondwana Research 23, 394–402.
Dada, S.S., 2008. Proterozoic evolution of the Nigeria-Borborema Province. In: Pankhurst, R.J., Trouw, R.A.J., Brito Neves, B.B., De Wit, M.J. (Eds.), West Gondwana. Pre-Cenozoic Correlations Across the South Atlantic Region. Geological Society (London), Special Publication 294, pp. 121–136.
De Wit, M., Stankiewicz, J., Reeves, C., 2008. Restoring Pan-African-Brasiliano connections: more Gondwana controll, less tran-Atlantic corruption. In: Pankhurst, R.J., Trouw, R.A.J., Brito Neves, B.B., De Wit, M.J. (Eds.), West Gondwana. Pre-Cenozoic Correlations Across the South Atlantic Region. Geological Society (London), Special Publication 294, pp. 399–412.
DePaolo, D.J., 1981. Nd isotopic studies: some new perspectives on earth structure and evolution. Eos 62, 137–145.
DePaolo, D.J., Linn, A.M., Schubert, G., 1991. The continental crust age distribution methods of determining mantle separation ages from Sm–Nd isotopic data and application the southwestern United States. Journal of Geophysical Research 9, 2071–2088.
Eiler, J.M., 2001. Oxygen-isotope variations of basaltic lavas and upper mantle rocks. In: Valley, J.M., Cole, D.R. (Eds.), Stable Isotope GeochemistryReviews in Mineralogy and Geochemistry, 43. Mineralogical Society of America/Geochemical Society, Washington, DC, pp. 319–364.
Eiler, J.M., McInnes, B., Valley, J.W., Graham, C.M., Stolper, E.M., 1998. Oxygen isotope evidence for slab-derived fluids in the sub-arc mantle. Nature 393, 777–781.
Evensen, N.M., Hamilton, P.J., Onions, R.K., 1978. Rare-earth abundances in chondritic meteorites. Geochimica et Cosmochimica Acta 42, 1199–1212.
Ewart, A.E., 1979. A review of the mineralogy and chemistry of the tertiary-recent dacitic, latitic, rhyolitic and related salic volcanic rocks. In: Barker, F. (Ed.), Trondhjemites, Dacites and Related Rocks. Elsevier, Amsterdam, pp. 13–121.
Ewart, A.E., 1981. The mineralogy and petrology of tertiary-recent orogenic volcanic rocks: with special reference to the andesitic-basaltic compositional range. In: Thorpe, R.S. (Ed.), Orogenic Andesites and Related Rocks. John Wiley and Sons Ltd, pp. 25–95.
Ferreira, V.P., Sial, A.N., Jardim de Sá, E.F., 1998. Geochemical and isotopic signatures of the Proterozoic granitoids in terranes of the Borborema Province, northeastern Brazil. Journal of South American Earth Sciences 11, 439–455.
Ferreira, V.P., Sial, A.N., Pimentel, M.M., Armstrong, R., Guimarães, I.P., Silva Filho, A.F., Lima, M.M.C., Silva, T.R., 2015. Reworked old crust-derived shoshonitic magma: the Guarany pluton, northeastern Brazil. Lithos 232, 150–161.
Frost, B.R., Frost, C.D., 2008. A geochemical classification for feldspathic igneous rocks. Journal of Petrology 49, 1955–1969.
Frost, B.R., Arculus, R.J., Barnes, C.G., Collins, W.J., Ellis, D.J., Frost, C.D., 2001. A geochemical classification of granitic rocks. Journal of Petrology 42, 2033–2048.
Ganade de Araujo, C.E., Weinberg, R.F., Cordani, U.G., 2014. Extruding the Borborema Province (NE-Brazil): a two-stage Neoproterozoic collision process. Terra Nova 26, 157–168.
Green, T.H., Watson, E.B., 1982. Crystallization of apatite in natural magmas under high pressure, hydrous conditions, with particular reference to orogenic rock series. Contributions to Mineralogy and Petrology 79, 96–105.
Guimarães, I.P., Van Schmus, W.R., Brito Neves, B.B., Bittar, S.M.B., Silva Filho, A.F., Armstrong, R., 2012. U–Pb zircon ages of orthogneisses and supracrustal rocks of the Cariris Velhos belt: onset of Neoproterozoic rifting in the Borborema Province, NE Brazil. Precambrian Research 192, 52–77.
Guimarães, I.P., Brito, M.F.L., Lages, G.A., Silva Filho, A.F., Santos, L., Brasilino, R.G., 2015. Tonian granitic magmatism of the Borborema Province, NE Brazil: a review. Journal of South American Earth Sciences 68, 97–112.
Hanson, G.N., 1980. Rare earth elements in petrogenetic studies of igneous systems. Annual Review of Earth and Planetary Sciences 8, 371–405.
Harmon, R.S., Hoefs, J., 1995. Oxygen isotope heterogeneity of the mantle deduced from global ^{18}O systematic of basalts from different geotectonic settings. Contributions to Mineralogy and Petrology 120, 95–114.
Harmon, R.S., Halliday, A.N., Clayburn, J.A.P., Stephens, W.E., 1984. Chemical and isotopic systematics of the Caledonian intrusions of Scotland and northern England: a guide to magma source region and magma crust interaction. Philosophical Transactions of the Geological Society of London A310, 439–456.
Harris, N.B.W., Pearce, J.A., Tindle, A.G., 1986. Geochemical characteristics of collision-zone magmatism. In: Coward, M.P., Ries, A.C. (Eds.), Collision Tectonics. Geological Society Special Publication, London vol. 19, pp. 67–81.
Harrison, T.M., Watson, E.B., 1984. The behaviour of apatite during crustal anatexis: equilibrium and kinetic considerations. Geochimica et Cosmochimica Acta 48, 1467–1477.
Hawkesworth, C.J., Kemp, A.I.S., 2006. Using hafnium and oxygen isotopes in zircons to unravel the record of crustal evolution. Chemical Geology 226, 144–162.
Hoefs, J., 2009. Stable Isotope Geochemistry. 5th ed. Springer-Verlag, Berlin, Heidelberg (244 pp.).
Hoskin, P.W.O., Black, L.P., 2000. Metamorphic zircon formation by solid-state recrystallization of protolith igneous zircon. Journal of Metamorphic Geology 18, 423–439.
Hoskin, P.W.O., Schaltegger, U., 2003. The composition of zircon and igneous and metamorphic petrogenesis. Reviews in Mineralogy and Geochemistry 53, 27–62.
Kawashita, K., 1972. O método Rb–Sr Em Rochas Sedimentares PhD thesis Instituto de Geociências, IGc–USP, Brazil (111 pp, in Portuguese).
Lackey, J.S., Valley, J.W., Chen, J.H., Stockli, D.F., 2008. Dynamic magma systems, crustal recycling, and alteration in the Central Sierra Nevada batholith: the oxygen isotope record. Journal of Petrology 49, 1397–1426.
Liégeois, J.P., Navez, J., Hertogen, J., Black, R., 1998. Contrasting origin of post-collisional high-K calc-alkalic and shoshonitic versus alkalic and peralkalic granitoids. The use of sliding normalization. Lithos 45, 1–28.
Lima, M.M.C., 2013. Caracterização geoquímica, isotópica e geotectônica dos complexos Araticum e Arapiraca, faixa Sergipana–Alagoas. Unpublished Master thesis dissertation, Federal University of Pernambuco, Recife, Brazil, 89 pp, (in Portuguese).
Lima, M.M.C., Silva, T.R., Ferreira, V.P., Silva, J.M.R., 2014. Metasedimentary rocks of the northern part of the Macururé domain, Sergipano Belt (northeastern Brazil): geochemical characterization of their protoliths and tectonic implications. Estudios Geológicos 24, 89–107.
Ludwig, K.R., 2009. User's Manual for Isoplot/Ex, Version 3.71: A Geochronological Toolkit for Microsoft Excel: Berkeley Geochronology Center Special Publication, N° 5.
Martin, H., Smithies, R.H., Rapp, R., Moyen, J.F., Champion, D., 2005. An overview of adakite, tonalite-trondhjemiten-granodiorite (TTG), and sanukitoid: relationships and some implications for crustal evolution. Lithos 79, 1–24.
Neves, S.P., 2003. Proterozoic history of the Borborema Province (NE Brazil): correlations with neighboring cratons and Pan-African belts, and implications for the evolution of western Gondwana. Tectonics 22, 1031–1044.
Neves, S.P., Vauchez, A., Archanjo, C.J., 1996. Shear zone-controlled magma emplacement or magma-assisted nucleation of shear zones? Insights from northeast Brazil. Tectonophysics 262, 349–364.
Neves, S.P., Bruguier, O., Vauchez, A., Bosch, D., Silva, J.M.R., Mariano, G., 2006. Timing of crust formation, deposition of supracrustal sequences, and Transamazonian and Brasiliano metamorphism in the East Pernambuco belt (Borborema Province, NE Brazil): implications for western Gondwana assembly. Precambrian Research 149, 197–216.
Neves, S.P., Bruguier, O., Bosch, D., Silva, J.M.R., Mariano, G., 2008. U–Pb ages of plutonic and metaplutonic rocks in southern Borborema Province (NE Brazil): timing of Brasiliano deformation and magmatism. Journal of South American Earth Sciences 25, 285–297.
Neves, S.P., Monié, P., Bruguier, O., Silva, J.M.R., 2012. Geochronological, thermochronological and thermobarometric constraints on deformation, magmatism and thermal regimes in eastern Borborema Province (NE Brazil). Journal of South American Earth Sciences 38, 129–146.
Neves, S.P., Bruguier, O., Bosch, D., Silva, J.M.R., Mariano, G., Silva Filho, A.F., Teixeira, C.M.L., 2015. From extension to shortening: dating the onset of the Brasiliano orogeny in eastern Borborema Province (NE Brazil). Journal of South American Earth Sciences 58, 238–256.

Oliveira, E.P., Toteu, S.F., Araújo, M.N.C., Carvalho, M.J., Nascimento, R.S., Bueno, J.F., McNaughton, N., Basilici, G., 2006. Geologic correlation between the Neoproterozoic Sergipano belt (NE Brazil) and the Yaoundé schist belt (Cameroon, Africa). Journal of African Earth Sciences 44, 470–478.

Oliveira, E.P., Windley, B.F., Araújo, M.N.C., 2010. The Neoproterozoic Sergipano orogenic belt, NE Brazil: a complete plate tectonic cycle in western Gondwana. Precambrian Research 181, 64–84.

O'Neil, J., Shaw, S.F., Flood, R.H., 1977. Oxygen and hydrogen isotope compositions of granite genesis in the New England batholith, Australia. Contributions to Mineralogy and Petrology 62, 313–325.

Patiño Douce, A.E., Beard, J.S., 1995. Dehydration-melting of biotite gneiss and quartz amphibolite from 3 to 15 kbar. Journal of Petrology 36, 707–738.

Pearce, J., 1996. Sources and settings of granitic rocks. Episodes 19, 120–125.

Pearce, J., Harris, N.B.W., Tindle, A.D., 1984. Trace element discrimination diagrams for the tectonic interpretation of granitic rocks. Journal of Petrology 25, 956–983.

Peccerillo, A., 1985. Roman comagmatic province (central Italy): evidence for subduction-related magma genesis. Geology 13, 103–106.

Rapp, R.P., Watson, E.B., 1995. Dehydration melting of metabasalt at 8–32 kbar: implications for continental growth and crust–mantle recycling. Journal of Petrology 36, 891–931.

Rapp, R.P., Shimizu, N., Norman, M.D., 2003. Growth of early continental crust by partial melting of eclogite. Nature 425, 605–609.

Rogers, N.W., Hawkesworth, C.J., Parker, R.J., Marsh, J.S., 1985. The geochemistry of potassic lavas from Vulsini, central Italy and implications for mantle enrichment processes beneath the Roman region. Contributions to Mineralogy and Petrology 90, 244–257.

Santos, E.J., 1995. O complexo granítico de Lagoa das Pedras: acresção e colisão na região de Floresta (PE), Província Borborema. Unpublished PhD thesis, University of São Paulo, São Paulo, Brazil, 219 pp, (in Portuguese).

Sato, K., Tassinari, C.G., Kawashita, K., Petronilho, L., 1995. O método Geocronológico Sm–Nd no IG/USP e suas aplicações. Anais da Academia Brasileira de Ciências 67 (3), 313–336.

Scaillet, B., Holtz, F., Pichavant, M., 2016. Experimental constraints on the formation of silicic magmas. Elements 12, 109–114.

Sial, A.N., 1986. Granite-types in northeast Brazil: current knowledge. Revista Brasileira de Geociencias 16, 54–72.

Sial, A.N., Ferreira, V.P., 2015. Magma associations in Ediacaran granitoids of the Cachoeirinha–Salgueiro and Alto Pajeú terranes, northeastern Brazil: forty years of studies. Journal of South American Earth Sciences 68, 113–133.

Sial, A.N., Vasconcelos, P.M., Ferreira, V.P., Pessoa, R.R., Brasilino, R.G., Morais Neto, J.M., 2008. Geochronological and mineralogical constraints on depth of emplacement and ascension rates of epidote-bearing magmas from northeastern Brazil. Lithos 105, 225–238.

Silva Filho, A.F., Guimarães, I.P., Van Schmus, W.R., 2002. Crustal evolution of the Pernambuco–Alagoas complex, Borborema Province, NE Brazil: Nd isotopic data from neoproterozoic granitoids. Godwana Research 5, 409–422.

Silva Filho, A.F., Guimarães, I.P., Ferreira, V.P., Armstrong, R., Sial, A.N., 2010. Ediacaran Águas Belas pluton, northeastern Brazil: evidence on age, emplacement and magma sources during Gondwana amalgamation. Gondwana Research 17, 676–687.

Silva Filho, A.F., Guimarães, I.P., Van Schmus, W.R., Dantas, E.L., Armstrong, R., Cocentino, L.M., Lima, D.R., 2013. Long-lived Neoproterozoic high-K magmatism in the Pernambuco–Alagoas domain, Borborema Province, Northeast Brazil. International Geology Review 55, 1280–1299.

Silva Filho, A.F., Guimarães, I.P., Van Schmus, W.R., Armstrong, R., Silva, J.M.R., Cocentino, L.M., Osako, L.S., 2014. SHRIMP U–Pb zircon geochronology and Nd signatures of supracrustal sequences and orthogneisses constrain the Neoproterozoic evolution of the Pernambuco–Alagoas domain, southern part of Borborema Province, NE Brazil. International Journal of Earth Sciences (Geol Rundsch) 103, 2155–2190.

Silva Filho, A.F., Guimarães, I.P., Santos, L., Armstrong, R., Van Schmus, W.R., 2016. Geochemistry, U–Pb geochronology, Sm–Nd and O isotopes of ca. 50 Ma long Ediacaran high-K syn-collisional magmatism in the Pernambuco–Alagoas domain, Borborema Province, NE Brazil. Journal of South American Earth Sciences 68, 134–154.

Silva, L.C., Armstrong, R., Pimentel, M.M., Scandolara, J., Ramgrab, G., Wildner, W., Angelim, L.A.A., Vasconcelos, A.M., Rizzoto, G., Quadros, M.L.E.S., Sander, A., Rosa, A.L.Z., 2002. Reavaliação da evolução geológica em terrenos pré-cambrianos brasileiros com base em novos dados U–Pb SHRIMP, Parte III: Províncias Borborema, Mantiqueira meridional e Rio Negro-Juruena. Revista Brasileira de Geociencias 32, 529–544.

Silva, T.R., Ferreira, V.P., Lima, M.M.C., Sial, A.N., Silva, J.M.R., 2015. Synkinematic emplacement of the magmatic epidote bearing Major Isidoro tonalite-granite batholith: relicts of an Ediacaran continental arc in the Pernambuco–Alagoas domain, Borborema Province, NE Brazil. Journal of South American Earth Sciences 64, 1–13.

Sisson, T., Ratajeski, K., Hankins, W., Glazner, A., 2005. Voluminous granitic magmas from common basaltic sources. Contributions to Mineralogy and Petrology 148, 635–661.

Thompson, R.N., 1982. Magmatism of the British tertiary volcanic province. Scottish Journal of Geology 18, 50–107.

Trompette, R., 1997. Neoproterozoic (~600 Ma) aggregation of western Gondwana: a tentative scenario. Precambrian Research 82, 101–112.

Valley, J.W., Chiarenzelli, J.R., McLelland, J.M., 1994. Oxygen isotope geochemistry of zircon. Earth and Planetary Science Letters 126, 187–206.

Valley, J.W., Kitchen, N.E., Kohn, M.J., Niendorf, C.R., Spicuzza, M.J., 1995. UWG-2, a garnet standard for oxygen isotope ratio: strategies for high precision and accuracy with laser heating. Geochimica et Cosmochimica Acta 59, 5223–5231.

Valley, J.W., Kinny, P.D., Schulze, D.J., Spicuzza, M.J., 1998. Zircon megacrysts from kimberlite: oxygen isotope variability among mantle melts. Contributions to Mineralogy and Petrology 133, 1–11.

Valley, J.W., Bindeman, I.N., Peck, W.H., 2003. Calibration of oxygen isotope fractionations in zircon. Geochimica et Cosmochimica Acta 67, 3257–3266.

Valley, J.W., Lackey, J.S., Cavosie, A.J., Clechenko, A., Spicuzza, M.J., Basei, M.A.S., Bindeman, I.N., Ferreira, V.P., Sial, A.N., King, E.M., Peck, W.H., Sinha, A.K., Wei, C., 2005. 4.4 billion years of crustal maturation from oxygen isotope ratios of zircon. Contributions to Mineralogy and Petrology 15, 561–580.

Van Schmus, W.R., Brito Neves, B.B., Hackspacher, P.C., Babinsky, M., 1995. U/Pb and Sm/Nd geochronologic studies of the eastern Borborema Province, NE Brazil. Journal of South American Earth Sciences 8, 267–288.

Van Schmus, W.R., Oliveira, E.P., Silva Filho, A.F., Toteu, S.F., Penaye, J., Guimarães, I.P., 2008. Proterozoic links between the Borborema Province, NE Brazil and the Central African Fold Belt. Geological Society, London, Special Publications 294, 69–99.

Weinberg, R.F., Sial, A.N., Mariano, G., 2004. Close spatial relationship between plutons and shear zones. Geology 32, 377–380.

Weinberg, R.F., Sial, A.N., Mariano, G., 2005. Close spatial relationship between plutons and shear zones: comment and reply: REPLY. Geology 33, e74. http://dx.doi.org/10.1130/0091-7613-33.1.e73.

Whitney, D.L., Evans, B.W., 2010. Abbreviations for names of rock-forming minerals. American Mineralogist 95, 185–187.

Williams, I.S., 1998. U–Th–Pb geochronology by ion microprobe. In: McKibben, M.A., Shanks, W.C., Ridley, W.I. (Eds.), In Applications of Microanalytical Techniques to Understanding Mineralizing Processes: Reviews in Economic Geology 7, pp. 1–35.

Williams, I.S., Claesson, S., 1987. Isotopic evidence for the Precambrian provenance and Caledonian metamorphism of high grade paragneisses from the Seve Nappes, Scandinavian Caledonides II. Ion microprobe zircon U–Pb–Th. Contributions to Mineralogy and Petrology 97, 205–217.

Wilson, M., 1989. Igneous Petrogenesis: a Global Tectonic Approach. Unwin Hyman, London (466 pp.).

Wones, D.R., 1989. Significance of the assemblage titanite + magnetite + quartz in granitic rocks. American Mineralogist 74, 744–749.

Zen, E.-a., Hammarstrom, J.M., 1984. Magmatic epidote and its petrologic significance. Geology 12, 515–518.

IJES-D-1….: Submission Confirmation for Isotope evidence for mantle-derived source rock of high-K calc-alkaline granites,...
Yahoo/Entrada

From: Editorial Office, IJES <em@editorialmanager.com>

To: Thyego Roberto da Silva

5 de dez de 2017 às 17:16

Dear Dr Silva,

Your submission entitled "Isotope evidence for mantle-derived source rock of high-K calc-alkaline granites, Pernambuco-Alagoas Domain, northeastern Brazil" has been received by journal International Journal of Earth Sciences

The submission id is: IJES-D-1…

Please refer to this number in any future correspondence.

You will be able to check on the progress of your paper by logging on to Editorial Manager as an author. The URL is http://ijes.edmgr.com/.

Thank you for submitting your work to this journal.

Kind regards,

International Journal of Earth Sciences

Now that your article will undergo the editorial and peer review process, it is the right time to think about publishing your article as open access. With open access your article will become freely available to anyone worldwide and you will easily comply with open access mandates. Springer's open access offering for this journal is called Open Choice (find more information on www.springer.com/openchoice). Once your article is accepted, you will be offered the option to publish through open access. So you might want to talk to your institution and funder now to see how payment could be organized; for an overview of available open access funding please go to www.springer.com/oafunding.

Although for now you don't have to do anything, we would like to let you know about your upcoming options.

6 ISOTOPE EVIDENCE FOR MANTLE-DERIVED SOURCE ROCK OF HIGH-K CALC-ALKALINE GRANITES, PERNAMBUCO–ALAGOAS DOMAIN, NORTHEASTERN BRAZIL (submitted to International Journal of Earth Sciences)

Thyego R. Silva*, Valderez P. Ferreira, Mariucha Maria C. Lima, Alcides N. Sial
NEG–LABISE, Department of Geology, Federal University of Pernambuco, Recife, PE, Brazil

---

ABSTRACT

We report whole-rock major, trace, mineral and isotope chemistries of the Jacaré dos Homens, and Santo Antonio granites from the Águas Belas–Canindé batholith, Pernambuco–Alagoas Domain, northeastern Brazil. These rocks exhibit low-angle foliation, suggesting emplacement under a regional strain field, associated with transpressive deformation. Both plutons are dominantly made up of K-feldspar, quartz, and plagioclase with biotite as the main mafic phase and minor hornblende. The Jacaré dos Homens pluton (642.4 ± 3 Ma) displays magnesian, slightly peraluminous and alkali-calcic character while the Santo Antonio granite (636.1 ± 4 Ma) is magnesian, metaluminous to slightly-moderately peraluminous and alkali-calcic. These two plutons are enriched in alkalis (up to 10.28 wt.%), Mg#, Rb, Ba, Sr, Th and LREE, and depleted in HFSE, with distinct Nb, Ta, and Ti depletion. The isotope data for the Jacaré dos Homens pluton yielded an Nd-model age of 1.21 Ga with slightly negative $\varepsilon Nd_{(642\ Ma)}$ of −1.58, initial $^{87}Sr/^{86}Sr$ ratios of 0.7068, and $\delta^{18}O$ (zircon) value of +7.0‰ $_{VSMOW}$. The isotope data for Santo Antonio pluton yielded Nd-model ages from 0.96 to 1.05 Ga, with $\varepsilon Nd_{(636\ Ma)}$ from +1.17 to −0.67, initial $^{87}Sr/^{86}Sr$ ratios from 0.7050 to 0.7052, and $\delta^{18}O$ (zircon) value of + 5.0 to 5.9‰ $_{VSMOW.}$ Altogether, the petrological, geochemical and isotopic data are consistent with the hypothesis that the studied granitoids were derived from basaltic lower crust of Stenian/Tonian (Jacaré dos Homens) or Tonian (Santo Antonio) ages. We envisage that partial melting was triggered by the uplift of asthenosphere and underplating of lithospheric mantle. After generation at depth, granite magmas evolved by fractional crystallization; the buoyancy-driven ascent to their present level was favored by shear zone.

Keywords: high-K calc-alkaline magmatism; basaltic-source rocks; U–Pb ages; Sr–Nd–O isotopes; northeastern Brazil

---

* Corresponding author: NEG–LABISE, Dept. of Geology, Av. da Arquitetura s/n, Cidade Universitária, Recife, PE, 50740-550, Brazil; phone/fax: +55 81 2126 8243; e-mail: rthyego@yahoo.com

INTRODUCTION

Widespread emplacement of Neoproterozoic–Cambrian granitoids, many of them associated with a network of E–W and NE–SW shear zones, marked the Brasiliano orogeny in the Borborema Province (e.g. VAUCHEZ et al. 1995; FERREIRA et al. 1998, 2004; GUIMARÃES et al. 2004). Structural, geochemical, and geochronological data of granitoids from the Borborema Province allow their classification into four main groups (FERREIRA et al. 2004; BRITO NEVES et al. 2000; GANADE DE ARAUJO et al. 2014; GUIMARÃES et al. 2011; NEVES et al. 2015; VAN SCHMUS et al. 2011; and references therein): (I) Calc-alkaline to high-K calc-alkaline I-type granitoids with ages that vary from 640 to 610 Ma (mostly with t_{DM} ages from 1.0–1.5 and $\varepsilon Nd_{(t)}$ varying from −2 to −14) , emplaced during compressional deformation; (II) Calc-alkaline and shoshonitic granitoids with ages ranging from 595 to 575 Ma (t_{DM} ages varying from 1.7–2.2 with $\varepsilon Nd_{(t)}$ = −10 to −20), related to the main period of transcurrence; (III) Alkaline and shoshonitic post-transcurrent granitoids with ages that range from 573 to 550 Ma (t_{DM} ages from 1.9–2.6 with $\varepsilon Nd_{(t)}$ = −14 to −25), marking the period of relaxation after collision; and (IV) A-type post-orogenic extension-related granitoids with ages ranging from 540 to 510 Ma (t_{DM} ages from 2.0–2.5 with $\varepsilon Nd_{(t)}$ = −17 to −20), associated to the subvolcanic bimodal magmatism.

High-K, calc-alkaline I-type granitoids (group I) abound in the Borborema Province, especially in the Pernambuco–Alagoas Domain (SILVA FILHO et al. 2002, 2013, 2014, 2016; SILVA et al. 2015, 2016). Their magmatic emplacement could have been post-collisional in a decompressional regime associated with crustal thinning (e.g. BONIN et al. 1998; LIÉGEOIS et al. 1998), or in a compressional regime associated with crustal thickening (e.g. BONIN 1990; BARBARIN 1999). We shall establish that in the Pernambuco–Alagoas Domain, the latter scenario is more likely.

In this study, we combine geology, major, trace and isotope chemistry to constrain the sources of two high-K granitoids of the Águas Belas–Canindé batholith in the Pernambuco–Alagoas Domain, and discuss the role of melting conditions and fractional crystallization process. This study concerns the Jacaré dos Homens and Santo Antonio granitic plutons, emplaced next to the boundary between the Pernambuco–Alagoas and Sergipano terranes, which have preserved information on the timing and convergence

between them.

GEOLOGIC SETTING

In the traditional concept, the Borborema Province (ALMEIDA et al. 1981) is subdivided into domains separated by major shear zones. Currently, six crustal segments are recognized (VAN SCHMUS et al. 2008 and references therein) (Fig. 1a). This study focuses one part of the Pernambuco–Alagoas segment (Fig. 1b).

In the Pernambuco–Alagoas Domain, large granitic batholiths (BRITO NEVES et al. 2000; SILVA FILHO et al. 2002, 2013) are emplaced into basement consisting of orthogneiss and high-grade, commonly migmatized metasedimentary rocks. The Buíque–Paulo Afonso, Águas Belas–Canindé, Marimbondo–Correntes, Ipojuca–Atalaia, and Garanhuns batholiths, each consisting of various plutons, are of Neoproterozoic–Cambrian age (SILVA FILHO et al. 2002).

VAN SCHMUS et al. (2008) proposed five distinct model age subdivisions for the Pernambuco–Alagoas Domain, as follows: (1) t_{DM} older than 2.40 Ga, represented by several local occurrences of gneisses and migmatites, (2) t_{DM} between 2.00 and 2.20 Ga, represented by large areas in the northeastern half of the Pernambuco–Alagoas Domain, (3) t_{DM} between 1.70 and 2.00 Ga, represented by several plutons in the northeastern corner of the domain, (4) t_{DM} between 1.20 and 1.50 Ga, represented by large parts of the southwestern half of the Pernambuco–Alagoas Domain and (5) t_{DM} between 0.90 and 1.20 Ga, represented mainly by the Buique–Paulo Afonso and Águas Belas–Canindé batholiths. Based on new Sm–Nd isotopic data from granitoids, orthogneisses, and supracrustal rocks, SILVA FILHO et al. (2014) proposed a further subdivision of the Pernambuco–Alagoas Domain into the Garanhuns, Água Branca, and Palmares sub-domains. In the Garanhuns sub-domain in the north, rocks are derived predominately from older crustal sources, whereas in the Água Branca and Palmares sub-domains in the south, rocks derived mostly from substantially younger sources.

Large granitoid intrusions in the Pernambuco–Alagoas Domain are mainly shoshonitic (BRITO et al. 2009; FERREIRA et al. 2015; SILVA FILHO et al. 2013, 2016), and calc-alkaline to high-K calc-alkaline (NEVES et al. 2008, 2012, 2015; SILVA FILHO et al. 2010, 2013, 2014, 2016; SILVA et al. 2015, 2016).

U–Pb crystallization ages of zircon lie in the 636 to 572 Ma time interval that can be classified into two groups (e.g. SILVA FILHO et al. 2013): (i) older plutons between 636 and 610 Ma whose Nd t_{DM} model ages range from 1.0 to 2.04 Ga, mostly < 1.5 Ga,

and (ii) younger plutons between 592 and 572 Ma whose Nd t_{DM} model ages range from 1.74 to 2.18 Ga.

GEOLOGY AND PETROGRAPHY

Jacaré dos Homens pluton

The Jacaré dos Homens orthogneiss is an NE-striking elongate pluton emplaced and deformed along a shear zone of the same name that divides the Pernambuco–Alagoas from the Sergipano Domain. This orthogneiss is a coarse-grained, granodioritic to granitic, equigranular to augen gneiss (Fig. 2a–d), locally displaying a facies with alternately mafic-and felsic-rich layers (Fig. 2a). Potassic feldspar porphyroclasts are up to 3 cm long. The layering exhibits low to moderate dip (Fig. 2a); shear criteria suggest top-to-the-southeast tectonic transport (Fig. 2b), and slightly asymmetric potassic feldspar porphyroclasts indicate sinistral shear. In places, a northwest-plunging stretching lineation is better developed than the foliation (Fig. 2c). Mafic magmatic enclaves (MME), of dioritic composition, are relatively abundant showing pseudo-rapakivi structures (Fig. 2d), and field relationships with the host granodiorite suggest sustained coexistence of magmas, with local mixing and mingling. The modal composition includes potassic feldspar, plagioclase, quartz, biotite, and titanite, amphibole, allanite, apatite, opaque minerals, epidote, and zircon. Anhedral to subhedral plagioclase occurs with variable sericitization commonly contains minor inclusions of biotite, apatite, zircon, and opaque minerals. Anhedral to subhedral coarse-grained perthitic microcline porphyroclasts with typical cross-hatched twinning, and anhedral quartz crystals contain inclusions of biotite and opaque minerals. Mild solid-state deformation created chessboard extinction in quartz, and myrmekitic intergrowths around potassic feldspar. Pleochroic anhedral to subhedral biotite contains inclusions of apatite, allanite, titanite, and opaque minerals, and biotite together with pleochroic anhedral to subhedral green amphibole define the foliation. Titanite occurs as slightly pleochroic subhedral crystals, up to a few millimeters long, and as secondary fine-grained crystals associated with biotite and opaque minerals. Epidote occurs as anhedral to subhedral grains as low-grade alteration products of plagioclase and biotite. Euhedral allanite, apatite, and zircon crystals may be isolated, or be included in other minerals.

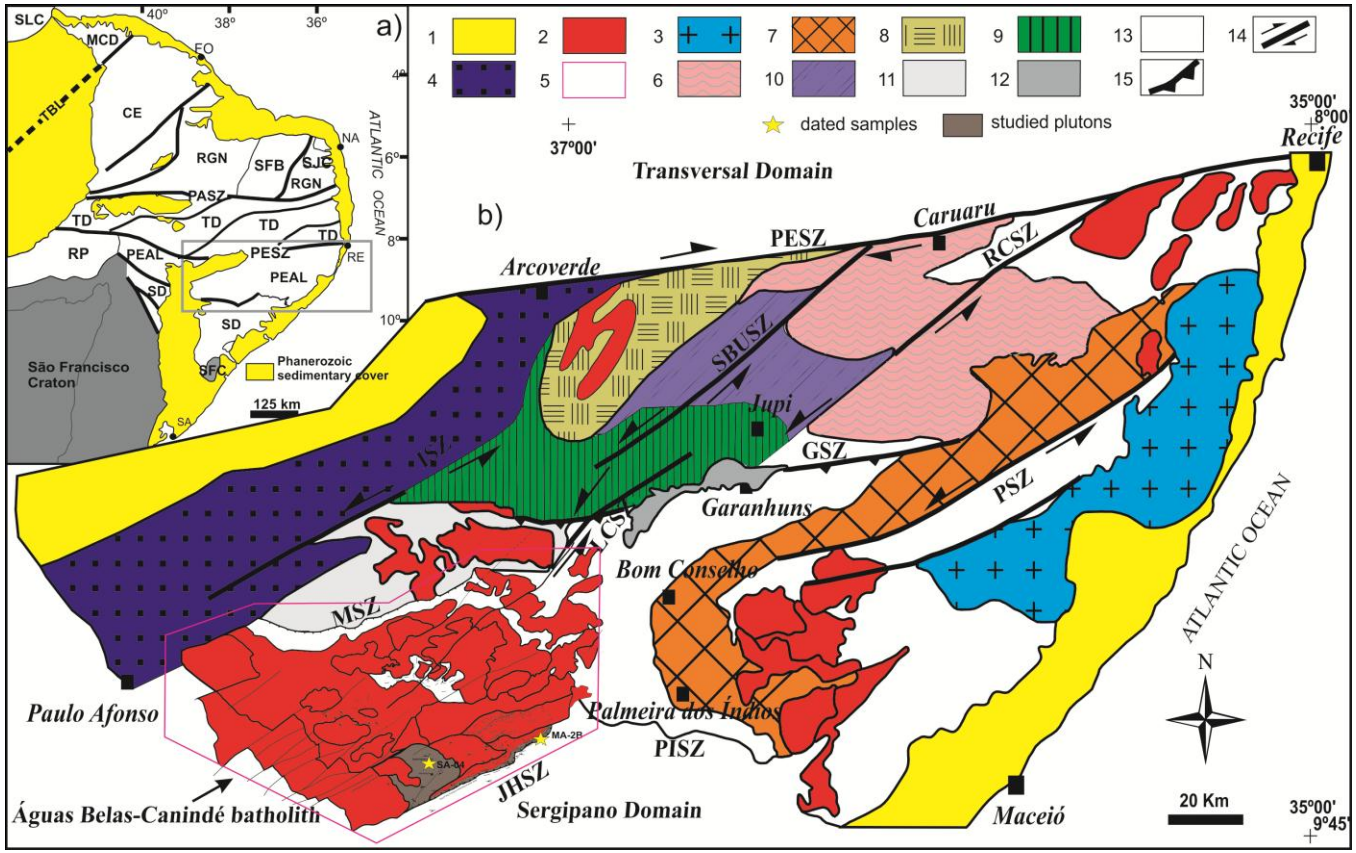

Figure 1. (a) Borborema Province. Major domains: MCD - Médio Coreaú; CE - Ceará; RGN - Rio Grande do Norte (SFB - Seridó Fold Belt; SJC - São José do Campestre Archaean nucleus); TD - Transversal; PEAL - Pernambuco–Alagoas; RP - Riacho do Pontal; SD - Sergipano; SFC - São Francisco Craton; SLC - São Luís Craton; Faults and shear zones: PASZ - Patos shear zone; PESZ - Pernambuco shear zone; TBL - Transbrasiliano Lineament. Cities and towns: Fo - Fortaleza; Na - Natal; Re - Recife; Sa - Salvador (VAN SCHMUS et al. 2008). (b) Geologic map of the Pernambuco–Alagoas Domain. 1 - Phanerozoic sedimentary cover; 2 – other Brasiliano granitoids; 3 - Ipojuca–Atalaia batholith; 4 - Buíque–Paulo Afonso batholith; 5 - Águas Belas–Canindé batholith; 6 - Granitoids and orthognaisses; 7 - Palmares Sequence; 8 - Rio Una (Unit 1) Sequence; 9 - Rio Una (Unit 2) Sequence; 10 - Rio Una (Unit 3) Sequence; 11 - Inhapi Sequence; 12 - Garanhuns quartzites; 13 - basement-migmatites; 14 - transcurrent shear zones (PESZ - Pernambuco; RCSZ - Rio da Chata; PSZ - Palmares; LCSZ - Limitão-Caetés; ISZ - Itaíba; SBUSZ - São Bento do Una); 15 - compressive shear zones (GSZ - Garanhuns; MSZ - Maravilha; ZCJH - Jacaré dos Homens; PISZ – Palmeira dos Índios) (modified from SILVA FILHO et al. 2002, 2010, 2014).

Santo Antonio granite

The Santo Antonio granitic pluton is bounded on the south by the Jacaré dos Homens transpressional shear zone, to the east it is in sharp contact with the Monteirópolis pluton (SILVA et al. 2016), to the west with the Serra do Catú batholith (BRITO et al. 2009; SILVA FILHO et al. 2013, 2016), and to the north with other Neoproterozoic granitic plutons of the Águas Belas–Canindé batholith (Fig. 2b). Santo Antonio is a leucocratic, fine- to medium-grained biotite granite. It contains amphibole-rich clots up to a few decimeters long, and diorite enclaves that show occasional crenulate to lobate contacts with the host granite, with partly digested boundaries. Fine-grained quartz-feldspar E–W trending dikes cut the pluton. The Santo Antonio pluton also shows a low-angle magmatic, mafic-felsic foliation and shape-preferred orientation of potassic feldspar and aggregates of biotite. Essential minerals are quartz, alkali feldspar, plagioclase, and biotite, with accessory titanite, amphibole, apatite, zircon, epidote, and opaque minerals. Biotite and plagioclase manifest some weathering and low temperature (subsolidus) alteration into chlorite, muscovite, and epidote. Anhedral quartz shows chessboard extinction. Subhedral plagioclase, with typical polysynthetic twinning, exhibits variable degrees of sericitization. Potassic feldspar, with Carlsbad twinning, exhibits coarse perthitic texture. Myrmekite intergrowths are common. Epidote occurs with both secondary and primary textural relationships.

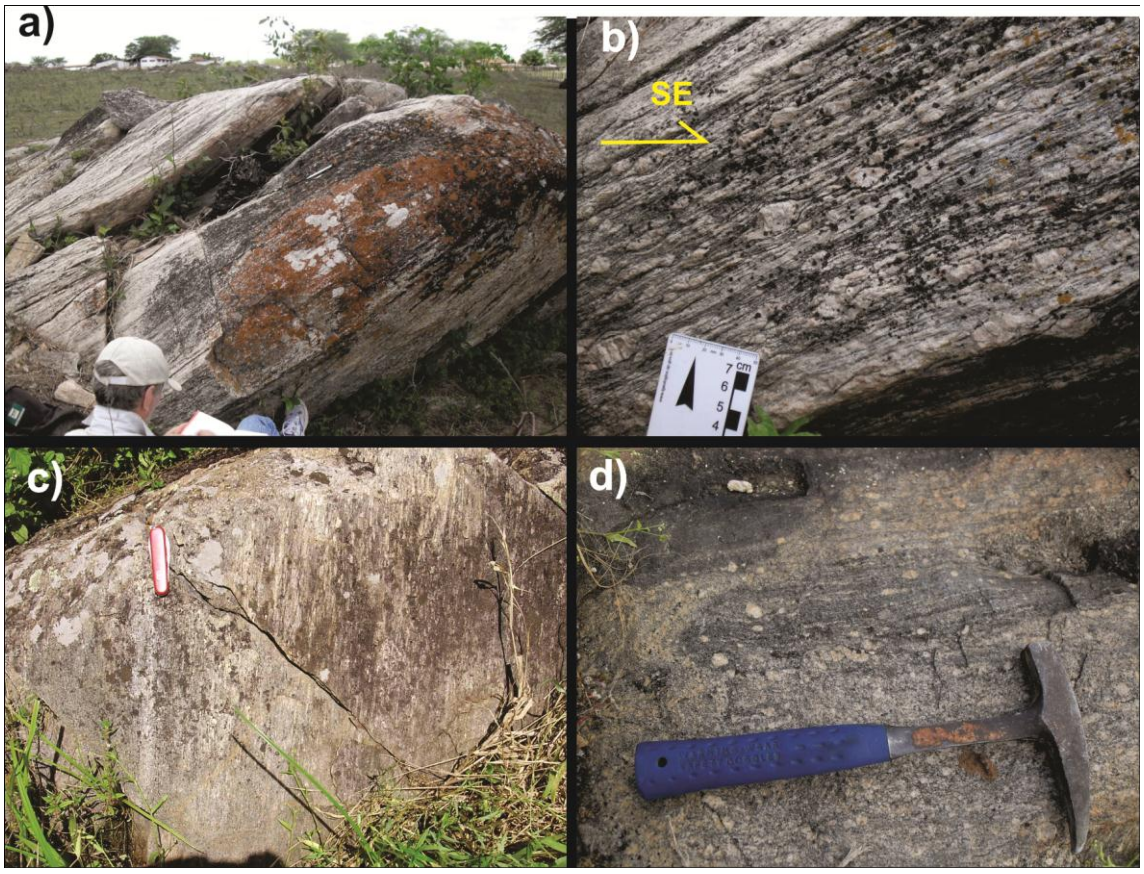

Figure 2. Field and structural aspects of the Jacaré dos Homens orthogneiss: (a) Hornblende-biotite granite augen gneiss with subhorizontal foliation. (b) K-feldspar porphyroclasts indicating top-to-the-SE tectonic transport. (c) Subhorizontal foliation with stretching lineation (parallel to the pocket knife). (d) Mixing of felsic and mafic magmas, with pseudo-rapakivi structures in feldspars.

ANALYTICAL PROCEDURES

Whole-rock major and some trace element chemical analyses were performed by X-ray fluorescence (XRF) with a fully automated Rigaku RIX-3000 XRF spectrometer at the NEG–LABISE, Federal University of Pernambuco, Recife, Brazil, by the calibration-curves method prepared using certified reference standards. Rare-earth element analyses were done by ICP-OES at the SGS-Geosol Laboratory, Belo Horizonte, Brazil. Table 1 lists representative whole-rock chemical analyses. Mineral chemistry analyses were performed at the Electron Microprobe Laboratory, University of Brasilia, Brazil, using a Superprobe JEOL JXA-8230 equipped with WDS, with a current of 10 ηA and 15Kv, with a 5μ diameter beam. Counting times were 10s on peak and 5s on background for all elements. Tables 2 and 3 contain some representative chemical analyses.

Zircon grains were separated from the whole-rock sample using standard crushing, sieving, and heavy liquid methods. Heavy mineral concentrates were subsequently processed by magnetic separation on a Frantz isodynamic separator at the NEG–

LABISE. Zircon samples were cleaned in cold hydrofluoric acid, and then cold sulfuric acid, and hot nitric acid if sulfides were present. This procedure has been shown to remove mineral impurities and radiation-damaged zircons without altering $\delta^{18}O$ of the residual zircon (KING et al. 1998; VALLEY et al. 1994). Representative zircon grains were hand-picked from the non-magnetic fraction under a binocular microscope, and were placed onto double-sided tape and mounted together with chips of reference zircons in epoxy disks, ground to half thickness, and polished with 3 μm and 1 μm diamond paste in order to expose the internal structure. A conductive gold-coating was applied just prior to analysis. The grains were photographed in reflected and transmitted light, and cathodoluminescence (CL) images were produced by scanning electron microscope to reveal the internal structures of the zircon crystals, to characterize different populations, and to ensure that an analyzed spot was wholly within a zone of a single age. The analyses were carried out on the SHRIMP IIe at the University of São Paulo, following the SATO et al. (2014) analytical procedures. Abundances of U, Th, and Pb, and Pb isotope ratios were normalized using the SL13 zircon standard (U=238 ppm; WILLIAMS 1998). Correction for common Pb was made using measured ^{204}Pb. U–Pb isotope ratios were collected in sets of five scans throughout the masses, and the TEMORA 2 reference zircon ($^{206}Pb/^{238}U$ age = 416.8 ± 0.3 Ma; BLACK et al. 2004) was measured after every third analysis of an unknown. Errors in the isotopic ratios and ages are quoted at a ± 1 sigma level. Data reduction was performed using SQUID/Excel macro (LUDWIG 2009). See Tables 4 and 5.

Sr and Nd isotopic compositions were determined according to analytical procedures described by KAWASHITA (1972) and SATO et al. (1995), using a Thermo-Finnigan TRITON thermal ionization mass spectrometer (TIMS). Sm was determined using a Thermo-Finnigan MAT 262 thermal ionization mass spectrometer (TIMS). The replicate analyses of $^{87}Sr/^{86}Sr$ for the NBS987 standard gave a mean value of 0.710237 ± 0.000014 (2σ). Laboratory blanks for the chemical procedure, during the period of analyses, yielded maximum values of 109 pg for Sr, 0.4 ng for Nd and 0.7 ng for Sm. The averages of $^{143}Nd/^{144}Nd$ for La Jolla and BCR-1 standards were 0.511847 ± 0.00005 (2σ) and 0.512662 ± 0.00005 (2σ), respectively. Table 6 lists whole-rock Rb–Sr and Sm–Nd isotope data.

Oxygen isotope ratios of 2–3 mg of zircon grains were determined at the NEG–LABISE, using a Delta V Advantage Thermo-Finningan mass spectrometer. Precision is better than ±0.1‰. Oxygen was liberated in a CO_2 laser-based extraction line by

reaction with BrF_5, reacted with hot graphite, and converted into CO_2 for mass spectrometer analysis following procedures described by VALLEY et al. (1995).

ANALYTICAL RESULTS

Whole-rock geochemistry

The Jacaré dos Homens pluton shows SiO_2 concentrations ranging from 61.19 to 69.23 wt.%. They display high K_2O contents (3.12–5.10 wt.%) and high $Na_2O + K_2O$ (7.58–8.46 wt.%) and intermediate Mg# (32–42). Granites of the Santo Antonio pluton show SiO_2 ranging from 60.55 to 74.92 wt.%. In Harker diagrams, SiO_2 correlates with major- and trace-elements for the Santo Antonio granites (Fig. 3 and 4), negative trends with large negative values of correlation coefficient (r) are observed, and point to a single-stage process (ROLLINSON 1993). These high-K calc-alkaline granites show higher K_2O contents (3.66 to 5.96 wt.%), and high total alkali contents (7.69 to 10.28 wt.%) and K_2O/Na_2O (0.68 to 1.40) that are typical for I-type granitoids: (0.4–1.7; CHAPPELL 1999; GREEN & ADAM 2002). Zr/Hf (28 to 43) is similar to primitive mantle (36; SUN & MCDONOUGH 1989), and Th/U (3 to 13) are generally higher than in either primitive mantle or continental crust (RUDNICK & FOUNTAIN 1995), suggesting that the source contains continental crustal material.

The Jacaré dos Homens rocks are magnesian, alkali-calcic, and slightly peraluminous while the Santo Antonio granites are magnesian, and alkali-calcic to alkalic, according to the FROST et al. (2001) classification, characteristics that are consistent with high-K calc-alkaline rocks, and metaluminous to slightly-peraluminous. The association of magnesian nature with alkali-calcic composition corresponds to granitoids that formed either in arc or post-collisional environments (FROST & FROST 2008).

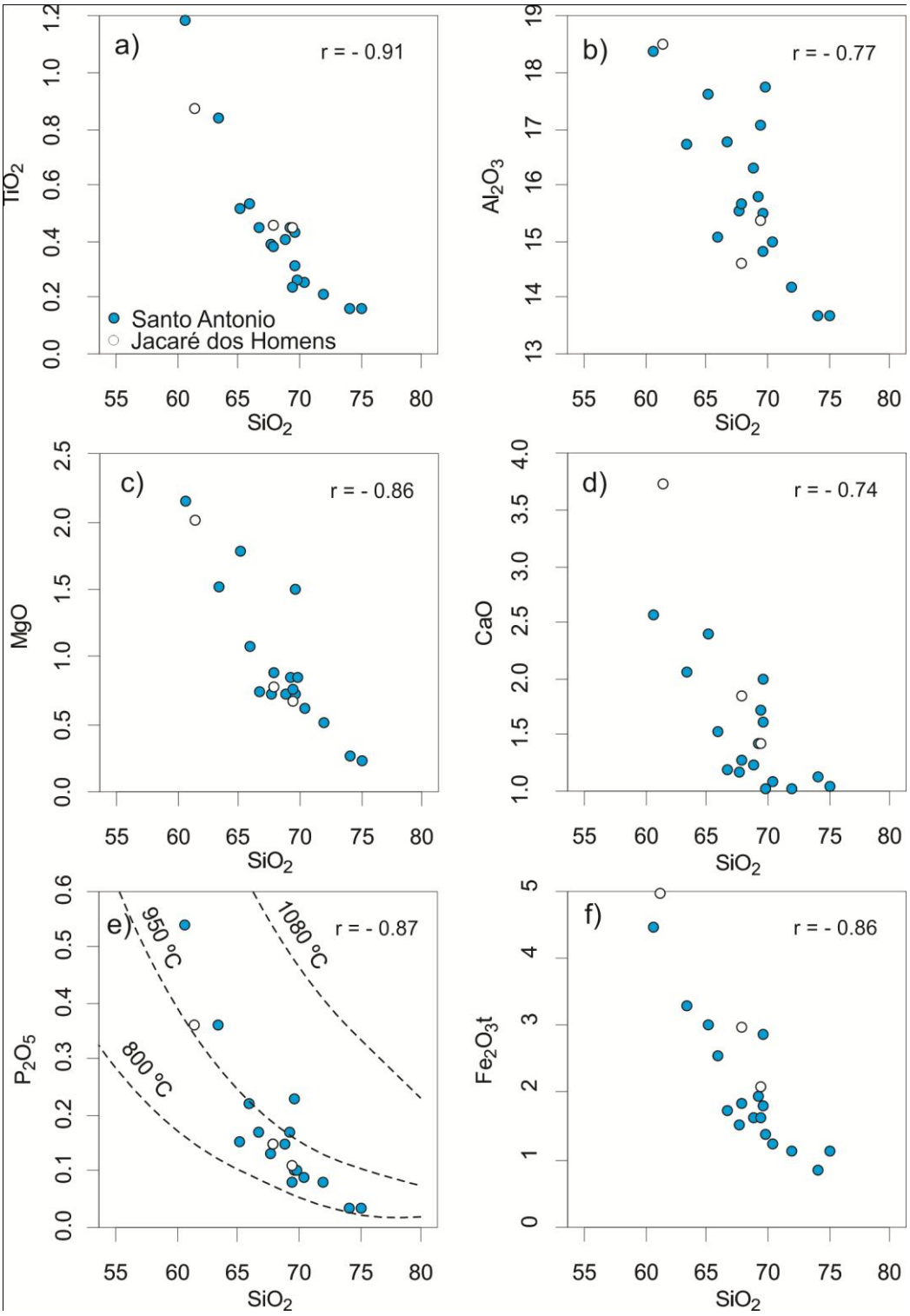

Figure 3. Oxide Harker diagrams of the studied samples. Dashed lines in the P_2O_5 versus SiO_2 plot correspond to isotherms as proposed by GREEN & WATSON (1982) at P = 7.5 kb. Data for experimentally-determined pure crustal partial melts from: RAPP & WATSON (1995) (low-K basaltic rocks at 8–16 kbar and 1000–1050 °C), and PATIÑO DOUCE & JOHNSTON (1991) (pelitic rocks at 7–13 kbar and 825–950 °C). Symbols are the same for the following figures.

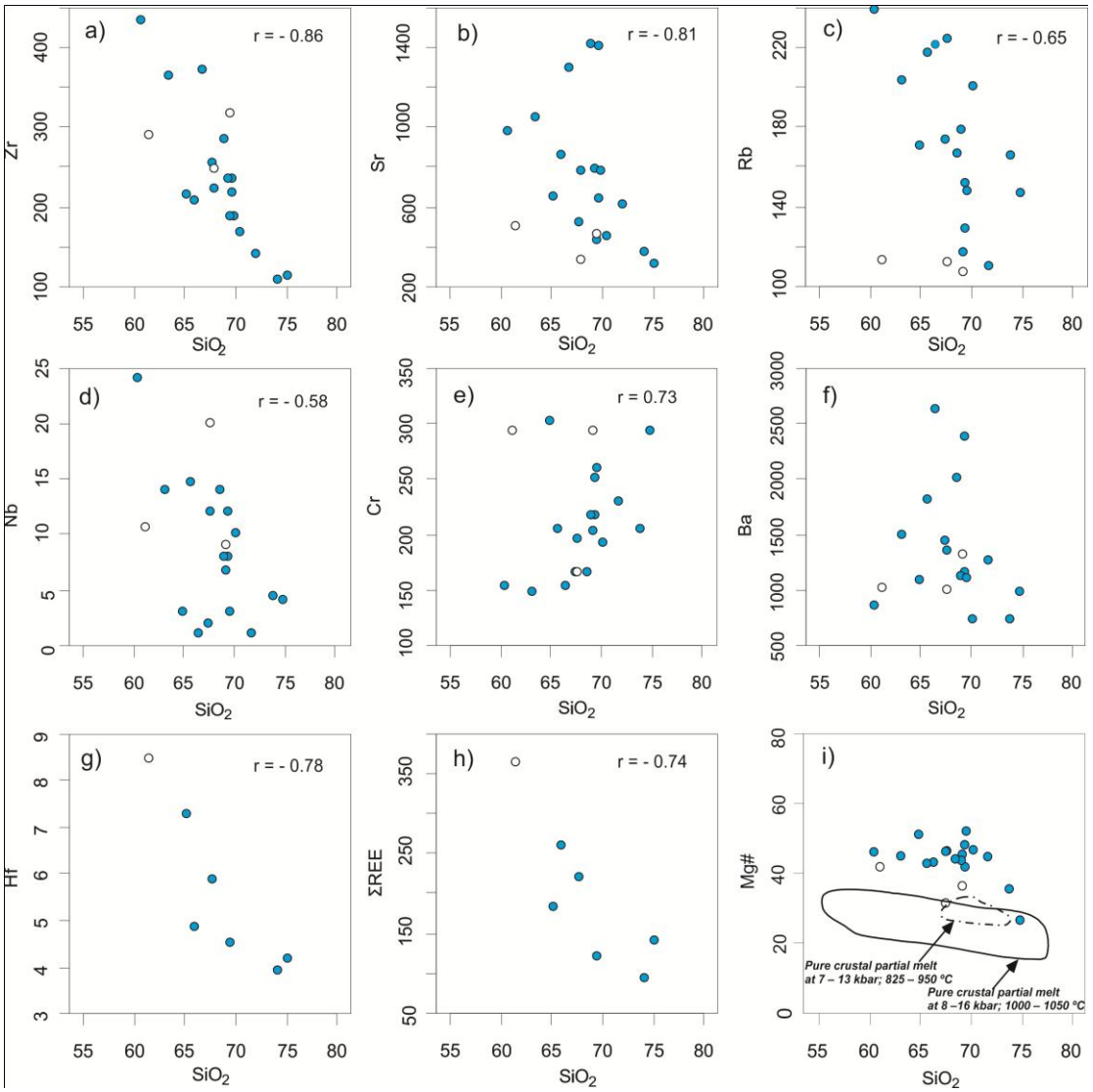

Figure 4. Trace elements Harker diagrams of the studied samples. In the calculated Cr and Sr correlation coefficients (r) sample SA–04, and samples SA–02, SA–13 and SA–33, respectively, were excluded.

Rare earth element (REE) concentrations, normalized to primitive mantle (MCDONOUGH & SUN 1995), show slight relative enrichment of light rare earth elements (LREE) more pronounced for the Santo Antonio pluton (La_N/Yb_N = 19.25–101.57) than for the Jacaré dos Homens pluton (La_N/Yb_N= 10.06). Eu/Eu* hovers slightly negative or positive in both plutons (Fig. 5a). Incompatible-element variation diagrams exhibit deep Nb–Ta and Ti troughs for the Santo Antonio pluton, negative Nb, Ta, Ti and Sr for the Jacaré dos Homens pluton and positive Rb–Th anomalies (Fig. 5b). The pronounced Nb, Ta, and Ti anomalies are similar to those of magmatic arc (e.g. CONDIE & KRÖNER 2013), and we interpret them as product of subduction zone fluids that affected the original basaltic source rocks. Enrichment in large-ion lithophile elements (LILE) relative to high field strength elements (HFSE) is a general characteristic of calc-alkaline granitoids.

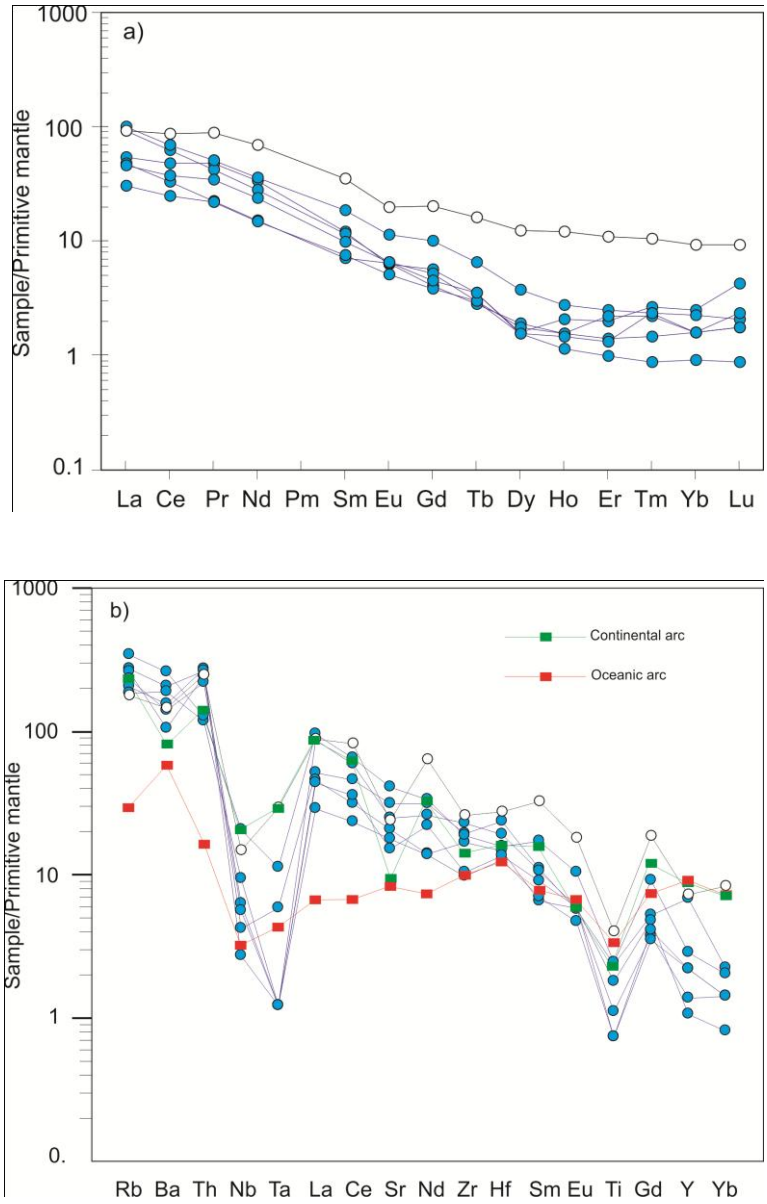

Figure 5. (a) Primitive mantle-normalized rare earth elements (normalization values are from MCDONOUGH & SUN 1995). (b) Primitive mantle-normalized incompatible-element abundances. (normalization values are from SUN & MCDONOUGH 1989). Continental and oceanic arcs are after CONDIE & KRÖNER (2013).

Table 1. Geochemical data of the Santo Antonio (SA) and Jacaré dos Homens (JH) plutons, and temperature estimates from zircon (TZr) and apatite (TAp) saturation thermometry.

Sample	SA–04	SA–02	SA–13	SA–33	SA–36	SA–39	SA–43	SA–43.2	SA–44	SA–48	SA–55	SA–59	SA–61	SA–77	SA–78	SA–104	SA–105	SZ–24	SZ–10	MA–2B
Rock type	SA	SA	SA	SA	SA	AS	SA	SA	SA	SA	SA	SA	SA	SA	SA	SA	SA	JH	JH	JH
SiO_2	64.98	69.48	66.43	68.56	69.43	67.53	60.55	69.06	70.24	69.64	63.22	69.23	71.74	65.77	67.73	73.84	74.92	69.23	61.19	67.6
TiO_2	0.52	0.43	0.45	0.41	0.31	0.39	1.19	0.45	0.25	0.26	0.84	0.24	0.21	0.53	0.38	0.16	0.16	0.45	0.87	0.46
Al_2O_3	17.62	15.52	16.79	16.29	14.83	15.54	18.4	15.79	15	17.77	16.74	17.05	14.2	15.09	15.69	13.69	13.67	15.39	18.52	14.62
Fe_2O_3t	3.36	3.18	1.92	1.81	2	1.68	4.96	2.16	1.38	1.52	3.66	1.8	1.24	2.82	2.04	0.93	1.26	2.31	5.55	3.31
MnO	0.09	0.05	0.02	0.02	0.03	0.02	0.09	0.03	0.03	0.03	0.06	0.05	0.01	0.04	0.03	0.02	0.02	0.05	0.1	0.07
MgO	1.79	1.5	0.74	0.72	0.73	0.73	2.15	0.85	0.61	0.84	1.52	0.76	0.51	1.08	0.89	0.26	0.23	0.67	2.02	0.77
CaO	2.39	1.99	1.19	1.24	1.61	1.16	2.56	1.43	1.09	1.02	2.07	1.71	1.03	1.54	1.28	1.12	1.05	1.42	3.74	1.85
Na_2O	4.03	5.08	4.54	4.32	4.05	4.57	5.81	5.32	4.63	4.19	4.68	4.18	3.73	4.64	4.3	4.04	3.66	3.36	4.46	3.29
K_2O	3.66	3.93	5.63	5.96	4.59	5.1	3.96	4.58	4.66	4.64	5.06	3.73	4.56	4.05	4.9	4.55	5.12	5.1	3.12	5.07
P_2O_5	0.15	0.23	0.17	0.15	0.1	0.13	0.54	0.17	0.09	0.1	0.36	0.08	0.08	0.22	0.15	0.03	0.03	0.11	0.36	0.15
LOI	1.02	0.93	0.59	0.61	0.66	0.59	0.93	0.63	0.5	0.72	0.64	1.6	1.1	0.79	0.64	0.78	0.4	0.94	0.92	0.36
Total	99.6	102.32	98.47	100.09	98.34	97.44	101.14	100.47	98.48	100.73	98.85	100.43	98.41	96.57	98.03	99.42	100.52	99.03	100.85	97.55
Trace elements																				
Ba	1082	2372	2629	1996	1151	1437	856	1112	732	1094	1495	1317	1259	1810	1351	732	977	1322	1017	994
Rb	130	151	221	166	129	173.1	240	178	234	148	203	117.1	110	216.9	224	165.4	147	107	112.8	112
Sr	660	1409	1294	1419	643	523	980	799	455	781	1050	437	620	861	787	374	318	464	504	342
Zr	216	236	372	286	219	256	434	235	170	189	366	188	141	210	224	109	116	317	290	249
Nb	3	8	1	14	12	1.94	24	8	10	3	14	6.68	1	14.67	12	4.47	3.99	9	10.53	20
Ni	31	37	14	15	19	14	24	27	24	16	14	8	15	18	16	21	12	21	24	23
Co	17			23		4.5	13	18				3.6		8.1		3.7	3		15.6	
Zn	71			76		38	50	85				42	23	70		22	33		101	
Cr	301	250	154	166	216	165	154	216	192	259	148	203	229	205.2	196	205.2	292	292	292	166
La	35.3					59.7						31.3		65.6		19.8	30		60.6	
Ce	81.2					104.8						55.6		115.4		41.4	63.1		145.6	
Pr	12.19					10.88						5.76		13.01		5.56	8.71		22.41	
Nd	42.3					35.1						18.9		45.2		18.6	29.7		86.1	
Sm	4.9					4.7						2.9		7.6		3.1	4		14.4	
Eu	0.96					1						0.98		1.74		0.79	1		3.03	
Gd	3.11					2.84						2.23		5.43		2.09	2.44		11.08	

Tb	0.35					0.3						0.28		0.65		0.3	0.35		1.6	
Dy	1.06					1.04						1.3		2.55		1.19	1.04		8.4	
Ho	0.31					0.17						0.23		0.41		0.23	0.22		1.8	
Er	0.87					0.43						0.62		1.1		0.96	0.58		4.81	
Tm	0.18					0.06						0.1		0.16		0.15	0.16		0.71	
Yb	1.1					0.4						0.7		1		0.7	0.7		4.1	
Lu	0.29					0.06						0.12		0.14		0.16	0.12		0.63	
Y	31	32	31	40	41	4.84	51	37	38	36	45	6.25	27	13.02	44	10	10	35	33	38
Cs	4.68					2.68						3.06		8.93		5.56	3.92		4.29	
Ta	0.24					0.05						0.05		0.46		0.05	0.05		1.2	
Hf	7.28					5.9						4.53		4.86		3.92	4.18		8.49	
Ga	24.1					25.4						18.8		27.4		20.8	22.8		24.5	
Th	23.1					22.4						10		10.8		20.6	18.6		21	
U	5.33					2.56						0.78		3.4		5.37	4.01		1.24	
ΣREE	184					221						121		260		95	142		365	
Mg#	51	48	43	44	42	46	46	44	47	52	45	46	45	43	46	36	27	36	42	32
Eu/Eu*	0.75					0.84						1.18		0.95		0.98			0.73	
Rb/Sr	0.2	0.11	0.17	0.12	0.2	0.33	0.24	0.22	0.51	0.19	0.19	0.27	0.18	0.25	0.28	0.44	0.46	0.23	0.22	0.33
Ba/Rb	8.32	15.71	11.9	12.02	8.92	8.3	3.57	6.25	3.13	7.39	7.36	11.25	11.45	8.34	6.03	4.43	6.65	12.36	9.02	8.88
Th/U	4					9						13		3		4	5		17	
Zr/Hf	30					43						42		43		28	28		34	
Na_2O+K_2O	7.69	9.01	10.17	10.28	8.64	9.67	9.77	9.9	9.29	8.83	9.74	7.91	8.29	8.69	9.2	8.59	8.78	8.46	7.58	8.36
Fe#	0.63	0.66	0.7	0.69	0.71	0.67	0.67	0.7	0.67	0.62	0.68	0.68	0.69	0.7	0.67	0.76	0.83	0.76	0.71	0.79
MALI	5.29	7.02	8.98	9.04	7.03	8.51	7.21	8.47	8.2	7.81	7.67	6.2	7.26	7.15	7.92	7.47	7.73	7.04	3.84	6.51
ASI	1.19	0.97	1.08	1.04	1.02	1.04	1.03	0.98	1.03	1.3	1.01	1.22	1.1	1.03	1.08	1.01	1.02	1.14	1.08	1.03
K_2O/Na_2O	0.91	0.77	1.24	1.38	1.13	1.12	0.68	0.86	1.01	1.11	1.08	0.89	1.22	0.87	1.14	1.13	1.4	1.52	0.7	1.54
T_{Zr} (ºC)	813	801	856	828	807	819	845	803	785	815	837	810	780	799	811	752	758	853	819	818
T_{Ap} (ºC)	894	990	923	932	898	906	1003	951	896	900	979	874	899	946	923	832	842	906	955	922

Major elements in wt.%, trace elements in ppm.. Eu/Eu* = $Eu_N/\sqrt{[(Sm_N).(Gd_N)]}$ (TAYLOR & MCLENNAN 1985). LOI (Loss on ignition). $Mg^{\#} = 100MgO/(MgO+FeO_T)$ (molar).

$T_{Ap} = \{[8400 + 26400(SiO_2 – 0.5)] / [\ln(42/P_2O_5) + 3.1 + 12.4(SiO_2 – 0.5)] – 273.15\}$ (HARRISON & WATSON 1984); $T_{Zr} = \{(12900) / [\ln(497644/Zr) + 3.8 + 0.85(M – 1)] – 273.15\}$ where M = 100(Na + K + 2Ca) / Al.Si. (WATSON & HARRISON 1983).

MINERAL CHEMISTRY

Micas

The annite–siderophyllite–phlogopite–eastonite quadrilateral is commonly used to illustrate the total Al and Fe# [Fe/(Fe + Mg)] compositional relationships of trioctahedral micas from igneous rock suites (SPEER 1984). Occupancies of the octahedral positions range from 5.41 to 5.63 atoms per formula unit (apfu), corresponding to typical values of fresh biotite. In this diagram (not shown), the studied mica samples consist of biotite (annite-rich) in the sense of DEER et al. (2013) (i.e., Fe# > 0.33). Biotite in these rocks has total Al contents in the range of 2.71 to 2.85 apfu. Biotite from the Santo Antonio pluton is more Fe-rich (Fe# values in the range of 0.57 to 0.59) than biotite in the Jacaré dos Homens pluton (0.54 to 0.55). Chemical data of biotites from the studied granites plot in the calc-alkaline field of the FeO–MgO–Al_2O_3 diagram (Fig. 6) of ABDEL-RAHMAN (1994) to discriminating biotite from alkaline (A), calc-alkaline (C), and peraluminous (P) granite suites.

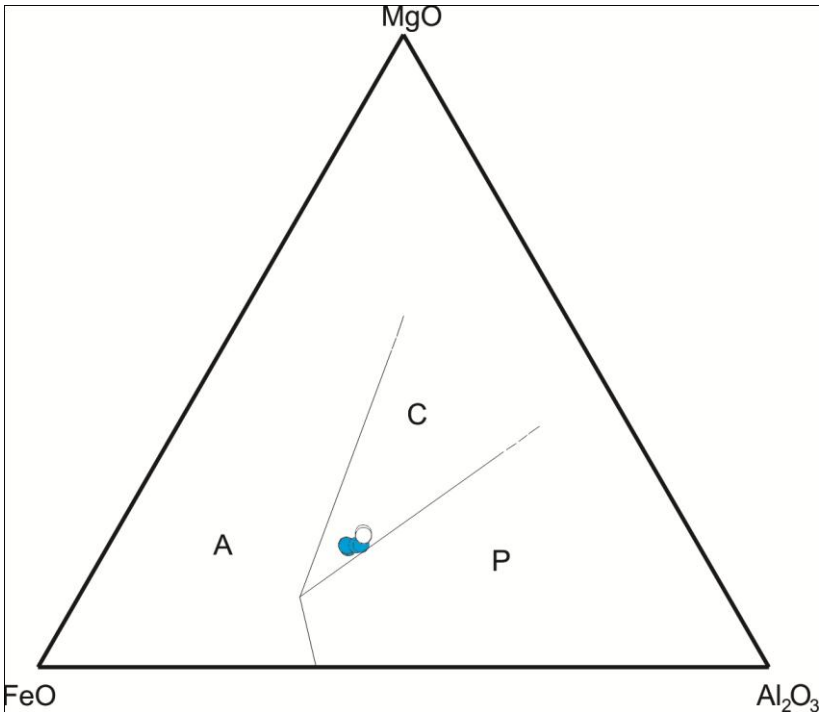

Figure 6. MgO x FeO x Al_2O_3 diagram of ABDEL-RAHMAN (1994). C = calc-alkaline; P = peraluminous; A = alkaline.

Table 2. Microprobe chemical analyses of biotite from the Jacaré dos Homens (MA) and Santo Antonio (SA) plutons.

Sample	MA–2B	MA–2B	MA–2B	MA–2B	SA–59	SA–59	SA–60	SA–60	SA–59	SA–59
Location	Core	Rim	Core	Rim	Core	Rim	Core	Rim	Core	Rim
SiO_2	36.903	36.443	36.673	36.558	35.608	35.918	35.763	35.841	36.596	36.68
TiO_2	2674	2.664	2.669	2.667	3.246	3.088	3.167	3.128	3.007	2.634
Al_2O_3	15.386	15.626	15.506	15.566	15.091	15.017	15.054	15.036	15.251	15.82
Cr_2O_3	0.035	0.092	0.064	0.078	0.049	0.058	0.054	0.056	0	0.024
FeO	20.372	20.603	20.488	20.545	21.994	22.241	22.118	22.179	22.006	22.118
MnO	0.651	0.531	0.591	0.561	0.615	0.792	0.704	0.748	0.598	0.708
MgO	9.641	9.46	9.551	9.505	8.602	8.928	8.765	8.847	7.675	7.871
V_2O_3	0.038	0	0.019	0.01	0.014	0.034	0.024	0.029	0.135	0.088
CaO	0.031	0.054	0.043	0.048	0.114	0.049	0.082	0.065	0.099	0.062
Na_2O	0.109	0.081	0.095	0.088	0.081	0.103	0.092	0.098	0.042	0.118
K_2O	9.998	9.803	9.901	9.852	9.445	9.633	9.539	9.586	9.626	9.748
SrO	0	0	0	0	0.043	0	0.022	0.011	0	0.03
NiO	0.044	0.011	0.028	0.019	0.026	0.004	0.015	0.01	0.027	0
BaO	0.275	0.176	0.226	0.201	0.109	0	0.055	0.027	0	0.097
F	0.735	0.861	0.798	0.83	0.56	0.605	0.583	0.594	0.46	0.392
Cl	0	0.033	0.017	0.025	0.036	0.046	0.041	0.044	0.014	0.034
Total	96.892	96.438	96.665	96.552	95.633	96.516	96.075	96.295	95.536	96.424
Structural formulae on the basis of 22 oxygens										
Si	5.648	5.578	5.613	5.596	5.45	5.498	5.474	5.486	5.601	5.614
Al^{IV}	2.352	2.422	2.387	2.404	2.55	2.502	2.526	2.514	2.399	2.386
Z site	8	8	8	8	8	8	8	8	8	8
Al^{VI}	0.424	0.397	0.41	0.403	0.172	0.206	0.189	0.198	0.352	0.468
Ti	0.308	0.307	0.307	0.307	0.374	0.355	0.365	0.36	0.346	0.303
Cr	0.004	0.011	0.008	0.009	0.006	0.007	0.006	0.007	0	0.003
Fe	2.608	2.637	2.622	2.63	2.815	2.847	2.831	2.839	2.689	2.703
Mn	0.084	0.069	0.077	0.073	0.08	0.103	0.091	0.097	0.078	0.092
Mg	2.2	2.159	2.179	2.169	1.963	2.037	2	2.019	1.979	2.024
V	0.005	0	0.002	0.001	0.002	0.004	0.003	0.004	0.017	0.011
Y site	5.632	5.579	5.606	5.592	5.411	5.56	5.486	5.523	5.461	5.604
Ca	0.005	0.009	0.007	0.008	0.019	0.008	0.013	0.011	0.016	0.01
Na	0.032	0.024	0.028	0.026	0.024	0.031	0.027	0.029	0.012	0.035
K	1.952	1.914	1.933	1.924	1.844	1.881	1.863	1.872	1.684	1.708
Ba	0.016	0.011	0.014	0.012	0.007	0	0.003	0.002	0	0.006
X site	2.006	1.958	1.982	1.97	1.894	1.92	1.907	1.913	1.713	1.759
Total cat	15.639	15.537	15.588	15.562	15.305	15.479	15.392	15.436	14.921	14.982
F	0.356	0.419	0.387	0.403	0.277	0.296	0.287	0.291	0.23	0.196
Cl	0.000	0.009	0.004	0.006	0.010	0.012	0.011	0.011	0.004	0.009
Fe/(Fe+Mg)	0.542	0.55	0.546	0.548	0.589	0.583	0.586	0.584	0.576	0.572
Mg/(Mg+Fe)	0.458	0.45	0.454	0.452	0.411	0.417	0.414	0.416	0.424	0.428
FeO/MgO	2.113	2.178	2.145	2.161	2.557	2.491	2.523	2.507	2.421	2.381
Al^{tot}	2.776	2.819	2.797	2.808	2.722	2.709	2.716	2.712	2.751	2.854

Epidote

In the Santo Antonio granite, subhedral magmatic epidote is partially rimmed by biotite surrounding allanite euhedral core, a textural relationship that resembles “type II” epidote in the Cryogenian–Ediacaran calc-alkalic granites from the Cachoeirinha-Salgueiro Belt (SIAL 1990, 1993; SIAL et al. 1999, 2008; FERREIRA et al. 2003;

SIAL & FERREIRA 2016). Two epidote grains analyzed in this study have shown pistacite contents (Ps = 100 x molar [Fe^{3+} /(Fe^{3+} + Al)]) between 28 and 29, and TiO_2 contents < 0.2 wt%, characteristics that support magmatic origin (TULLOCH 1979, 1986; EVANS & VANCE 1987).

Table 3. Microprobe chemical analyses of epidote from the Santo Antonio pluton.

Table 9. Microprobe chemical analyses of epidote from the Santo Antonio pluton.				
Sample	SA–59	SA–59	SA–59	SA–59
Location	Core	Rim	Core	Rim
MgO	0.079	0.057	0.035	0.046
Al_2O_3	22.637	22.714	22.791	22.753
SiO_2	36.930	37.200	37.470	37.335
CaO	22.574	23.028	23.482	23.255
K_2O	0.002	0.024	0.046	0.035
TiO_2	0.000	0.049	0.098	0.074
MnO	0.285	0.348	0.411	0.380
SrO	0.000	0.040	0.080	0.060
NiO	0.000	0.015	0.030	0.023
Fe_2O_3	14.413	14.254	14.095	14.175
V_2O_3	0.047	0.029	0.011	0.020
Total	96.980	97.766	98.552	98.159
Structural formulae on the basis of 12.5 oxygens				
Mg	0.010	0.007	0.004	0.006
Al	2.155	2.162	2.170	2.166
Si	2.983	3.005	3.027	3.016
Ca	1.954	1.993	2.032	2.013
K	0.000	0.002	0.005	0.004
Ti	0.000	0.003	0.006	0.004
Mn	0.019	0.024	0.028	0.026
Sr	0.000	0.002	0.004	0.003
Ni	0.000	0.001	0.002	0.001
Fe	0.876	0.866	0.857	0.862
V	0.003	0.002	0.001	0.001
Total	8.002	8.068	8.135	8.102
Pistacite = 100 x Fe/(Fe+Al)	28.9	28.6	28.3	28.5

U–Pb SHRIMP GEOCHRONOLOGY

Jacaré dos Homens pluton

SEM and CL imaging of 120 to 300 μm colorless to light yellow zircons from Jacaré dos Homens granodiorite orthogneiss sample MA–2B reveal an igneous oscillatory-zoned edge (Fig. 7). Zoning in cores and rims can be pronounced, to very weak or diffuse. Mostly euhedral (but some corroded) grains are equant to elongated

(aspect ratio 1 to > 7:2), commonly with bi-pyramidal terminations typical of magmatic growth.

U–Pb SHRIMP analyses performed on cores and an oscillatory-zoned edge provide a weighted $^{206}Pb/^{238}U$ mean age of 642.4 ± 3.4 Ma (n=12, MSWD= 0.20) (Fig. 8). High Th/U ratios, ranging from 0.53 to 1.47, are typical of magmatic zircons (HOSKIN & BLACK 2000; HOSKIN & SCHALTEGGER 2003; WILLIAMS & CLAESSON 1987). We interpret this age to refer to crystallization and emplacement of the orthogneiss.

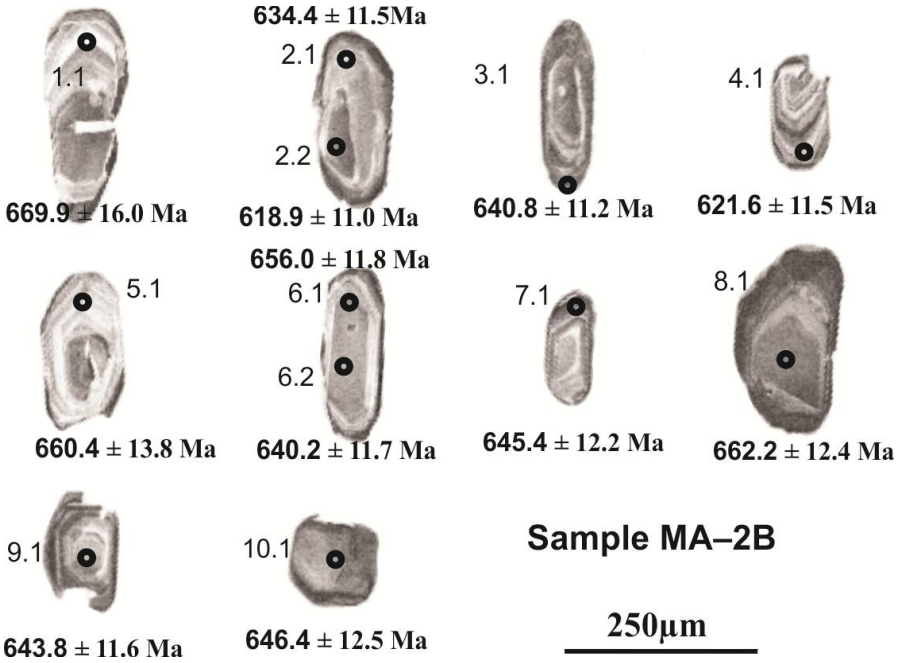

Figure 7. Cathodoluminescence (CL) images of the zircon crystals from the Jacaré dos Homens pluton. Circles indicate the position of the U–Pb analysis listed in Table 4.

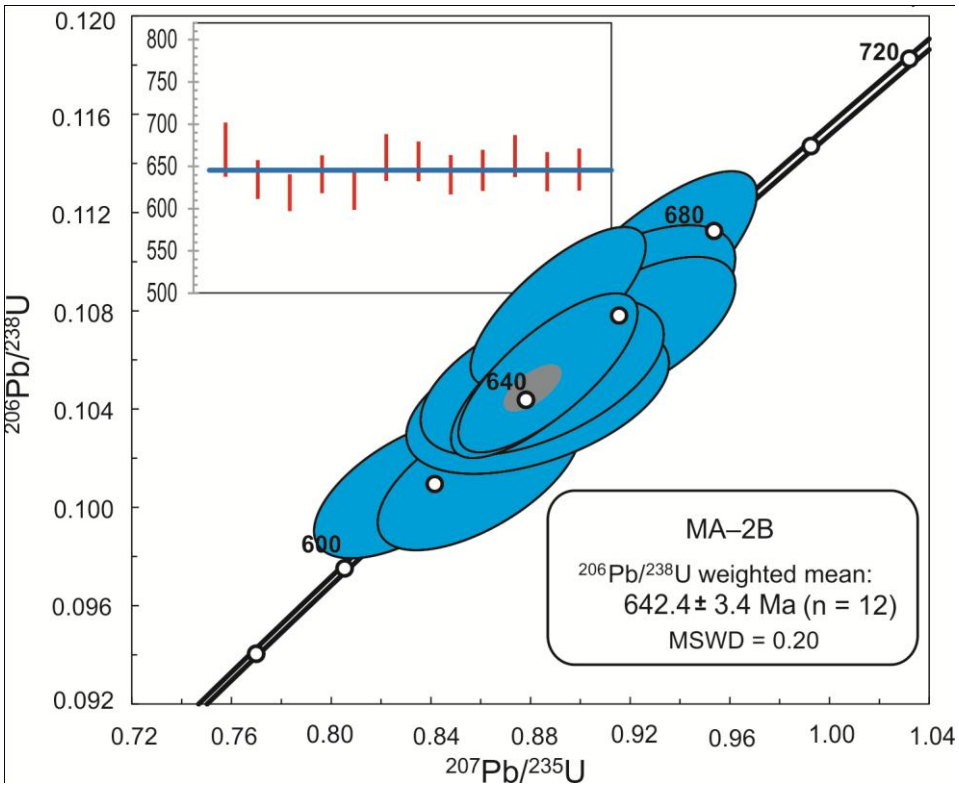

Figure 8. Concordia diagram for SHRIMP 204-corrected, zircon analyses from the Jacaré dos Homens pluton. Inset: $^{206}Pb/^{238}Pb$ weighted mean plots.

Table 4. Summary of SHRIMP U–Pb zircon data of the Sample MA–02B from the Jacaré dos Homens pluton.

Grain. Spot	% $^{206}Pb_c$	U ppm	Th ppm	$^{232}Th/^{238}U$	$^{206}Pb^*$ ppm	(1) $^{206}Pb/^{238}Pb$ Age		(1) $^{207}Pb/^{206}Pb$ Age		% Dis	(1) $^{207}Pb^*/^{206}Pb^*$	±%	(1) $^{207}Pb^*/^{235}Pb$	±%	(1) $^{206}Pb^*/^{238}Pb$	±%	Erro corr
1.1	0.00	156	157	1.04	14.7	669.9	± 16.0	650	± 44	-3	0.0613	2.0	0.93	3.2	0.1095	2.5	0.777
2.1	0.29	154	108	0.72	13.7	634.4	± 11.5	657	± 50	4	0.0615	2.3	0.88	3.0	0.1034	1.9	0.632
2.2	0.20	288	168	0.60	25.0	618.9	± 11.0	598	± 52	-3	0.0598	2.4	0.83	3.0	0.1008	1.9	0.612
3.1	0.00	258	261	1.05	23.1	640.8	± 11.2	634	± 33	-1	0.0609	1.5	0.88	2.4	0.1045	1.8	0.769
4.1	0.37	183	185	1.05	15.9	621.6	± 11.5	659	± 53	6	0.0616	2.4	0.86	3.1	0.1012	1.9	0.620
5.1	0.16	113	101	0.93	10.5	660.4	± 13.8	653	± 60	-1	0.0614	2.8	0.91	3.5	0.1079	2.2	0.621
6.1	0.22	180	181	1.04	16.6	656.0	± 11.8	684	± 50	4	0.0623	2.4	0.92	3.0	0.1071	1.9	0.626
6.2	0.54	165	192	1.20	14.9	640.2	± 11.7	651	± 74	2	0.0613	3.4	0.88	3.9	0.1044	1.9	0.487
7.1	0.24	149	108	0.75	13.5	645.4	± 12.2	637	± 66	-1	0.0609	3.0	0.88	3.6	0.1053	2.0	0.546
8.1	0.00	217	308	1.47	20.2	662.2	± 12.4	594	± 37	-10	0.0597	1.7	0.89	2.6	0.1082	2.0	0.757
9.1	0.00	218	243	1.15	19.7	643.8	± 11.6	636	± 37	-1	0.0609	1.7	0.88	2.6	0.1050	1.9	0.743
10.1	0.14	284	147	0.53	25.8	646.4	± 12.5	639	± 38	-1	0.0610	1.8	0.89	2.7	0.1055	2.0	0.756

Errors are 1–sigma; Pbc and Pb* indicate the common and radiogenic portions, respectively. 1) Common Pb corrected using measured ^{204}Pb.

Santo Antonio granite

Euhedral to subhedral, short to elongated, pink to yellow zircon crystals with bi-pyramidal terminations, are 155 to 300 μm long, and with aspects ratios of 1 to ≥ 5:2. Santo Antonio zircons comprise cores and rims with normal magmatic zoning (Fig. 9).

Of thirteen analyzed zircon grains, data from eleven cluster close to concordia, providing a weighted $^{206}Pb/^{238}U$ mean age of 636.1 ± 3.6 Ma, with MSWD of 0.12 (Fig. 10). These grains show high Th/U ratios ranging from 0.43 to 1.45, typical of magmatic zircon. Anomalous data of zircon grain #8.1 with Th/U = 0.49, plots moderately concordantly at ca. 461 Ma (% disc = 14), likely to Pb loss. Zircon grain #6.1, with $t_{206/238}$ = 664 ± 12.5 Ma, is possibly inherited from an older source.

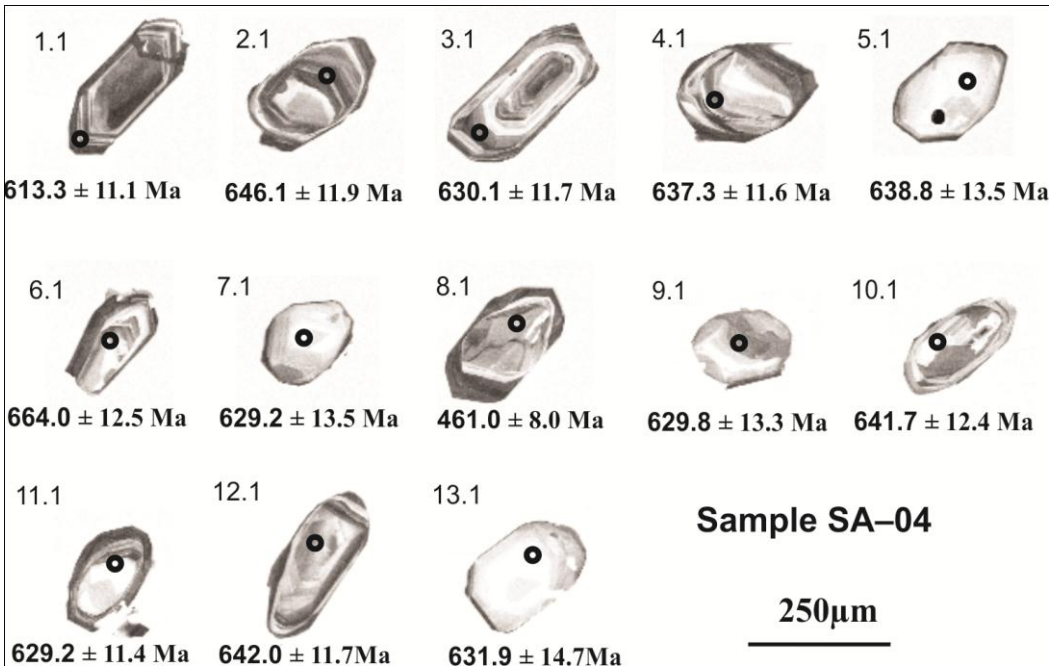

Figure 9. Cathodoluminescence (CL) images of the zircon crystals from the Santo Antonio granite. Circles indicate the position of the U–Pb analysis listed in Table 5.

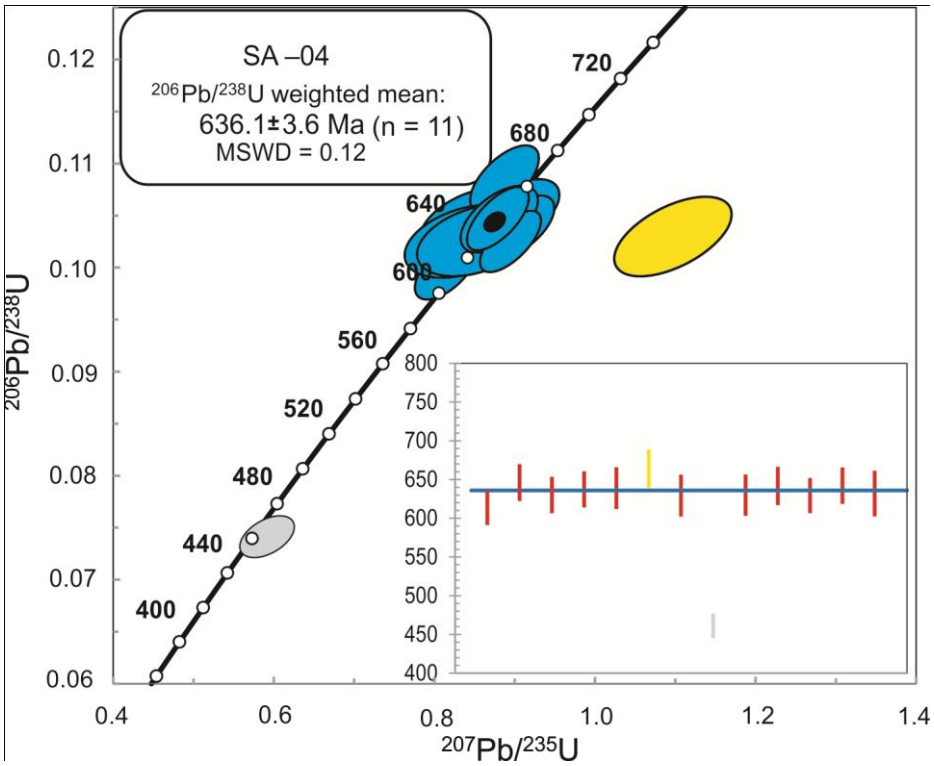

Figure 10. Concordia diagram for SHRIMP 204-corrected, zircon analyses from the Santo Antonio granite. Blue ellipses indicate protolith crystallization; yellow ellipse indicates inheritance; light gray ellipse indicates Pb loss. Inset: $^{206}Pb/^{238}Pb$ weighted mean plots.

Table 5. Summary of SHRIMP U–Pb zircon data of the Sample SA–04 from the Santo Antonio granite.

Grain. Spot	% ^{206}Pbc	U ppm	Th ppm	^{232}Th/ ^{238}U	^{206}Pb* ppm	(1) ^{206}Pb/^{238}Pb Age		(1) ^{207}Pb/^{206}Pb Age		% Dis	(1) ^{207}Pb*/ ^{206}Pb*	±%	(1) ^{207}Pb*/ ^{235}Pb	±%	(1) ^{206}Pb*/ ^{238}Pb	±%	Erro corr
1.1	0.13	165	68	0.43	14.2	613.3	± 11.1	573	54	-7	0.0592	2.5	0.81	3.1	0.0998	1.9	0.609
2.1	0.16	174	119	0.71	15.8	646.1	± 11.9	681	69	5	0.0622	3.2	0.90	3.8	0.1054	1.9	0.512
3.1	0.23	128	110	0.89	11.3	630.1	± 11.7	637	68	1	0.0609	3.1	0.86	3.7	0.1027	2.0	0.528
4.1	-0.18	153	133	0.90	13.7	637.3	± 11.6	716	54	12	0.0632	2.5	0.91	3.2	0.1039	1.9	0.604
5.1	0.50	57	54	0.98	5.1	638.8	± 13.5	571	104	-11	0.0591	4.7	0.85	5.3	0.1042	2.2	0.423
6.1	0.00	111	133	1.24	10.3	664.0	± 12.5	579	54	-13	0.0593	2.5	0.89	3.2	0.1085	2.0	0.621
7.1	0.40	56	55	1.01	5.0	629.2	± 13.5	577	118	-8	0.0593	5.4	0.84	5.9	0.1025	2.3	0.383
8.1	0.76	468	221	0.49	30.0	461.0	± 8.0	526	73	14	0.0579	3.3	0.59	3.8	0.0741	1.8	0.472
9.1	0.46	78	98	1.29	6.9	629.8	± 13.3	611	114	-3	0.0602	5.2	0.85	5.7	0.1026	2.2	0.389
10.1	0.21	161	92	0.59	14.5	641.7	± 12.4	641	64	0	0.061	3.0	0.88	3.6	0.1047	2.0	0.563
11.1	-0.09	160	139	0.90	14.1	629.2	± 11.4	718	44	14	0.0633	2.1	0.89	2.8	0.1025	1.9	0.676
12.1	0.00	154	217	1.45	13.9	642.0	± 11.7	635	47	-1	0.0609	2.2	0.88	2.9	0.1047	1.9	0.664
13.1	-1.13	50	46	0.94	4.4	631.9	± 14.7	1128	73	79	0.0773	3.6	1.10	4.4	0.1030	2.5	0.557

Errors are 1–sigma; Pbc and Pb* indicate the common and radiogenic portions, respectively. 1) Common Pb corrected using measured ^{204}Pb.

WHOLE-ROCK Rb–Sr AND Sm–Nd ISOTOPES

The U–Pb ages of igneous crystallization were used to calculate εNd and Nd model ages for the studied granites. The calculated t_{DM} age for the Jacaré dos Homens pluton is 1.2 Ga, and $\varepsilon Nd_{(642\ Ma)}$ is slightly negative (−1.58). Initial $^{87}Sr/^{86}Sr$, back-calculated to 642 Ma, is 0.7068. These model calculations suggest the presence of a continental crust component in the source. For the Santo Antonio pluton, the model calculations are homogeneous, t_{DM} ranging from 0.96 to 1.05 Ga, and $\varepsilon Nd_{(636\ Ma)}$ from +1.17 to −0.67 (Fig. 11a). Initial $^{87}Sr/^{86}Sr_{636\ Ma}$ varies from 0.7050 to 0.7052. Nd and Sr isotope data for these plutons plot along the mantle array or near it in the εNd(t) *vs*. $^{87}Sr/^{86}Sr$(i) diagram and fit well within the isotopic field of the Lachlan Fold Belt I-type granites (Fig. 11b).

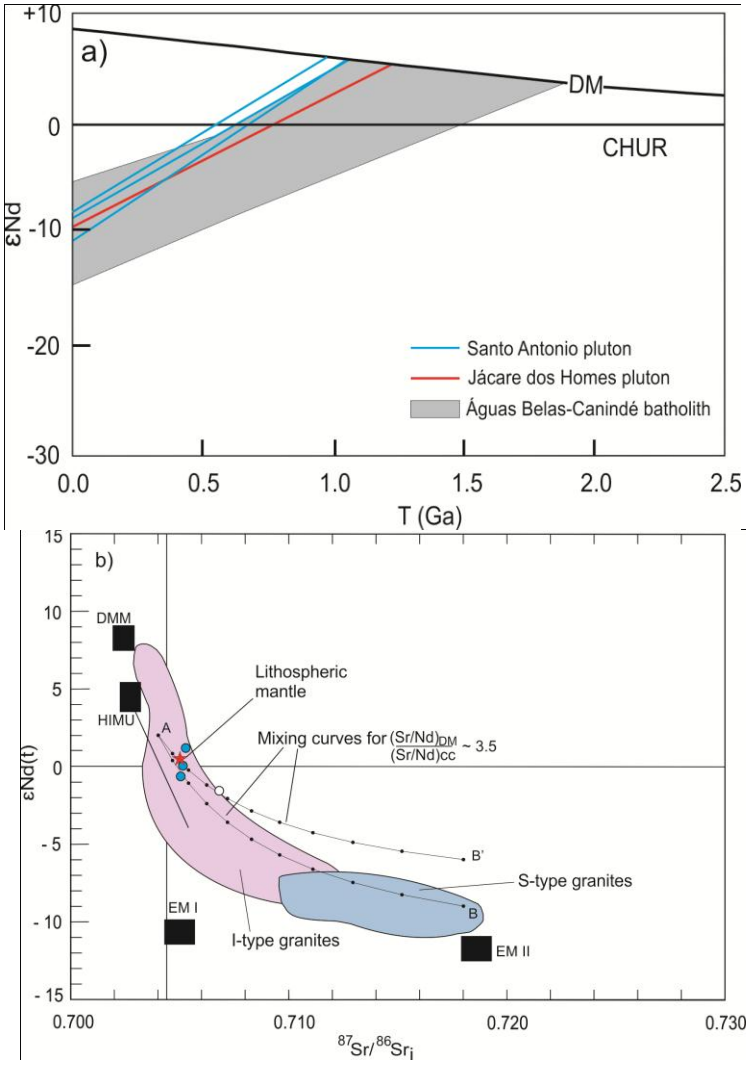

Figure 11. (a) $T_{(Ga)}$ and (b) $^{87}Sr/^{86}Sr_I$ *vs*. εNd(t) diagrams for the studied granites. Águas Belas–Canindé batholith data are from SILVA FILHO et al. (2014). Two calculated mixing hyperbolas (after FAURE 1986; ALLÈGRE 2008) illustrate the possible effect of bulk-assimilation of continental crust. The depleted mantle-like component used in modeling has εNd = +2, $^{87}Sr/^{86}Sr$ = 0.704, Sr_{DMC} = 318 ppm, Nd_{DMC} = 18 ppm. The crustal components are (B) εNd = -9, $^{87}Sr/^{86}Sr$ = 0.718, Ndcc = 28 ppm, Srcc = 140 ppm, and (B') εNd = -6, $^{87}Sr/^{86}Sr$ = 0.718, Ndcc = 28 ppm, Srcc = 140 ppm. The curvature of the mixing curves is controlled by the ratio $(Sr/Nd)_{DMC}/(Sr/Nd)cc$ ~ 3.5. Modeling curves are marked in 10%

increments. Fields for I- and S-type granites of the Lachlan Fold Belt are after HEALY et al. (2004). End-member mantle reservoirs modified from: ZINDLER & HART (1986) and HART et al. (1986) [DMM (depleted "MORB" mantle), EM I (enriched mantle type 1) and EM II (enriched mantle type 2) and HIMU (high U/Pb mantle)]. Isotopic composition of the lithospheric mantle is from LIU et al. (2014). Linear HIMU-EM I array (LoNd array) is from HART et al. (1986).

CRYSTALLIZATION INTENSIVE PARAMETERS

Temperature

WATSON & HARRISON (1983) developed an experimental model relating the concentration of Zr in a melt equilibrated with zircon to major-element composition and temperature. This model assumes that zircon was early to crystallize and it was not a cumulate phase, xenocrystic, or otherwise inherited. Variations of pressure (up to 25 kbar) or variable water content exert no observable influence (BOEHNKE ET AL. 2013). Accordingly, calculated temperatures for the Santo Antonio granite range from 856 to 800 ºC, except for a few samples. The Jacaré dos Homens pluton presented slightly higher calculated temperatures of 853 to 818 ºC. The zircon saturation temperatures for the studied rocks are higher than 800°C and suggest that these plutons are high-temperature granites (MILLER et al. 2003; CHAPPELL et al. 2004).

GREEN & WATSON (1982) and HARRISON & WATSON (1984) demonstrated a close dependence between apatite saturation and silica content of the magma, which is temperature dependent, but independent of pressure up to 25 kbar (GREEN & ADAM 2002), and any effect of iron or oxidation state (TOLLARI et al. 2006). Compositions of the studied rocks lie within the stipulated calibration range. For the Santo Antonio granite, apatite saturation temperatures range from 1003 to 832 ºC, and for the Jacaré dos Homens pluton, from 955 to 906 ºC (Fig. 3e). Apatite is an early phase relative to zircon in the crystallization sequence and apatite exhibits higher saturation temperatures (e.g. ANDERSON et al. 2008).

Table 6. Sr–Nd isotopes for the Santo Antonio (SA–04, SA–104 and SA–105) and Jacaré dos Homens plutons (JH–10).

Sample	Nd ppm	Sm ppm	$^{147}Sm/^{143}Nd$	$^{143}Nd/^{144}Nd$	Erro (2σ)	εNd (Today)	εNd (T)	T_{DM} (Ga)	Rb ppm	Sr ppm	87Rb/ 86Sr	erro (1s)	87Sr/ 86Sr	erro (2σ)	(87Sr/ 86Sr)i	εSr (Today)	εSr (T)
JH–10	11.383	66.749	0.10312	0.512162	0.0000097	-9.28	-1.58	1.21	118.06	540.94	0.6319	0.009	0.71249	0.000042	0.706799	113.44	43.25
SA–04	3.982	31.835	0.07563	0.512099	0.0000113	-10.51	-0.67	1.04	172.36	485.962	1.0271	0.016	0.71419	0.000062	0.705029	137.61	18.00
SA–104	2.166	14.285	0.09168	0.512203	0.0000100	-8.49	0.05	1.05	175.03	409.636	1.2376	0.015	0.71616	0.000068	0.705116	165.51	19.24
SA–105	3.151	22.543	0.08453	0.512230	0.0000096	-7.96	1.17	0.96	148.61	339.606	1.2675	0.009	0.71657	0.000074	0.705254	171.26	21.21

Initial compositions recalculated to crystallization ages.
The present-day composition of the CHUR is $^{147}Sm/^{144}Nd_{CHUR} = 0.1967$ and $^{143}Nd/^{144}Nd_{CHUR} = 0.512638$ (JACOBSEN & WASSERBURG, 1980; PATCHETT et al., 2004).
The Nd isotopic compositions were normalized to $^{146}Nd/^{144}Nd = 0.7219$. $\lambda_{147Sm} = 6.54 \times 10^{-12}$ y^{-1} (LUGMAIR & MARTI 1978). The calculations of the model ages were based on the depleted-mantle evolution model of DEPAOLO (1981) and DEPAOLO et al. (1991).
The present-day composition of the UR is $^{87}Rb/^{86}Sr_{UR} = 0.0827$ and $^{87}Sr/^{86}Sr_{UR} = 0.7045$ (DEPAOLO 1988). The Sr isotopic ratios were normalized to $^{86}Sr/^{88}Sr = 0.1194$.
$\lambda_{87Rb} = 1.3968 \times 10^{-11}$ y^{-1} (ROTENBERG et al., 2012).

Redox conditions

It is difficult to estimate oxygen fugacity (fO_2) of the source to silicic magmatic rocks (e.g. WONES 1989). Oxygen fugacity exerts far more control on mineral compositions in granitic rocks than other intensive parameters, such as P and T (ANDERSON 1996). The assemblage titanite + magnetite + quartz ± amphibole (as in the studied rocks) implies a relatively high oxygen fugacity (WONES 1989): near to the TMQAI buffer (NOYES 1983; WONES 1989). For epidote in the Santo Antonio pluton, pistacite (Ps_{28} to Ps_{29}) suggests relatively oxidizing conditions, between the NNO and HM buffers (e.g. LIOU 1973; SIAL et al. 1999, 2008). All of these indicators point to a high oxygen fugacity.

DISCUSSION

For the Jacaré dos Homens pluton, all of the characteristics discussed above—whole rock, major and accessory mineral compositions, and Rb–Sr and Sm–Nd isotope data—are consistent with an I-type magma that has incorporated minor, possibly altered, crustal material. It is an overall pattern similar to that of the Sierra Nevada batholith (e.g. LACKEY et al. 2008). Value of $\delta^{18}O$ in zircon (7.0 ‰) is higher than those of mantle-derived zircon (5 to 6.0‰, HAWKESWORTH & KEMP 2006; VALLEY et al. 1998, 2005; CAVOSIE et al. 2009), but lower than those of metasedimentary rocks (≈10‰, GAO et al. 2016 and references therein). Value of whole-rock $\delta^{18}O$ inferred from $\delta^{18}O$ in zircon (LACKEY et al. 2008) is ≈ 8.6‰ that points to an I-type magma (values for typical I-type granites vary from 6.0 to 10‰, according to O'NEIL et al. 1977 and EILER 2001).

The major and trace-elements patterns in Harker diagrams define curved or broken lines for the Santo Antonio pluton, a characteristic that enables us to reject mixing as main process. On the contrary, these patterns indicate their derivation from magmatic differentiation by partial melting or fractional crystallization. During differentiation, with increase of silica, fractional crystallization leads to drastic reduction of concentration for the compatible elements, differently to partial melting. Bi-log diagrams (compatible x incompatible elements) separated well magmatic liquids generated by fractional crystallization that will show a straight sub-vertical line from those produced by partial melting that will exhibit a sub-horizontal one, and also from magma mixing which may give a large range of curves but with an inverse concavity with respect to that of partial melting (COCHERIE 1986). Log compatible (Nb, Zr, Rb,

Sr) vs log incompatible (Ba, Cr) elements show for the studied granitic rocks sub-vertical trends that point to a fractional crystallization process (Fig. 12). The negative correlations between SiO_2 and MgO, CaO, TiO_2, Fe_2O_3T, and Al_2O_3 indicate fractionation dominated by ferromagnesian phases (Fig. 3), while trace elements (e.g. Zr, P, Hf, and ΣREE) inversely related to SiO_2 suggest fractionation of accessory minerals (Fig. 4).

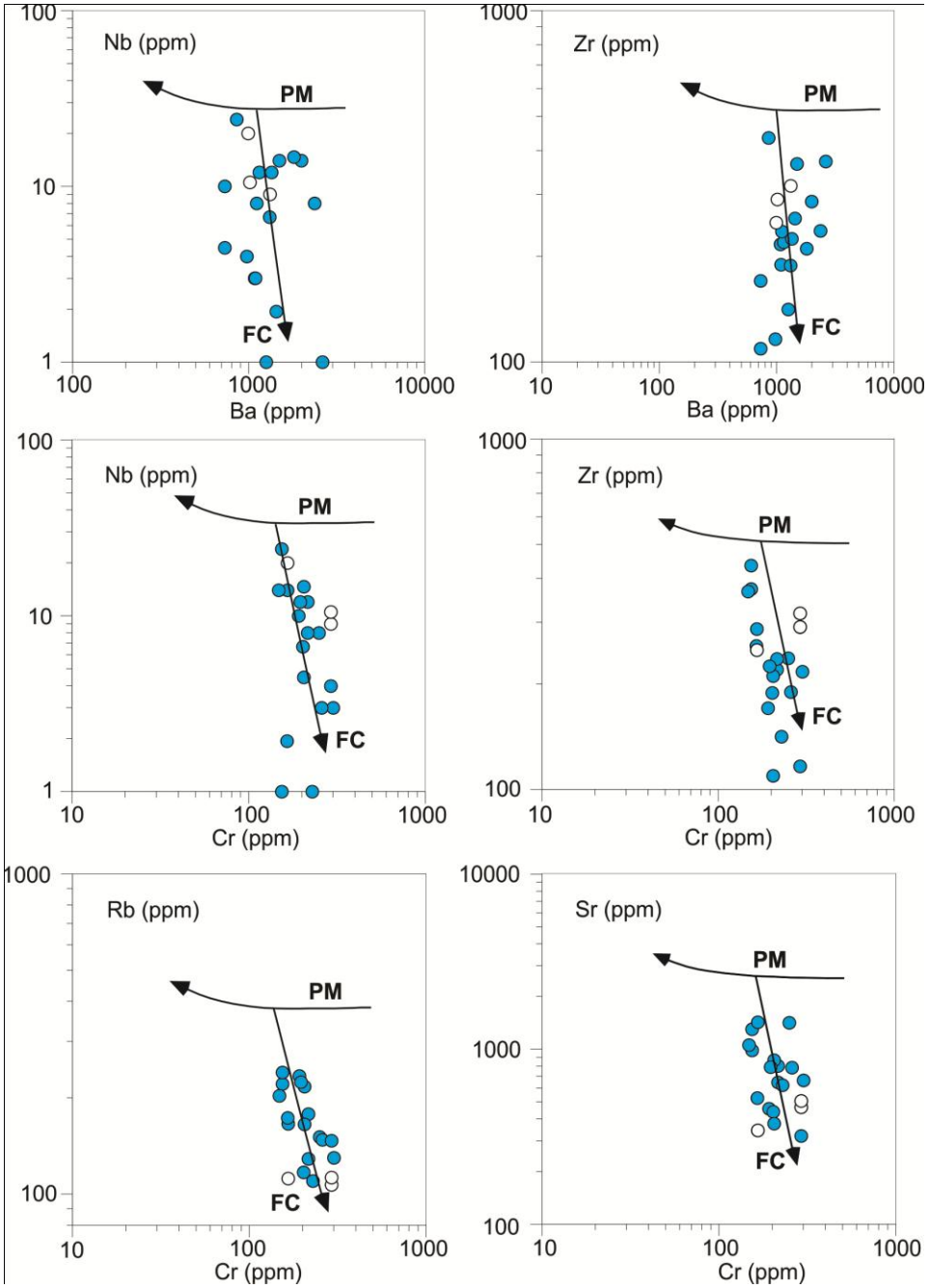

Figure 12. Bi-log diagrams correlating compatible (y-axis) *vs.* incompatible (x-axis) behavior of some elements from the studied rocks. These set of correlations suggests fractional crystallization as the main process of evolution. PM = Partial Melting; FC = Fractional Crystallization.

Various petrologic indicators (A/CNK, etc.) point to I-type characteristics, but Santo Antonio is quite aluminous. Fractionation of amphibole or assimilation of metasedimentary host rock will relatively increase aluminum (BARBARIN 1999; FROST & FROST 2008; CHAPPELL et al. 2012). Melting experiments indicate that melting of metaluminous basaltic to andesitic rocks (Al-poor; i.e. metaluminous amphibole-dominated sources) (e.g. BEARD & LOFGREN 1991; ROBERTS & CLEMENS 1993; PATIÑO DOUCE & BEARD 1995; WOLF & WYLLIE 1994; SISSON et al. 2005; NANDEDKAR et al. 2014) can create strongly peraluminous granitoid magma, as can fractional crystallization (e.g. MILLER 1985; ZEN 1986; CHAPPELL 1999; CHAPPELL et al. 2012).

Depleted HREE patterns (Fig. 5a) for the Santo Antonio granites illustrate that garnet was residual in the source, consistent with partial melting at the garnet stability field (WILSON 1989; TEPPER et al. 1993; PETFORD & ATHERTON 1996). Lack of significant Eu anomalies (Eu/Eu*=0.75 to 1.18; average = 0.94) at this pluton may also suggest that partial melting took place at pressures above the stability field of plagioclase. Magmatic epidote crystallized under relatively oxidizing conditions suggests mid-crustal pressure of crystallization (ZEN & HAMMARSTRON 1984; SCHMIDT & THOMPSON 1996; SCHMIDT & POLI 2004).

The Mg# values (most of them > 42) for the studied granitic rocks are higher than experimentally-determined crustal partial melts (e.g. RAPP & WATSON 1995), possibly revealing a mantle-derived magma component in the source (Fig. 4i). In a plot of K_2O and Na_2O versus silica (Fig. 13a–b) with fields for experimental melts compiled from literature by CHEN et al. (2013), our samples show compositions that are similar to those of melts produced by the partial melting of medium-to high-K basaltic rocks (SISSON et al. 2005), and suggest that the Santo Antonio and Jacaré dos Homens magmas probably were derived from partial remelting of mantle-derived medium-to high-K basaltic rocks. The high content of K_2O in the studied granites require a potassic mineral in the source region such as phlogopite, potassic amphibole or potassic feldspar. The absence of Eu anomalies and positive correlation between Eu/Eu* and SiO_2 (not shown) preclude K-feldspar as the potassic phase in the source rocks. FURMAN & GRAHAM (1999) suggested that melts in equilibrium with phlogopite have high Rb/Sr (> 0.1) and low Ba/Rb (< 15) ratios compared to melts in equilibrium with amphibole (Rb/Sr < 0.06 and Ba/Rb > 15). Rb/Sr ratios for the studied granites are higher than 0.1 and vary from 0.11 to 0.33 (a few up to 0.46); Ba/Rb values (3.1 to 15.7; average = 9)

are higher than crustal estimate (6.7, RUDNICK & FOUNTAIN 1995) and slightly lower-average primitive mantle estimate (~11, HOFMANN & WHITE 1983; SUN & MCDONOUGH 1989; HOFMANN 2003). These ratios suggest that phlogopite rather than potassic amphibole was present in the source rocks of the studied granites (Fig. 13c) (FURMAN & GRAHAM 1999; LI et al. 2009; LI et al. 2016).

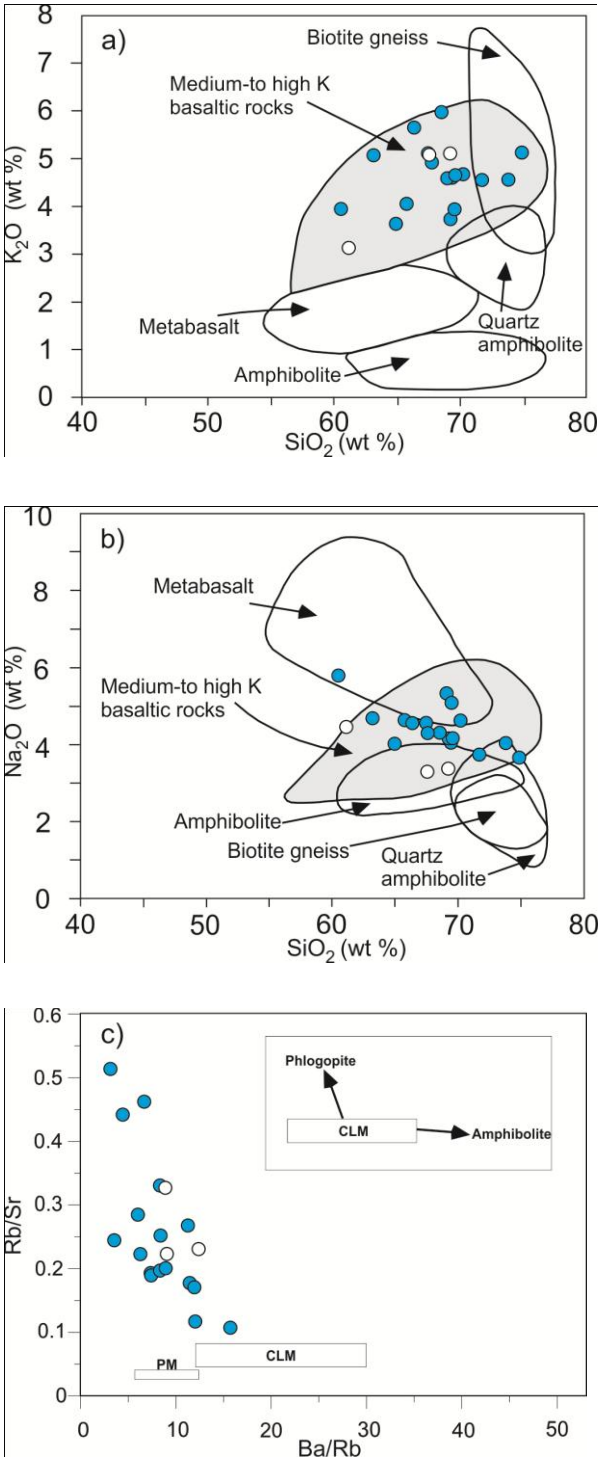

Figure 13. (a) K_2O and (b) Na_2O *vs*. SiO_2. Data for experimental melts from: BEARD & LOFGREN (1991) (Amphibolites; 1, 3, 6, 9 kb; 800–1000 °C); RAPP & WATSON (1995) (Metabasalt; 8–32 kb;

1000–1125 °C); PATIÑO DOUCE & BEARD (1995) (Quartz amphibolites; 3–15 kb; 850–930 °C); PATIÑO DOUCE & BEARD (1995) (Biotite gneiss; 3–15 kb; 850–930 °C) and SISSON et al. (2005) (Medium to high K basaltic rocks; 700 Mpa; 825–975 °C). (c) Rb/Sr *vs*. Ba/Rb. PM (primitive mantle) and CLM (continental lithospheric mantle) fields are from SUN & MCDONOUGH (1989) and Furman and GRAHAM (1999), respectively. Inset: high Ba/Rb values indicate abundant amphibole in the lithospheric mantle, whereas high Rb/Sr values indicate phlogopite in the lithospheric mantle source.

The Santo Antonio pluton has mantle-like initial $^{87}Sr/^{86}Sr$ (0.7050–0.7052). These values are similar to typical EM I type mantle ($^{87}Sr/^{86}Sr \geq 0.7040$; e.g. ZINDLER & HART 1986; SUN & MCDONOUGH 1989). Mantle separation ages for this pluton are in a narrow interval of 0.96 to 1.05 Ga, with positive to slightly negative $\varepsilon Nd_{(636\ Ma)}$ values from +1.17 to −0.67, and $\delta^{18}O_{zircon}$ = 5.0 to 5.9‰. These data comprise evidence that the protolith was likely formed either by (a) partial melting of an enriched/depleted Tonian (1.0 Ga) mantle, or (b) by mixing of Late Cryogenian-Early Ediacaran mantle-derived rocks (juvenile component of ca. 636 Ma) and an older (crustal) component. Simple Sr–Nd numerical modeling (after FAURE 1986; ALLÈGRE 2008) with two-component mixing between depleted mantle-like and crustal components suggests that the studied plutons are predominantly made up of mantle-derived magmas. The Jacaré dos Homens pluton was modeled as a 64:36 mix of mantle- and crustal-derived magmas, while the Santo Antonio pluton was modeled as an 84:16 mix (Fig. 11b). Chemical variation trends (Harker diagrams), and bi-log diagrams rule out mixing as main magmatic process (see discussion above) on the contrary, suggest that the crystal fractionation was the major process that operated after partial melting. Mixing must have occurred at the source, before or during partial melting, whereas fractionation was the dominant process generating chemical variation during differentiation. Similarly to the isotopic data, the low Rb/Ba (0.06–0.28) and Rb/Sr (0.11–0.46) ratios of the studied plutons also reveal large fraction of a mafic component (Fig. 14). Mantle-derived possible sources within the Pernambuco–Alagoas Domain are mainly Tonian, Cryogenian juvenile source rocks being largely or entirely absent (SILVA FILHO et al. 2014). The t_{DM} ages of the Santo Antonio granites correspond to the ages of the extensional Cariris Velhos event, which occurs elsewhere in the Borborema Province (e.g. GUIMARÃES et al. 2012, 2016; NEVES 2015; VAN SCHMUS et al. 1995, 2008).

Uplift of the asthenosphere may have provided the necessary heat for partial melting from Tonian/Stenian lower continental crust (including the source rocks of the studied plutons) during collision of the São Francisco and Pernambuco–Alagoas plates in the onset of the Brasiliano orogeny (e.g. OLIVEIRA et al. 2015a, 2015b).

Notwithstanding, extension prevailed before the beginning of the Brasiliano orogeny (at least, between 715–650 Ma; OLIVEIRA et al. 2010) and decompression also could have allowed partial melting of the asthenosphere and generation of basaltic magmas. These basaltic magmas underplated under the lower continental crust and triggered partial melting of the source rocks of the studied plutons (e.g. HUPPERT & SPARKS 1988; ANNEN & SPARKS 2002; ANNEN et al. 2006; SCHUBERT et al. 2013). Another possibility for the heat source to promote partial melting in the Borborema Province has been raised as heat-producing elements in the lithospheric mantle (NEVES et al. 2004, 2008).

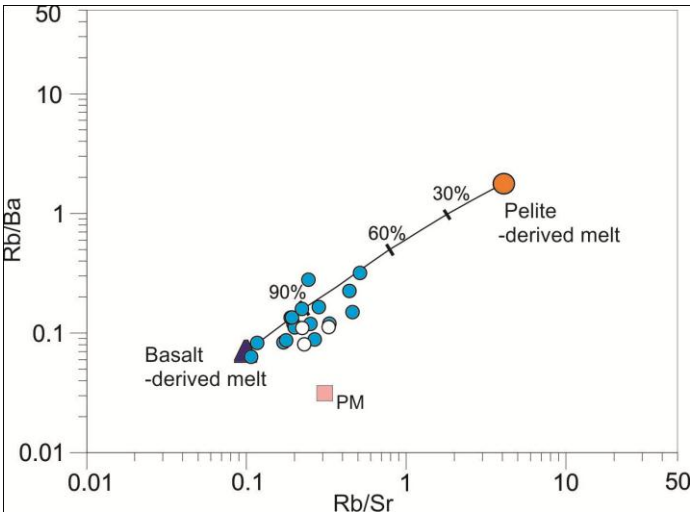

Figure 14. Rb/Sr *vs.* Rb/Ba for the studied plutons. A calculated mixing line shows the effect of mixing basalt and pelite-derived melts. Increments marked along the mixing line show the proportion of basalt-derived melt. PM field is from SUN & MCDONOUGH (1989).

An origin by a juvenile mantle-derived melt for the Santo Antonio granite can be ruled out; its origin is more compatible with remelting after ca. 350 Ma crustal residence time of mantle-derived rocks that evolved by fractional crystallization. A multi-stage process for the formation of the Santo Antonio granite could be suggested, including melting, assimilation, storage and homogenization (MASH) or deep crustal hot zones at the crust-mantle transition (HILDRETH & MOORBATH 1988, 1991; ANNEN et al. 2006; LACKEY et al. 2008). After that, fractional crystallization must have occurred during magma ascent, as supported by correlated variation on whole-rock major and trace elements and relatively similar Sr–Nd isotopic compositions, suggesting minor crustal assimilation during magma ascent. Crystal fractionation of hydrous mantle-derived basalts is well known as a fundamental mechanism by which arc

magmas evolve towards silicic compositions (e.g. SISSON et al. 2005; LEE & BACHMANN 2014; FODEN et al. 2015, KELLER et al. 2015). Magma mixing and/or mingling should have played some role (secondary) within the studied plutons as evidenced by the presence of mafic magmatic enclaves (e.g. POLI & TOMMASINI 1991).

A flat lying foliation is ubiquitous in basement gneiss, metasedimentary rocks, and early Brasiliano plutons throughout the Borborema Province (NEVES et al. 2005, 2006, 2012, 2015; VAN SCHMUS et al. 2008, 2011; SILVA FILHO et al. 2014, 2016; OLIVEIRA et al. 2015a, 2015b; among others). The studied plutons intruded along the Jacaré dos Homens shear zone, and also display a low-angle magmatic/gneissic foliation suggesting these bodies were intruded coeval with the period of formation of the flat-lying fabrics (640 to 610 Ma) associated with the compressive stage of the Brasiliano orogeny, probably during the top-to-the southeast tectonic in the region.

The mechanisms by which granite magma ascent through the crust remain debated (BROWN 2013). However, within the Borborema Province the close spatial relationship and temporal link between synkinematic granitic plutons and continental-scale shear zones have long been recognized as constituting the main mechanism of granite emplacement into the upper crust (NEVES et al. 1996, 2000, 2006; VAUCHEZ et al. 1995, 1997; WEINBERG et al. 2004). Some of these shear zones transect the entire crust and must have favored upward melt migration from different lithospheric levels (VAUCHEZ & EGYDIO-SILVA 1992; VAUCHEZ et al. 1995; DE OLIVEIRA 2008; SANTOS et al. 2014). The Jacaré dos Homens shear zone probably represents one of these deep- seated lithospheric shear zones rooted in the upper mantle that must have facilitated mantle-derived melts to rise, contributing to generate the Santo Antonio and Jacaré dos Homens plutons.

Available geophysical data shows that the Jacaré dos Homens shear zone coincides with a magnetic anomaly, and a negative–positive paired Bouguer anomaly oriented in an NE–SW direction, which displays an up to 30 mGal peak-to-peak difference, with predominantly negative anomalies towards north, and positive gravity anomalies toward south (DE OLIVEIRA 2008). Paired gravity anomalies are considered as an indication of suture zones (GIBB & THOMAS 1976; GUPTA et al. 2014). The Jacaré dos Homens shear zone together with the Palmeira dos Índios shear zone, which has a cryptic signature in the sense that no clear surface indications of continuity has yet been recognized (e.g. NEVES et al. 2016; MARTINS 2017), might represent the suture zone

between the south domain and the São Francisco-Congo plate. These shears could be the trace of a major ocean (i.e., Sergipano-Oubanguides) closure, with the subduction–collision–accretion tectonics along these zones related to the amalgamation of the Gondwana supercontinent (TROMPETTE 1997; OLIVEIRA et al. 2010; MERDITH et al. 2017).

CONCLUSIONS

The Jacaré dos Homens and Santo Antonio plutons have been studied to constrain their ages, sources, and petrogenesis.

(1) Petrological, geochemical and isotopic characteristics of the studied bodies are typical of high-K, calc-alkaline I-type granites;

(2) Isotopic data of the Jacaré dos Homens pluton ($^{87}Sr/^{86}Sr_I$ = 0.7068, and εNd_t = −1.58, and $\delta^{18}O_{zircon}$ = 7.0‰) suggest that the source rock was likely formed either by hybridization of an enriched Tonian mantle source with a felsic crustal rock component, or partial melting of Stenian (t_{DM} = 1.2 Ga) high-K basaltic lower continental crust. On the other hand, the isotopic characteristics of the Santo Antonio pluton are relatively unevolved ($^{87}Sr/^{86}Sr_I$ < 0.7052, εNd_t ~ − 0.67 to + 1.17 and $\delta^{18}O_{zircon}$ = 5.0 to 5.9‰) and together with the t_{DM} age of ca. 1.0 Ga reveal that these rocks were possibly generated by partial melting of Tonian lower crustal rocks derived from lithospheric mantle;

(3) Zircon SHRIMP U–Pb dating indicates that the Jacaré dos Homens and the Santo Antonio plutons were, respectively, formed at ca. 642 Ma and ca. 636 Ma, and ages likely correlated to early stages of the Brasiliano orogeny, probably associated with the assembly of the Gondwana supercontinent.

ACKNOWLEDGMENTS

We are indebted to Prof. José Maurício Rangel da Silva for geological discussions in the field. Constructive suggestions and comments from Maria de Lourdes da Silva Rosa, Julio Cezar Mendes, Adejardo Francisco da Silva Filho and Anelise Losângela Bertotti of an early version of this manuscript contributed to improve it. We are grateful for patient analysis and critical comments from Prof. Leon Long (University of Texas at Austin) and Prof. Michael Roden (University of Georgia) who spotted several imperfections and helped us to re-examine assumptions and to clarify ideas presented in this manuscript. Thanks are also due to Gilsa M. Santana and Vilma Sobral Bezerra for the assistance with oxygen isotope analyses, Severina Paulina for assistance with

chemical analyses at the Stable Isotope Laboratory (LABISE) in the Federal University of Pernambuco, Brazil, and Bruna Maria Borba de Carvalho for mineral analyses at the Electron Microprobe Laboratory in the University of Brasília, Brazil. TRS and MMCL are especially grateful to Kei Sato for the help and guidance with the U–Pb analysis on the SHRIMP IIe at the University of São Paulo, Brazil. VPF and ANS acknowledge the continuous financial support from the CNPq and FACEPE through several grants (PRONEX/FACEPE APQ-0479-1.07/06, APQ-0727-1.07/08, APQ-1738-1.07/12 and CNPq 478554/2009–5, 472842/2010-2, 471034/2012–6). This is the NEG–LABISE contribution n. 285.

REFERENCES

ABDEL-RAHMAN AFM (1994) Nature of Biotites from Alkaline, Calc-alkaline, and Peraluminous Magmas. Journal of Petrology 35(2):525–541

ALLÈGRE CJ (2008) Isotope Geology. Cambridge University Press, Cambridge, New York, Melbourne, Madrid, Cape Town, Singapore, São Paulo

ALMEIDA FFM, HASUI Y, BRITO NEVES, BB, FUCK, RA (1981) Brazilian Structural Provinces: An Introduction. Earth-Science Reviews 17(1–2):1–29

ANDERSON JL (1996) Status of thermobarometry in granitic batholiths. Transactions of the Royal Society of Edinburgh: Earth Sciences 87(1–2):125–138

ANDERSON JL, BARTH AP, WOODEN JL, MAZDAB F (2008) Thermometry and Thermobarometers in Granitic Systems. In: Putirka KD, Tepley III FJ (eds) Minerals, Inclusions and Volcanic Processes. Reviews in Mineralogy and Geochemistry 69, pp 121–142

ANNEN C, SPARKS RSJ (2002) Effects of repetitive emplacement of basaltic intrusions on thermal evolution and melt generation in the crust. Earth and Planetary Science Letters 203(3–4):937–955

ANNEN C, BLUNDY JD, SPARKS RSJ (2006) The genesis of intermediate and silicic magmas in deep crustal hot zones. Journal of Petrology 47(3):505–539

BARBARIN B (1999) A review of the relationships between granitoid types, their origins and their geodynamic environments. Lithos 46(3):605–626

BEARD JS, LOFGREN GE (1991) Dehydration Melting and Water-Saturated Melting of Basaltic and Andesitic Greenstones and Amphibolites at 1, 3, and 6.9 kb. Journal of Petrology 32(2):365–401

BLACK LP, KAMO SL, ALLEN CM, DAVIS DW, ALEINIKOFF JN, VALLEY JW, MUNDIL R, CAMPBELL IH, KORSCH RJ, WILLIAMS IS, FOUDOULIS C (2004) Improved $^{206}Pb/^{238}U$ microprobe geochronology by the monitoring of a trace-element-

related matrix effect; SHRIMP, ID-TIMS, ELA-ICP-MS and oxygen isotope documentation for a series of zircon standards. Chemical Geology 205(1–2):115–140

BOEHNKE P, WATSON EB, TRAIL D, HARRISON TM, SCHMITT AK (2013) Zircon saturation re-revisited. Chemical Geology 351:324–334

BONIN B (1990) From orogenic to anorogenic settings: Evolution of granitoid suites after a major orogenesis. Geological Journal 25(3–4):261–270

BONIN B, AZZOUNI-SEKKAL A, BUSSY F, FERRAG S (1998) Alkali-calcic and alkaline post-orogenic (PO) granite magmatism: petrologic constraints and geodynamic settings. Lithos 45(1–4):45–70

BRITO NEVES BB, SANTOS EJ, VAN SCHMUS WR (2000) Tectonic History of the Borborema Province, Northeastern Brazil. In: Cordani U, Milani EJ, Thomaz Filho A, Campos DA (eds) Tectonic Evolution of South America. International Geological Congress, 31st, Rio de Janeiro, Brazil, pp 151–182

BRITO MFL, SILVA FILHO AF, GUIMARÃES IP (2009) Geologia isotópica do batólito shoshonítico-ultrapotássico Neoproterozóico Serra do Catú e implicações na evolução da interface dos Domínios Canindé e Pernambuco–Alagoas. Revista Brasileira de Geociências 39(2):324–337

BROWN M (2013) Granite: From: Genesis to emplacement. Geological Society of American Bulletin 125(7–8):1079–1113

CAVOSIE AJ, KITA NT, VALLEY JW (2009) Primitive oxygen-isotope ratio recorded in magmatic zircon from the Mid-Atlantic Ridge. American Mineralogist 94:926–934

CHEN J-Y, YANG J-H, ZHANG J-H, SUN J-F, WILDE SA (2013) Petrogenesis of the Cretaceous Zhangzhou batholith in southeastern China: Zircon U–Pb age and Sr–Nd–Hf–O isotopic evidence. Lithos 162–163:140–156

CHAPPELL BW (1999) Aluminium saturation in I- and S-type granites and the characterization of fractionated haplogranites. Lithos 46(3):535–551

CHAPPELL BW, BRYANT CJ, WYBORN D (2012) Peraluminous I-type granites. Lithos 153:142–153

CHAPPELL BW, WHITE AJR, WILLIAMS IS, WYBORN D (2004) Low- and high-temperature granites. Transactions of the Royal Society of Edinburgh: Earth Sciences 95(1–2):125–140

COCHERIE A (1986) Systematic use of trace element distribution patterns in log-log diagrams for plutonic suites. Geochimica et Cosmochimica Acta 50(11):2517–2522

CONDIE KC, KRÖNER A (2013) The building blocks of continental crust: Evidence for a major change in the tectonic setting of continental growth at the end of the Archean. Gondwana Research 23(2):394–402

DEER WA, HOWIE RA, ZUSSMAN J (2013) An Introduction to the Rock-Forming Minerals. 3rd edn. Mineralogical Society, London

DE OLIVEIRA RG (2008) Arcabouço geofísico, isostasia e causas do magmatismo Cenozóico da Província Borborema e de sua margem continental (Nordeste do Brasil). PhD thesis, Federal University of Rio Grande do Norte, Brazil (in Portuguese with English abstract)

DEPAOLO D.J (1981) Neodymium isotopes in the Colorado Front Range and crust–mantle evolution in the Proterozoic. Nature 291:193–196

DEPAOLO DJ, Linn AM, Schubert G (1991) The continental crust age distribution: Methods of determining mantle separation ages from Sm–Nd isotopic data and application to the southwestern United States. Journal of Geophysical Research 96:2071–2088

DEPAOLO, D.J., 1988. Neodymium Isotope Geochemistry. An Introduction. Springer–Verlag, Berlin, Heidelberg

EILER JM (2001) Oxygen-isotope variations of basaltic lavas and upper mantle rocks. In: Valley JM, Cole DR (eds) Stable Isotope Geochemistry. Reviews in Mineralogy and Geochemistry 43, pp 319–364

EVANS BW, VANCE JA (1987) Epidote phenocrysts in dacitic dikes, Boulder County, Colorado. Contributions to Mineralogy and Petrology 96(2):178–185

FAURE G (1986) Principles of Isotope Geology. 2nd edn. John Wiley, New York

FERREIRA VP, SIAL AN, JARDIM de SÁ EF (1998) Geochemical and isotopic signatures of the Proterozoic granitoids in terranes of the Borborema Province, northeastern Brazil. Journal of South American Earth Sciences 11(5):439–455

FERREIRA VP, SIAL AN, PIMENTEL MM, MOURA CAV (2004) Acidic to intermediate magmatism and crustal evolution in the Transversal Zone, northeastern Brazil. In: Mantesso-Neto V, Bartorelli A, Carneiro CDR, Brito Neves BB (eds) Geologia do Continente Sul-americano: a evolução da obra de Fernando Flávio Marques de Almeida. Beca, São Paulo, pp 189–201

FERREIRA VP, SIAL AN, PIMENTEL MM, ARMSTRONG R, GUIMARÃES IP, SILVA FILHO AF, LIMA MMC, SILVA TR (2015) Reworked old crust-derived shoshonitic magma: The Guarany pluton, Northeastern Brazil. Lithos 232:150–161

FERREIRA VP, VALLEY JW, SIAL AN, SPICUZZA MJ (2003) Oxygen isotope compositions and magmatic epidote from two contrasting metaluminous granitoids, NE Brazil. Contributions to Mineralogy and Petrology 145(2):205–216

FODEN J, SOSSI PA, WAWRYK CM (2015) Fe isotopes and the contrasting petrogenesis of A-, I- and S-type granite. Lithos 212–215:32–44

FROST BR, BARNES CG, COLLINS WJ, ARCULUS RJ, ELLIS DJ, FROST CD (2001) A Geochemical Classification for Granitic Rocks. Journal of Petrology 42(11):2033–2048

FROST BR, FROST CD (2008) A Geochemical Classification for Feldspathic Igneous Rocks. Journal of Petrology 49(11):1955–1969

FURMAN T, GRAHAM D (1999) Erosion of lithospheric mantle beneath the East African Rift system: geochemical evidence from the Kivu volcanic province. Lithos 48:237–262

GANADE DE ARAUJO, CE, WEINBERG, RF, CORDANI UG (2014) Extruding the Borborema Province (NE-Brazil): a two-stage Neoproterozoic collision process. Terra Nova 26:157–168

GAO P, ZHENG Y-F, ZHAO Z-F (2016) Distinction between S-type and peraluminous I-type granites: Zircon versus whole-rock geochemistry. Lithos 258–259:77–91

GIBB RA, THOMAS MD (1976) Gravity signature of fossil plate boundaries in the Canadian Shield. Nature 262:199–200. doi:10.1038/262199a0

GREEN TH, ADAM J (2002) Pressure effect on Ti- or P-rich accessory mineral saturation in evolved granitic melts with differing K_2O/Na_2O ratios. Lithos 61(3–4):271–282

GREEN TH, WATSON EB (1982) Crystallization of Apatite in Natural Magmas Under High Pressure, Hydrous Conditions, with Particular Reference to 'Orogenic' Rock Series. Contributions to Mineralogy and Petrology 79(1):96–105

GUIMARÃES IP, SILVA FILHO AF, ALMEIDA CN, MACAMBIRA MB, ARMSTRONG R (2011) U–Pb SHRIMP data constraints on calc-alkaline granitoids with 1.3–1.6 Ga Nd T_{DM} model ages from the central domain of the Borborema province, NE Brazil. Journal of South American Earth Sciences 31:383–396

GUIMARÃES, I.P., SILVA FILHO, A.F., ALMEIDA, C.N., VAN SCHMUS, W.R., ARAÚJO, J.M.M., MELO, S.C., MELO, E,B., 2004. Brasiliano (Pan-African) granitic magmatism in the Pajeú-Paraíba belt, Northeast Brazil: an isotopic and geochronological approach. Precambrian Research 135(1–2), 23–53.

GUIMARÃES IP, BRITO MFL, LAGES GA, SILVA FILHO AF, SANTOS L, BRASILINO RG (2016) Tonian granitic magmatism of the Borborema Province, NE Brazil: A review. Journal of South American Earth Sciences 68:97–112

GUIMARÃES IP, VAN SCHMUS WR, BRITO NEVES BB, BITTAR SMB, SILVA FILHO AF, ARMSTRONG R., (2012) U–Pb zircon ages of orthogneisses and supracrustal rocks of the Cariris Velhos belt: onset of Neoproterozoic rifting in the Borborema Province, NE Brazil. Precambrian Research 192–195:52–77

GUPTA S, MOHANTY WK, MANDAL A, MISRA S (2014) Ancient terrane boundaries as probable seismic hazards: A case study from the northern boundary of the Eastern Ghats Belt, India. Geoscience Frontiers 5:17 –24

HARRISON TM, WATSON EB (1984) The behavior of apatite during crustal anatexis: Equilibrium and kinetic considerations. Geochimica et Cosmochimica Acta 48(7):1467–1477

HART S.R, GERLACH DC, WHITE WM (1986) A possible new Sr–Nd–Pb mantle array and consequences for mantle mixing. Geochimica et Cosmochimica Acta 50:1551–1557

HAWKESWORTH CJ, KEMP AIS (2006) Using hafnium and oxygen isotopes in zircons to unravel the record of crustal evolution. Chemical Geology 226:144–162

HEALY B, COLLINS WJ, RICHARDS SW (2004) A hybrid origin for Lachlan S-type granites: the Murrumbidgee Batholith example. Lithos 78(1–2):197–216

HILDRETH W, MOORBATH S (1988) Crustal contributions to arc magmatism in the Andes of Central Chile. Contributions to Mineralogy and Petrology 98(4):455–489

HILDRETH W, MOORBATH S (1991) Reply to Comment on "Crustal contributions to arc magmatism in the Andes of Central Chile" by W. Hildreth and S. Moorbath. Contributions to Mineralogy and Petrology 108(1–2):247–252

HOFMANN AW, WHITE WM (1983) Ba, Rb, and Cs in the Earth's mantle. Zeitschrift für Naturforschung A 38(2):256–266

HOFMANN AW (2003) Sampling mantle heterogeneity through oceanic basalts: Isotopes and trace elements. In: Holland HD, Turekian KK (eds) The Mantle and Core. Treatise on Geochemistry 2, pp 1–44. doi:10.1016/B0-08-043751-6/02123-X

HOSKIN PWO, BLACK LP (2000) Metamorphic zircon formation by solid-state recrystallization of protolith igneous zircon. Journal of Metamorphic Geology 18(4):423–439

HOSKIN PWO, SCHALTEGGER U (2003) The Composition of Zircon and Igneous and Metamorphic Petrogenesis. In: Hanchar JM, Hoskin PWO (eds) Zircon. Reviews in Mineralogy and Geochemistry 53, pp 27–62

HUPPERT HE, SPARKS RS (1988) The Generation of Granitic Magmas by Intrusion of Basalt into Continental Crust. Journal of Petrology 29(3):599–624

JACOBSEN SB, WASSERBURG GJ (1980) Sm–Nd isotopic evolution of chondrites. Earth and Planetary Science Letters 50(1):139–155

KAWASHITA K (1972) O método Rb–Sr em rochas sedimentares. PhD thesis, University of São Paulo, Brazil (in Portuguese with English abstract)

KELLER CB, SCHOENE B, BARBONI M, SAMPERTON KM, HUSSON JM (2015) Volcanic–plutonic parity and the differentiation of the continental crust. Nature 523, 301–307. doi:10.1038/nature14584

KING EM, VALLEY JW, DAVIS DW, EDWARDS G.R (1998) Oxygen isotope ratios of Archean plutonic zircons from granite-greenstone belts of the Superior Province: indicator of magmatic source. Precambrian Research 92(4):365–387

LACKEY JS, VALLEY JW, CHEN JH, STOCKLI DF (2008) Dynamic Magma Systems, Crustal Recycling, and Alteration in the Central Sierra Nevada Batholith: the Oxygen Isotope Record. Journal of Petrology 49(7):1397–1426

LEE C-TA, BACHMANN O (2014) How important is the role of crystal fractionation in making intermediate magmas? Insights from Zr and P systematics. Earth and Planetary Science Letters 393:266–274

LI B, JIANG S-Y, LU A-H, ZHAO H-X, YANG T-L, HOU M-L (2016) Zircon U–Pb dating, geochemical and Sr–Nd–Hf isotopic characteristics of the Jintonghu monzonitic rocks in western Fujian Province, South China: Implication for Cretaceous crust–mantle interactions and lithospheric extension. Lithos 260:413–428

LI XH, LI WX, WANG XC, LI QL, LIU Y, TANG GQ (2009) Role of mantle-derived magma in genesis of early Yanshanian granites in the Nanling Range, South China: in situ zircon Hf–O isotopic constraints. Science in China Series D: Earth Sciences 52(9):1262–1278

LIÉGEOIS JP, NAVEZ J, HERTOGEN J, BLACK R (1998) Contrasting origin of post-collisional high-K calc-alkaline and shoshonitic versus alkaline and peralkaline granitoids. The use of sliding normalization. Lithos 45(1–4):1–28

LIOU JG (1973) Synthesis and Stability Relations of Epidote, $Ca_2Al_2FeSi_3O_{12}(OH)$. Journal of Petrology 14(3):381–413

LIU D, ZHAO Z, ZHU D-C, NIU Y, DEPAOLO DJ, HARRISON TM, MO X, DONG G, ZHOU S, SUN C, ZHANG Z, LIU J (2014) Postcollisional potassic and ultrapotassic rocks in Southern Tibet: Mantle and crustal origins in response to India–Asia collision and convergence. Geochimica et Cosmochimica Acta 143:207–231

LUDWIG KR (2009) User´s Manual for Isoplot/Ex, version 3.71: A Geochronological Toolkit for Microsoft Excel. Berkeley Geochronology Center, Special Publication 5

LUGMAIR GW, MARTI K (1978) Lunar initial $^{143}Nd/^{144}Nd$: Differential evolution of the lunar crust and mantle. Earth and Planetary Science Letters 39(3):349–357

MARTINS EP (2017) Análises geométrica e cinemática meso-microscópica das zonas de cisalhamento Palmeira dos Índios e Jacaré dos Homens: Significância geodinâmica destas estruturas para a zona de limite entre o Domínio Pernambuco–Alagoas e a Faixa Sergipana. Dissertation, Federal University of Pernambuco, Brasil (in Portuguese with English abstract)

MCDONOUGH WF, SUN S-S (1995) The composition of the Earth. Chemical Geology 120(3–4):223–253

MERDITH AS, COLLINS AS, WILLIAMS SE, PISAREVSKY S, FODEN JD, ARCHIBALD DB, BLADES ML, ALESSIO BL, ARMISTEAD S, PLAVSA D, CLARK C, MÜLLER RD (2017) A full-plate global reconstruction of the Neoproterozoic. Gondwana Research 50:84–134

MILLER CF (1985) Are Strongly Peraluminous Magmas Derived from Pelitic Sedimentary Sources? Journal of Geology 93(6):673–689

MILLER CF, MCDOWELL SM, MAPES RW (2003) Hot and cold granites? Implications of zircon saturation temperatures and preservation of inheritance. Geology 31(6):529–532

NANDEDKAR RH, ULMER P, MÜNTENER O (2014) Fractional crystallization of primitive, hydrous arc magmas: an experimental study at 0.7 GPa. Contributions to Mineralogy and Petrology 167:1015

NEVES SP (2015) Constraints from zircon geochronology on the tectonic evolution of the Borborema Province (NE Brazil): Widespread intracontinental Neoproterozoic reworking of a Paleoproterozoic accretionary orogen. Journal of South American Earth Sciences 58:150–164

NEVES SP, BRUGUIER O, BOSCH D, SILVA JMR, MARIANO G (2008) U–Pb ages of plutonic and metaplutonic rocks in southern Borborema Province (NE Brazil): Timing of Brasiliano deformation and magmatism. Journal of South American Earth Sciences 25(3):285–297

NEVES SP, BRUGUIER O, BOSCH D, SILVA JMR, MARIANO G, SILVA FILHO AF, TEIXEIRA CML (2015) From extension to shortening: Dating the onset of the Brasiliano Orogeny in eastern Borborema Province (NE Brazil). Journal of South American Earth Sciences 58:238–256

NEVES SP, BRUGUIER O, VAUCHEZ A, BOSCH D, SILVA JMR, MARIANO, G (2006) Timing of crust formation, deposition of supracrustal sequences, and Transamazonian and Brasiliano metamorphism in the East Pernambuco belt (Borborema Province, NE Brazil): Implications for western Gondwana assembly. Precambrian Research 149(3–4):197–216

NEVES SP, MARIANO G (2004) Heat-producing elements-enriched continental mantle lithosphere and Proterozoic intracontinental orogens: Insights from Brasiliano/Pan-African belts. Gondwana Research 7:427–436

NEVES SP, MONIÉ P, BRUGUIER O, SILVA JMR (2012) Geochronological, thermochronological and thermobarometric constraints on deformation, magmatism and thermal regimes in eastern Borborema Province (NE Brazil). Journal of South American Earth Sciences 38:129–146

NEVES SP, SILVA JMR, BRUGUIER O (2016) The transition zone between the Pernambuco–Alagoas Domain and the Sergipano Belt (Borborema Province, NE Brazil): Geochronological constraints on the ages of deposition, tectonic setting and metamorphism of metasedimentary rocks. Journal of South American Earth Sciences 72:266–278

NEVES SP, SILVA JMR, MARIANO G (2005) Oblique lineations in orthogneisses and supracrustal rocks: vertical partitioning of strain in a hot crust (eastern Borborema Province, NE Brazil). Journal of Structural Geology 27(8):1513–1527

NEVES SP, TOMMASI A, VAUCHEZ A, HASSANI R (2008) Intraplate continental deformation: Influence of a heat-producing layer in the lithospheric mantle. Earth and Planetary Science Letters 274:392–400

NEVES SP, VAUCHEZ A, ARCHANJO CJ (1996) Shear zone-controlled magma emplacement or magma-assisted nucleation of shear zones? Insights from northeast Brazil. Tectonophysics 262(1–4):349–364

NEVES SP, VAUCHEZ A, FÉRAUD G (2000) Tectono-thermal evolution, magma emplacement, and shear zone development in the Caruaru area (Borborema Province, NE Brazil). Precambrian Research 99(1–2):1–32

NOYES HJ, FREY FA, WONES DR (1983) A Tale of Two Plutons: Geochemical Evidence Bearing on the Origin and Differentiation of the Red Lake and Eagle Peak Plutons, Central Sierra Nevada, California. Journal of Geology 91(5):487–509

OLIVEIRA EP, BUENO JF, MCNAUGHTON N, SILVA FILHO AF, NASCIMENTO RS, DONATTI-FILHO JP (2015a) Age, composition, and source of continental arc- and syncollision granites of the Neoproterozoic Sergipano Belt, Southern Borborema Province, Brazil. Journal of South American Earth Sciences 58:257–280

OLIVEIRA EP, MCNAUGHTON NJ, WINDLEY BF, CARVALHO MJ, NASCIMENTO RS (2015b) Detrital zircon U–Pb geochronology and whole-rock Nd-isotope constraints on sediment provenance in the Neoproterozoic Sergipano orogen, Brazil: From early passive margins to late foreland basins. Tectonophysics 662:183–194

OLIVEIRA EP, WINDLEY BF, ARAÚJO MNC (2010) The Neoproterozoic Sergipano orogenic belt, NE Brazil: A complete plate tectonic cycle in western Gondwana. Precambrian Research 181(1–4):64–84

O'NEIL JR, SHAW SE, FLOOD RH (1977) Oxygen and hydrogen isotope compositions as indicators of granite genesis in the New England batholith, Australia. Contributions to Mineralogy and Petrology 62(3):313–325

PATCHETT PJ, VERVOORT JD, SÖDERLUND U, SALTERS VJM (2004) Lu–Hf and Sm–Nd isotopic systematics in chondrites and their constraints on the Lu–Hf properties of the Earth. Earth and Planetary Science Letters 222(1):29–41

PATIÑO DOUCE AE, BEARD JS (1995) Dehydration-melting of Biotite Gneiss and Quartz Amphibolite from 3 to 15 kbar. Journal of Petrology 36(3):707–738

PATIÑO DOUCE AE, JOHNSTON AD (1991) Phase equilibria and melt productivity in the pelitic system: implications for the origin of peraluminous granitoids and aluminous granulites. Contributions to Mineralogy and Petrology 107(2):202–218

PETFORD N, ATHERTON M (1993) Na-rich Partial Melts from Newly Underplated Basaltic Crust: the Cordillera Blanca Batholith, Peru. Journal of Petrology 37(6):1491–1521

POLI GE, TOMMASINI S (1991) Model for the Origin and Significance of Microgranular Enclaves in Calc-alkaline Granitoids. Journal of Petrology 32(3):657–666

RAPP RP, WATSON EB (1995) Dehydration Melting of Metabasalt at 8–32 kbar: Implications for Continental Growth and Crust–Mantle Recycling. Journal of Petrology 36(4):891–931

ROBERTS MP, CLEMENS JD (1993) Origin of high-potassium, calc-alkaline, I-type granitoids. Geology 21(9):825–828

ROLLINSON H (1993) Using Geochemical Data: Evaluation, Presentation, Interpretation. Longman Scientific and technical, London

ROTENBERG E, DAVIS DW, AMELIN Y, GHOSH S, BERGQUIST BA (2012) Determination of the decay-constant of ^{87}Rb by laboratory accumulation of ^{87}Sr. Geochimica et Cosmochimica Acta 85:41–57

RUDNICK RL, FOUNTAIN DM (1995) Nature and composition of the continental crust: A lower crustal perspective. Reviews of Geophysics 33(3):267–309

SANTOS ACL, PADILHA AL, FUCK RA, PIRES ACB, VITORELLO I, PÁDUA MB (2014) Deep structure of a stretched lithosphere: Magnetotelluric imaging of the southeastern Borborema province, NE Brazil. Tectonophysics 610:39–50

SATO K, TASSINARI CCG, KAWASHITA K, PETRONILHO L (1995) O método Geocronológico Sm–Nd no IG/USP e suas aplicações. Anais da Academia Brasileira de Ciências 67(3):313–336

SATO K, TASSINARI CCG, BASEI MAS, SIGA Jr O, ONOE AT, SOUZA MD (2014) Sensitive High Resolution Ion Microprobe (SHRIMP IIe/MC) of the Institute of Geosciences of the University of São Paulo, Brazil: analytical method and first results. Geologia USP: Série Cientifica 14(3):3–18

SCHUBERT M, DRIESNER T, GERYA TV, ULMER P (2013). Mafic injection as a trigger for felsic magmatism: a numerical study. Geochemistry, Geophysics, Geosystems 14(6):1910–1928

SCHMIDT MW, POLI S (2004) Magmatic Epidote. Reviews in Mineralogy and Geochemistry 56, pp 399–430

SCHMIDT MW, THOMPSON AB (1996) Epidote in calc-alkaline magmas: An experimental study of stability, phase relationships, and the role of epidote in magmatic evolution. American Mineralogist 81:462–474

SIAL AN (1990) Epidote-bearing calc-alkalic granitoids in Northeast Brazil. Revista Brasileira de Geociências 20(1–4):88–100

SIAL AN (1993) Contrasting metaluminous magmatic epidote-bearing granitic suites from two Precambrian Foldbelts in Northeast Brazil. Anais da Academia Brasileira de Ciências 65 (suppl.):141–162

SIAL AN, TOSELLI AJ, SAAVEDRA J, PARADA MA, FERREIRA VP (1999) Emplacement, petrological and magnetic susceptibility characteristics of diverse magmatic epidote-bearing granitoid rocks in Brazil, Argentina and Chile. Lithos 46(3):367–392

SIAL AN, VASCONCELOS PM, FERREIRA VP, PESSOA RR, BRASILINO RG, MORAIS NETO JM (2008) Geochronological and mineralogical constraints on depth of emplacement and ascension rates of epidote-bearing magmas from northeastern Brazil. Lithos 105(3–4):225–238

SIAL AN, FERREIRA VP (2016) Magma associations in Ediacaran granitoids of the Cachoeirinha–Salgueiro and Alto Pajeú terranes, northeastern Brazil: Forty years of studies. Journal of South American Earth Sciences 68:113–133

SILVA FILHO AF, GUIMARÃES IP, VAN SCHMUS WR (2002) Crustal Evolution of the Pernambuco–Alagoas Complex, Borborema Province, NE Brazil: Nd Isotopic Data from Neoproterozoic Granitoids. Gondwana Research 5(2):409–422

SILVA FILHO AF, GUIMARÃES IP, FERREIRA VP, ARMSTRONG R, SIAL, A.N (2010) Ediacaran Águas Belas pluton, Northeastern Brazil: Evidence on age, emplacement and magma sources during Gondwana amalgamation. Gondwana Research 17(4):676–687

SILVA FILHO AF, GUIMARÃES IP, VAN SCHMUS WR, DANTAS E, ARMSTRONG R, COCENTINO L, LIMA D (2013) Long–lived Neoproterozoic high-K magmatism in the Pernambuco–Alagoas Domain, Borborema Province, Northeast Brazil. International Geology Review 55(10):1280–1299

SILVA FILHO AF, GUIMARÃES IP, VAN SCHMUS WR, ARMSTRONG RA, SILVA JMR, COCENTINO LM, OSAKO LS (2014) SHRIMP U–Pb zircon geochronology and Nd signatures of supracrustal sequences and orthogneisses constrain the Neoproterozoic evolution of the Pernambuco–Alagoas Domain, southern part of Borborema Province, NE Brazil. International Journal of Earth Sciences 103(8):2155–2190

SILVA FILHO AF, GUIMARÃES IP, SANTOS L, ARMSTRONG R, VAN SCHMUS WR (2016) Geochemistry, U–Pb geochronology, Sm–Nd and O isotopes of ca. 50 Ma long Ediacaran High-K Syn-Collisional Magmatism in the Pernambuco Alagoas

Domain, Borborema Province, NE Brazil. Journal of South American Earth Sciences 68:134–154

SILVA TR, FERREIRA VP, LIMA MMC, SIAL AN (2016) Two stage mantle-derived granitic rocks and the onset of the Brasiliano orogeny: Evidence from Sr, Nd, and O isotopes. Lithos 264:189–200

SILVA TR, FERREIRA VP, LIMA MMC, SIAL AN, SILVA JMR (2015) Synkinematic emplacement of the magmatic epidote bearing Major Isidoro tonalite-granite batholith: Relicts of an Ediacaran continental arc in the Pernambuco–Alagoas domain, Borborema Province, NE Brazil. Journal of South American Earth Sciences 64:1–13

SISSON TW, RATAJESKI K, HANKINS WB, GLAZNER AF (2005) Voluminous granitic magmas from common basaltic sources. Contributions to Mineralogy and Petrology 148(6):635–661

SPEER JA (1984) Micas in igneous rocks. Reviews in Mineralogy 13, pp 299–356

SUN S-S, MCDONOUGH WF (1989) Chemical and isotopic systematics of oceanic basalts: implications for mantle composition and processes. In: Saunders AD, Norry MJ (eds) Magmatism in the Ocean Basins. Geological Society, London, Special Publications 42, pp 313–345

TAYLOR SR, MCLENNAN SM (1985) The continental crust: Its composition and evolution. Blackwell Scientific Publications, Oxford

TEPPER JH, NELSON BK, BERGANTZ GW, IRVING AJ (1993) Petrology of the Chilliwack batholith, North Cascades, Washington: generation of calc-alkaline granitoids by melting of mafic lower crust with variable water fugacity. Contributions to Mineralogy and Petrology 113(3):333–351

TOLLARI N, TOPLIS MJ, BARNES S-J (2006) Predicting phosphate saturation in silicate magmas: An experimental study of the effects of melt composition and temperature. Geochimica et Cosmochimica Acta 70(6):1518–1536.

TROMPETTE R (1997) Neoproterozoic (~600 Ma) aggregation of Western Gondwana: a tentative scenario. Precambrian Research 82(1–2):101–112

TULLOCH AJ (1979) Secondary Ca–Al Silicates as Low-Grade Alteration Products of Granitoid Biotite. Contributions to Mineralogy and Petrology 69(2):105–117

TULLOCH AJ (1986) Comment on “Implications of magmatic epidote-bearing plutons on crustal evolution in the accreted terranes of northwestern North America” and “Magmatic epidote and its petrologic significance”. Geology 14(2):186–187

VALLEY JW, CHIARENZELLI JR, MCLELLAND JM (1994) Oxygen isotope geochemistry of zircon. Earth and Planetary Science Letters 126(4):187–206

VALLEY JW, KINNY PD, SCHULZE DJ, SPICUZZA MJ (1998) Zircon megacrysts from kimberlite: oxygen isotope variability among mantle melts. Contributions to Mineralogy and Petrology 133(1–2):1–11

VALLEY JW, KITCHEN N, KOHN MJ, NIENDORF CR, SPICUZZA MJ (1995) UWG-2, a garnet standard for oxygen isotope ratios: Strategies for high precision and accuracy with laser heating. Geochimica et Cosmochimica Acta 59(24):5223–5231

VALLEY JW, LACKEY JS, CAVOSIE AJ, CLECHENKO CC, SPICUZZA MJ, BASEI MAS, BINDEMAN IN, FERREIRA VP, SIAL AN, KING EM, PECK WH, SINHA AK, WEI CS (2005) 4.4 billion years of crustal maturation: oxygen isotope ratios of magmatic zircon. Contributions to Mineralogy and Petrology 150(6):561–580

VAN SCHMUS WR, BRITO NEVES BB, HACKSPACHER PC, BABINSKY M (1995) U/Pb and Sm/Nd geochronologic studies of the eastern Borborema Province, NE Brazil. Journal of South American Earth Sciences 8(3–4):267–288

VAN SCHMUS WR, OLIVEIRA EP, SILVA FILHO AF, TOTEU SF, PENAYE J, GUIMARÃES IP (2008) Proterozoic links between the Borborema Province, NE Brazil and the Central African Fold Belt. In: Pankhurst RJ, Trouw RAJ, Brito Neves BB, De Wit MJ (eds) West Gondwana: Pre-Cenozoic Correlations Across the South Atlantic Region. Geological Society, London, Special Publications 294, pp 69–99. doi:10.1144/SP294.5

VAN SCHMUS WR, KOZUCH M, BRITO NEVES BB (2011) Precambrian history of the Zona Transversal of the Borborema Province, NE Brazil: Insights from Sm–Nd and U–Pb geochronology. Journal of South American Earth Sciences 31(2–3):227–252

VAUCHEZ A, NEVES S, CABY R, CORSINI M, EGYDIO-SILVA M, ARTHAUD M, AMARO V (1995) The Borborema shear zone system, NE Brazil. Journal of South American Earth Sciences 8(3–4):247–266

VAUCHEZ A, EGYDIO-SILVA M (1992) Termination of a continental-scale strike-slip fault in partially melted crust: The West Pernambuco shear zone, northeast Brazil. Geology 20(11):1007–1010

WATSON EB, HARRISON TM (1983) Zircon saturation revisited: temperature and composition effects in a variety of crustal magma types. Earth and Planetary Science Letters 64(2):295–304

WEINBERG RF, SIAL AN, MARIANO G (2004) Close spatial relationship between plutons and shear zones. Geology 32(5):377–380

WILLIAMS IS (1998) U–Th–Pb geochronology by ion microprobe. In: McKibben MA, Shanks WC, Ridley WI (eds) Applications of Microanalytical Techniques to Understanding Mineralizing Processes. Reviews in Economic Geology 7, pp 1–35

WILLIAMS IS, CLAESSON S (1987) Isotopic evidence for the Precambrian provenance and Caledonian metamorphism of high grade paragneisses from the Seve

Nappes, Scandinavian Caledonides II. Ion microprobe zircon U–Pb–Th. Contribution to Mineralogy and Petrology 97(2):205–217

WILSON M (1989) Igneous Petrogenesis–A Global Tectonic Approach. Chapman and Hall, London

WOLF MB, WYLLIE PJ (1994) Dehydration-melting of amphibolite at 10 kbar: the effects of temperature and time. Contributions to Mineralogy and Petrology 115(4):369–383

WONES DR (1989) Significance of the assemblage titanite + magnetite + quartz in granitic rocks. American Mineralogist 74(7–8)744–749

ZEN E-A (1986) Aluminum Enrichment in Silicate Melts by Fractional Crystallization: Some Mineralogic and Petrographic Constraints. Journal of Petrology 27(5):1095–1117

ZEN E-A, HAMMARSTROM JM (1984) Magmatic epidote and its petrologic significance. Geology 12(9):515–518

ZINDLER A, HART S (1986) Chemical geodynamics. Annual Reviews of Earth and Planetary Science 14:493–571

6 MINERALOGY AND MINERAL CHEMISTRY OF THE CALC-ALKALINE EPIDOTE-BEARING MAJOR ISIDORO AND MONTEIRÓPOLIS PLUTONS, BORBOREMA PROVINCE, NE BRAZIL (to submit)

Thyego R. Silva, Valderez P. Ferreira, Mariucha Maria C. Lima, Alcides N. Sial
NEG-LABISE, Department of Geology, Federal University of Pernambuco, Recife, PE, Brazil

---

ABSTRACT

We report mineralogy and mineral chemistry from two new discovery magmatic epidote-bearing plutons (Major Isidoro and Monteirópolis) that were emplaced along the NE-SW-trending Jacaré dos Homens transpressional shear zone, at the boundary between the Sergipano and Pernambuco–Alagoas domains, during the onset of the Brasiliano orogeny at circa 626 Ma. These rocks are composed of medium-to-porphyritic granite to tonalite that show flat-lying foliation, with abundant dioritic enclaves. The mineral assemblage comprises quartz, K-feldspar and plagioclase as essential phases, and biotite, amphibole, titanite, epidote, apatite, zircon, and Fe–Ti phases as accessory minerals. Micas from both plutons are classified as biotite from calc-alkaline granitoids. Pistacite [100 x Fe^{3+}/ $(Fe^{3+} + Al)_{Molar}$] in the Major Isidoro pluton is in the interval of 27 to 29 mol% and in the Monteirópolis pluton range from 29 to 31 mol%, and TiO_2 in both of them is < 0.30% by weight, which are typical from magmatic epidote (mEp). Hornblende in the Monteirópolis pluton is edenite to ferro-edenite, whereas in the granitoids and enclaves of the Major Isidoro pluton it is hastingsite and magnesiohastingsite, respectively. Al-in-hornblende barometry and hornblende-plagioclase thermometry for granites and enclaves of the Major Isidoro pluton indicates pressure of 5.3 to 7.71 kbar and 5.83 to 5.96 kbar at a temperature (H&B, 1994TB) of 684 to 720 ºC and 730 to 735 °C, respectively. For granites of the Monteirópolis pluton hornblende solidified between 4.3–5.34 kbar (15–17.3 km depth), at 660 to 696 °C. The coexistent mineral assemblage, pistacite contents of the magmatic epidote, and Fe# [$Fe^{Amp}/(Fe^{Amp} + Mg^{Amp})$] ratios ranging from 0.55 to 0.639 suggest magma crystallization under high fO_2. Calculated near-liquidus Zr temperatures from the Major Isidoro and Monteirópolis plutons are respectively 740 to 868 °C and 763 to 856 °C. The Jacaré dos Homens shear zone must have acted faciliting rapid upward transport through the continental crust during onset of the Brasiliano orogeny (650–620

Ma) as indicated by partial dissolution of epidote. Partial corrosion occurred during 15.6 to 32 years (Major Isidoro), and 27–49 years (Monteirópolis) corresponding to upward transport rates of 365 to 750, and 395 to 635 m.years^{-1} respectively.

Keywords: Borborema Province, calc-alkaline orogenic rocks, Magmatic epidote, crystallization conditions

---

* Corresponding author: NEG–LABISE, Dept. of Geology, Av. Acadêmico Hélio Ramos s/n, Cidade Universitária, Recife, PE, 50740-550, Brazil; phone/fax: +55 81 2126 8243; e-mail: rthyego@yahoo.com

INTRODUCTION

The Borborema Province comprises several magma associations that were recognized as contain magmatic epidote (mEp) (SIAL, 1990, 1993; GALINDO et al., 1995; BRASILINO et al., 1999; SIAL et al., 1999, 2008; FERREIRA et al., 1998; 2003, 2004, 2011; CAMPOS et al., 2005; LONG et al., 2005; SIAL & FERREIRA 2015; CAMPOS et al., 2016; among others). Early studies on mineral chemistry of natural and experimental assemblages showed that ferromagnesian and coexisting phases constitute a way for estimating intensive crystallization parameters of granitoids (e.g., ANDERSON et al., 2008; among many others). Biotite composition has been largely used as a redox and tectonomagmatic indicators (e.g., WONES & EUGSTER 1965; NACHIT et al., 1985; ADDEL-RAHMAN 1994; SHABANI & LALONDI 2003; among others). Calcic amphiboles are of special interest because of their compositional diversity and common occurrence that provide huge potential to investigate magmatic process (PUTIRKA 2016) and this phase has been successfully employed as a geobarometry and together with plagioclase (the pair amphibole-plagioclase) as a powerful geothermometry (e.g., HAMMARSTRON & ZEN 1986; HOLLISTER et al., 1987; SCHMIDT 1992; HOLLAND & BLUNDY 1994; among others). Titanite shows potential to quantitative estimates of pressure and temperature (e.g., ENAMI et al., 1993). Magmatic epidote was initially ascribed as indicating high-pressures of crystallization in intermediate calc-alkaline rocks (> 0.5 GPa; ZEN & HAMMARSTRON 1984). However, this phase is strongly dependent on oxygen fugacity and bulk composition. Thus, at fO_2 buffered by HM (hematite-magnetite) the stability of epidote is shifted to more low pressure (> 0.3 GPa; FERREIRA et al., 2003; SCHMIDT & THOMPSON 1996; SCHMIDT & POLI 2004). This phase has been successfully employed to measure the ascension rate of epidote-bearing magma (e.g.,

SIAL et al., 1999, 2008; BRASILINO et al., 2011). The presence of mEp within the Pernambuco–Alagoas Domain was discovery late (cf., SILVA et al., 2015, 2016; FERREIRA et al., 2015) and its presence in the Águas Belas–Canindé batholith was described on the basis of textural criteria by SILVA et al. (2015) for the Major Isidoro pluton.

Mineral and whole rock chemistries constitute an important way to assess intensive crystallization parameters and know the nature, source, and evolution of the magmatism. In this work, we deal with chemical data from biotite, hornblende, plagioclase, titanite, and epidote from two calc-alkaline mEp-bearing plutons (named Major Isidoro and Monteirópolis) in order to estimate the physical conditions at which they were crystallized.

GEOLOGICAL BACKGROUND

The Borborema Province (NE Brazil) is characterized by widespread Neoproterozoic-Cambrian granitic magmatism associated to shear zones control (FERREIRA et al., 1998, 2004; GUIMARÃES et al., 2004; NEVES et al., 1995; 2006, 2012; VAUCHEZ et al., 1995; VAN SCHMUS et al., 1995; 2008) which could be divided into six main domains: one of them named Pernambuco–Alagoas (Fig. 1). Within this domain were identified three granitoid associations; shoshonitic, calc-alkaline and high-K calc-alkaline (e.g., BRITO et al., 2009; FERREIRA et al., 2015; NEVES et al., 2008, 2012; SILVA FILHO et al., 2002, 2016; SILVA et al., 2015, 2016). SILVA FILHO et al. (2014) divided this domain into the Garanhuns, Água Branca, and Palmares sub-domains. Rocks of the Garanhuns sub-domain (northern portion) are derived predominantly from older sources, whereas the others sub-domains (southern portion) contain rocks derived from substantially younger sources. The Buíque–Paulo Afonso, Águas Belas–Canindé and Ipojuca–Atalaia granitic batholiths (SILVA FILHO et al., 2002), each consisting of various plutons, intruded Paleoproterozoic migmatitic gneisses (SILVA et al., 2002; NEVES et al., 2004). Most of these composite batholiths occur into the Água Branca and Palmares sub-domains.

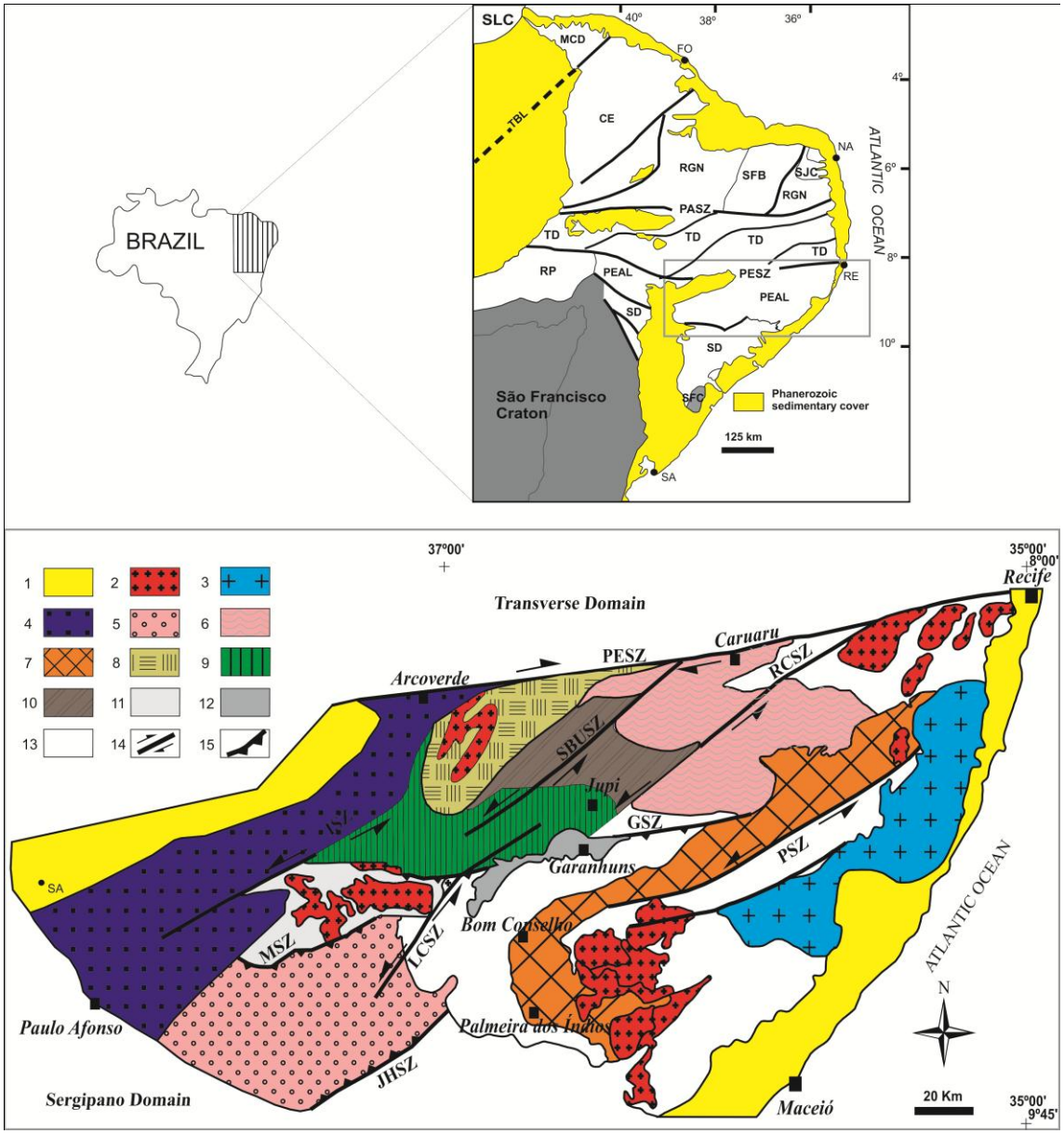

Figure 2. Borborema Province. Major domains: MCD - Médio Coreaú; CE - Ceará; RGN - Rio Grande do Norte (SFB - Seridó Fold Belt; SJC - São José do Campestre Archaean nucleus); TD - Transverse; PEAL - Pernambuco–Alagoas; RP - Riacho do Pontal; SD - Sergipano; SFC - São Francisco Craton; SLC - São Luís Craton; Faults and shear zones: PASZ - Patos shear zone; PESZ - Pernambuco shear zone; TBL - Transbrasiliano Lineament. Cities and towns: Fo - Fortaleza; Na - Natal; Re - Recife; Sa - Salvador (VAN SCHMUS et al., 2008). Geologic map of the Pernambuco–Alagoas Domain. 1 - Phanerozoic sedimentary cover; 2 – other Brasiliano granitoids; 3 - Ipojuca–Atalaia batholith; 4 - Buíque–Paulo Afonso batholith; 5 - Águas Belas–Canindé batholith; 6 - Granitoids and orthognaisses; 7 - Palmares Sequence; 8 - Rio Una (Unit 1) Sequence; 9 - Rio Una (Unit 2) Sequence; 10 - Rio Una (Unit 3) Sequence; 11 - Inhapi Sequence; 12 - Garanhuns quartzites; 13 - basement-migmatites; 14 - transcurrent shear zones (PESZ - Pernambuco; RCSZ - Rio da Chata; PSZ - Palmares; LCSZ - Limitão-Caetés; ISZ - Itaíba; SBUSZ - São Bento do Una); 15 - compressive shear zones (GSZ - Garanhuns; MSZ - Maravilha; ZCJH - Jacaré dos Homens) (modified from SILVA FILHO et al., 2002, 2016).

FIELD RELATIONSHIPS AND PETROGRAPHY

The Major Isidoro pluton is in sharp contact to the north with the Poço da Cacimba (LIMA et al., in preparation), and to the west with the Monteirópolis plutons (SILVA et al., 2016). The Monteirópolis and Major Isidoro plutons constitute NE–SW elongate intrusions along the boundary of the Pernambuco–Alagoas and Sergipano domains, limited to the south/southeast by the Jacaré dos Homens transpressional shear zone (Fig. 2) (DE OLIVEIRA 2008; MENDES et al., 2009). The Major Isidoro pluton presents two main facies: biotite granite and epidote-amphibole-biotite tonalite that are pink-gray leucocratic to mesocratic, coarse-grained to porphyritic with alkali-feldspar up to 5 cm in length. It shows a well-developed moderately to low-angle dipping foliation that strikes northwest. Diorite elliptical enclaves that reach 0.5 meters long occur elsewhere into this pluton, and sometimes they appear along with the foliation suggesting that they were dykes disrupted in a plastic stage. It may have happened due to local shearing or to intense convective forces generated during the early stages of granite emplacement that displaced into smaller rounded blobs (e.g., COBBING 2000). The Major Isidoro pluton had undergone partial melting, segregation, and deformation that suggest high-strain synkinematic emplacement. Some parts of this that were migmatized preserves the main foliation and constitute the metatexite migmatites, however the majority are the diatexite migmatites (cf. SAWYER 2008). The last one shows heterogeneous schlieren up to 1 meter. The schlierens are gray due to the presence of biotite-rich domains separated by quartz-feldspar domains. The Jacaré dos Homens shear zone (also known as Belo Monte Jeremoabo shear zone; SILVA FILHO et al., 2014) may have acted with far-field stresses that could have contributed to melt segregation by shear-enhanced compaction (e.g., WEINBERG et al., 2015).

The Monteirópolis pluton constitutes leucocratic amphibole-biotite alkali feldspar granite to granodiorite with texture medium-to- coarse grained, sometimes porphyritic with zoned alkali feldspar crystals that reach 4.5 cm in length. This pluton has a magmatic foliation that dominantly dips gentle (normally < 30º, but sometimes up to 55º) to the northwest. Diorite enclaves and amphibole-rich clots, typically a few centimeters to about 25 cm long, are present mainly in the eastern portion of the batholith. These enclaves have sharp contacts with the host granite and show regular, generally oval, but occasionally lobate or diffuse contours.

The Major Isidoro and Monteirópolis plutons have very similar mineralogical characteristics that are made up of quartz, plagioclase and alkali feldspar as essential phases. Biotite and amphibole are the main mafic phases and together with the shape-preferred orientation of alkali feldspar define the magmatic/metamorthic foliation of these plutons. Accessory minerals are titanite, zircon, allanite, apatite, magmatic epidote and Fe-Ti oxides. Minor saussurite was observed as products of post-magmatic transformations.

The mineral assemblage of quartz + alkali feldspar + plagioclase + biotite ± hornblende + titanite ± magnetite ± epidote ± ilmenite is common within both investigated plutons.

AGE AND Sr–Nd–O ISOTOPIC COMPOSITIONS

SILVA et al. (2015) and SILVA et al. (2016) presented an integrated study of Sr, Nd, Pb, and O isotopes for the calc-alkaline Major Isidoro and Monteirópolis intrusions. U–Pb SHRIMP zircon crystallization ages of the Major Isidoro and Monteirópolis batholiths are respectively 626.6 ± 4.1 Ma and 625.8 ± 3.7 Ma. Inherited zircon cores from the Major Isidoro yielded ages varying from 800 to 1000 Ma. These crystallization ages tied the emplacement of them to early stages of the Brasiliano orogeny. For the Major Isidoro granites Nd-model ages (t_{DM1}) vary from 1.1 to 1.4 with $\varepsilon Nd_{(627\ Ma)}$ of −1.09 to −2.12 and $^{87}Sr/^{86}Sr_{(627\ Ma)}$ varies from 0.7069 to 0.7086. The Monteirópolis pluton shows homogeneous model age of 1.0 Ga and $\varepsilon Nd_{(625\ Ma)}$ values of −0.78 to +1.06 (avg. = +0.14), and initial $^{87}Sr/^{86}Sr_{(625\ Ma)}$ values of 0.7050–0.7052. Bulk zircon oxygen values for the Major Isidoro granites vary from 6.95 to 7.02 ‰ and lie between zircon crystallized from mantle-derived magmas (5.3 ± 0.3‰; VALLEY et al., 2005) and zircon originated from partial melting of metasedimentary rocks (> 8.8 ‰; GAO et al., 2016). For the Monteirópolis pluton $\delta^{18}O$ in zircon varies from 5.0 to 5.9 ‰ and suggest crystallization in high-temperature equilibrium with mantle-derived magmas. The Major Isidoro and Monteirópolis granites were plausibly produced by partial melting of a reworked Tonian lower continental crust and by Tonian mantle-derived rocks, respectively.

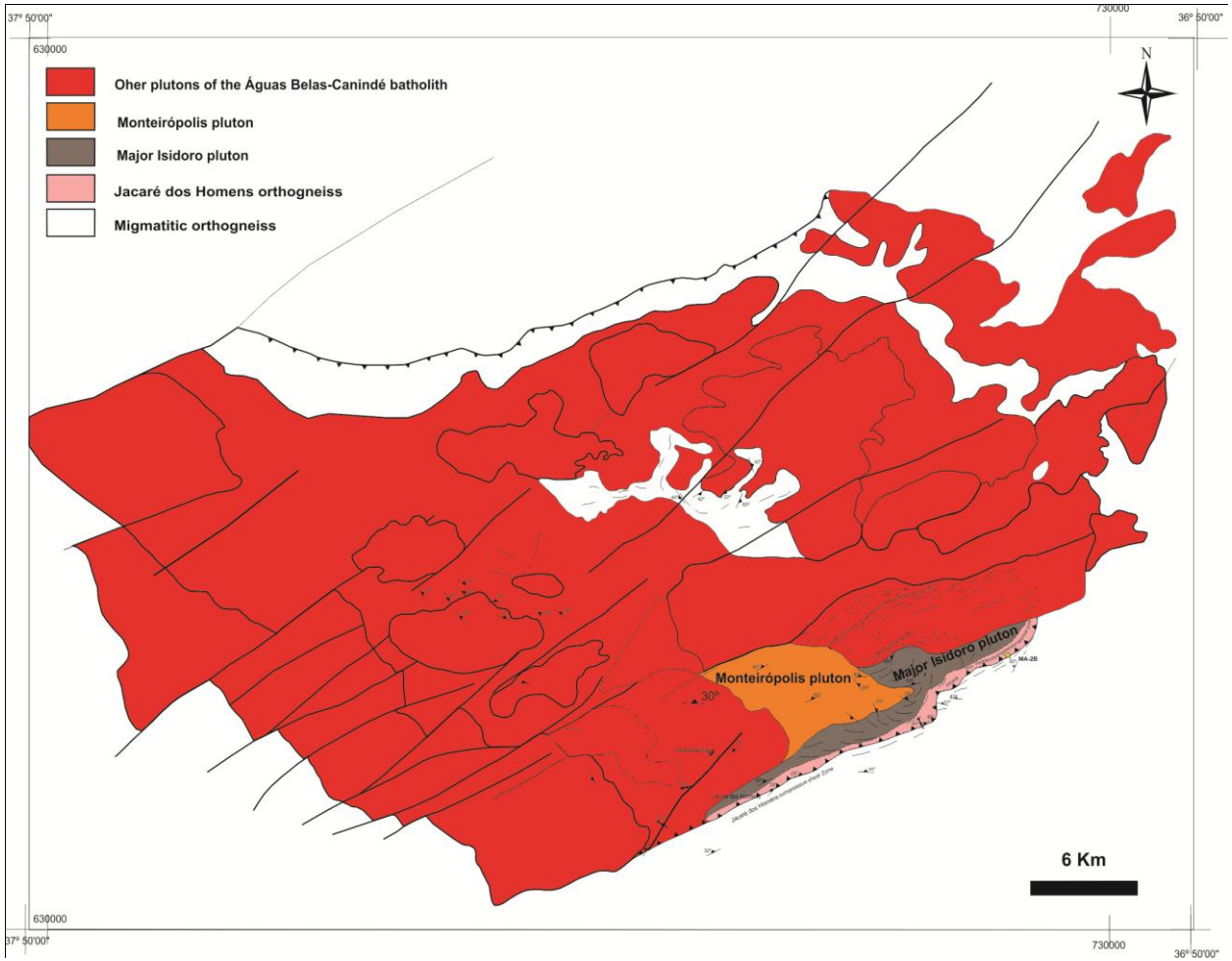

Figure 2. Geological map of the Águas Belas–Canindé batholith showing the studied plutons.

ANALYTICAL PROCEDURES

Whole-rock major and some trace element chemical analyses were performed by X-ray fluorescence (XRF) with a fully automated Rigaku RIX-3000 XRF spectrometer and some of them with a Rigaku ZSX Primus II at the NEG–LABISE, Federal University of Pernambuco, Recife, Brazil, by the calibration -curves method prepared using certified reference standards.

Mineral chemistry analyses were performed at the Electron Microprobe Laboratory, University of Brasilia, Brazil, using a Superprobe JEOL JXA-8230 equipped with WDS, with an accelerating potential of 15 kV and a current of 10 ηA, with a 5μ diameter beam. The crystals were analyzed using the following standards: albite (Na), forsterite (Mg), topaz (F), microcline (Al, Si, K), andradite (Ca), vanadinite (V, Cl), $MnTiO_3$ (Ti, Mn), Cr_2O_3 (Cr), $SrSO_4$ (Sr), NiO (Ni), andradite (Fe), $BaSO_4$ (Ba). Counting times were 10s on peak and 5s on background for all elements. Structural formulae of plagioclase, amphibole, titanite, biotite, and epidote were calculated on the basis of 32, 23, 5, 22 and 12 oxygens, respectively (DEER et al., 2013). Tables 1 to 5 contain representative microprobe chemical analyses.

MINERAL CHEMISTRY

Plagioclase

Microprobe analyses of plagioclase of the Monteirópolis pluton show compositions varying between $An_{16–19}$ (oligoclase), while for plagioclase of granites and enclaves of the Major Isidoro pluton compositions range between $An_{23–35}$ (oligoclase–andesine) and $An_{34–40}$ (andesine), respectively (Fig. 3; Table 13). They show a normal zoning with the nuclei slightly enriched in Ca compared to rim.

Table 1. Microprobe analyses and structural formulae for feldspar of the studied granites.

Sample	TR–89	TR–89	TR–89	TR–89	TR–22	TR–22	TR–22	TR–22	TR–30	TR–30
Location	Core	Rim	Core	Rim	Core	Rim	Core	Rim	Core	Rim
Na_2O	9.351	9.371	9.075	9.553	8.64	8.782	7.299	8.223	6.958	7.726
MgO	0	0.022	0	0	0	0	0	0.01	0.01	0
Al_2O_3	22.192	22.173	22.634	21.882	23.67	22.984	24.995	23.937	26.073	25.079
SiO_2	64.441	64.406	64.396	64.649	61.411	62.278	58.947	61.056	57.576	59.502
CaO	3.531	3.449	4.03	3.308	5.176	4.775	7.308	6.015	8.204	7.045
K_2O	0.184	0.139	0.13	0.187	0.262	0.235	0.113	0.151	0.164	0.165
Cl	0	0	0	0	0	0.011	0	0.002	0.023	0
TiO_2	0.026	0.028	0	0	0.064	0.024	0.024	0	0	0
Cr_2O_3	0	0	0.048	0.024	0	0	0	0	0.061	0.011
MnO	0	0	0.034	0	0	0.026	0	0	0	0.007

SrO	0.111	0.324	0.024	0.22	0	0.161	0.18	0	0.088	0.124
NiO	0.041	0	0.035	0	0	0	0.017	0	0.009	0.077
FeO	0.043	0.066	0.011	0	0.073	0.12	0.027	0.329	0.147	0.198
BaO	0	0.033	0.095	0.017	0.096	0	0	0	0.071	0
V_2O_3	0.073	0	0.011	0	0.014	0.012	0.011	0	0	0.018
Total	99.993	100.011	100.523	99.84	99.406	99.408	98.921	99.723	99.384	99.952
				Structural formulae on the basis of 32 oxygens						
Na	0.79984	0.80213	0.77261	0.81834	0.74882	0.76000	0.63873	0.71163	0.60912	0.67015
Mg	0	0	0	0	0	0	0	0.00067	0.00067	0
Al^{tot}	1.15385	1.15369	1.17134	1.13944	1.24702	1.20908	1.32959	1.25922	1.38746	1.32231
Si	2.84287	2.84337	2.82761	2.85631	2.74512	2.77973	2.66051	2.72522	2.59963	2.66193
Ca	0.16690	0.16314	0.18960	0.15659	0.24790	0.22835	0.35340	0.28765	0.39688	0.33768
K	0.01036	0.00783	0.00728	0.01054	0.01494	0.01338	0.00651	0.00860	0.00945	0.00942
Cl	0	0	0	0	0	0.00083	0	0.00015	0.00176	0
Ti	0.00086	0.00093	0	0	0.00215	0.00081	0.00081	0	0	0
Cr	0	0	0.00167	0.00084	0	0	0	0	0.00218	0.00039
Mn	0	0	0.00126	0	0	0.00098	0	0	0	0.00027
Sr	0.00284	0.00829	0.00061	0.00564	0	0.00417	0.00471	0	0.00230	0.00322
Ni	0.00145	0	0.00124	0	0	0	0.00062	0	0.00033	0.00277
Fe	0.00159	0.00244	0.00040	0	0.00273	0.00448	0.00102	0.01228	0.00555	0.00741
Ba	0	0.00057	0.00163	0.00029	0.00168	0	0	0	0.00126	0
V	0.00258	0	0.00039	0	0.00050	0.00043	0.00040	0	0	0.00065
Sum	4.983	4.984	4.976	4.988	5.011	5.002	4.996	5.005	5.017	5.016
% An	16.69	16.31	18.96	15.66	24.79	22.84	35.34	28.77	39.69	33.77
% Ab	79.98	80.21	77.26	81.83	74.88	76.00	63.87	71.16	60.91	67.01
% Or	1.04	0.78	0.73	1.05	1.49	1.34	0.65	0.86	0.94	0.94

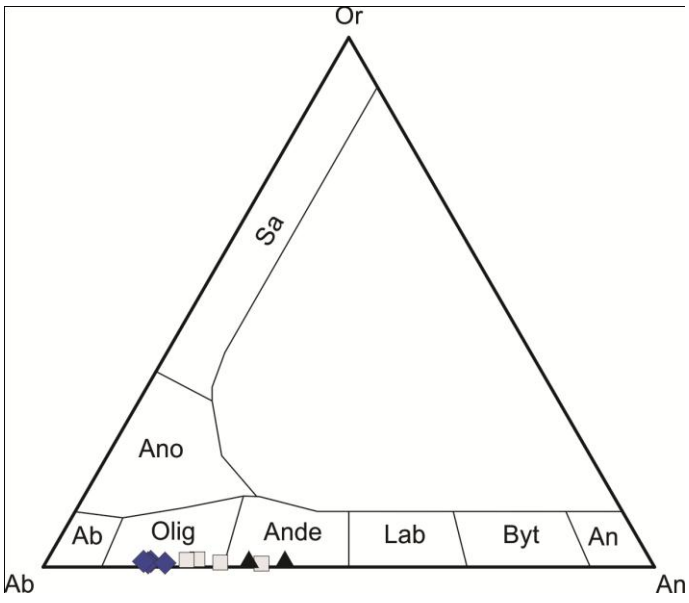

Figure 3. Plagioclase classification from the studied plutons. Ab – Albite; Olig – Oligoclase; Ande – Andesine; Lab – Labradorite; Byt – Bytownite; An – Anorthite; Ano – Anorthoclase; Sa – Sanidine.

Table 2. Microprobe analyses and structural formulae for amphibole of the studied granites.

Sample	TR–89_C2	TR–89_C2	TR–89_C2	TR–89_C2	TR–89_C5	TR–89_C5	TR–22_C5	TR–22_C5	TR–22_C3	TR–22_C3	TR–22_C2	TR–30_C1	TR–30_C1
Location	Core	Rim	Core	Rim	Core	Rim	Core	Rim	Core	Rim	Rim	Core	Rim
SiO_2	43.573	43.361	43.269	42.743	43.942	44.12	42.114	41.355	41.047	42.145	41.519	41.25	41.603
TiO2	0.926	0.93	1.025	0.49	0.592	0.632	1.067	1.065	0.672	0.877	0.377	1.227	1.445
Al_2O_3	8.913	8.83	8.833	9.545	9.02	9.19	10.211	10.471	11.104	10.806	12.898	11.776	11.438
FeO*	19.885	20.21	20.219	20.478	20.043	19.926	20.528	20.528	21.7	20.975	22.08	19.192	18.791
MgO	8.984	8.99	9.101	8.493	9.465	9.09	8.447	8.379	7.75	7.715	7.013	9.153	8.959
MnO	0.742	0.643	0.714	0.614	0.607	0.844	0.594	0.592	0.697	0.735	0.772	0.309	0.489
CaO	11.349	11.102	11.219	11.399	11.337	11.176	11.264	11.311	11.488	11.482	11.362	11.933	11.733
Na_2O	1.691	1.637	1.697	1.6	1.548	1.655	1.394	1.426	1.414	1.429	1.356	1.216	1.406
K_2O	1.249	1.281	1.245	1.297	1.178	1.32	1.36	1.36	1.362	1.394	1.395	1.666	1.666
F	0.48	0.43	0.426	0.458	0.532	0.539	0.298	0.204	0.285	0.216	0.318	0.231	0.185
Cl	0.024	0.017	0.045	0.021	0.007	0.018	0.04	0.059	0.062	0.027	0.073	0.053	0.053
Total	97.816	97.431	97.793	97.138	98.271	98.51	97.317	96.75	97.581	97.801	99.163	98.006	97.768
Structural formulae on the basis of 23 oxygens													
T-sites													
Si	6.639	6.624	6.590	6.565	6.624	6.660	6.434	6.356	6.283	6.432	6.246	6.225	6.309
Al^{iv}	1.361	1.376	1.410	1.435	1.376	1.340	1.566	1.644	1.717	1.568	1.754	1.775	1.691
Al(total)	1.601	1.590	1.586	1.728	1.603	1.636	1.839	1.897	2.004	1.944	2.288	2.095	2.045
M1,2,3 sites													
Al^{vi}	0.240	0.214	0.175	0.293	0.227	0.296	0.274	0.253	0.287	0.376	0.534	0.320	0.354
Ti	0.106	0.107	0.117	0.057	0.067	0.072	0.123	0.123	0.077	0.101	0.043	0.139	0.165
Fe^{3+}	0.431	0.516	0.544	0.537	0.621	0.475	0.642	0.707	0.820	0.534	0.757	0.682	0.478
Mg	2.040	2.047	2.066	1.944	2.126	2.045	1.923	1.919	1.768	1.755	1.572	2.059	2.025
Mn	0.096	0.083	0.092	0.080	0.078	0.108	0.077	0.077	0.090	0.095	0.098	0.039	0.063
Fe^{2+}	2.088	2.034	2.005	2.089	1.880	2.005	1.962	1.921	1.957	2.140	1.995	1.740	1.906
Ca	0.000	0.000	0.000	0.000	0.000	0.000	0.000	0.000	0.000	0.000	0.000	0.021	0.010
Sum	5	5	5	5	5	5	5	5	5	5	5	5	5
M4 site													
Fe	0.015	0.032	0.026	0.004	0.026	0.036	0.020	0.011	0.001	0.004	0.025	0.000	0.000
Ca	1.853	1.817	1.831	1.876	1.831	1.808	1.844	1.863	1.884	1.878	1.832	1.909	1.897
Na	0.132	0.151	0.143	0.120	0.143	0.156	0.136	0.127	0.115	0.119	0.143	0.091	0.103

Sum	2	2	2	2	2	2	2	2	2	2	2	2	2
A site													
Ca	0.000	0.000	0.000	0.000	0.000	0.000	0.000	0.000	0.000	0.000	0.000	0.000	0.000
Na	0.368	0.334	0.358	0.357	0.309	0.328	0.277	0.298	0.304	0.304	0.253	0.265	0.310
K	0.243	0.250	0.242	0.254	0.227	0.254	0.265	0.267	0.266	0.271	0.268	0.321	0.322
Sum A	0.611	0.584	0.600	0.611	0.536	0.582	0.542	0.565	0.570	0.576	0.520	0.585	0.632
OH site													
O	0.000	0.000	0.000	0.000	0.000	0.000	0.000	0.000	0.000	0.000	0.000	0.000	0.000
OH	1.760	1.785	1.781	1.769	1.741	1.735	1.843	1.884	1.843	1.887	1.827	1.874	1.897
F	0.233	0.210	0.208	0.225	0.257	0.260	0.146	0.101	0.140	0.105	0.154	0.112	0.090
Cl	0.006	0.004	0.012	0.006	0.002	0.005	0.011	0.016	0.016	0.007	0.019	0.014	0.014
Sum	2	2	2	2	2	2	2	2	2	2	2	2	2
Sum cations	15.611	15.584	15.600	15.611	15.536	15.582	15.542	15.565	15.570	15.576	15.520	15.585	15.632
$Fe^{\#}$	0.554	0.558	0.555	0.575	0.543	0.552	0.577	0.579	0.611	0.604	0.639	0.541	0.541
Mg/Fe^{2+}	0.970	0.991	1.017	0.929	1.116	1.002	0.971	0.993	0.903	0.819	0.778	1.183	1.063
Mg/Fe	0.805	0.793	0.802	0.739	0.842	0.813	0.733	0.727	0.636	0.655	0.566	0.850	0.850
$Mg/(Mg+Fe^{2+})$	0.492	0.498	0.504	0.481	0.527	0.501	0.493	0.498	0.474	0.450	0.438	0.542	0.515
T (B&H,1990)	720	725	734	728	719	707	770	791	806	761	787	879	842
T (H&B, 1994TA)	724	732	758	714	722	692	740	766	767	712	695	778	765
T (H&B, 1994TB)	672	685	696	662	672	660	710	720	716	684	686	735	730
P (A&S, 1995)	4.64	4.46	4.30	5.34	4.65	4.92	5.27	5.36	5.91	6.14	7.71	5.96	5.83
P (S, 1992)	4.61	4.56	4.54	5.22	4.62	4.78	5.74	6.02	6.53	6.24	7.88	6.96	6.72

Amphiboles

Analyzed hornblendes (Table 14) were classified according to nomenclature scheme proposed by LEAKE et al. (1997; 2003) and based on this classification they are member of the calcic group in which $(Ca + Na)_B \geq 1.50$, and $Na_B \leq 0.50$. Amphiboles from the Monteirópolis pluton has Si contents in the range of 6.56 to 6.66 atoms per formula unit (apuf), Al^{VI} contents in the range of 0.17 to 0.29 apfu, and show Ti contents in a narrow range of 0.06 to 0.11 apfu and they are classified as ferro-edenite to edenite (Fig. 4). Amphiboles from the Major Isidoro granite and enclave show slightly lower Si content compared to the Monteirópolis pluton that vary from 6.25 to 6.43 apfu and has higher Al^{VI} contents in the range of 0.25 to 0.534 apfu, and Ti content varies from 0.04 to 0.12 apfu. Hornblendes from granite and enclave are respectively classified as hastingsite and mg-hastingsite (Fig. 4). Based on the new classification and nomenclature scheme for the amphiboles (HAWTHORNE et al., 2012) all analyzed hornblendes classify as pargasite. Hornblende compositions were plotted (Fig. 5a–b) in order to test the role of Edenite and Tschermak exchange and clearly compositional variations could be partially explained for both exchange mechanisms in these plutons. Similar observations were made for hornblende compositions of the Mount Stuart batholith, Fish Canyon magmatic system (e.g., ANDERSON & SMITH 1995; BACHMANN & DUNGAN 2002).

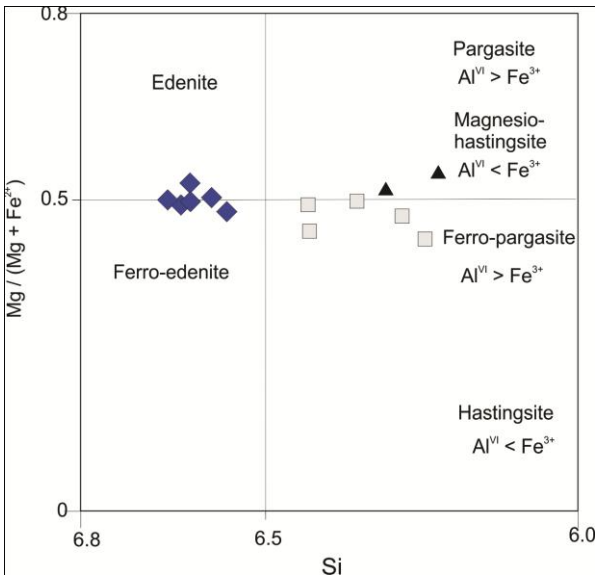

Figure 4. Amphibole classification from the studied plutons. Fields after LEAKE et al. (1997).

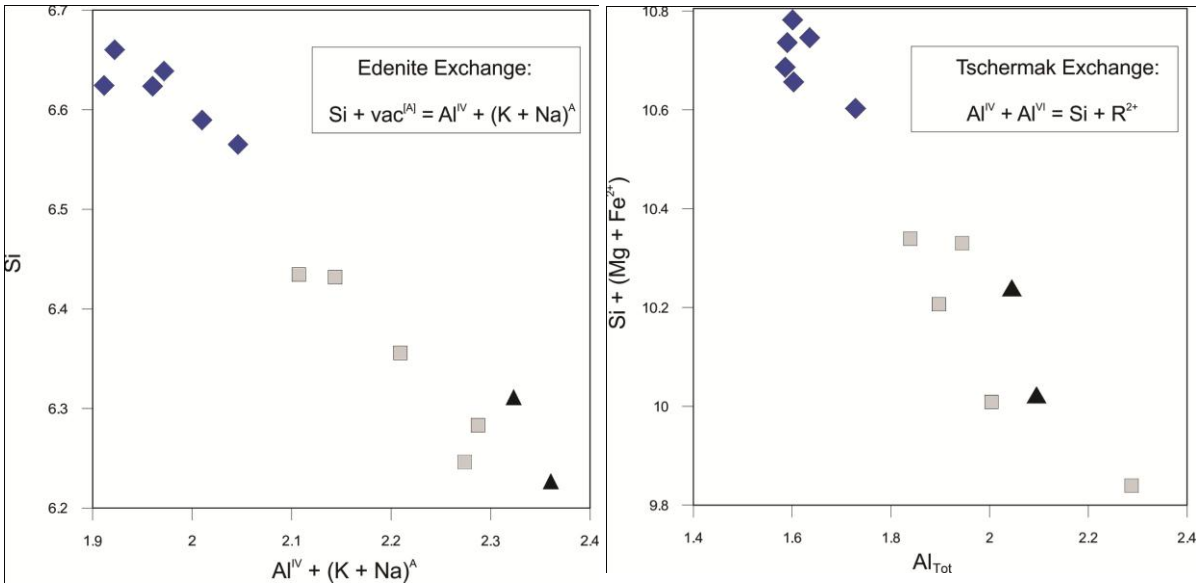

Figure 5. (a) Si vs. Al^{IV}+ $(K + Na)^{A}$ and (b) Si + R^{2+} vs. Al_{Tot}.

Titanite

Titanite composition depends upon temperature and pressure; and so, titanite crystals having Al + Fe^{3+} < 0.35 apfu indicates crystallization at temperatures higher than ~700 ºC (ENAMI et al., 1993). Both studied plutons show very low Al + Fe^{3+} (Table 15) and point to crystallization within the range for typical high-temperature titanites, which is consistent to early crystallization of euhedral titanite in these plutons.

Table 3a. Microprobe analyses and structural formulae for titanite of the Major Isidoro granites.

Sample	TR–13	TR–13	TR–22	TR–22	TR–22	TR–22
Location	Core	Rim	Core	Rim	Core	Rim
Na_2O	0.037	0.026	0.047	0.035	0.031	0.017
MgO	0	0.008	0.033	0.006	0.012	0.013
F	0.488	0.58	0.409	0.402	0.46	0.342
Al_2O_3	2.233	2.364	1.425	1.443	1.421	1.374
SiO_2	30.709	30.576	30.504	29.627	30.536	30.116
CaO	28.786	28.672	28.638	27.768	28.175	27.63
K_2O	0.015	0	0	0.013	0	0
Cl	0.022	0.007	0	0.008	0.008	0
TiO_2	35.321	36.512	35.014	35.654	35.897	37.125
Cr_2O_3	0	0	0.174	0.06	0	0.053
MnO	0.088	0.047	0.123	0.205	0.116	0.221
SrO	0.058	0	0.034	0.056	0	0.075
NiO	0	0	0.011	0	0	0
FeO	0.66	0.654	1.085	1.284	1.147	1.275
Fe_2O_3	0.733	0.727	1.206	1.427	1.275	1.417
BaO	0.008	0.066	0.21	0.185	0.124	0.081
V_2O_3	0.326	0.374	0.376	0.357	0.29	0.333

Total	99.484	100.613	99.289	98.530	99.492	100.072
Structural formulae on the basis of 5 oxygens						
Na	0.0024	0.0017	0.0031	0.0023	0.0020	0.0011
Mg	0.0000	0.0004	0.0016	0.0003	0.0006	0.0006
F	0.0512	0.0602	0.0433	0.0431	0.0486	0.0359
Altot	0.0873	0.0914	0.0563	0.0576	0.0559	0.0538
Si	1.0188	1.0036	1.0222	1.0035	1.0196	1.0008
Ca	1.0232	1.0083	1.0283	1.0077	1.0080	0.9837
K	0.0006	0.0000	0.0000	0.0006	0.0000	0.0000
Cl	0.0012	0.0004	0.0000	0.0005	0.0005	0.0000
Ti	0.8812	0.9012	0.8824	0.9081	0.9014	0.9278
Cr	0.0000	0.0000	0.0046	0.0016	0.0000	0.0014
Mn	0.0025	0.0013	0.0035	0.0059	0.0033	0.0062
Sr	0.0011	0.0000	0.0007	0.0011	0.0000	0.0014
Ni	0.0000	0.0000	0.0003	0.0000	0.0000	0.0000
Fe^{3+}	0.0183	0.0180	0.0304	0.0364	0.0320	0.0354
Ba	0.0001	0.0008	0.0028	0.0025	0.0016	0.0011
V	0.0087	0.0098	0.0101	0.0097	0.0078	0.0089

Table 3b. Microprobe analyses and structural formulae for titanite of the Monteirópolis granites.

Sample	TR–89	TR–89	TR–89	TR–89	TR–89	TR–89	TR–01	TR–01	TR–01	TR–01	TR–30
Location	Core	Rim	Core	Rim	Core	Rim	Core	Rim	Core	Rim	Core
Na_2O	0.052	0.027	0.05	0.274	0.054	0.166	0	0	0.057	0.047	0.039
MgO	0.053	0.031	0.03	0.032	0.018	0.063	0.026	0.004	0.003	0.002	0
F	0.499	0.451	0.183	0.506	0.439	0.607	0.342	0.602	0.442	0.774	0.293
Al_2O_3	1.345	1.544	1.217	1.469	1.412	1.72	1.506	1.662	1.412	1.664	1.181
SiO_2	29.655	29.89	29.006	30.69	30.677	31.77	30.369	30.441	30.44	30.704	30.021
CaO	26.923	27.611	26.277	25.713	27.981	26.992	27.067	28.888	27.72	28.607	28.766
K_2O	0.034	0.015	0	0.169	0.006	0.087	0.005	0.001	0.01	0	0
Cl	0.024	0.012	0.087	0.068	0.013	0.094	0.004	0	0	0.004	0.028
TiO_2	35.544	36.427	35.198	35.313	35.417	32.818	36.414	37.241	36.475	34.467	39.37
Cr_2O_3	0.06	0.036	0	0	0	0	0.026	0.098	0	0.161	0.051
MnO	0.13	0.186	0.076	0.087	0.101	0.241	0.282	0.131	0.21	0.176	0.033
SrO	0	0.021	0	0.062	0	0	0.078	0.023	0	0	0.018
NiO	0	0.024	0	0.085	0.021	0.089	0	0	0.017	0.03	0
FeO	2.411	1.573	1.762	1.599	1.534	1.937	1.513	1.265	1.455	1.269	0.755
Fe_2O_3	2.679	1.748	1.958	1.777	1.705	2.153	1.681	1.406	1.617	1.410	0.839
BaO	0	0.092	0.182	0.166	0.115	0.212	0.184	0.18	0.16	0.227	0.152
V_2O_3	0.314	0.406	0.294	0.466	0.382	0.327	0.385	0.386	0.33	0.301	0.376
Total	99.723	100.094	96.320	98.476	99.875	99.276	99.882	102.328	100.348	99.843	101.922
Structural formulae on the basis of 5 oxygens											
Na	0.0034	0.0017	0.0034	0.0180	0.0035	0.0108	0.0000	0.0000	0.0037	0.0031	0.0025
Mg	0.0027	0.0015	0.0016	0.0016	0.0009	0.0032	0.0013	0.0002	0.0001	0.0001	0.0000
F	0.0534	0.0476	0.0201	0.0541	0.0464	0.0647	0.0361	0.0622	0.0464	0.0820	0.0301
Altot	0.0537	0.0608	0.0498	0.0585	0.0556	0.0683	0.0592	0.0639	0.0553	0.0657	0.0453
Si	1.0037	0.9984	1.0068	1.0377	1.0245	1.0708	1.0126	0.9938	1.0114	1.0283	0.9762
Ca	0.9763	0.9881	0.9772	0.9316	1.0012	0.9747	0.9669	1.0105	0.9869	1.0265	1.0022
K	0.0015	0.0006	0.0000	0.0073	0.0003	0.0037	0.0002	0.0000	0.0004	0.0000	0.0000
Cl	0.0014	0.0007	0.0051	0.0039	0.0007	0.0054	0.0002	0.0000	0.0000	0.0002	0.0015
Ti	0.9047	0.9150	0.9188	0.8980	0.8895	0.8318	0.9130	0.9143	0.9114	0.8681	0.9628
Cr	0.0016	0.0010	0.0000	0.0000	0.0000	0.0000	0.0007	0.0025	0.0000	0.0043	0.0013
Mn	0.0037	0.0053	0.0022	0.0025	0.0029	0.0069	0.0080	0.0036	0.0059	0.0050	0.0009
Sr	0.0000	0.0004	0.0000	0.0012	0.0000	0.0000	0.0015	0.0004	0.0000	0.0000	0.0003
Ni	0.0000	0.0006	0.0000	0.0023	0.0006	0.0024	0.0000	0.0000	0.0005	0.0008	0.0000

Fe^{3+}	0.0682	0.0439	0.0511	0.0452	0.0428	0.0546	0.0422	0.0345	0.0404	0.0355	0.0205
Ba	0.0000	0.0012	0.0025	0.0022	0.0015	0.0028	0.0024	0.0023	0.0021	0.0030	0.0019
V	0.0085	0.0109	0.0082	0.0126	0.0102	0.0088	0.0103	0.0101	0.0088	0.0081	0.0098

Biotite

Biotite from the Major Isidoro granites has higher Al^{tot} contents of 2.67 to 2.94 atoms per formula unit (apfu) and Fe# (i.e., Fe/(Mg+Fe)) of 0.50 to 0.58 compared to biotite in Monteirópolis granites that has Al^{tot} varying from 2.49 to 2.85 apuf, and Fe# of 0.44 to 0.55 (Fig. 6; Table 16).

NACHIT et al. (1985) used mica composition in granitoids to relate magma types in which biotite crystallized. In Al^{tot} versus Mg classification diagram, the analyzed samples from both plutons plot within the calc-alkaline field (Fig. 7). ABDEL-RAHMAN (1994) proposed discrimination diagrams between alkaline (A), calc-alkaline (C), and peraluminous (P) granite suites based on the biotite chemistry. In the MgO x FeO and MgO x FeO x Al_2O_3 diagrams, biotite plot predominantly in the calc-alkaline field (Fig. 8a–b).

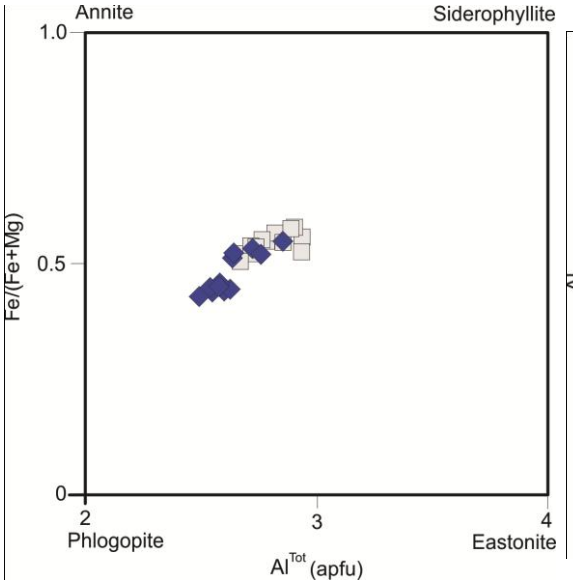

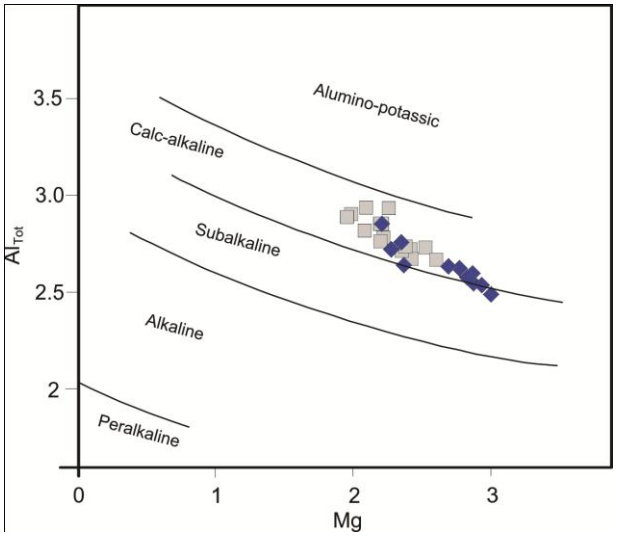

Figure 6. Fe / (Fe + Mg) *vs.* Al_{Tot} diagram.

Figure 7. Al_{Tot} *vs.* Mg diagram.

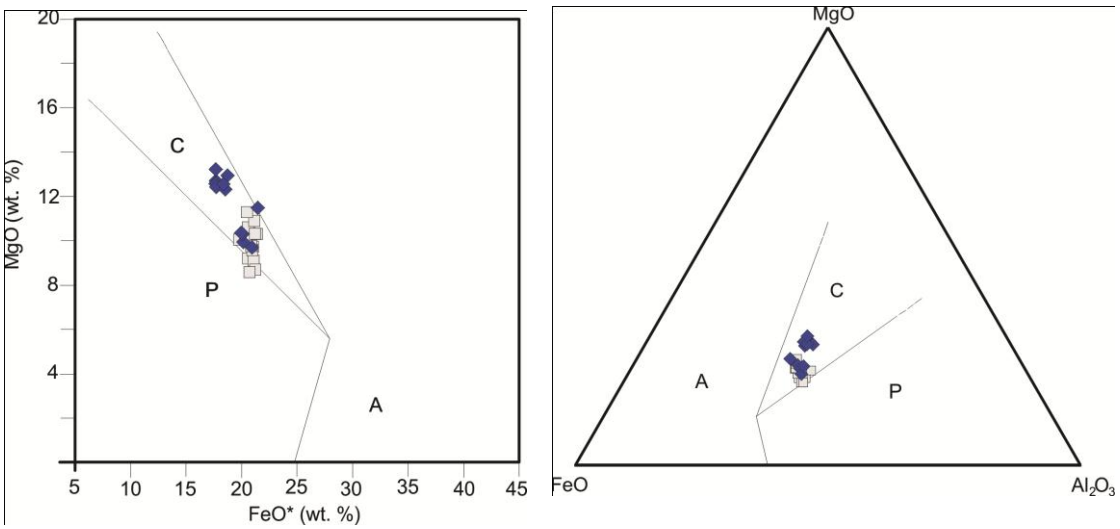

Figure 8. (a) MgO vs. FeO and (b) MgO x FeO x Al_2O_3 diagrams of ABDEL-RAHMAN (1994). C – calc-alkaline; P – peraluminous; A – alkaline.

Epidote

According to chemical criteria of TULLOCH (1979, 1986), JOHNSTON & WYLLIE (1988), and VYHNAL et al. (1991), magmatic epidote has pistacite contents (Ps = molar [Fe^{3+} /(Fe^{3+} + Al)] x 100) between 25 to 29 mol%, however epidote phenocrysts in high-K calc-alkaline dacitic dykes of Colorado which are considered to be unequivocally magmatic epidote have Ps contents between 19 to 24 mol% (EVANS & VANCE 1987; DAWES & EVANS 1991) and mEp grains described in the Borborema Province have Ps contents up to 33 mol% (SIAL et al., 1999, 2008; FERREIRA et al., 2003, 2011, 2015; among others). The analyzed crystals of the Major Isidoro yielded values of 27 to 29 mol%, which are within that range proposed by these authors, while the analyzed grains of the Monteirópolis plutons showed Ps values of 29 to 31 mol% suggesting crystallization under higher fO_2 conditions compared to that of the Major Isidoro pluton. Magmatic epidote according to EVANS & VANCE (1987) has TiO_2 contents < 0.6 wt%, while secondary epidote replacing biotite has TiO_2 contents > 0.6 wt.%. The analyzed crystals present values ranging from 0.0 to 0.3 wt.% for both plutons (Table 17) suggesting that they are primary, in accordance with the Tulloch's criteria based on pistacite contents.

Table 4a. Microprobe analyses and structural formulae for biotite of the Major Isidoro granites.

Sample	TR–13	TR–13	TR–13	TR–13	TR–13	TR–13	TR–13	TR–13	TR–22	TR–22	TR–22	TR–22	TR–22	TR–22
Location	Core	Rim	Core	Rim	Core	Rim	core	Rim	Core	Rim	Core	Rim	Core	Rim
Na_2O	0.094	0.105	0.095	0.06	0.081	0.123	0.085	0.091	0.077	0.133	0.12	0.138	0.08	0.095
MgO	9.186	9.716	9.083	9.565	9.749	10.034	8.685	8.573	10.539	10.591	10.293	10.303	10.883	11.279
F	0.599	0.827	0.864	0.679	0.883	0.808	0.683	0.596	0.536	0.718	0.633	0.537	0.552	0.617
Al_2O_3	16.355	15.454	15.601	15.259	16.028	16.538	16.13	16.089	15.057	14.813	15.056	15.017	14.919	14.65
SiO_2	36.416	36.528	36.662	36.383	37.031	36.929	36.794	36.604	36.621	36.924	36.789	36.317	35.956	36.294
CaO	0.049	0.06	0.034	0.067	0.042	0.032	0.011	0.044	0.026	0.082	0.021	0.023	0.031	0.039
K_2O	9.755	9.591	9.653	9.634	9.894	9.763	9.722	9.871	9.663	9.728	9.612	9.703	9.565	9.721
Cl	0.05	0.025	0.056	0.057	0.044	0.055	0.058	0.087	0.049	0.062	0.043	0.059	0.065	0.018
TiO_2	3.358	3.24	3.113	3.288	2.948	3.146	2.91	3.804	2.498	2.531	2.287	2.051	1.835	1.968
Cr_2O_3	0	0	0.037	0	0	0	0	0	0	0	0	0.118	0	0.06
MnO	0.265	0.318	0.388	0.294	0.265	0.3	0.475	0.425	0.458	0.369	0.567	0.37	0.463	0.501
SrO	0	0.104	0.005	0.023	0.005	0	0	0.06	0	0	0.033	0	0	0
NiO	0	0.011	0	0	0	0.063	0.05	0.037	0.09	0.048	0.078	0	0	0.063
FeO	20.626	21.047	21.111	20.999	20.895	19.818	21.256	20.74	20.703	20.605	21.409	21.226	21.166	20.523
BaO	0.055	0.055	0.004	0.136	0.15	0.118	0.142	0	0.104	0.226	0.101	0.197	0.143	0.059
V_2O_3	0.048	0.038	0.086	0.11	0.074	0.042	0.041	0.09	0.034	0.022	0.1	0.055	0.035	0.069
Total	96.856	97.119	96.792	96.554	98.089	97.769	97.042	97.111	96.455	96.852	97.142	96.114	95.693	95.956
Structural formulae on the basis of 22 oxygens														
Na	0.028	0.031	0.028	0.018	0.024	0.036	0.025	0.027	0.023	0.039	0.036	0.041	0.024	0.028
Mg	2.086	2.213	2.075	2.190	2.195	2.252	1.977	1.946	2.410	2.416	2.346	2.374	2.519	2.598
F	0.289	0.400	0.419	0.330	0.422	0.385	0.330	0.287	0.260	0.348	0.306	0.263	0.271	0.301
Altot	2.937	2.782	2.818	2.762	2.853	2.934	2.903	2.888	2.722	2.672	2.713	2.736	2.730	2.667
Si	5.548	5.580	5.619	5.588	5.593	5.559	5.619	5.574	5.616	5.651	5.625	5.614	5.583	5.607
Ca	0.008	0.010	0.006	0.011	0.007	0.005	0.002	0.007	0.004	0.013	0.003	0.004	0.005	0.006
K	1.896	1.869	1.887	1.888	1.907	1.875	1.894	1.918	1.891	1.899	1.875	1.913	1.895	1.916
Cl	0.013	0.006	0.015	0.015	0.011	0.014	0.015	0.022	0.013	0.016	0.011	0.015	0.017	0.005
Ti	0.385	0.372	0.359	0.380	0.335	0.356	0.334	0.436	0.288	0.291	0.263	0.238	0.214	0.229
Cr	0.000	0.000	0.004	0.000	0.000	0.000	0.000	0.000	0.000	0.000	0.000	0.014	0.000	0.007
Mn	0.034	0.041	0.050	0.038	0.034	0.038	0.061	0.055	0.059	0.048	0.073	0.048	0.061	0.066
Sr	0.000	0.009	0.000	0.002	0.000	0.000	0.000	0.005	0.000	0.000	0.003	0.000	0.000	0.000

Ni	0.000	0.001	0.000	0.000	0.000	0.008	0.006	0.005	0.011	0.006	0.010	0.000	0.000	0.008
Fe	2.628	2.689	2.706	2.697	2.639	2.495	2.715	2.641	2.655	2.637	2.738	2.744	2.749	2.651
Ba	0.003	0.003	0.000	0.008	0.009	0.007	0.008	0.000	0.006	0.014	0.006	0.012	0.009	0.004
V	0.006	0.005	0.011	0.014	0.009	0.005	0.005	0.011	0.004	0.003	0.012	0.007	0.004	0.009
Al^{IV}	2.452	2.420	2.381	2.412	2.407	2.441	2.381	2.426	2.384	2.349	2.375	2.386	2.417	2.393
Al^{VI}	0.484	0.362	0.437	0.351	0.447	0.493	0.523	0.462	0.338	0.323	0.339	0.350	0.314	0.274
OH	1.698	1.594	1.567	1.655	1.567	1.601	1.655	1.690	1.727	1.636	1.683	1.722	1.712	1.694
Fe/(Fe+Mg)	0.557	0.549	0.566	0.552	0.546	0.526	0.579	0.576	0.524	0.522	0.538	0.536	0.522	0.505

Table 4b.. Microprobe analyses and structural formulae for biotite of the Monteirópolis granites.

Sample	TR–89	TR–89	TR–89	TR–89	TR–89	TR–89	TR–89	TR–89	TR–01	TR–01	TR–01	TR–01
Location	Core	Rim	Core	Rim	Core	Rim	Core	Rim	Core	Rim	Core	Rim
Na_2O	0.043	0.086	0.032	0.119	0.042	0.037	0.066	0.115	0.123	0.075	0.16	0.123
MgO	12.693	12.56	12.412	11.47	12.304	12.928	12.54	13.206	9.931	10.29	9.685	10.344
F	1.193	1.182	1.135	1.062	1.118	1.243	1.193	1.288	0.675	0.749	0.601	0.8
Al_2O_3	14.242	14.417	14.887	14.22	14.24	14.159	14.461	13.868	15.061	14.549	15.876	15.401
SiO_2	38.274	37.954	38.601	35.452	37.703	38.159	38.294	38.223	37.107	36.967	36.246	37.111
CaO	0.048	0.044	0.071	0.084	0.053	0.031	0.091	0.13	0.045	0	0.018	0.047
K_2O	9.747	9.761	9.943	9.328	9.783	9.708	9.69	9.653	9.633	9.719	9.972	9.586
Cl	0	0.013	0	0	0	0	0.003	0.024	0.037	0.024	0.028	0.018
TiO_2	1.631	1.312	2.13	1.495	1.23	1.112	1.728	1.46	2.721	2.779	3.059	2.836
Cr_2O_3	0.069	0.13	0.104	0	0	0	0	0	0	0.115	0.079	0
MnO	0.625	0.512	0.373	0.478	0.44	0.457	0.416	0.357	0.507	0.413	0.47	0.619
SrO	0.083	0.029	0	0	0	0	0.019	0	0	0.047	0.013	0.02
NiO	0.039	0.059	0.026	0.024	0	0.039	0	0.044	0.059	0	0	0.013
FeO	17.715	17.674	17.745	21.489	18.562	18.763	18.392	17.702	20.186	20.127	20.966	19.994
BaO	0.182	0	0.209	0.039	0.139	0.198	0	0.133	0.19	0.116	0.099	0.154
V_2O_3	0.065	0.043	0.073	0.057	0.137	0.011	0.063	0.046	0.034	0.085	0.076	0.061
Total	96.649	95.776	97.741	95.317	95.751	96.845	96.956	96.249	96.309	96.055	97.348	97.127
Structural formulae on the basis of 22 oxygens												
Na	0.013	0.025	0.009	0.036	0.013	0.011	0.019	0.034	0.037	0.022	0.047	0.036

Mg	2.870	2.862	2.766	2.687	2.817	2.929	2.825	2.997	2.269	2.361	2.201	2.343
F	0.572	0.571	0.537	0.528	0.543	0.597	0.570	0.620	0.327	0.365	0.290	0.384
Altot	2.546	2.597	2.623	2.633	2.578	2.536	2.575	2.488	2.721	2.639	2.853	2.757
Si	5.804	5.801	5.771	5.570	5.791	5.799	5.786	5.819	5.688	5.690	5.526	5.638
Ca	0.008	0.007	0.011	0.014	0.009	0.005	0.015	0.021	0.007	0.000	0.003	0.008
K	1.886	1.903	1.897	1.870	1.917	1.882	1.868	1.875	1.884	1.908	1.940	1.858
Cl	0.000	0.003	0.000	0.000	0.000	0.000	0.001	0.006	0.010	0.006	0.007	0.005
Ti	0.186	0.151	0.239	0.177	0.142	0.127	0.196	0.167	0.314	0.322	0.351	0.324
Cr	0.008	0.016	0.012	0.000	0.000	0.000	0.000	0.000	0.000	0.014	0.010	0.000
Mn	0.080	0.066	0.047	0.064	0.057	0.059	0.053	0.046	0.066	0.054	0.061	0.080
Sr	0.007	0.003	0.000	0.000	0.000	0.000	0.002	0.000	0.000	0.004	0.001	0.002
Ni	0.005	0.007	0.003	0.003	0.000	0.005	0.000	0.005	0.007	0.000	0.000	0.002
Fe	2.247	2.259	2.219	2.824	2.384	2.385	2.324	2.254	2.588	2.591	2.673	2.540
Ba	0.011	0.000	0.012	0.002	0.008	0.012	0.000	0.008	0.011	0.007	0.006	0.009
V	0.008	0.005	0.009	0.007	0.017	0.001	0.008	0.006	0.004	0.010	0.009	0.007
Al^{IV}	2.196	2.199	2.229	2.430	2.209	2.201	2.214	2.181	2.312	2.310	2.474	2.362
Al^{VI}	0.350	0.398	0.395	0.203	0.369	0.336	0.361	0.308	0.409	0.329	0.379	0.395
OH	1.428	1.425	1.463	1.472	1.457	1.403	1.429	1.374	1.663	1.629	1.703	1.611
Fe/(Fe+Mg)	0.439	0.441	0.445	0.512	0.458	0.449	0.451	0.429	0.533	0.523	0.548	0.520

Table 5. Microprobe analyses, structural formulae, and pistacite contents for epidote of the studied plutons.

Sample	TR–89	TR–89	TR–89	TR–89	TR–89	TR–22	TR–22	TR–22	TR–22	TR–22	TR–22
Location	Core	Rim	Core	Rim	Rim	Core	Rim	Core	Rim	Core	Rim
Na_2O	0.017	0.031	0.049	0	0.047	0.041	0	0.016	0	0.016	0.024
MgO	0.005	0.037	0.019	0.011	0.049	0.084	0	0.044	0.011	0	0.003
Al_2O_3	21.634	22.018	21.456	22.502	22.2	21.968	22.612	22.376	22.798	22.555	22.81
SiO_2	38.213	37.667	37.938	38.328	36.143	36.531	37.717	37.741	37.687	37.88	36.206
CaO	23.366	23.448	23.21	23.143	23.267	23.428	23.646	23.442	23.598	23.421	23.14
K_2O	0	0	0.018	0.005	0	0.017	0.003	0	0	0	0
TiO_2	0.152	0	0.009	0.06	0.122	0.07	0.104	0.188	0.296	0.162	0.005
Cr_2O_3	0	0	0.107	0.071	0.059	0.071	0	0.06	0	0	0.025
MnO	0.186	0.198	0.242	0.106	0.268	0.423	0.367	0.412	0.425	0.261	0.435
SrO	0.32	0.456	0.443	0.424	0.193	0.149	0.143	0.096	0.154	0.1	0.059
NiO	0.007	0.087	0	0.041	0.031	0.066	0.026	0	0	0	0.059
Fe_2O_3	15.481	15.231	15.020	14.273	15.055	13.923	13.896	14.330	13.419	13.878	14.507
BaO	0	0.023	0.133	0.041	0.075	0.05	0.017	0	0.017	0	0.04
V_2O_3	0.067	0.069	0.107	0.051	0.044	0.037	0.055	0.054	0.054	0.101	0.069
Total	99.448	99.265	98.751	99.056	97.553	96.858	98.586	98.759	98.459	98.374	97.382
Structural formulae on the basis of 12 oxygens											
Na	0.0025	0.0046	0.0073	0.0000	0.0071	0.0062	0.0000	0.0024	0.0000	0.0024	0.0036
Mg	0.0006	0.0042	0.0022	0.0012	0.0057	0.0098	0.0000	0.0050	0.0013	0.0000	0.0003
Al	1.9382	1.9802	1.9390	2.0144	2.0352	2.0222	2.0360	2.0127	2.0525	2.0311	2.0878
Si	2.9048	2.8744	2.9090	2.9113	2.8113	2.8532	2.8814	2.8803	2.8789	2.8943	2.8118
Ca	1.9030	1.9171	1.9068	1.8834	1.9391	1.9605	1.9355	1.9168	1.9314	1.9173	1.9254
K	0.0000	0.0000	0.0018	0.0005	0.0000	0.0017	0.0003	0.0000	0.0000	0.0000	0.0000
Ti	0.0087	0.0000	0.0005	0.0034	0.0071	0.0041	0.0060	0.0108	0.0170	0.0093	0.0003
Cr	0.0000	0.0000	0.0065	0.0043	0.0036	0.0044	0.0000	0.0036	0.0000	0.0000	0.0015
Mn	0.0120	0.0128	0.0157	0.0068	0.0177	0.0280	0.0237	0.0266	0.0275	0.0169	0.0286
Sr	0.0141	0.0202	0.0197	0.0187	0.0087	0.0067	0.0063	0.0042	0.0068	0.0044	0.0027
Ni	0.0004	0.0053	0.0000	0.0025	0.0019	0.0041	0.0016	0.0000	0.0000	0.0000	0.0037
Fe	0.8855	0.8746	0.8667	0.8158	0.8812	0.8183	0.7989	0.8230	0.7714	0.7980	0.8478
Ba	0.0000	0.0007	0.0040	0.0012	0.0023	0.0015	0.0005	0.0000	0.0005	0.0000	0.0012
V	0.0041	0.0042	0.0066	0.0031	0.0027	0.0023	0.0034	0.0033	0.0033	0.0062	0.0043
Total	7.6739	7.6984	7.6857	7.6667	7.7237	7.7231	7.6936	7.6888	7.6905	7.6799	7.7190
Ps = 100 x Fe/(Fe+Al)	31	31	31	29	30	29	28	29	27	28	29

INTENSIVE CRYSTALLIZATION PARAMETERS

Solidus temperature

BLUNDY & HOLLAND (1990) proposed a hornblende-plagioclase thermometer with estimated uncertainties of ± 75 ºC, in a temperature range of 500–1100ºC for quartz-saturated rocks. In a later paper, HOLLAND & BLUNDY (1994) extend the formulation of BLUNDY & HOLLAND (1990) to embrace more amphibole-plagioclase parageneses. The calibration based on the equilibrium: edenite + albite = richterite + anorthite (reaction B) of HOLLAND & BLUNDY (1994) show the lowest values and are considered to be the most reliable because they more precisely reproduce the T estimated by other independent methods (ANDERSON 1996; BACHMANN & DUNGAN 2002). This thermometer works well (±35–40 ºC) in the range 400–1000 ºC and 1 to 15 kbar over a broad range of bulk compositions. MOLINA et al. (2015) calibrated an empirical amphibole/liquid Mg partitioning thermometer using robust regression methods and observed that their T estimates are consistent with those of the edenite-albite-richterite-anorthite thermometer from HOLLAND & BLUNDY (1994). Near-solidus hornblende-plagioclase temperatures (HB94TB) for the Major Isidoro and Monteirópolis plutons range from 684 to 720 ºC and 660 to 696 ºC, respectively. Diorite enclaves of the Major Isidoro pluton crystallized under temperature of 732 (± 2) º C.

Liquidus temperature

GREEN & WATSON (1982) and HARRISON & WATSON (1984) determined P_2O_5 levels at a given silica value and temperature at which that composition may be expected to crystallize apatite. This model could be used between 45% and 75% silica and, 0 and 10% water, and for the range of pressures expected in the crust (up to 25 kbar; GREEN & ADAM 2002). Iron content of the liquid or oxidation state play insignificant effects on phosphate saturation (TOLLARI et al., 2006). According to HARRISON & WATSON (1984) the following expression could have been used to estimate the minimum liquidus temperature: $T\ (°C) = \{[8400 + 26400(SiO_2 - 0.5)]/[\ln(42/P_2O_5) + 3.1 + 12.4(SiO_2 - 0.5)] - 273.15\}$. Accordingly, the granites of the Major Isidoro pluton have temperatures that vary between 863 to 1000 °C (average = 936 °C) while rocks of the Monteirópolis pluton presented calculated temperature of 814 to 1023 °C (Table 18).

WATSON & HARRISON (1983) developed a solubility model based on the relationship of zircon crystallization and melt composition and defined the saturation

behavior of zircon as a function of temperature and composition. This model could be used when zircon was one of the earliest minerals to crystallize and assumes that zircon was not a cumulate phase, xenocrystic or inherited of the source region. Sensitivity tests reinforce previous thoughts (see WATSON & HARRISON op. cit.) and indicate that temperature and composition are the two dominant controls on zircon solubility in crustal melts with no observable effects due to pressure (up to 25 kbar) or variable water content (BOEHNKE et al., 2013). Estimates of the near liquidus could be obtained by the equation: $T_{Zr}(°C) = \{(12900) / [\ln(497644/Zr) + 3.8 + 0.85(M - 1)] - 273.15\}$ where the parameter $M = (Na + K + 2Ca)/(Al \cdot Si)$. For the studied rocks M values are within the experimental calibration range of WATSON & HARRISON (1983) and MILLER et al., 2003 (1.3 to 1.9), except for two samples of the Monteirópolis pluton that have granodioritic to tonalitic compositions (Table 18). Some authors extrapolated the experimental calibration range to apply this model to tonalitic composition rocks (e.g., HANSMANN & OBERTI 1991). According to this method the calculated temperatures recorded for the Major Isidoro pluton vary between 740 to 868 °C (avg. 818 °C) and the Monteirópolis pluton gives temperature estimates ranging from 763 to 856 °C (avg. 805 °C).

Table 6. Temperature estimates from apatite (T_{Ap}) and zirconium (T_{Zr}) saturation thermometry. Major elements in wt.%, and Zr in ppm.

Major Isidoro pluton										
Sample\Elements	SiO_2	Al_2O_3	CaO	Na_2O	K_2O	P_2O_5	Zr	T_{Zr}(ºc)	T_{Ap}(°C)	M
TR-13	70.05	14.08	2.14	4.09	4.20	0.24	262	817	1000	1.57
TR-18	68.87	14.43	2.69	3.51	3.58	0.26	408	868	998	1.47
TR-20	67.08	14.41	2.88	4.01	2.12	0.09	95	740	863	1.43
TR-22	59.13	16.90	4.58	5.24	2.07	0.49	364	824	972	1.86
TR 24	69.23	15.39	1.42	3.36	5.10	0.11	317	857	906	1.30
TR-25	68.68	14.91	2.41	3.55	4.95	0.17	305	832	947	1.55
TR-26	67.86	15.34	3.25	4.62	1.59	0.14	120	756	917	1.47
TR-37	66.58	15.62	2.36	3.66	4.60	0.17	281	831	927	1.48
TR-38	65.61	15.40	2.84	4.10	2.20	0.22	273	836	944	1.38
TR-39	65.09	16.10	3.05	4.90	2.00	0.25	260	822	954	1.50
Monteirópolis pluton										
TR–01	59.72	17.50	3.70	5.78	3.04	0.40	455	835	951	1.92
TR–43	67.50	13.81	2.09	3.14	5.44	0.18	221	796	940	1.61
TR–45	69.44	14.41	1.55	3.39	5.39	0.11	267	825	907	1.46
TR–46	71.86	14.45	1.31	4.04	4.27	0.05	158	787	857	1.37
TR–48	62.72	15.18	2.52	3.07	6.79	0.52	515	856	1023	1.83
TR–49	71.49	15.82	1.18	4.20	4.66	0.09	128	772	908	1.32
TR–50	73.43	14.56	0.74	3.87	5.05	0.03	112	763	828	1.31
TR–51	71.27	15.19	1.06	4.42	4.47	0.13	121	764	944	1.37
TR–52	64.53	17.14	2.43	5.12	3.77	0.45	388	848	1023	1.62

TR–73	71.04	14.78	1.53	3.66	5.68	0.18	323	840	977	1.51
TR–74	66.47	15.74	1.89	4.22	5.21	0.22	294	824	954	1.59
TR–76	68.78	16.19	2.08	4.54	4.84	0.18	280	821	954	1.58
TR–77	70.77	13.92	1.38	4.19	4.43	0.17	220	806	965	1.50
TR–78	70.68	14.94	1.21	4.73	4.42	0.15	164	781	953	1.49
TR–79	70.23	15.31	0.20	5.73	3.22	0.04	159	793	814	1.29
TR–80	71.27	15.27	1.56	3.71	4.53	0.08	210	814	895	1.34
TR–85	67.43	15.10	2.19	4.11	3.92	0.24	176	782	974	1.53
TR–88	66.19	19.56	1.55	4.27	3.58	0.11	146	797	872	1.13
TR–89	63.73	14.51	2.65	4.84	4.92	0.34	295	791	976	2.02

Major elements in wt.%, and Zr in ppm. T_{Zr}(°C) = {(12900) / [ln(497644/Zr) + 3.8 + 0.85(M – 1)] – 273.15} where M = 100(Na + K + 2Ca) / Al.Si. (WATSON & HARRISON 1983); TAp(°C) = {[8400 + 26400(SiO_2 – 0.5)] / [ln(42/P_2O_5) + 3.1 + 12.4(SiO_2 – 0.5)] – 273.15} (HARRISON & WATSON 1984).

Amphibole barometry

An empirical igneous barometer based on Al-in-hornblende was proposed by HAMMARSTRON & ZEN (1986) for estimate pressures of crystallization of calc-alkaline plutons and HOLLISTER et al. (1987) reduced the ± 3 kbar error to 1 kbar in the main range 2–8 kbar. This barometer was subject to experimental calibration that confirms the linear relation between aluminum in hornblende and total pressure of intrusion that can be used from 2.5 to 13 kbar (JOHNSON & RUTHERFORD 1989; SCHMIDT 1992). The experimental calibration delivered by SCHMIDT (1992) was made using epidote-bearing tonalite and some authors argue that its calibration is expected to be the most appropriate for mEp bearing plutons (e.g., SIAL et al., 1999, 2008) although others factors control the amphibole's chemistry. The Al-in-Hornblende barometry should be applied to rocks that have the mineral assemblage plagioclase + K-feldspar + quartz + hornblende + biotite + titanite + magnetite ± ilmenite + melt + fluid phase (e.g., HAMMARTRON AND ZEN 1986; HOLLISTER et al., 1987; JOHNSON & RUTHERFORD 1989; SCHMIDT 1992; RUTHERFORD & JOHNSON 1992; ANDERSON & SMITH 1995; ANDERSON 1996; among others). The barometer is sensitive to variations in fO_2, f_{H_2O}, and temperature (HAMMARSTRON & ZEN 1986; SCHMIDT 1992; ANDERSON & SMITH 1995; ANDERSON 1996). ANDERSON & SMITH (1995) delivered a revised expression for the Al in hornblende barometer incorporating the effect of temperature from the hornblende-plagioclase thermometer of HOLLAND & BLUNDY (1994) and using the experimental data from JOHNSON & RUTHERFORD (1989b) and SCHMIDT (1992). The resulting equation is P (± 0.6 kbar) = 4.76Al – 3.01 – {[T (ºC) – 675]/85} x {0.530Al + 0.005294 [T (ºC) – 675]}. The presence of the buffer assemblage into the studied granitoids, at first, ensure to apply the Al-in-hornblende barometer of ANDERSON & SMITH (1995). These authors recommend that T must be < 800 ºC. When applied to the epidote-bearing Major Isidoro

and Monteirópolis plutons we found calculated pressures of 5.27–7.71 kbar and 4.3–5.34 kbar, respectively. These pressures of crystallization are within the lower limit of stability of magmatic epidote (0.3 to 0.7; ZEN & HAMMARSTRON 1984; SCHMIDT & POLI 2004). In order to compare the obtained results of the Al-in-hornblende barometer of SCHMIDT (1992) and ANDERSON & SMITH (1995), the calculated values are portrayed in Table 14. These values are equal within the uncertainty of ± 0.6 kbar. ANDERSON (1996) proposed two groups of granitic plutons as a function of Al_2O_3 contents. The Major Isidoro granites and dioritic enclave have high-alumina hornblende (Al_2O_3 > 10 wt.%), while the Monteirópolis granites have intermediate-alumina hornblende (Al_2O_3 = 8.83 to 9.54 wt.%).

Oxygen fugacity

Oxygen fugacity by far exerts the strongest control on mafic silicate mineral chemistry (ANDERSON & SMITH 1995; ANDERSON 1996). This parameter is difficult to estimate in silicic rocks, especially those that contain only one Fe-Ti oxide mineral (WONES 1989). The presence of titanite + magnetite + quartz assemblage has long been known as suggestive of relatively high fO_2 in siliceous magmas (ENAMI et al., 1993; WONES 1989 and references therein). According to WONES (1989), when this assemblage occurs along with clinopyroxene or amphibole with intermediate or higher Mg# ((Mg/(Mg + Fe)) ratios, relatively high fO_2 are implied. Based on the recognition of this primary assemblage he proposed an equation that involves the intensive parameters temperature (in Kelvins) and pressure (in bars) [$\log fO_2 = -30930/T + 14.98 + 0.142(P - 1)/T$] to estimate of relative oxygen fugacity. Accordingly, the Major Isidoro pluton shows the highest $\log fO_2$ values of – 16.4 to – 14.9 and the Monteirópolis presents the lowest $\log fO_2$ values of – 17.4 to −16.3. ANDERSON & SMITH (1995) suggested that amphibole Fe# ratios ($Fe^{Amp}/(Fe^{Amp} + Mg^{Amp})$) for barometry studies should be in the range of 0.40–0.65 (Mg-rich amphiboles) and for the Major Isidoro and Monteirópolis plutons Fe# ratios vary from 0.577–0.639 and 0.552–0.575, respectively, consistent with moderate to high oxygen fugacity (Fig. 9). This exceptional condition remains to be validity (cf., PUTIRKA 2016). Plutons that crystallized to low oxygen fugacity with Fe-rich amphiboles are not amenable to hornblende barometry even though the full mineral assemblage is present and yield anomalous elevated pressures. Fe-rich amphiboles should not have $Fe^{3+}/(Fe^{3+} + Fe^{2+})$ ratios lower than 0.20 to apply hornblende barometry (SCHMIDT 1992; ANDERSON

& SMITH 1995), however exceptions occur (e.g., PAPOUTSA & PE-PIPER 2014; CAMPOS et al., 2016). For the studied granitoids, hornblende $Fe^{3+}/(Fe^{3+} + Fe^{2+})$ ratios are within the limiting value except to one core and one rim analyzed of the Monteirópolis pluton. The whole-rock Fe# [Fe/(Fe + Mg)] ratio varies independently of Fe# ratio of amphibole and biotite, and with the increase of fO_2 the Fe# ratio of these minerals notably decrease (e.g., ANDERSON & SMITH 1995; ANDERSON et al., 2008). ANDERSON et al. (2008) proposed an approximate fO_2 relative to the quartz-fayalite-magnetite buffer (Δ_{QFM}) depending upon fe# [Fe/(Fe + Mg)] in biotite. For the Major Isidoro pluton, fe# in biotite ranges from 0.50 to 0.58, and for Monteirópolis from 0.43 to 0.55, corresponding to Δ_{QFM} = + 1 to < + 2.5. This result is similar to those for granites in the northern Borborema Province obtained by CAMPOS et al. (2016), who also observed that biotite with high fO_2 (Δ_{QFM} = + 0.8 to + 2.0) crystallizes together with amphibole at similar high oxidizing conditions.

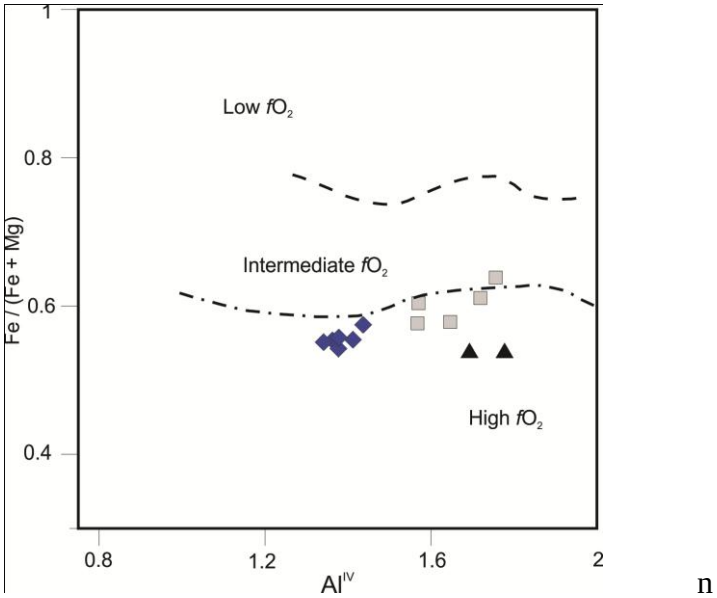

Figure 9. Al^{IV} *vs.* (Fe/(Fe + Mg) plot. fO_2 fields after ANDERSON & SMITH (1995).

Magma transport estimates

BRANDON et al. (1996) suggested that epidote survival in granitic rocks at lower pressures is due to fast armoring of epidote from contact with the melt during low-pressure crystallization by mineral aggregates, and due to fast upward transport probably by dyking. The textural relationships of epidote with other minerals (Fig. 10) yield information an upward magma transport (DAWES & EVANS 1991; BRANDON et al., 1996). SIAL et al. (2008) based on dissolution kinetic experiments on epidote from BRANDON et al. (1996) and estimating the size of partially corroded subhedral

epidote crystals proposed a way to estimate magma transport rates that follow the approach detailed below:

1) Select mEp on the basis of their mol.% Ps, consisting of highly corroded subhedral grains that are partially shielded by plagioclase, biotite or K-feldspar (Fig. 10);
2) Infer the original shapes of corroded grains and measure the maximum dissolution zone width;
3) Estimate the duration of corrosion by using the minimum apparent diffusion coefficient of 5×10^{-17} m^2/s for Si, Al, Ca and Fe between tonalitic magma and epidote at 750 °C (BRANDON et al., 1996) as follows:

$d_z = \sqrt{[D_{app} \text{ x } t]}$

where

d_z width of dissolution zone (m);

D_{app} apparent diffusion coefficient (5×10^{-17} m^2/s); and

t time for partial dissolution of epidote (s)

Accordingly,

$t = d_z{}^2/(5\times10^{-17}\ m^2/s)$

4) Depth of host magma emplacement is inferred from Al-in hornblende barometry;

5) The rate of magma transport is the ratio of the route length (difference between the emplacement depth and the source depth) to the average time of corrosion of epidote exposed to the host melt. For a tonalite melting, at water-saturated conditions and fO_2 buffered by NNO, plagioclase and epidote may coexist from a depth ~10 kbar (SCHMIDT & THOMPSON 1996, Fig. 2). We infer the route length as the difference between 10 kbar and the emplacement depth. Accordingly,

$T_r = L_r/t$

where

T_r transport rate (m/year)

L_r $(10-P_e)\cdot10^4/3$ (m)

L_r length route (m)

P_e pressure of emplacement (kbar)

t time of partial dissolution of epidote (year)

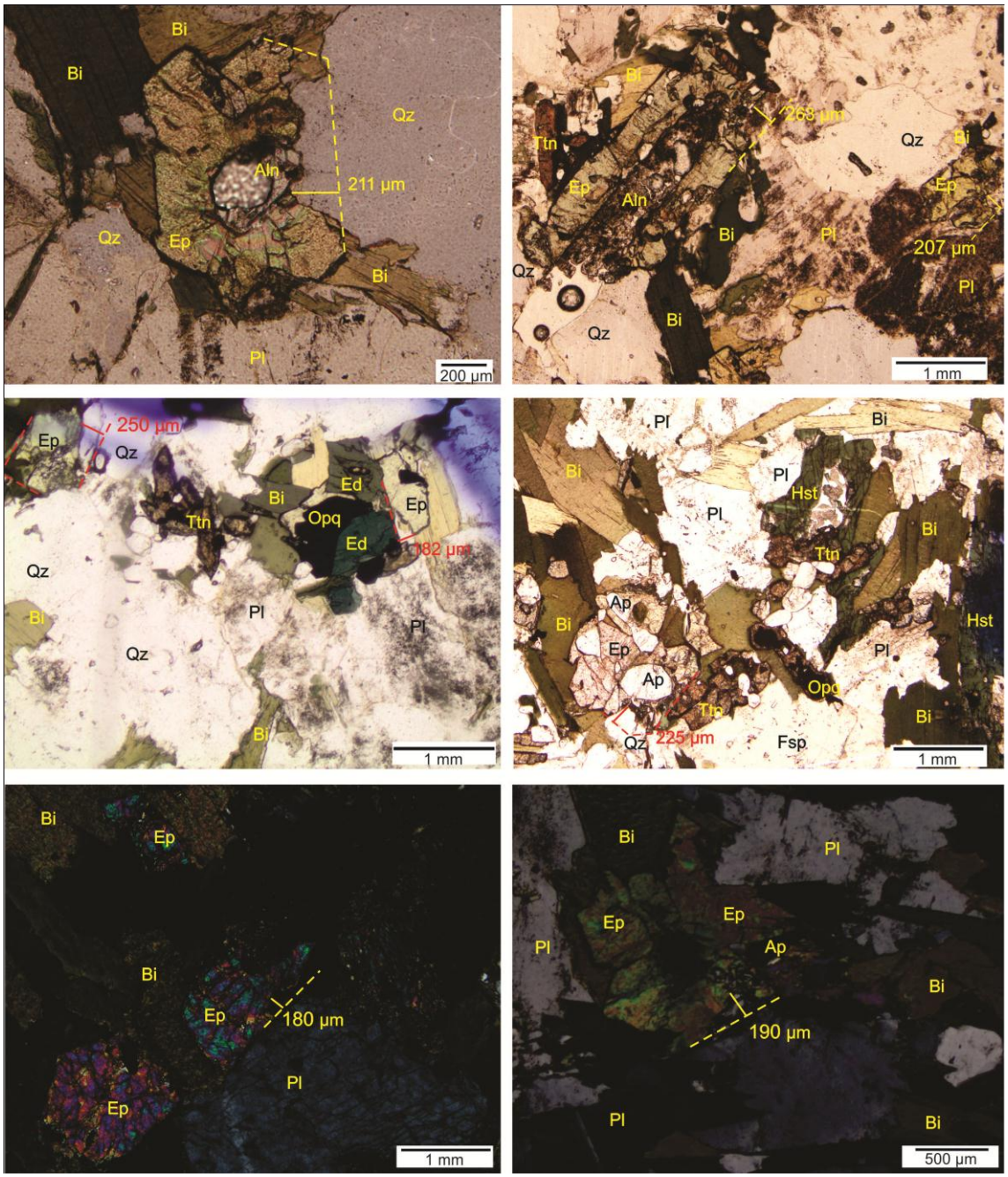

Figure 10. Textural aspects showed by magmatic epidote from the Monteirópolis (a, b, c) and Major Isidoro (d, e, f) granites. a) Euhedral epidote partially dissolved by the host granitic magma; b) Euhedral magmatic epidote with allanite core embayed or totally dissolved where in contact with the quartz-feldspathic matrix; c) Euhedral epidote armored from total dissolution by biotite, and edenite from reaction with host magma; d) Subhedral epidote armored by biotite; included occur euhedral apatite crystals. e) Subhedral epidote grains armored by biotite, and feldspar with minor corroded embayment. f) Euhedral magmatic epidote with allanite core included in biotite. Parallel polarizers except for photo e and f. dashed lines are an attempt to reconstruct original shape of epidote crystals, indicating how much some of them have been dissolved by host magma. Mineral abbreviations after WHITNEY & EVANS (2010) are: All = allanite; Bt = biotite; Ep = epidote; Pl = plagioclase; Ttn = titanite; Ed = edenite; Hst = hastingsite; Ap = apatite; Qz = quartz; Opc = opaque mineral; Fsp = feldspar.

Based on this approach we can obtain the time for dissolution width of magmatic epidote, and the maximum upward ascension rates of the magmas that originated the Major Isidoro and Monteirópolis plutons. For the Major Isidoro granites the width of dissolution reported of 0.157 to 0.225 mm occurred during 15.6 to 32 years of partial corrosion, which correspond to ascent rates of 365 to 750 m.year^{-1}, while for the Monteirópolis granites the dissolution zones reported of 0.207 to 0.263 mm occurred during 27–49 years of partial corrosion, which correspond to ascent rates of 395 to 635 m.year^{-1}.

DISCUSSION AND CONCLUSION

The studied granites share similar chemistry and mineralogy. The plutonic rocks from Major Isidoro pluton are medium-to high-K calc-alkaline while the rocks from the Monteirópolis pluton are high-K calc-alkaline, both of them magnesian, and slightly peraluminous to metaluminous (SILVA et al., 2015, 2016). The mineral assemblage of magnetite, titanite, hornblende, biotite, quartz, and ± epidote in both plutons suggests that the original magmas were oxidized (e.g. WONES 1989).

Early crystallized subhedral to euhedral epidote crystals with or without allanite core mainly armored by biotite, feldspar, and titanite or included in the former are typical of magmatic epidote, and minor secondary alteration reinforces it. Pistacite contents of the analyzed epidote crystals from the Major Isidoro granites (27 to 29) and from the Monteirópolis granites (29 to 31) also indicate a magmatic origin and suggest oxidizing conditions between the NNO-HM buffers (e.g. LIOU 1973; NANEY 1983; SCHMIDT & POLI 2004) as suggested by the coexistent mineral assemblage. Pistacite contents are different from epidote derived from plagioclase alteration that shows Ps ranging from 0 to 20, and that originated from biotite alteration has 30 to 50 (e.g. TULLOCH 1979).

Epidote from these plutons shows corroded margins suggestive of dissolution with the host magma before final solidification that together with the geological location next to the Jacaré dos Homens shear zone, which probably represents one deep- seated lithospheric shear zone rooted in the upper mantle that must have facilitated magmas to rise, are consistent with the rapid upward magma migration (e.g. BRANDON et al., 1996; SIAL et al., 1999, 2008; BRASILINO et al., 2011).

The aluminum-in-hornblende barometer indicates emplacement depth of 15 to 17.3 km (4.3 to 5.3 kbar) to the Monteirópolis granites and of 17 to 25 km (5.3 to 7.7 kbar) to

the Major Isidoro granitic rocks. These pressures estimated by Al–in–hornblende correlates with the compositional variations of coexisting epidote; being high pressure to the Major Isidoro granites that have lower pistacite contents, and more lower pressure to the Monteirópolis granites that have pistacite-rich compositions. Hornblende-plagioclase thermometry for Major Isidoro granites gave solidified temperatures between 684 to 720 ºC, while for Monteirópolis granites provided slightly lower temperatures between 660 to 696 °C. The Zr saturation temperatures (i.e., liquidus temperature) from both plutons are higher than 800 ºC, except to a few samples that are more silica-rich, and suggest that these plutons are high-temperature granites in the sense of MILLER et al. (2003) however, the dated samples clearly presented inherited zircon cores that point to low-temperature granites (c.f. CHAPPELL et al., 2004).

The inferred primary melt of the studied granites was a high-K basalt. After partial melting from source rocks, fractional crystallization must have occurred during magma ascent, as supported relatively similar Sr–Nd isotopic compositions, suggesting minor crustal assimilation during magma ascent.

ACKNOWLEDGMENTS

We thank Edward Sawyer for discussion on the geology from the Major Isidoro pluton. Nilson M. Botelho is thanked for mineral chemistry laboratory facilities.We are grateful to Bruna Maria Borba de Carvalho for acquisition of mineral chemistry at the Electron Microprobe Laboratory in the University of Brasília, Brazil, and Anderson de Abreu da Silva for assistance with chemical analyses at the Stable Isotope Laboratory (LABISE) in the Federal University of Pernambuco, Brazil. VPF and ANS acknowledge the continuous financial support from the CNPq and FACEPE.

REFERENCES

ABDEL-RAHMAN, A.F.M., 1994. Nature of Biotites from Alkaline, Calc-alkaline, and Peraluminous Magmas. Journal of Petrology 35, 525–541.

ANDERSON, J.L., 1996. Status of thermobarometry in granitic batholiths. Transactions of the Royal Society of Edinburgh: Earth Sciences, 87,125–138.

ANDERSON, J.L., BARTH, A.P., WOODEN, J.L., MAZDAB, F., 2008. Thermometry and Thermobarometers in Granitic Systems. Reviews in Mineralogy and Geochemistry 69, 121–142.

ANDERSON, J.L., SMITH, D.R., 1995. The effects of temperature and fO_2 on the Al-in-hornblende barometer. American Mineralogist 80, 549–559.

BACHMANN, O., DUNGAN, M., 2002. Temperature-induced Al-zoning in hornblendes of the Fish Canyon magma, Colorado. American Mineralogist, 87, 1062–1076.

BLUNDY, J.D., HOLLAND, T.J.B., 1990. Calcic amphibole equilibria and a new amphibole-plagioclase geothermometer. Contributions to Mineralogy and Petrology 104, 208–224

BOEHNKE, P., WATSON, E.B., TRAIL, D., HARRISON, T.M., SCHMITT, A., 2013. Zircon saturation re-revisited. Chemical Geology 351, 324–334.

BRANDON, A.D., CREASER, R.A., CHACKO, T., 1996. Constraints on Rates of Granitic Magma Transport from Epidote Dissolution Kinetics. Science 271, 1845–1848.

BRASILINO, R.G., SIAL, A.N., FERREIRA, V.P., PIMENTEL, M.M., 2011. Bulk rock and mineral chemistries and ascent rates of high-K calc-alkalic epidote-bearing magmas, Northeastern Brazil. Lithos 127, 441–454.

BRASILINO, R.G., SIAL, A.N., LAFON, J.M., 1999. Magmatic epidote, hornblende barometric estimates of the Conceição das Creoulas pluton, Alto Pajeu Terrane, NE Brazil. Anais da Academia Brasileira de Ciências 71, 3–16.

BRITO, M.F.L., SILVA FILHO, A.F., GUIMARÃES, I.P., 2009. Geologia isotópica do batólito shoshonítico-ultrapotássico Neoproterozóico Serra do Catú e implicações na evolução da interface dos Domínios Canindé e Pernambuco–Alagoas. Revista Brasileira de Geociências 39, 324–337.

CAMPOS, T.F.C., NEIVA, A.M.R., NARDI, L.V.S., PEREIRA, L.S., BONZANINI, L.F., PETTA, R.A., MEYER, F.M., 2005. Magmatic epidote and amphibole from the Rio Espinharas Hybrid Complex, Northeastern Brazil. Pesquisas em Geociências 32 (2), 41–55.

CAMPOS, B.C.S., VILALVA, F.C.J., NASCIMENTO, M.A.L., GALINDO, A.C., 2016. Crystallization conditions of porphyritic high-K calc-alkaline granitoids in the extreme northeastern Borborema Province, NE Brazil, and geodynamic implications. Journal of South American Earth Sciences 70, 224–236.

CHAPPELL, B.W., WHITE, A. J. R., WILLIAMS, I.S., WYBORN, D., 2004. Low- and high-temperature granites. Transactions of the Royal Society of Edinburgh: Earth Sciences 95, 125–140.

COBBING, J., 2000. The Geology and Mapping of Granite Batholiths. Lecture Notes in Earth Sciences 96, Springer, Berlin Heidelberg New York, 121 pp.

DAWES, R.L., EVANS, B.W., 1991. Mineralogy and geothermobarometry of magmatic epidote-bearing dikes, Front Range, Colorado. Geological Society of America Bulletin 103, 1017–1031.

DEER, W.A., HOWIE, R.A., ZUSSMAN, J., 2013. An Introduction to the Rock-Forming Minerals. 3rd. Edition. London: Mineralogical Society, 498 pp.

DE OLIVEIRA, R.G., 2008. Arcabouço geofísico, isostasia e causas do magmatismo Cenozóico da Província Borborema e de sua margem continental (Nordeste do Brazil). Unpublished PhD thesis, Federal University of Rio Grande do Norte, Rio Grande do Norte, Brazil, 411 pp, (in Portuguese with English abstract).

ENAMI, M., SUZUKI, K., LIOU, J.G., BIRD, D.K., 1993. $Al–Fe^{3+}$ and F–OH substitutions in titanite and constraints on their P–T dependence. European Journal of Mineralogy 5, 219–231.

EVANS, B.W., VANCE, J.A., 1987. Epidote phenocrysts in dacitic dikes, Boulder County, Colorado. Contributions to Mineralogy and Petrology 96, 178–185.

FERREIRA, V.P., SIAL, A.N., JARDIM DE SÁ, E.F., 1998. Geochemical and isotopic signatures of the Proterozoic granitoids in terranes of the Borborema Province, northeastern Brazil. Journal of South American Earth Sciences 11, 439–455.

FERREIRA, V.P., SIAL, A.N., PIMENTEL, M.M., ARMSTRONG, R., GUIMARÃES, I.P., SILVA FILHO., A.F., LIMA, M.M.C., SILVA, T.R., 2015. Reworked old crust-derived shoshonitic magma: The Guarany pluton, Northeastern Brazil. Lithos 232, 150–161.

FERREIRA, V.P., SIAL, A.N., PIMENTEL, M.M., ARMSTRONG, R., SPICUZZA, M.J., GUIMARÃES, I.P., SILVA FILHO, A.F., 2011. Contrasting sources and P-T crystallization conditions of epidote-bearing granitic rocks, northeastern Brazil: O, Sr, and Nd Isotopes. Lithos 121, 189–201.

FERREIRA, V.P., SIAL, A.N., PIMENTEL, M.M., MOURA, C.A.V., 2004. Acidic to intermediate magmatism and crustal evolution in the Transversal Zone, northeastern Brazil. In: Mantesso, Neto, Bartorelli, V., Carneiro, A., Dal Re, C., e Brito Neves, B.B. (Eds.), Geologia do Continente Sul-americano: a evolução da obra de Fernando Flávio Marques de Almeida. Editora São Paulo, USP, pp. 189–201. chapter XII,.

FERREIRA, V.P., VALLEY, J.W., SIAL, A.N, SPICUZZA, M.J., 2003. Oxygen isotope compositions and magmatic epidote from two contrasting metaluminous granitoids, NE Brazil. Contributions to Mineralogy and Petrology 145, 205–216.

GALINDO, A.C., DALL'AGNOL, R., MCREATH, I., LAFON, J.M., TEIXEIRA, N., 1995. Evolution of Brasiliano-age granitoid types in a shear-zone environment, Umarizal-Caraubas region, Rio Grande do Norte, northeast Brazil. Journal of South American Earth Sciences 8, 79–95.

GAO, P., ZHENG, Y-F., ZHAO, Z-F., 2016. Distinction between S-type and peraluminous I-type granites: Zircon versus whole-rock geochemistry. Lithos 258–259, 77–91.

GREEN, T.H., ADAM, J., 2002. Pressure effect on Ti- or P-rich accessory mineral saturation in evolved granitic melts with differing K_2O/Na_2O ratios. Lithos 61(3–4), 271–282.

GREEN, T.H., WATSON, E.B., 1982. Crystallization of Apatite in Natural Magmas Under High Pressure, Hydrous Conditions, with Particular Reference to 'Orogenic' Rock Series. Contributions to Mineralogy and Petrology 79, 96–105.

GUIMARÃES, I.P., SILVA FILHO, A.F., ALMEIDA, C.N., VAN SCHMUS, W.R., ARAÚJO, J.M.M., MELO, S.C., MELO, E.B., 2004. Brasiliano (Pan-African) granitic magmatism in the Pajeú-Paraíba belt, Northeast Brazil: an isotopic and geochronological approach. Precambrian Research 135, 23–53.

HAMMARSTRON, J.M., ZEN, E.-A., 1986. Aluminum in hornblende: An empirical igneous geobarometer. American Mineralogist 71, 1297–1313.

HANSMANN W, OBERLI F (1991) Zircon inheritance in an igneous rock suite from the southern Adamello batholith (Italian Alps). Contributions to Mineralogy and Petrology 107, 501–518.

HARRISON, T.M., WATSON, E.B., 1984. The behavior of apatite during crustal anatexis: Equilibrium and kinetic considerations. Geochimica et Cosmochimica Acta 48, 1467–1477.

HAWTHORNE, F.C., OBERTI, R., HARLOW, G.E., MARESCH, W.V., MARTIN, R.F., SCHUMACHER, J.C., WELCH, M.D., 2012. IMA Report: Nomenclature of the amphibole supergroup. American Mineralogist 97, 2031–2048.

HOLLAND, T., BLUNDY, J., 1994. Non-ideal interactions in calcic amphiboles and their bearing on amphibole-plagioclase thermometry. Contributions to Mineralogy and Petrology 116, 433–447.

HOLLISTER, L.S., GRISSOM, G.C., PETERS, E.K., STOWELL, H.H., SISSON, V.B., 1987. Confirmation of the empirical correlation of Al in hornblende with pressure of solidification of calc-alkaline plutons. American Mineralogist 72, 231–239.

JOHNSON, M.C., RUTHERFORD, M.J., 1989. Experimental calibration of the aluminum-in-hornblende geobarometer with application to Long Valley caldera (California) volcanic rocks. Geology 17, 837–841.

JOHNSTON, A.D., WYLLIE, P.J., 1988. Interaction of granitic and basic magmas: experimental observations on contamination processes at 10 kbar with H_2O. Contributions to Mineralogy and Petrology 98, 352–362.

LEAKE, B.E., WOOLLEY, A.R., ARPS, C.E.S., BIRCH, W.D., GILBERT, M.C., GRICE, J.D., HAWTHORNE, F.C., KATO, A., KISCH, H.J., KRIVOVICHEV, V.G., LINTHOUT, K., LAIRD, J., MANDARINO, J., MARESCH, W.V., NICKEL, E.H., ROCK, N.M.S., SCHUMACHER, J.C., SMITH, D.C., STEPHENSON, N.C.N., UNGARETTI, L., WHITTAKER, E.J.W., YOUZHI, G., 1997. Nomenclature of amphiboles: Report of the Subcommittee on Amphiboles of the International Mineralogical Association Commission on New Minerals and Mineral Names. European Journal of Mineralogy 9, 623–651.

LEAKE, B.E., WOOLLEY, A.R., BIRCH, W.D., BURKE, E.A.J., FERRARIS, G., GRICE, J.D., HAWTHORNE, F.C., KISCH, H.J., KRIVOVICHEV, V.G., SCHUMACHER, J.C., STEPHENSON, N.C.N., WHITTAKER, E.J.W., 2003. Nomenclature of amphiboles: Additions and revisions to the International Mineralogical Association's 1997 recommendations. The Canadian Mineralogist 41, 1355–1362.

LIOU, J.G., 1973. Synthesis and stability relations of epidote, $Ca_2Al_2FeSiO_{12}(OH)$. Journal of Petrology 14, 381–413.

LONG, E.L., CASTELLANA, C.H., SIAL, A.N., 2005. Age, Origin and Cooling History of the Coronel João Sá Pluton, Bahia, Brazil. Journal of Petrology 46, 255–273.

MENDES, V., BRITO, M.F.L, PAIVA, I.P., 2009. Folha Arapiraca (SC.24-X-D, escala 1:250000). Integration Geological (Geologic map). Brazilian Geological Survey (CPRM), Recife-PE, Brazil.

MILLER, C.F., MCDOWELL, S.M., MAPES, R.W., 2003. Hot and cold granites? Implications of zircon saturation temperatures and preservation of inheritance. Geology 31, 529–532.

MOLINA, J.F., MORENO, J.A., CASTRO, A., RODRÍGUEZ, C., FERSHTATER, G.B., 2015. Calcic amphibole thermobarometry in metamorphic and igneous rocks: New calibrations based on plagioclase/amphibole Al-Si partitioning and amphibole/liquid Mg partitioning. Lithos 232, 286–305.

NACHIT, H., RAZAFIMAHEFA, N., STUSSI, J.M., CARRON, J.P., 1985. Composition chimique des biotites et typologie magmatique des granitoids. Comptes rendus de l'Académie des sciences de la Terre et des planetes. Earth and Planetary Sciences 11 (II), 813–818.

NANEY, M.T., 1983. Phase equilibria of rocks-forming ferromagnesian silicates in granitic systems. American Mineralogy 283, 993–1033.

NEVES, S.P., BRUGUIER, O., BOSCH, D., SILVA, J.M.R., MARIANO, G., 2008. U–Pb ages of plutonic and metaplutonic rocks in southern Borborema Province (NE Brazil): timing of Brasiliano deformation and magmatism. Journal of South American Earth Sciences 25, 285–297.

NEVES, S.P., BRUGUIER, O., VAUCHEZ, A., BOSCH, D., SILVA, J.M.R., MARIANO, G., 2006. Timing of crust formation, deposition of supracrustal sequences, and Transamazonian and Brasiliano metamorphism in the East Pernambuco belt (Borborema Province, NE Brazil): Implications for western Gondwana assembly. Precambrian Research 149, 197–216.

NEVES, S.P., MELO, S.C., MOURA, C.A.V., MARIANO, G., SILVA, J.M.R., 2004. Zircon Pb-Pb Geochronology of the Caruaru area, Northeastern Brazil: Temporal Constraints on the Proterozoic Evolution of Borborema Province. International Geology Review 46, 52–63.

NEVES, S.P., MONIÉ, P., BRUGUIER, O., SILVA, J.M.R., 2012. Geochronological, thermochronological and thermobarometric constraints on deformation, magmatism and thermal regimes in eastern Borborema Province (NE Brazil). Journal of South American Earth Sciences 38, 129–146.

NEVES, S.P., VAUCHEZ, A., 1995. Magma emplacement and shear zone nucleation and development in Northeast Brazil (Fazenda Nova and Pernambuco shear zones, State of Pernambuco). Journal of South American Earth Sciences 8, 289–298.

PAPOUTSA, A., PE-PIPER, G., 2014. Geochemical variation of amphiboles in A-type granites as an indicator of complex magmatic systems: Wentworth pluton, Nova Scotia, Canada. Chemical Geology 384, 120–134.

PUTIRKA., 2016. Amphibole thermometers and barometers for igneous systems and some implications for eruption mechanisms of felsic magmas at arc volcanoes. American Mineralogist 101, 841–858.

RUTHERFORD, M.J., JOHNSON, M.C., 1992. Comment on Blundy and Holland's (1990) "Calcic amphibole equilibria and a new amphibole-plagioclase geothermometer. Contributions to Mineralogy and Petrology

SAWYER, E.W., 2008. Atlas of Migmatites. The Canadian Mineralogist, Special Publication 9. NRC Research Press, Ottawa, Ontario, Canada 371 pp.

SCHMIDT, M, W., 1992. Amphibole composition in tonalite as a function of pressure: an experimental calibration of the Al-in-hornblende barometer. Contributions to Mineralogy and Petrology 110, 304–310.

SCHMIDT, M.W., POLI, S., 2004. Magmatic Epidote. Reviews in Mineralogy and Geochemistry 56, 399–430.

SCHMIDT, M.W., THOMPSON, A.B., 1996. Epidote in calc-alkaline magmas: An experimental study of stability, phase relationships, and the role of epidote in magmatic evolution. American Mineralogist 81, 462–474.

SHABANI, A.A.T., LALONDE, A.E., 2003. Composition of biotite from granitic rocks of the Canadian Appalachian Orogen: a potential tectonomagmatic indicator? The Canadian Mineralogist 41, 1381–1396.

SIAL, A.N., 1990. Epidote-bearing calc-alkalic granitoids in Northeast Brazil. Revista Brasileira de Geociências 20(1–4), 88–100.

SIAL, A.N., 1993. Contrasting metaluminous magmatic epidote-bearing granitic suites from two Precambrian Foldbelts in Northeast Brazil. Anais da Academia Brasileira de Ciências 65 (supl.), 141–162.

SIAL, A.N., FERREIRA, V.P., 2015. Magma associations in Ediacaran granitoids of the Cachoeirinha–Salgueiro and Alto Pajeú terranes, northeastern Brazil: Forty years of studies. Journal of South American Earth Sciences 68, 113–133.

SIAL, A.N., TOSELLI, A.J., SAAVEDRA, J., PARADA, M.A., FERREIRA, V.P., 1999. Emplacement, petrological and magnetic susceptibility characteristics of diverse magmatic epidote-bearing granitoid rocks in Brazil, Argentina and Chile. Lithos 46, 367–392.

SIAL, A.N., VASCONCELOS, P.M., FERREIRA, V.P., PESSOA, R.R., BRASILINO, R.G., MORAIS NETO, J.M., 2008. Geochronological and mineralogical constraints on depth of emplacement and ascension rates of epidote-bearing magmas from northeastern Brazil. Lithos 105, 225–238.

SILVA, L.C., ARMSTRONG, R., PIMENTEL, M.M., SCANDOLARA, J., RAMGRAB, G., WILDNER, W., ANGELIM, L.A.A., VASCONCELOS, A.M., RIZZOTO, G., QUADROS, M.L.E.S., SANDER,A., ROSA, A.L.Z., 2002. Reavaliação da evolução geológica em terrenos pré-cambrianos brasileiros com base em novos dados U–Pb SHRIMP, Parte III: Províncias Borborema, Mantiqueira meridional e Rio Negro-Juruena. Revista Brasileira de Geociências 32, 529–544.

SILVA, T.R., FERREIRA, V.P., LIMA, M.M.C., SIAL, A.N., 2016. Two stage mantle-derived granitic rocks and the onset of the Brasiliano orogeny: Evidence from Sr, Nd, and O isotopes. Lithos 264, 189–200.

SILVA, T.R., FERREIRA, V.P., LIMA, M.M.C., SIAL, A.N., SILVA., J.M.R., 2015. Synkinematic emplacement of the magmatic epidote bearing Major Isidoro tonalite-granite batholith: Relicts of an Ediacaran continental arc in the Pernambuco–Alagoas domain, Borborema Province, NE Brazil. Journal of South American Earth Sciences 64, 1–13.

SILVA FILHO, A.F., GUIMARÃES, I.P., SANTOS, L., ARMSTRONG, R., VAN SCHMUS, W.R., 2016. Geochemistry, U–Pb geochronology, Sm–Nd and O isotopes of ca. 50 Ma long Ediacaran High-K Syn-Collisional Magmatism in the Pernambuco Alagoas Domain, Borborema Province, NE Brazil. Journal of South American Earth Sciences 68, 134–154.

SILVA FILHO, A.F., GUIMARÃES, I.P., VAN SCHMUS, W.R., 2002. Crustal Evolution of the Pernambuco–Alagoas Complex, Borborema Province, NE Brazil: Nd Isotopic Data from Neoproterozoic Granitoids. Gondwana Research 5, 409–422.

SILVA FILHO, A.F., GUIMARÃES, I.P., VAN SCHMUS, W.R., ARMSTRONG, R., SILVA, J.M.R., COCENTINO, L.M., OSAKO, L.S., 2014. SHRIMP U–Pb zircon geochronology and Nd signatures of supracrustal sequences and orthogneisses constrain the Neoproterozoic evolution of the Pernambuco–Alagoas domain, southern part of Borborema Province, NE Brazil. International Journal of Earth Sciences 103, 2155–2190.

TOLLARI, N., TOPLIS, M.J., BARNES, S.J., 2006. Predicting phosphate saturation in silicate magmas: An experimental study of the effects of melt composition and temperature. Geochimica et Cosmochimica Acta, 70, 1518–1536.

TULLOCH, A.J., 1979. Secondary Ca–Al Silicates as Low-Grade Alteration Products of Granitoid Biotite. Contributions to Mineralogy and Petrology 69, 105–117.

TULLOCH, A.J., 1986. Comments and Reply on "Implications of magmatic epidote-bearing plutons on cirustal evolution in the accreted terranes of northwestern North America" and "Magmatic epidote and its petrologie significance". Geology 14, 186–187.

VALLEY, J.W., LACKEY, J.S., CAVOSIE, A.J., CLECHENKO, C.C., SPICUZZA, M.J., BASEI, M.A.S., BINDEMAN, I.N., FERREIRA, V.P., SIAL, A.N., KING, E.M., PECK, W.H., SINHA, A.K., WEI, C.S., 2005. 4.4 billion years of crustal maturation: oxygen isotope ratios of magmatic zircon. Contributions to Mineralogy and Petrology 150, 561–580.

VAN SCHMUS, W.R., BRITO NEVES, B.B., HACKSPACHER, P., BABINSKI, M., 1995. U/Pb and Sm/Nd geochronologic studies of the eastern Borborema Province, northeastern Brazil: initial conclusions. Journal of South American Earth Scieces 8, 267–288.

VAN SCHMUS, W.R., OLIVEIRA, E.P., SILVA FILHO, A.F., TOTEU, S.F., PENAYE, J., GUIMARÃES, I.P., 2008. Proterozoic links between the Borborema Province, NE Brazil and the Central African Fold Belt. In: Geological Society, London, Special Publications 294, 69–99.

VAUCHEZ, A., NEVES, S.P., CABY, R., CORSINI, M., EGYDIO-SILVA, M., ARTHAUD, M.H., AMARO, V., 1995. The Borborema shear zone system, NE Brazil. Journal of South American Earth Sciences 8, 247–266.

VYHNAL, C.R., MCSWEEN JR., H.Y., SPEER, J.A., 1991. Hornblende chemistry in southern Appalachian granitoids: Implication for aluminum hornblende thermo barometry and magmatic epidote stability. American Mineralogist 76, 176–188.

WATSON, E.B., HARRISON, T.M., 1983. Zircon saturation revisited: temperature and composition effects in a variety of crustal magma types. Earth and Planetary Science Letters 64, 295–304.

WEINBERG, R.F., VEVEAKIS, E., LIEB, R., 2015. Compaction-driven melt segregation in migmatites. Geology 43, 471–474.

WHITNEY, D.L., EVANS, B.W., 2010. Abbreviations for names of rock-forming minerals. American Mineralogist 95, 185–187.

WONES, D.R., 1989. Significance of the assemblage titanite + magnetite + quartz in granitic rocks. American Mineralogist 74, 744–749.

WONES, D.R., EUGSTER, H.P., 1965. Stability of biotite: experiment, theory and application. American Mineralogist 50, 1228–1272.

ZEN, E.-A., HAMMARSTROM, J.M., 1984. Magmatic epidote and its petrologic significance. Geology 12, 515–518.

7 DISCUSSÃO E CONCLUSÕES

7.1 DISCUSSÃO DOS ARTIGOS

O artigo 1 “Synkinematic emplacement of the magmatic epidote bearing Major Isidoro tonalite-granite batholith: Relicts of an Ediacaran continental arc in the Pernambuco–Alagoas Domain, Borborema Province, NE Brazil. Journal of South American Earth Sciences 64, 1–13” aborda as relações de campo e estruturais, a carecterização petrográfica a geoquímica, a geocronologia e as assinaturas isotópicas do pluton Major Isidoro.

O pluton Major Isidoro corresponde a um corpo alongado de direção NE–SW que apresenta uma foliação de baixo ângulo de mesma direção que mergulha para noroeste. O mesmo registra áreas que sofreram fusão parcial o que sugere que o alojamento deste pluton foi sin-cinemático contemporâneo ao pico de metarmofismo relacionado à orogênese Brasiliana. Este pluton possui uma composição granítica a tonalitica e apresenta enclaves máficos. Essas rochas contêm biotita, anfibólio, titanita e epidoto que muitas vezes mostra um núcleo alanita como principais fases minerais máficas.

Os dados de geoquímica caracterizaram estas rochas como metaluminosas, cálcio-alcalinas de médio-K e magnesianas. Estas apresentam anomalias negativas de Nb–Ta e Ti que são típicas de magmas relacionados a zonas de subducção e possuem química de rochas formadas em ambiente de arco continental (em todos os diagramas tectônicos comuns).

Dados U–Pb SHRIMP em zircão forneceram uma idade de cristalização e alojamento de 627 Ma (Th/U = 0,25 a 0,60). Nos cristais de zircão da amostra datada foram observados diversos núcleos de zircão herdados arredondados com idades variando de 798 a 1007 Ma com razões Th/U variando de 0,37 a 0,72 que estão dentro das razões típicas de fontes ígneas.

Idades t_{DM} variam de 1,1 a 1,4 Ga com valores de $\varepsilon Nd_{(627Ma)}$ −1,09 a −2,12. Razões iniciais de $^{87}Sr/^{86}Sr$ variam de 0,7069 a 0,7086. Enquanto que os valores de $\delta^{18}O_{(zircão)}$ variam de 6,95‰ a 7,02‰ e são mais altos que os valores encontrados em zircão de rochas ígneas derivadas do manto. Estes dados em conjunto sugerem que o pluton Major Isidoro pode ter sido derivado de uma crosta continental inferior retrabalhada de idade Toniana com provável contribuição de material derivado do manto.

O artigo 2 “Two stage mantle-derived granitic rocks and the onset of the Brasiliano orogeny: evidence from Sr, Nd, and O isotopes. Lithos 264, 189–200” trata das relações

de campo e das relações estruturais, da geoquímica, das assinaturas isotópicas, da petrogênese do batólito granítico Monteirópolis, e da cronologia do início da orogênese Brasiliana.

O batólito Monteirópolis apresenta uma área de 270 km² que aflora ao longo da zona do limite com o Domínio Sergipano. Este batólito é limitado na margem sudoeste pela zona de cisalhamento Jacaré dos Homens e mostra uma foliação de fluxo magmático definida pela forma da orientação preferencial de feldspato potássico e pelos agregados de biotita e anfibólio. Enclaves microgranulares máficos são abundantes neste corpo que possui uma composição predominante granítica a granodiorítica e apresenta titanita e epidoto magmático (mEp) como minerais traços.

As rochas deste batólito são cálcio-alcalinas de alto-K, metaluminosas a levemente peraluminosas, magnesianas com uma assinatura geoquímica indicativa de arco vulcânico. Marcantes anomalias negativas de Nb, Ta e Ti são interpretadas como refletindo uma assinatura relacionada a subducção. Ausencia de anomalias de Eu* sugerem que fusão parcial aconteceu a pressões acima do campo de estabilidade de plagioclásio e/ou cristalização a alta fugacidade de oxigênio que permitiu a preservação de mEp.

Os altos valores de Na_2O e K_2O neste batólito mostram composições similares a fusões produzidas experimentalmente de rochas basálticas de médio a alto-K (SISSON et al., 2005). Estas mostram composições distintas daquelas fusões produzidas pela fusão parcial de anfibolitos que possuem baixos valores de K e variáveis conteúdos de Na_2O e CaO.

Para o batólito Monteirópolis foi obtida uma idade t_{DM} uniforme de 1,0 Ga no qual $\varepsilon Nd_{(0,626\ Ga)}$ é positivo a ligeiramente negativo (+1,06 a −0,78), razões $^{87}Sr/^{86}Sr_{(0,626\ Ga)}$ variando de 0,7050 a 0,7052 e razões de $\delta^{18}O_{zircão}$ (5,0 a 5,94) próximas dos valores de zircão cristalizados de magmas derivados do manto. Estes valores integrados sugerem que este batólito foi produzido por fusão parcial de rochas Tonianas derivadas do manto em dois estágios (*two stage*). Provavelmente durante o evento extensional? "Cariris Velhos" a rocha fonte do Monteirópolis foi adicionada a crosta inferior e durante o Brasiliano *underplating* (possivelmente relacionado à subducção de crosta oceânica; P. ex. OLIVEIRA et al., 2010) de magma basáltico correspondeu a fonte de calor (*heat source*) para fundir parcialmente esta crosta e originar este corpo.

Os cristais de zircão analisados por U–Pb SHRIMP de uma amostra da porção leste deste batólito forneceram uma idade de 625.8 ± 3.7 Ma (Th/U = 0,32 a 1,82) que é

interpretada como a idade de cristalização e alojamento. Este dado em conjunto com os dados da literatura permitiu estabelecer a entrada da orogenia Brasiliana no Domínio Pernambuco–Alagoas entre 642 e 626 Ma.

O artigo 3 “Isotope evidence for mantle-derived source rock of high-k calc-alkaline granites, Pernambuco–Alagoas Domain, northeastern Brazil (submitted to International Journal of Earth Sciences” aborda as relações geológicas e estruturais de um ortognaisse granítico e um pluton granítico, a geoquímica, a química mineral das fases biotita e epidoto, a idade e a petrogênese destes.

O ortognaisse Jacaré dos Homens constituísse em um corpo alongado que intrudiu ao longo da zona de cisalhamento de mesmo nome enquanto que o pluton Santo Antonio é delimitado ao sul por esta zona de cisalhamento. Ambos plutons mostram enclaves máficos e preservam uma foliação/bandamento de baixo ângulo, com o pluton Jacaré dos Homens mostrando critérios de cisalhamento sugerindo transporte tectônico de topo para sudeste.

Petrograficamente ambos os plutons são predominantemente constituídos por feldspato potássico, quartzo e plagioclásio com biotita como principal fase máfica e menor hornblende, atestando para a natureza metaluminosa e cálcio-alcalina destes. No entanto, epidoto magmático foi reconhecido no pluton Santo Antonio com teores de pistacita no intervalo de 28 a 29 que são típicos desta fase.

A classificação geoquímica deste plutons mostra que os mesmos são cálcio-alcalinos de alto-K, magnesiano e metaluminos a moderadamente peraluminosos. Estes apresentam distintas anomalias negativas de Nb, Ta, e Ti que é consistente com magmatismo em ambiente relacionado à subducção (similares aos plutons anteriores discutidos). Os padrões de elementos incompatíveis destas rochas mostra enriquecimento de LILE em relação aos elementos HFSE (típico em granitos cálcio-alcalinos). Empobrecimento de HREE sugere fusão parcial no campo de estabilidade da granada. A assinatura geoquímica das amostras analisadas favorece um ambiente de arco continental.

Biotitas analisadas de ambos os plutons dispõe-se em grande maioria no campo cálcio-alcalino consistente com a química de rocha total.

A geocronologia U–Pb SHRIMP em zircão nos plutons Jacaré dos Homens e Santo Antonio mostraram idades de 642.4 ± 3.4 Ma e 636.1 ± 3.6 Ma, respectivamente, que são interpretadas como idade de cristalização estando estas intimamente associadas ao inicio da orogênese Brasiliana.

Varios critérios geoquímicos (Mg# destas rochas em geral são > 42 e altos valores de Cr por exemplo) e isotópicos destes plutons sugerem uma conecção com o manto. As idades de separação do manto para o pluton Santo Antonio estão no intervalo de 0,96 a 1,05 com uma amostra deste pluton apresentando o valor mais alto, até agora, de $\varepsilon Nd_{(t)}$ (+1.17 a −0.67) encontrado para uma rocha no Domínio Pernambuco–Alagoas. As razões $^{87}Sr/^{86}Sr$ deste são similares ao manto do tipo EM I e a média de $\delta^{18}O_{zircão}$ = 5.45‰ esta compatível com valores obtidos em zircão cristalizados de magmas devivados do manto ($\delta^{18}O$ = 5.3 ± 0.3‰; P. ex. VALLEY et al., 2005). Para o Jacaré dos Homens os dados isotópicos são mais evoluídos ($^{87}Sr/^{86}Sr_t$ = 0.7068, e εNd_t = −1.58, com $\delta^{18}O_{zircon}$ = 7.0‰) possivelmente refletem a presença de mais material crustal.

Um processo de vários estágios para a formação dos plutons estudados pode ser sugerido, incluindo fusão, assimilação, armazenamento e homogeneização (MASH) na transição crosta–manto (P ex. HILDRETH & MOORBATH 1988). Depois disso, cristalização fracionada deve ter ocorrido durante a subida do magma, como suportado pela correlacão de elementos maiores e menores (em diagramas tipo Harker), e composições isotópicas Sr–Nd relativamente semelhantes, sugerindo menor assimilação crustal durante a ascenção do magma.

No artigo 4 “Mineralogy and mineral chemistry of the calc-alkaline epidote-bearing Major Isidoro and Monteirópolis plutons, Borborema Province, NE Brazil. (to submit)” são apresentados dados petrográficos e de química mineral exclusivamente dos plutons Major Isidoro e Monteirópolis.

A assembleia mineral de quartz + feldspato potássico + plagioclásio + biotita ± hornblenda ± magnetita ± titanita ± epidoto ± ilmenita é comum em ambos os plutons investigados. A coexistência da assembleia mineral acima sugere que cristalização deve ter ocorrido a condições de alta fugacidade de oxigênio. As razões de Fe# [$Fe^{Amp}/(Fe^{Amp} + Mg^{Amp}$)] que se estendem de 0,55 a 0,639 e os teores de pistacita (27 a 31) reforçam esta conclusão.

As condições médias de pressão e temperatura que os plutons Major Isidoro e Monteirópolis se alojaram foram respectivamente de 6,1 Kbar a ca.703ºC e 4,7 Kbar a ca. 674ºC.

7.2 INTERPRETAÇÃO GEODINÂMICA

Em reconstruções *pre-drift*, a Província Borborema (PB) fica adjacente ao cinturão Pan-Africano e ao bloco cratônico da África ocidental. O início da Orogênese

Brasiliano-Pan-Africano na Província de Borborema pode ser limitado entre 640 e 625 Ma. A partir de uma revisão dos dados geocronológicos e isotópicos disponíveis para ortognaisses e rochas graníticas, é possível identificar que a deformação regional e o metamorfismo foram síncronos no leste da Província Borborema, com o desenvolvimento inicial de uma foliação de baixo ângulo (ex., BRITO NEVES et al., 2003; SIAL 1993; GUIMARÃES et al., 2004, 2011; FERREIRA et al., 2004, 2011; VAN SCHMUS et al., 2011; CRUZ & ACCIOLY 2012; NEVES et al., 2006, 2008, 2012, 2015b; SILVA FILHO et al., 2013, 2014, 2016; BUENO et al., 2009; LONG et al., 2005; OLIVEIRA et al., 2015a; SILVA et al., 2015, 2016; Tabela 1). Idades similares às encontradas na PB foram registradas em granitoides sintectônicos, metagranitóides e em minerais metamórficos entre 640–620 Ma em Camarões (TOTEU 1990; TOTEU et al., 1994, 2001, 2006, NJIEKAK et al., 2008). Em Camarões, este período também foi interpretado como um estágio de convergência, durante o qual uma foliação de baixo ângulo foi desenvolvida sob metamorfismo de alto grau e em associação com o plutonismo calc-alcalino (ex., PENAYE et al., 1993, 2006; TOTEU et al. , 2001, 2004; BOUYO HOUKETCHANG et al., 2009, 2013).

O modelo tectônico proposto para a evolução da área de estudo e adjacências a partir dos dados desta tese e os advindos da literatura durante a orogênese Brasiliana é discutido a seguir:

Magmatismo relacionado à extensão provavelmente começou a cerca de 715 Ma atrás (granito Garrote do tipo A) e continuou pelo menos até ca. 641 Ma (granito Boa Esperança com textura rapakivi) no Cinturão de Dobramento Sergipano (OLIVEIRA et al., 2010) (Fig. 1a). Um evento extensional Criogeniano, dentro do intervalo 850–631 Ma também foi sugerido por SILVA FILHO et al. (2014) para seqüências metasedimentares (Rio Una e Inhapi) do Domínio Pernambuco–Alagoas.

O fechamento do oceano Sergipano–Oubanguides entre o norte do Craton São Francisco-Congo e o sul da Província Borborema (Domínio Pernambuco–Alagoas) deve ter começado na transição Criogeniano–Ediacarano e não é mais tardia que o inicio do Ediacarano (~ 625 Ma), conforme inferido pelos magmas com assinatura geoquímica de arco da porção sul do batólito Aguas Belas–Canindé e pelas idades de zircão detriticos mais jovens dos cinturões de dobramentos Sergipano e Yaoundé (BOUYO HOUKETCHANG et al., 2015; OLIVEIRA et al., 2006, 2010, 2015b, VAN SCHMUS et al., 2008). As idades de zircão detriticos mais jovens (650–630 Ma) indicam que a deposição terminou imediatamente antes ou provavelmente no início da orogenia

Brasiliana.

Entre ca. 642 e 626 Ma, crosta oceânica (Sergipano–Oubanguides) pode ter sofrido subducção com polaridade para o norte sob o Domínio Pernambuco–Alagoas, formando os plutons Poço da Cacimba (640,9 ± 3,7 Ma, LIMA et al., 2016), Santo Antonio (636,1 ± 3,6 Ma, esta tese), Serra do Catú (632 ± 4; SILVA FILHO et al., 2013, 2016), Major Isidoro (626,6 ± 4,1 Ma; SILVA et al., 2015) e Monteirópolis (625,8 ± 3,7 Ma; SILVA et al., 2016). Isto foi seguido pelas intrusões dos plutons Santana do Ipanema (618 ± 6; SILVA FILHO et al., 2016), Serra da Caiçara (616 ± 4; SILVA FILHO et al., 2013), Água Branca (610 ± 4; SILVA FILHO et al., 2016), Mata Grande (612 ± 7; SILVA FILHO et al., 2013, 2016) e Correntes (603 ± 5; SILVA FILHO et al., 2016). Estes granitos se intrudiram em um embasamento Toniano (ao menos para o batólito Águas Belas–Canindé) como sugerido pelas idades U–Pb em zircão de orthogneisses que variam entre 958 a 972 Ma (LIMA, comunicação verbal e SILVA FILHO et al., 2014, respectivamente) e conforme a presença de núcleos de zircão herdados dentro de alguns desses plutons com idades variando entre 800 e 1100 Ma (Ex., plutons Major Isidoro, Serra do Catú e Água Branca; SILVA et al., 2015 e SILVA FILHO et al., 2016); Este embasamento provavelmente se formou durante o evento Cariris Velhos (1.1–0.8 Ga).

A colisão culminou com o fechamento do oceano Sergipano–Oubanguides levando ao magmatismo (sin-colisonal) com assinaturas relacionadas a construção de um arco magmático (Ex., BUENO et al., 2009; OLIVEIRA et al., 2010.; SILVA et al., 2015), e com a formação concomitante do Cinturão de Dobramento Sergipano–Yaoundé (P. ex.. BRITO NEVES et al., 1977; TROMPETE 1997, 2000, OLIVEIRA et al., 2006, 2010, 2015a, 2015b, VAN SCHMUS et al., 2008), e a formação da zona de cisalhamento Jacaré dos Homens, que representa uma possível paleo sutura (SILVA et al., 2015; SILVA et al., submetido), e finalmente implicou em progressivo espessamento da crosta continental.

As intrusões mais antigas na área estudada têm seu eixo maior em geral paralelo a direção da foliação do Cinturão de Dobramento Sergipano e mostram uma foliação de baixo ângulo que corresponde à deformação regional D_2, que produziu dobras reclinadas no Domínio Pernambuco-Alagoas (Ex.,, SILVA FILHO et al., 2014), e que representa o clímax do máximo evento de encurtamento crustal durante a colisão (BUENO et al., 2009; SILVA FILHO et al., 2014; OLIVEIRA et al., 2015a, 2015b).

Entre o intervalo de 642 e 626 Ma, *slab break-off* (DAVIES & BLANCKENBURG 1995), que causa a ruptura da crosta oceânica e fascilita a ascenção

da astenosfera ou *slab tearing* podem ter ocorrido (Fig. 1b), assim como material do manto pode ter sido aprisionado (*underpleted*) na base da crosta, e pode ter metassomatizado o manto litosférico sobrejacente. Este material derivado do manto pode ter se tornado a rocha fonte dos enclaves, que são bastante comuns nos plutons da parte sudeste do domínio. Ascensão astenosférica e *underplating* de magma do manto litosférico forneceram o calor necessário para a fusão parcial do material basáltico de alto-K adicionado a crosta continental inferior durante o Toniano (t_{DM} = 0,96 a 1,2 Ga) provavelmente durante o evento Cariris Velhos (P. ex. GUIMARÃES et al., 2012, 2016).

O período durante a colisão continental foi marcado por extensiva migmatização que foi registrada no Domínio Pernambuco–Alagoas (P. ex. NEVES et al., 2008; SILVA FILHO et al., 2002, 2014; SILVA et al., 2015). Os dados geocronológicos disponíveis, mostram que as intrusões desses plutons são também contemporâneas com as condições de pico de metamorfismo nos domínios Transversal e Pernambuco–Alagoas (NEVES et al., 2006, 2008, 2009, 2012, 2015b; SILVA FILHO et al., 2014) Estes dados também sugerem que deformação contracional continuou até pelo menos 600 Ma (Fig. 1c).

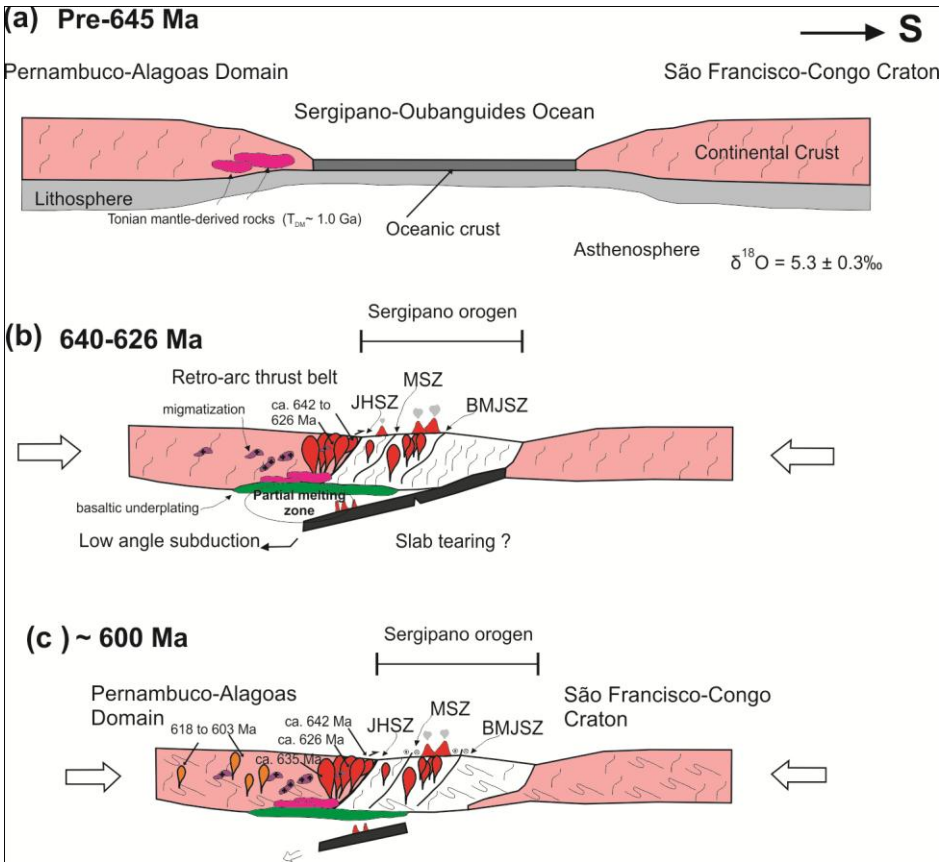

Figura 1. Modelo tectônico esquemático para evolução tectonica da area de estudo baseada em dados deste trabalho e da literature. Siglas; JHSZ = Zona de cisalhamento Jacaré dos Homens; MSZ = Zona de cisalhamento Macururé; BMJSZ = Zona de cisalhamento Belo Monte/Jeremoabo.

Tabela 1. Resumo dos dados geocronológicos U–Pb e Pb–Pb disponíveis para rochas ígneas e metaigneas dos domínios Sergipano, Transversal e Pernambuco–Alagoas, Província Borborema.

Rock type or unit	Mineral	Age (Ma)	Method	Sr i	ε Nd	T_{DM}(Ga)	δ^{18}Osmow (‰)	References	Age back-calculated
Sitios Novos granite	Zircon	631 ± 4	U–Pb (SHRIMP)	0.7116	−5.47	1.51		OLIVEIRA et al. (2015a)	625
Camara tonalite	Zircon	628 ± 12	U–Pb (SHRIMP)	0.7092	−7.45	1.71		BUENO et al. (2009)	628
Coronel João Sá granodiorite	Zircon	625 ± 2	U–Pb (SHRIMP)	0.7084 to 0.7100	−6.90 to −4.80	1.50 to 1.70		LONG et al. (2005)	625
Poço Redondo granite	Zircon	623 ± 7	U–Pb (SHRIMP)	0.7135 to 0.7142	−4.23 to −5.50	1.40 to 1.57		OLIVEIRA et al. (2015a)	625
Lajedinho granodiorite pluton	Zircon	619 ± 3	U–Pb (SHRIMP)		-1.10 to -0.08	1.14 to 1.22		OLIVEIRA et al. (2015a)	625
Queimada Grande pluton	Zircon	618 ± 4	U–Pb (SHRIMP)	0.7066 to 0.7079	−1.15 to −2.55	1.18 to 1.32		OLIVEIRA et al. (2015a)	625
Serra do Catú pluton	Zircon	632 ± 4	U–Pb (SHRIMP)		−3.80	1.40	7.10 to 9.18	SILVA FILHO et al. (2016)	600
Major Isidoro batholith	Zircon	626.6 ± 4	U–Pb (SHRIMP)	0.7069 to 0.7086	−2.12 to −1.09	1.10 to 1.40	6.95 to 7.02	SILVA et al. (2015)	627
Monteirópolis batholith	Zircon	625.8 ± 4	U–Pb (SHRIMP)	0.7050 to 0.7052	−0.78 to +1.06	1.00	5.00 to 5.94	SILVA et al. (2016)	626
Santana do Ipanema pluton	Zircon	618 ± 6	U–Pb (SHRIMP)		−8.11 to −4.10	1.33 to 2.00	4.94 to 7.06	SILVA FILHO et al. (2016)	600
Serra da Caiçara pluton	Zircon	616 ± 4	U–Pb (TIMS)		−5.20	1.43		SILVA FILHO et al. (2013)	600
Mata Grande pluton	Zircon	612 ± 7	U–Pb (SHRIMP)		−9.30	2.04		SILVA FILHO et al. (2013, 2016)	600
Água Branca pluton	Zircon	610 ± 4	U–Pb (SHRIMP)		−9.08 to −4.60	1.44 to 1.90		SILVA FILHO et al. (2016)	600
Correntes pluton	Zircon	603 ± 5	U–Pb (SHRIMP)		−8.20	1.81		SILVA FILHO et al. (2016)	600
Altinho Orthogneiss	Zircon	646 ± 13	U–Pb (LA-ICP-MS)	0.7047	−0.84	1.31		NEVES et al. (2015b)	646
Remédios pluton	Zircon	643 ± 2	Pb–Pb evaporation		−16.6	2.14		FERREIRA et al. (2004)	600
Syenitic Orthogneiss	Zircon	636 ± 3	U–Pb (LA-ICP-MS)	0.7047				NEVES et al. (2015b)	636
Conceição pluton	Zircon	635 ± 9	U–Pb (convencional)	0.7059	−1.23	1.22		BRITO NEVES et al. (2003); SIAL 1993	600
Migmatite leucosome	Zircon	626 ± 15	U–Pb (LA-ICP-MS)					NEVES et al. (2006)	
Praça Meio Mundo gneiss	Zircon	623 ± 5	U–Pb (SHRIMP)		−4.10	1.51		VAN SCHMUS et al. (2011)	600
Granitic orthogneiss	Zircon	622 ± 4	U–Pb (SHRIMP)					SILVA FILHO et al. (2014)	
Granitic orthogneiss	Zircon	620 ± 10	U–Pb (SHRIMP)					SILVA FILHO et al. (2014)	
Curral de Cima tonalite	Zircon	618 ± 5	U–Pb (SHRIMP)	0.7067 to 0.7099	−2.52 to −4.58	1.31 to 1.41	8.10 to 8.40	FERREIRA et al. (2011)	620
Timbaúba complex	Zircon	616 ± 5	U–Pb (SHRIMP)		−4.23 to −5.37	1.41 to 1.56		GUIMARÃEs et al. (2011)	600
Caruaru orthogneiss	Zircon	616 ± 4	U–Pb (LA-ICP-MS)					NEVES et al. (2012)	
Itapetim complex	Zircon	615.5 ± 8.7	U–Pb (SHRIMP)		−2.69 to −3.60	1.37 to 1.45		GUIMARÃES et al. (2011)	600
Olho d'água pluton	Zircon	613 ± 18	U–Pb (SHRIMP)		−2.60	1.42		VAN SCHMUS et al. (2011)	600
Caldeirão Verm. metagranitoid	Zircon	611 ± 14	U–Pb (LA-ICP-MS)		−19.73	2.08		CRUZ & ACCIOLY (2012)	611
Jupi orthogneiss	Zircon	606 ± 8	U–Pb (LA-ICP-MS)					NEVES et al. (2008)	

REFERÊNCIAS

ABDEL-RAHMAN AFM (1994) Nature of Biotites from Alkaline, Calc-alkaline, and Peraluminous Magmas. Journal of Petrology 35(2), 525–541.

ACCIOLY, A.C.A., MCREATH, I., SANTOS, E.J., GUIMARÃES, I.P., VANNUCI, R., BOTTAZZI, R., 2000. The passira meta-anorthositic complex and its tectonic implication, Borborema Province, Brazil. In: International Geological Congress, 31, Rio de Janeiro.

ALLÈGRE CJ (2008) Isotope Geology. Cambridge University Press, Cambridge, New York, Melbourne, Madrid, Cape Town, Singapore, São Paulo

ALMEIDA, F.F.M., HASUI, Y., BRITO NEVES, B.B., FUCK, R.A., 1981. Brazilian Structural Provinces: An Introduction. Earth-Science Reviews 17(1–2), 1–29.

ANDERSON, J.L., 1996. Status of thermobarometry in granitic batholiths. Transactions of the Royal Society of Edinburgh: Earth Sciences, 87,125–138.

ANDERSON, J.L., BARTH, A.P., WOODEN, J.L., MAZDAB, F., 2008. Thermometry and Thermobarometers in Granitic Systems. Reviews in Mineralogy and Geochemistry 69, 121–142.

ANNEN, C., SPARKS, R.S.J., 2002. Effects of repetitive emplacement of basaltic intrusions on thermal evolution and melt generation in the crust. Earth and Planetary Science Letters 203(3–4), 937–955.

ANNEN, C., BLUNDY, J.D., SPARKS, R.S.J., 2006. The genesis of intermediate and silicic magmas in deep crustal hot zones. Journal of Petrology 47(3), 505–539.

ANDERSON, J.L., SMITH, D.R., 1995. The effects of temperature and fO_2 on the Al-in-hornblende barometer. American Mineralogist 80, 549–559.

ARAÚJO, M.N., OLIVEIRA, E.P., ONOE, A.T., 2004. Geocronologia Ar/Ar de sucessivos episódios deformacionais em limite de terrenos da faixa sergipana. XLII Congresso Brasileiro de Geologia, Araxá, Brazil, CD-ROM.

ARCHANJO, C.J., BOUCHEZ, J.-L., CORSINI, M., VAUCHEZ, A., 1994. The Pombal granite pluton: Magnetic fabric, emplacement and relationships with the Brasiliano strike-slip setting of NE Brazil (Paraiba State). Journal of Structural Geology 16(3), 323–335.

ARCHANJO, C.J., HOLLANDA, M.H.B.M., RODRIGUES, S.W.O., BRITO NEVES, B.B., ARMSTRONG, R., 2008. Fabrics of pre- and syntectonic granite plutons and chronology of shear zones in the Eastern Borborema Province, NE Brazil. Journal of Structural Geology 30(3), 310–326.

BACHMANN, O., DUNGAN, M., 2002. Temperature-induced Al-zoning in hornblendes of the Fish Canyon magma, Colorado. American Mineralogist, 87, 1062–1076.

BARBARIN, B., 1990. Granitoids: main petrogenetic classifications in relation to origin and tectonic setting. Geological Journal 25, 227–238.

BARBARIN, B., 1999. A review of the relationships between granitoid types, their origins and their geodynamic environments. Lithos 46(3), 605–626.

BARKER, F., 1979. Trondhjemite: Definition, environment, and hypothesis of origin. In: Barker, F., (ed.). Trondhjemites, dacites, and related rocks. Amsterdam, Elsevier, pp. 1–12.

BEARD, J.S., LOFGREN, G.E., 1991. Dehydration melting and water-saturated melting of basaltic and andesitic greenstones and amphibolites at 1.3 and 6.9 kb. Journal of Petrology 32, 365–401.

BLACK, L.P., KAMO, S.L., ALLEN, C.M., DAVIS, D.W., ALEINIKOFF, J.N., VALLEY, J.W., MUNDIL, R., CAMPBELL, I.H., KORSCH, R.J., WILLIAMS, I.S., FOUDOULIS, C., 2004. Improved $^{206}Pb/^{238}U$ microprobe geochronology by the monitoring of a trace-element-related matrix effect; SHRIMP, ID-TIMS, ELA-ICP-MS and oxygen isotope documentation for a series of zircon standards. Chemical Geology 205(1–2), 115–140.

BLUNDY, J.D., HOLLAND, T.J.B., 1990. Calcic amphibole equilibria and a new amphibole-plagioclase geothermometer. Contributions to Mineralogy and Petrology 104, 208–224

BOEHNKE, P., WATSON, E.B., TRAIL, D., HARRISON, T.M., SCHMITT, A., 2013. Zircon saturation re-revisited. Chemical Geology 351, 324–334.

BONIN, B., 1990. From orogenic to anorogenic settings: evolution of granitoid suites after a major orogenesis. Geological Journal 25, 261–270.

BONIN, B., AZZOUNI-SEKKAL, A., BUSSY, F., FERRAG, S., 1998. Alkali-calcic and alkaline post-orogenic (PO) granite magmatism: petrologic constraints and geodynamic settings. Lithos 45(1–4), 45–70

BRANDON, A.D., CREASER, R.A., CHACKO, T., 1996. Constraints on rates of granitic magma transport from epidote dissolution kinetics. Science 271, 1845–1848.

BRASILINO, R.G., SIAL, A.N., FERREIRA, V.P., PIMENTEL, M.M., 2011. Bulk rock and mineral chemistries and ascent rates of high-K calc-alkalic epidote-bearing magmas, Northeastern Brazil. Lithos 127, 441–454.

BRASILINO, R.G., SIAL, A.N., LAFON, J.M., 1999. Magmatic epidote, hornblende barometric estimates of the Conceição das Creoulas pluton, Alto Pajeu Terrane, NE Brazil. Anais da Academia Brasileira de Ciências 71, 3–16.

BRITO, M.F.L., SILVA FILHO, A.F., GUIMARÃES, I.P., 2009. Geologia isotópica do batólito shoshonítico-ultrapotássico Neoproterozóico Serra do Catú e implicações na evolução da interface dos Domínios Canindé e Pernambuco–Alagoas. Revista Brasileira de Geociências 39, 324–337.

BRITO NEVES, B.B., 1975. Regionalização geotectônica do Precambriano nordestino. Unpublished PhD thesis, University of São Paulo, São Paulo, Brazil, 198 pp, (in Portuguese).

BRITO NEVES, B. B., CAMPOS NETO, M.C., VAN SCHMUS W.R., SANTOS E.J. 2001. O "Sistema" Pajeu-Paraiba e o "maciço" São José do Campestre no leste da Borborema. Revista Brasileira de Geociências 31, 173–184.

BRITO NEVES, B.B., FUCK, R.A, 2013. Neoproterozoic evolution of the basement of the South-American platform. Journal of South American Earth Sciences 47, 72–89.

BRITO NEVES, B. B., PASSARELI, C. R., BASEI, M. A. S., SANTOS, E. J., 2003. Idades U–Pb em zircões de alguns granitos clássicos da província Borborema. Geologia USP: Série Científica 3, 25–38.

BRITO NEVES, B.B., SANTOS, E.J., VAN SCHMUS, W.R., 2000. Tectonic History of the Borborema Province, Northeastern Brazil. In: Cordani U, Milani EJ, Thomaz Filho A, Campos DA (eds) Tectonic Evolution of South America. International Geological Congress, 31st, Rio de Janeiro, Brazil, pp 151–182.

BRITO NEVES, B.B., SIAL, A.N., RAND, H.M., MANSO, V.V., 1982. The Pernambuco–Alagoas massif, Northeastern Brazil. Revista Brasileira de Geociências 12, 240–250.

BRITO NEVES, B.B., VAN SCHMUS, W.R., FETTER, A., 2002. North-western Africa–North-eastern Brazil. Major tectonic links and correlation problems. Journal of African Earth Sciences 34(3–4), 275–278.

BROWN, G.C., 1977. Mantle origin of Cordilleran granites. Nature 265, 21–24.

BROWN, M., 2013. Granite: From: Genesis to emplacement. Geological Society of American Bulletin 125(7–8), 1079–1113.

BROWN, M., SOLAR, G.S., 1998. Shear-zone systems and melts: feedback relations and selforganization in orogenic belts. Journal of Structural Geology 20, 211–227.

BUCHOLZ, C.E., JAGOUTZ, O., SCHMIDT, M.W., SAMBUU, O., 2014. Fractional crystallization of high‐K arc magmas: biotite‐ versus amphibole‐dominated fractionation series in the Dariv Igneous Complex, Western Mongolia. Contributions to Mineralogy and Petrology 168:1072.

BUENO, J.F., OLIVEIRA, E.P., MCNAUGHTON, N., LAUX, J.H., 2009. U–Pb dating of granites in the Neoproterozoic Sergipano Belt, NE–Brazil, and implications for the timing and duration of continental collision. Gondwana Research 15, 86–97.

BOUYO HOUKETCHANG, M., TOTEU, S.F., DELOULE, E., PENAYE, J., VAN SCHMUS, W.R., 2009. U–Pb and Sm–Nd dating of high-pressure granulites from Tcholliré and Banyo regions: evidence for a Pan-African granulite facies metamorphism in northcentral Cameroon. Journal of African Earth Sciences 54, 144–154.

BOUYO HOUKETCHANG, M., PENAYE, J., BARBEY, P., TOTEU, S.F., WANDJI, P., 2013. Petrology of high-pressure granulite facies metapelites and metabasites from Tcholliré and Banyo regions: geodynamic implication for the Central African Fold Belt (CAFB) of north-central Cameroon. Precambrian Research 224, 412–433.
BOUYO HOUKETCHANG, M., ZHAO, Y., PENAYE, J., ZHANGA, S.H., NJEL, U.O., 2015 Neoproterozoic subduction-related metavolcanic and metasedimentary rocks from the Rey Bouba Greenstone Belt of north-central Cameroon in the Central African Fold Belt: New insights into a continental arc geodynamic setting. Precambrian Research 261, 40–53.

CAMPOS, T.F.C., NEIVA, A.M.R., NARDI, L.V.S., PEREIRA, L.S., BONZANINI, L.F., PETTA, R.A., MEYER, F.M., 2005. Magmatic epidote and amphibole from the Rio Espinharas Hybrid Complex, Northeastern Brazil. Pesquisas em Geociências 32 (2), 41–55.

CAMPOS, B.C.S., VILALVA, F.C.J., NASCIMENTO, M.A.L., GALINDO, A.C., 2016. Crystallization conditions of porphyritic high-K calc-alkaline granitoids in the extreme northeastern Borborema Province, NE Brazil, and geodynamic implications. Journal of South American Earth Sciences 70, 224–236.

CARMONA, L.C.M., 2000. Geologia, geoquímica e avaliação econômica do Migmatito Rosa Imperial, domínio meridional da Província Borborema, NE do Brasil. Master Thesis. Federal University of Pernambuco, Recife, Brazil, 187 pp (in Portuguese).

CARVALHO, M.J., 2005. Tectonic Evolution of the Marancó-Poço Redondo Domain: Records of the Cariris Velhos and Brasiliano Orogenesis in the Sergipano Belt, NE Brazil. Unpublished PhD Thesis. University of Campinas, Brazil, 202 pp (in Portuguese).

CAVOSIE, A.J., KITA, N. T., VALLEY, J. W., 2009. Primitive oxygen-isotope ratio recorded in magmatic zircon from the Mid-Atlantic Ridge. American Mineralogist 94, 926–934.

CAVOSIE, A.J., VALLEY, J.W., KITA, N.T., SPICUZZA, M.J., USHIKUBO, T. AND WILDE, S.A., 2011. The origin of high $\delta^{18}O$ zircons: marbles, megacrysts, and metamorphism. Contributions to Mineralogy and Petrology 162, 961–974.

CAXITO, F.A., UHLEIN, A., DANTAS, E.L., STEVENSON, R., SALGADO, S.S., DUSSIN, I.A., SIAL, A.N., 2016. A complete Wilson Cycle recorded within the Riacho do Pontal Orogen, NE Brazil: Implications for the Neoproterozoic evolution of the Borborema Province at the heart of West Gondwana. Precambrian Research 282, 97–120.

CHAPPELL, B.W., 1999. Aluminium saturation in I- and S-type granites and the characterization of fractionated haplogranites. Lithos 46(3), 535–551.

CHAPPELL, B.W., BRYANT, C.J., WYBORN, D., 2012. Peraluminous I-type granites. Lithos 153:142–153.

CHAPPELL, B.W., WHITE, A.J.R., 1974. Two contrasting granite types. Pacific Geology 8, 173–174.

CHAPPELL, B.W., WHITE, A.J.R., 1992. I- and S-types granites in Lachlan Fold Belt. Transactions of the Royal Society of Edinburgh: Earth Sciences 83, 1–26.

CHAPPELL, B.W., WHITE, A.J.R., 2001. Two contrasting granite types: 25 years later. Australian Journal of Earth Sciences 48, 489–499.

CHAPPELL, B.W., WHITE, A.J.R., WILLIAMS, I.S., WYBORN, D., 2004. Low- and high-temperature granites. Transactions of the Royal Society of Edinburgh: Earth Sciences 95(1–2), 125–140

CHAPPELL, B.W., WHITE, A.J.R., WYBORN, D., 1987. The importance of residual source material (restite) in granite petrogenesis. Journal of Petrology 28, 1111–1138.

CLEMENS, J.D., STEVENS, G., 2012. What controls chemical variation in granitic magmas? Lithos 134–135, 317–319.

CLEMENS, J.D., REGMI, K., NICHOLLS, I.A., WEINBERG, R., MAAS, R., 2016. The Tynong pluton, its mafic synplutonic sheets and igneous microgranular enclaves: the nature of the mantle connection in I-type granitic magma. Contributions to Mineralogy and Petrology 171:35.

CHEN, J.-Y., YANG, J.-H., ZHANG, J.-H., SUN, J.F., WILDE, S.A., 2013. Petrogenesis of the Cretaceous Zhangzhou batholith in southeastern China: Zircon U–Pb age and Sr–Nd–Hf–O isotopic evidence. Lithos 162–163, 140–156.

COBBING, J., 2000. The Geology and Mapping of Granite Batholiths. Lecture Notes in Earth Sciences 96, Springer, Berlin Heidelberg New York, 121 pp.

COCHERIE, A., 1986. Systematic use of trace element distribution patterns in log-log diagrams for plutonic suites. Geochimica et Cosmochimica Acta 50(11), 2517–2522.

CONDIE, K.C., 1989. Plate Tectonics and Crustal Evolution. 3rd. Edition. Pergamon Press, 476 pp.

CONDIE, K.C., KRÖNER, A., 2013. The building blocks of continental crust: Evidence for a major change in the tectonic setting of continental growth at the end of the Archean. Gondwana Research 23, 394–402.

CRUZ, R.F., ACCIOLY, A.C.A., 2012. Idade e litogeoquímica do metagranitoide Caldeirão Vermelho (Parnamirim–PE), Zona Transversal, Província Borborema. Estudos Geológicos 22, 129–148.

CRUZ, R.F., ACCIOLY, A.C.A., 2013. Petrografia, geoquímica e idade U/Pb do ortognaisse Rocinha, no Domínio Pernambuco-Alagoas W da Província Borborema. Estudos Geológicos 23, 3–27.

DADA, S.S., 2008. Proterozoic evolution of the Nigeria-Borborema Province. In: Pankhurst, R.J., Trouw, R.A.J., Brito Neves, B.B., De Wit, M.J., 2008 (Eds.).West Gondwana. Pre-Cenozoic correlations across the South Atlantic region. Geological Society (London), Special Publication 294, 121–136.

DANTAS, E.L., HACKSPACHER, P.C., VAN SCHMUS, W.R., BRITO NEVES, B.B., 1998. Archean accretion in the São José do Campestre Massif, Borborema province, northeast Brazil, Revista Brasileira de Geociências 28, 221–228.

DAVIES, J.H., VON BLANCKENBURG, F., 1995. Slab breakoff: a model of lithosphere detachment and its test in the magmatism and deformation of collisional orogens. Earth and Planetary Science Letters 129, 85–102.

DAWES, R.L., EVANS, B.W., 1991. Mineralogy and geothermobarometry of magmatic epidote-bearing dikes, Front Range, Colorado. Geological Society of America Bulletin 103, 1017–1031.

DEER, W.A., HOWIE, R.A., ZUSSMAN, J., 2013. An Introduction to the Rock-Forming Minerals. 3rd. Edition. London: Mineralogical Society, 498 pp.

DE OLIVEIRA, R.G., 2008. Arcabouço geofísico, isostasia e causas do magmatismo Cenozóico da Província Borborema e de sua margem continental (Nordeste do Brazil). Unpublished PhD thesis, Federal University of Rio Grande do Norte, Rio Grande do Norte, Brazil, 411 pp, (in Portuguese with English abstract).

DEPAOLO, D.J., 1980a. Crustal growth and mantle evolution: Inferences from models of element transport and Nd and Sr isotopes. Geochimica Cosmochimica Acta 44, 1185–1196.

DEPAOLO, D.J., 1980b. Sources of Continental Crust: Neodymium Isotope: Evidence from the Sierra Nevada and Peninsular Ranges. Science 209, 684–687.

DEPAOLO, D.J., 1981. Nd isotopic studies: Some New Perspectives on Earth Structure and Evolution. EOS 62,137–145

DEPAOLO, D.J., 1981a. Trace element and isotopic effects of combined wallrock assimilation and fractional crystallization. Earth and Planetary Science Letters 53, 189–202.

DEPAOLO, D.J., 1981b. Nd isotopes in the Colorado Front Range and crust-mantle evolution in the Proterozoic. Nature 291, 193–196.

DEPAOLO, D.J., 1981c. A Neodymium and Strontium Isotopic Study of the Mesozoic Calc Alkaline Granitic Batholiths of the Sierra Nevada and Peninsular Ranges, California. Journal of Geophysical Research 86, 10470–10488.

DEPAOLO, D.J., 1985. Isotopic studies of processes in mafic magma chambers. I. The Kiglapait intrusion, Labrador: Journal of Petrology 26, 925–951.

DEPAOLO, D.J., 1988. Neodymium Isotope Geochemistry: An Introduction, Springer-Verlag, Heidelberg, 187pp.

DEPAOLO, D.J., LINN, A.M., SCHUBERT, G., 1991. The continental crust age distribution methods of determining mantle separation ages from Sm–Nd isotopic data and application the southwestern United States. Journal of Geophysical Research 9, 2071–2088.

DEPAOLO, D.J., PERRY, F.V., BALDRIDGE, W.S., 1992. Crustal versus mantle sources of granitic magmas: a two-parameter model based on Nd isotopic studies. Transactions of the Royal Society of Edinburgh: Earth Sciences 83, 439–446.

DEPAOLO, D.J., WASSERBURG, G.J., 1979. Petrogenetic mixing models and Nd–Sr isotopic patterns. Geochimica Cosmochimica Acta 43, 615–627.

DE WIT, M., STANKIEWICZ, J., REEVES, C., 2008. Restoring Pan-African-Brasiliano connections: more Gondwana controll, less Tran-Atlantic corruption. In: Pankhurst, R.J., Trouw, R.A.J., Brito Neves, B.B., De Wit, M.J. 2008 (Eds.). West Gondwana. Pre-Cenozoic correlations across the South Atlantic region. Geological Society (London), Special Publication 294, 399–412.

EILER, J.M. 2001. Oxygen-isotope variations of basaltic lavas and upper mantle rocks. In J.W. Valley and D.R. Cole (Eds) Stable Isotope Geochemistry, Reviews in Mineralogy and Geochemistry, 43. Mineralogical Society of America/Geochemical Society, Washington, DC, 319–364.

EILER, J.M., MCINNES, B., VALLEY, J.W., GRAHAM, C.M., STOLPER, E.M., 1998. Oxygen isotope evidence for slab-derived fluids in the sub-arc mantle. Nature 393, 777–781.

ENAMI, M., SUZUKI, K., LIOU, J.G., BIRD, D.K., 1993. Al–Fe^{3+} and F–OH substitutions in titanite and constraints on their P–T dependence. European Journal of Mineralogy 5, 219–231.

EVANS, B.W., VANCE, J.A., 1987. Epidote phenocrysts in dacitic dikes, Boulder County, Colorado. Contributions to Mineralogy and Petrology 96, 178–185.

EVENSEN, N.M., HAMILTON, P.J., ONIONS, R.K., 1978. Rare-Earth Abundances in Chondritic Meteorites. Geochimica et Cosmochimica Acta 42, 1.199–1.212.

EWART, A.E., 1979. A review of the mineralogy and chemistry of theTertiary-Recent dacitic, latitic, rhyolitic and related salic volcanic rocks. In: Barker, F., (ed.). Trondhjemites, dacites and related rocks. Amsterdam, Elsevier, pp. 13–121.

EWART, A.E., 1981. The mineralogy and petrology of Tertiary-Recent orogenic volcanic rocks: with special reference to the andesitic-basaltic compositional range. In: Thorpe, R.S., (ed.). Orogenic andesites and related rocks. John Wiley and Sons Ltd, pp. 25–95.

FARMER, G.L., DEPAOLO, D.J., 1983. Origin of Mesozoic and Tertiary Granite in the Western U. S. and Implications for Pre-Mesozoic Crustal Structure. 1. Nd and Sr

Isotopic Studies in the Geocline of the Northern Great Basin: Journal of Geophysical Research 88, 3379–3401.

FAURE, G., 1986. Principles of Isotope Geology. 2nd edn. John Wiley, New York

FERREIRA, V.P., SIAL, A.N., JARDIM DE SÁ, E.F., 1998. Geochemical and isotopic signatures of the Proterozoic granitoids in terranes of the Borborema Province, northeastern Brazil. Journal of South American Earth Sciences 11, 439–455.

FERREIRA, V.P., SIAL, A.N., PIMENTEL, M.M., ARMSTRONG, R., GUIMARÃES, I.P., SILVA FILHO., A.F., LIMA, M.M.C., SILVA, T. R., 2015. Reworked old crust-derived shoshonitic magma: The Guarany pluton, Northeastern Brazil. Lithos 232, 150–161.

FERREIRA, V.P., SIAL, A.N., PIMENTEL, M.M., ARMSTRONG, R., SPICUZZA, M., GUIMARÃES, I.P., SILVA FILHO, A.F., 2011. Contrasting sources and P-T crystallization conditions of epidote-bearing granitic rocks, northeastern Brazil: O, Sr, and Nd Isotopes. Lithos 121, 189–201.

FERREIRA, V.P., SIAL, A.N., PIMENTEL, M.M., MOURA, C.A.V., 2004. Intermediate to acidic magmatism and crustal evolution in the Transversal Zone, northeastern Brazil. In: MANTESSO, NETO, BARTORELLI, V., CARNEIRO, A., DAL RE, C., BRITO NEVES, B.B. (Eds.),Geologia do Continente Sul-americano: a evolução da obra de Fernando Flávio Marques de Almeida. Editora São Paulo, USP, 189–201. chapter XII,.

FERREIRA, V.P., SIAL, A.N., WHITNEY, J.A., 1994. Large-scale silicate liquid immiscibility: a possible example from northeastern Brazil. Lithos 33, 285–302.

FERREIRA, V.P., VALLEY, J.W., SIAL, A.N., SPICUZZA, M., 2003. Oxygen isotope compositions and magmatic epidote from two contrasting metaluminous granitoids, NE Brazil. Contributions to Mineralogy and Petrology 145, 205–216.

FODEN, J., SOSSI, P.A., WAWRYK, C.M., 2015. Fe isotopes and the contrasting petrogenesis of A-, I- and S-type granite. Lithos 212–215, 32–44

FROST, B.R., FROST, C.D., 2008. A Geochemical Classification for Feldspathic Igneous Rocks. Journal of Petrology 49, 1955–1969.

FROST, B.R., LINDSLEY, D.H., 1991. "The occurrence of Fe-Ti oxides in igneous rocks. Oxide minerals: petrologic and magnetic significance. Mineralogical Society of America", Rev. Mineral 25, 433–486.

FROST, B.R., ARCULUS, R.J., BARNES, C.G., COLLINS, W.J., ELLIS, D.J., FROST, C.D., 2001. A geochemical classification of granitic rocks. Journal of Petrology 42, 2033–2048.

FURMAN, T., GRAHAM, D., 1999. Erosion of lithospheric mantle beneath the East African Rift system: geochemical evidence from the Kivu volcanic province. Lithos 48, 237–262.

GALINDO, A.C., DALL'AGNOL, R., MCREATH, I., LAFON, J.M., TEIXEIRA, N., 1995. Evolution of Brasiliano-age granitoid types in a shear-zone environment, Umarizal-Caraubas region, Rio Grande do Norte, northeast Brazil. Journal of South American Earth Sciences 8, 79–95.

GANADE DE ARAUJO, C.E., RUBATTO, R., HERMANN, J., CORDANI, U.G., CABY, R., BASEI, M.A.S., 2014a. Ediacaran 2500-km-long synchronous deep continental subduction in the West Gondwana Orogen, Nature Communications. Doi: 10.1038/ncomms6198.

GANADE DE ARAUJO, C.E., WEINBERG, R.F., CORDANI, U.G., 2014. Extruding the Borborema Province (NE-Brazil): a two-stage Neoproterozoic collision process. Terra Nova 26, 157–168.

GAO, P., ZHENG, Y-F., ZHAO, Z-F., 2016. Distinction between S-type and peraluminous I-type granites: Zircon versus whole-rock geochemistry. Lithos 258–259, 77–91.

GIBB, R.A., THOMAS, M.D., 1976. Gravity signature of fossil plate boundaries in the Canadian Shield. Nature 262:199–200. doi:10.1038/262199a0

GIOIA, S.M., PIMENTEL, M.M., 2000. A metodologia Sm–Nd no Laboratório de Geocronologia da Universidade de Brasília. Anais da Academia Brasileira de Ciências 72, 219–245.

GREEN, T.H., ADAM, J., 2002. Pressure effect on Ti- or P-rich accessory mineral saturation in evolved granitic melts with differing K_2O/Na_2O ratios. Lithos 61(3–4), 271–282.

GREEN, T.H., WATSON, E.B., 1982. Crystallization of Apatite in Natural Magmas Under High Pressure, Hydrous Conditions, with Particular Reference to Orogenic Rock Series. Contributions to Mineralogy and Petrology 79, 96–105.

GUIMARÃES, I.P., SILVA FILHO, A.F., ALMEIDA, C.N., MACAMBIRA, M.J.B., ARMSTRONG, R., 2011. U–Pb SHRIMP data constraints on calc-alkaline granitoids with 1.3–1.6 Ga Nd TDM model ages from the Central Domain of the Borborema Province, NE Brazil. Journal of South American Earth Sciences 31, 383–396.

GUIMARÃES, I.P., SILVA FILHO, A.F., ALMEIDA, C.N., VAN SCHMUS, W.R., ARAÚJO, J.M.M., MELO, S.C., MELO, E.B., 2004. Brasiliano (Pan-African) granitic magmatism in the PajeueParaiba belt, northeast Brazil: an isotopic and geochronological approach. Precambrian Research. 135, 23–53.

GUIMARÃES, I.P., BRITO, M.F.L., LAGES, G.A., SILVA FILHO, A.F., SANTOS, L., BRASILINO, R.G., 2016. Tonian granitic magmatism of the Borborema Province, NE Brazil: A review. Journal of South American Earth Sciences 68, 97–112.

GUIMARÃES, I.P., VAN SCHMUS, W.R., BRITO NEVES, B.B., BITTAR, S.M.B., SILVA FILHO, A.F., ARMSTRONG, R., 2012. U–Pb zircon ages of orthogneisses and

supracrustal rocks of the Cariris Velhos belt: onset of Neoproterozoic rifting in the Borborema Province, NE Brazil. Precambrian Research 192–195, 52–77.

GUPTA, S., MOHANTY, W.K., MANDAL, A., MISRA, S., 2014. Ancient terrane boundaries as probable seismic hazards: A case study from the northern boundary of the Eastern Ghats Belt, India. Geoscience Frontiers 5, 17 –24

HAMMARSTRON, J.M., ZEN, E.-A., 1986. Aluminum in hornblende: An empirical igneous geobarometer. American Mineralogist 71, 1297–1313.

HANSMANN W, OBERLI F (1991) Zircon inheritance in an igneous rock suite from the southern Adamello batholith (Italian Alps). Contributions to Mineralogy and Petrology 107, 501–518.

HANSON, G.N., 1980. Rare Earth Elements in Petrogenetic Studies of Igneous Systems. Annual Review of Earth and Planetary Sciences 8, 371–405.

HARMON, R.S., HALLIDAY, A.N., CLAYBURN, J.A.P., STEPHENS, W.E., 1984. Chemical and isotopic systematics of the Caledonian intrusions of Scotland and northern England: a guide to magma source region and magma crust interaction. Philosophical Transactions of the Geolological Society of London A310, 439–456.

HARMON, R.S., HOEFS, J., 1995. Oxygen isotope heterogeneity of the mantle deduced from global ^{18}O systematic of basalts from different geotectonic settings. Contributions to Mineralogy and Petrology 120, 95–114.

HARRIS, N.B.W., PEARCE, J.A., TINDLE, A.G., 1986. Geochemical characteristics ofcollision-zone magmatism. In: Coward, M.P., Ries, A.C. (Eds.), Collision Tectonics, Geological Society Special Publication, London, 19, 67–81.

HARRISON, T.M., WATSON, E.B., 1984. The behaviour of apatite during crustal anatexis: equilibrium and kinetic considerations. Geochimica et Cosmochimica Acta 48, 1467–1477.

HARRISON, T.M., WATSON, E.B., 1984. The behaviour of apatite during crustal anatexis: equilibrium and kinetic considerations. Geochimica et Cosmochimica Acta 48, 1467–1477.

HART, S.R., GERLACH, D.C., WHITE, W.M., 1986. A possible new Sr–Nd–Pb mantle array and consequences for mantle mixing. Geochimica et Cosmochimica Acta 50, 1551–1557.

HAWKESWORTH, C.J., KEMP, A.I.S., 2006. Using hafnium and oxygen isotopes in zircons to unravel the record of crustal evolution. Chemical Geology 226, 144–162.

HAWTHORNE, F.C., OBERTI, R., HARLOW, G.E., MARESCH, W.V., MARTIN, R.F., SCHUMACHER, J.C., WELCH, M.D., 2012. IMA Report: Nomenclature of the amphibole supergroup. American Mineralogist 97, 2031–2048.

HEALY, B., COLLINS, W.J., RICHARDS, S.W., 2004. A hybrid origin for Lachlan S-type granites: the Murrumbidgee Batholith example. Lithos 78(1–2), 197–216.

HILDRETH, W., MOORBATH, S., 1988. Crustal contributions to arc magmatism in the Andes of Central Chile. Contributions to Mineralogy and Petrology 98, 455–489.

HILDRETH, W., MOORBATH, S., 1991. Reply to Comment on "Crustal contributions to arc magmatism in the Andes of Central Chile" by W. Hildreth and S. Moorbath. Contributions to Mineralogy and Petrology 108(1–2), 247–252.

HOEFS, J., 2009. Stable Isotope Geochemistry, 5th ed. Springer-Verlag, Berlin, Heidelberg, 244 pp.

HOFMANN, A.W., WHITE, W.M., 1983. Ba, Rb, and Cs in the Earth's mantle. Zeitschrift für Naturforschung A 38(2), 256–266.

HOFMANN, A.W., 2003. Sampling mantle heterogeneity through oceanic basalts: Isotopes and trace elements. In: Holland HD, Turekian KK (eds) The Mantle and Core. Treatise on Geochemistry 2, pp 1–44. doi:10.1016/B0-08-043751-6/02123-X

HOLLAND, T., BLUNDY, J., 1994. Non-ideal interactions in calcic amphiboles and their bearing on amphibole-plagioclase thermometry. Contributions to Mineralogy and Petrology 116, 433–447.

HOLLISTER, L.S., GRISSOM, G.C., PETERS, E.K., STOWELL, H.H., SISSON, V.B., 1987. Confirmation of the empirical correlation of Al in hornblende with pressure of solidification of calc-alkaline plutons. American Mineralogist 72, 231–239.

HOSKIN, P.W.O., BLACK, L.P., 2000. Metamorphic zircon formation by solid-state recrystallization of protolith igneous zircon. Journal of Metamorphic Geology 18, 423–439.

HOSKIN, P.W.O., SCHALTEGGER, U., 2003. The Composition of Zircon and Igneous and Metamorphic Petrogenesis. Reviews in Mineralogy and Geochemistry 53, 27–62.

HUPPERT, H.E., SPARKS, R.S., 1988. The Generation of Granitic Magmas by Intrusion of Basalt into Continental Crust. Journal of Petrology 29(3), 599–624.

IRVINE, T.N., BARAGAR., W.R.A. 1971. A guide to chemical classification of common volcanic rocks. Canadian Journal of Earth Sciences 8, 523–548.

ISHIHARA, S., 1977. The magnetite-series and ilmenite-series granitic rocks. Mining Geology 27, 293–305.

JACOBSEN, S.B., WASSERBURG, G.J., 1980. Sm–Nd isotopic evolution of chondrites. Earth and Planetary Science Letters 50(1), 139–155.

JANOUŠEK, V., FARROW, C. M., ERBAN, V., 2006. Interpretation of Whole-rock Geochemical Data in Igneous Geochemistry: Introducing Geochemical Data Toolkit (GCDkit). Journal of Petrology 47, 1255–1259.

JARDIM DE SÁ, E.F., 1994. A Faixa Seridó (Província Borborema, NE do Brasil) e o seu significado geodinâmico na cadeia brasiliana/pan-africana. Unpublished PhD thesis, University of Brasília, Brasília, Brazil, 804 pp, (in Portuguese).

JOHNSON, M.C., RUTHERFORD, M.J., 1989. Experimental calibration of the aluminum-in-hornblende geobarometer with application to Long Valley caldera (California) volcanic rocks. Geology 17, 837–841.

JOHNSTON, A.D., WYLLIE, P.J., 1988. Interaction of granitic and basic magmas: experimental observations on contamination processes at 10 kbar with H_2O. Contributions to Mineralogy and Petrology 98, 352–362.

KALSBEEK, F., EKWUEME, B.N., PENAYE, J., SOUZA, Z.S., THRANE, K., 2013. Recognition of Early and Late Neoproterozoic supracrustal units in West Africa and North-East Brazil from detrital zircon geochronology. Precambrian Research 226, 105–115.]

KAWASHITA, K., 1972. O método Rb–Sr em rochas sedimentares. PhD thesis. Instituto de Geociências, IGc–USP, Brazil,111 pp, (in Portuguese).

KELLER, C.B,, SCHOENE, B., BARBONI, M., SAMPERTON, K.M., HUSSON, J.M., 2015. Volcanic–plutonic parity and the differentiation of the continental crust. Nature 523, 301–307.

KEMP, A.I.S., HAWKESWORTH, C.J., FOSTER, G.L., PATERSON, B.A., WOODHEAD, J.D., HERGT, J.M., GRAY, C.M., WHITEHOUSE, M.J., 2007. Magmatic and Crustal Differentiation History of Granitic Rocks from Hf–O Isotopes in Zircon. Science 315, 980–983.

KING, E.M., VALLEY, J.W., DAVIS, D.W., EDWARDS, G.R., 1998. Oxygen isotope ratios of Archean plutonic zircons from granite-greenstone belts of the Superior Province: indicator of magmatic source. Precambrian Research 92(4):365–387

KOZUCH, M., 2003, Isotopic and trace element geochemistry of early Neoproterozoic gneissic and metavolcanic rocks in the Cariris Velhos orogen of the Borborema Province, Brazil and their bearing tectonic setting [Ph.D. thesis]: Lawrence, Kansas University, 199 pp.

LACKEY, J.S., VALLEY, J.W., CHEN, J.H., STOCKLI, D.F., 2008. Dynamic magma systems, crustal recycling, and alteration in the Central Sierra Nevada Batholith: the oxygen isotope record. Journal of Petrology 49, 1397–1426.

LEAKE, B.E., WOOLLEY, A.R., ARPS, C.E.S., BIRCH, W.D., GILBERT, M.C., GRICE, J.D., HAWTHORNE, F.C., KATO, A., KISCH, H.J., KRIVOVICHEV, V.G., LINTHOUT, K., LAIRD, J., MANDARINO, J., MARESCH, W.V., NICKEL, E.H., ROCK, N.M.S., SCHUMACHER, J.C., SMITH, D.C., STEPHENSON, N.C.N.,

UNGARETTI, L., WHITTAKER, E.J.W., YOUZHI, G., 1997. Nomenclature of amphiboles: Report of the Subcommittee on Amphiboles of the International Mineralogical Association Commission on New Minerals and Mineral Names. European Journal of Mineralogy 9, 623–651.

LEAKE, B.E., WOOLLEY, A.R., BIRCH, W.D., BURKE, E.A.J., FERRARIS, G., GRICE, J.D., HAWTHORNE, F.C., KISCH, H.J., KRIVOVICHEV, V.G., SCHUMACHER, J.C., STEPHENSON, N.C.N., WHITTAKER, E.J.W., 2003. Nomenclature of amphiboles: Additions and revisions to the International Mineralogical Association's 1997 recommendations. The Canadian Mineralogist 41, 1355–1362.

LEAL, A.S., 1970. Inventário hidrogeológico do nordeste, folha 19, Aracajú-NE, [S.l.]: SUDENE,. 242 pp. (Série Hidrogeologia, 33).

LEE, C.-T.A., BACHMANN, O., 2014. How important is the role of crystal fractionation in making intermediate magmas? Insights from Zr and P systematics. Earth and Planetary Science Letters 393, 266–274.

LI, B., JIANG, S.-Y., LU, A.-H., ZHAO, H.-X., YANG, T.-L., HOU, M.-L., 2016. Zircon U–Pb dating, geochemical and Sr–Nd–Hf isotopic characteristics of the Jintonghu monzonitic rocks in western Fujian Province, South China: Implication for Cretaceous crust–mantle interactions and lithospheric extension. Lithos 260, 413–428.

LI, X.H., LI, W.X., WANG, X.C., LI, Q.L., LIU, Y., TANG, G.Q., 2009. Role of mantle-derived magma in genesis of early Yanshanian granites in the Nanling Range, South China: in situ zircon Hf–O isotopic constraints. Science in China Series D: Earth Sciences 52(9), 1262–1278.

LIÉGEOIS, J.P., NAVEZ, J., HERTOGEN, J., AND BLACK, R., 1998. Contrasting origin of postcollisional high-K calc-alkalic and shoshonitic versus alkalic and peralkalic granitoids. The use of sliding normalization. Lithos 45, 1–28.

LIMA M.M.C., 2013. Caracterização geoquímica, isotópica e geotectônica dos complexos Araticum e Arapiraca, faixa Sergipana-Alagoas. 2013. Unpublished MSc. dissertation, Federal University of Pernambuco, Recife, Brazil, 89pp, (in Portuguese).

LIMA, M.M.C., FERREIRA, V.P., SILVA, T.R., 2016. Age, composição and source of the Poço da Cacimba, Borborema Province-NE Brazil: Sr and Nd isotopic constraints. In: 48° Congresso Brasileiro de Geologia, Porto Alegre.

LIMA, M.M.C., SILVA, T. R., FERREIRA, V.P., SILVA, J.M.R., 2014. Metasedimentary rocks of the northern part of the Macururé Domain, Sergipano Belt (northeastern Brazil): geochemical characterization of their protoliths and tectonic implications. Estudos Geológicos 24, 89–107.

LIOU, J.G., 1973. Synthesis and stability relations of epidote, $Ca_2Al_2FeSiO_{12}(OH)$. Journal of Petrology 14, 381–413.

LIU, D., ZHAO, Z., ZHU, D.-C., NIU, Y., DEPAOLO, D.J., HARRISON, T.M., MO, X., DONG, G., ZHOU, S., SUN, C., ZHANG, Z., LIU, J., 2014. Postcollisional potassic

and ultrapotassic rocks in Southern Tibet: Mantle and crustal origins in response to India–Asia collision and convergence. Geochimica et Cosmochimica Acta 143, 207–231.

LONG, L.E., CASTELLANA, C.H., SIAL, A.N., 2005.Age, origin and cooling history of the Coronel João Sá Pluton, Bahia, Brazil. Journal of Petrology 46, 255–273.

LUDWIG, K.R., 2009. User´s Manual for Isoplot/Ex, version 3.71: A Geochronological Toolkit for Microsoft Excel. Berkeley Geochronology Center, Special Publication 5

LUGMAIR, G.W., MARTI, K., 1978. Lunar initial 143Nd/144Nd: Differential evolution of the lunar crust and mantle. Earth and Planetary Science Letters 39(3), 349–357.

MANIAR, P.D., PICOLLI, P.M., 1989. Tectonic discrimination of granitoids. Geological Society of America Bulletin 101, 635–643.

MARIANO, G., NEVES, S.P., SILVA FILHO, A.F., GUIMARÃES, I.P., 2001, Diorites of the high-K calc-alkalic association: Geochemistry and Sm–Nd isotope data and implications for the evolution of the Borborema Province, Northeast Brazil. International Geology Review 10, 921–929.

MARIANO, G., NEVES, S.P., SILVA, J.M.R., CORREIA, P.B., 2008. Programa Geologia do Brasil. Carta Geológica – Escala 1:100 000: Folha SC.25-X-B-III, Belo Jardim. CPRM – Serviço Geológico do Brasil.

MARTIN, H., SMITHIES, R.H., RAPP, R., MOYEN, J.F., CHAMPION, D., 2005. An overview of adakite, tonalite-trondhjemiten-granodiorite (TTG), and sanukitoid: Relationships and some implications for crustal evolution. Lithos 79, 1–24.

MARTINS, E.P., 2017. Análises geométrica e cinemática meso-microscópica das zonas de cisalhamento Palmeira dos Índios e Jacaré dos Homens: Significância geodinâmica destas estruturas para a zona de limite entre o Domínio Pernambuco–Alagoas e a Faixa Sergipana. Dissertation, Federal University of Pernambuco, Brasil (in Portuguese with English abstract)

MCCULLOCH, M.T., CHAPPELL, B.W., 1982. Nd isotopic characteristics of S- and I-type granites. Earth and Planetary Science Letters 58, 51–64.

MCDONOUGH, W.F., SUN, S.-S., 1995 The composition of the Earth. Chemical Geology 120(3–4):223–253

MEDEIROS, V., 1998. Folha Garanhuns, escala 1:250.000. CPRM, Programa PLGB, internal report, 22 pp.

MELO S.C., 2002. Estrutura, petrologia e geocronologia do batólito Brejo da Madre de Deus (Estado de Pernambuco): relações com a zona de cisalhamento Pernambuco leste. 2002. Unpublished PhD thesis, Federal University of Pernambuco, Recife, Brazil, 118 pp, (in Portuguese).

MENDES V.A., BRITO M.F.L., PAIVA I. P. 2008. Folha Arapiraca (SC.24-X-D, escala 1: 250,000). Integration Geological (Geologic map), Brazilian Geological Survey (CPRM), Recife-PE, Brazil.

MERDITH, A.S., COLLINS, A.S., WILLIAMS, S.E., PISAREVSKY, S., FODEN, J.D., ARCHIBALD, D.B., BLADES, M.L., ALESSIO, B.L., ARMISTEAD, S., PLAVSA, D., CLARK, C., MÜLLER, R.D., 2017. A full-plate global reconstruction of the Neoproterozoic. Gondwana Research 50, 84–134.

MIDDLEMOST, E., 1997. Magmas, Rocks and Planetary Development. A Survey of Magma/Igneous Rock Systems. Editora: Harlow: Longman, 1997.

MILLER, C.F., 1985. Are Strongly Peraluminous Magmas Derived from Pelitic Sedimentary Sources? Journal of Geology 93(6), 673–689.

MILLER, C.F., MCDOWELL, S.M., MAPES, R.W., 2003. Hot and cold granites? Implications of zircon saturation temperatures and preservation of inheritance. Geology 31, 529–532.

MOLINA, J.F., MORENO, J.A., CASTRO, A., RODRÍGUEZ, C., FERSHTATER, G.B., 2015. Calcic amphibole thermobarometry in metamorphic and igneous rocks: New calibrations based on plagioclase/amphibole Al-Si partitioning and amphibole/liquid Mg partitioning. Lithos 232, 286–305.

MORI, Y., MASHIMA, H., 2005. X-ray fluorescence analysis of major and trace elements in silicate rocks using 1:5 dilution glass beads. Bulletin of the Kitakyushu Museum of Natural History and Human History Ser. A 3, 1–12.

NACHIT, H., RAZAFIMAHEFA, N., STUSSI, J.M., CARRON, J.P., 1985. Composition chimique des biotites et typologie magmatique des granitoids. Comptes rendus de l'Académie des sciences de la Terre et des planetes. Earth and Planetary Sciences 11 (II), 813–818.

NANDEDKAR, R.H., ULMER, P., MÜNTENER, O., 2014. Fractional crystallization of primitive, hydrous arc magmas: an experimental study at 0.7 GPa. Contributions to Mineralogy and Petrology 167:1015.

NANEY, M.T., 1983. Phase equilibria of rocks-forming ferromagnesian silicates in granitic systems. American Mineralogy 283, 993–1033.

NELSON, B.K., DEPAOLO, D.J., 1985. Rapid production of continental crust 1.7–1.9 b.y. ago: Nd and Sr isotopic evidence from the basement of the North American midcontinent: Geological Society of America Bulletin 96, 746–754.

NEVES, S.P., 2003, Proterozoic history of the Borborema Province (NE Brazil): Correlations with neighboring cratons and Pan-African belts, and implications for the evolution of western Gondwana. Tectonics 22, 1031–1044.

NEVES, S.P., 2011. Atlantica revisited: new data and thoughts on the formation and evolution of a long-lived continent. International Geology Review 53, 1377–1391.

NEVES, S.P., 2015. Constraints from zircon geochronology on the tectonic evolution of the Borborema Province (NE Brazil): Widespread intracontinental Neoproterozoic reworking of a Paleoproterozoic accretionary orogen. Journal of South American Earth Sciences 58, 150–164.

NEVES S.P., BRUGUIER O., VAUCHEZ A., BOSCH D., SILVA J.M.R., MARIANO G., 2006. Timing of crust formation, deposition of supracrustal sequences, and Transamazonian and Brasiliano metamorphism in the East Pernambuco belt (Borborema Province, NE Brazil): implications for western Gondwana assembly. Precambrian Research 149, 197–216.

NEVES, S.P., BRUGUIER, O., BOSCH, D., SILVA, J.M.R., MARIANO, G., 2008. U–Pb ages of plutonic and metaplutonic rocks in southern Borborema Province (NE Brazil): timing of Brasiliano deformation and magmatism. Journal of South American Earth Sciences 25, 285–297.

NEVES, S.P., BRUGUIER, O., SILVA, J.M.R., BOSCH, D., ALCANTARA, V.C., LIMA, C.M., 2009. The age distributions of detrital zircons in metasedimentary sequences in eastern Borborema Province (NE Brazil): Evidence for intracontinental sedimentation and orogenesis? Precambrian Research 175, 187–205.

NEVES, S.P., MARIANO, G., 2004. Heat-producing elements-enriched continental mantle lithosphere and Proterozoic intracontinental orogens: Insights from Brasiliano/Pan-African belts. Gondwana Research 7, 427–436.

NEVES, S.P., MELO, S.C., MOURA, C.A.V., MARIANO, G., AND SILVA, J.M.R., 2004, Zircon Pb–Pb geochronology of the Caruaru area, northeastern Brazil: Temporal constraints on the Proterozoic evolution of Borborema Province: International Geology Review 46, 52–63.

NEVES, S.P., MONIÉ, P., BRUGUIER, O., SILVA, J.M.R., 2012. Geochronological, thermochronological and thermobarometric constraints on deformation, magmatism and thermal regimes in eastern Borborema Province (NE Brazil). Journal of South American Earth Sciences 38, 129–146.

NEVES, S.P., LAGES, G.A., BRASILINO, R.G., MIRANDA, A.W.A., 2015a. Paleoproterozoic accretionary and collisional processes and the build-up of the Borborema Province (NE Brazil): geochronological and geochemical evidence from the Central Domain. Journal of South American Earth Sciences 58, 165–187.

NEVES, S.P., BRUGUIER, O., SILVA, J.M.R., MARIANO, G., SILVA FILHO, A.F., TEIXEIRA, C.M.L.., 2015b. From extension to shortening: Dating the onset of the Brasiliano Orogeny in eastern Borborema Province (NE Brazil). Journal of South American Earth Sciences 58, 238–256.

NEVES, S.P., SILVA, J.M.R., BRUGUIER, O., 2016. The transition zone between the Pernambuco–Alagoas Domain and the Sergipano Belt (Borborema Province, NE Brazil): Geochronological constraints on the ages of deposition, tectonic setting and

metamorphism of metasedimentary rocks. Journal of South American Earth Sciences 72, 266–278.

NEVES, S.P., SILVA, J.M.R., BRUGUIER, O., 2017. Geometry, kinematics and geochronology of the Sertânia Complex (central Borborema Province, NE Brazil): Assessing the role of accretionary versus intraplate processes during West Gondwana assembly. Precambrian Research 298, 552–571.

NEVES, S.P., SILVA, J.M.R., MARIANO, G., 2005. Oblique lineations in orthogneisses and supracrustal rocks: vertical partitioning of strain in a hot crust (eastern Borborema Province, NE Brazil). Journal of Structural Geology 27(8), 1513–1527.

NEVES, S.P., TOMMASI, A., VAUCHEZ, A., HASSANI, R., 2008. Intraplate continental deformation: Influence of a heat-producing layer in the lithospheric mantle. Earth and Planetary Science Letters 274, 392–400.

NEVES, S.P., VAUCHEZ, A., 1995. Magma emplacement and shear zone nucleation and development in northeast Brazil (Fazenda Nova and Pernambuco shear zones; State of Pernambuco). Journal of South American Earth Sciences 8(3–4), 289–298.

NEVES, S.P., VAUCHEZ, A., ARCHANJO, C.J., 1996. Shear zone-controlled magma emplacement or magma-assisted nucleation of shear zones? Insights from northeast Brazil. Tectonophysics 262(1–4), 349–364.

NEVES, S.P., VAUCHEZ, A., FÉRAUD, G., 2000. Tectono-thermal evolution, magma emplacement, and shear zone development in the Caruaru area (Borborema Province, NE Brazil). Precambrian Research 99(1–2), 1–32.

NJIEKAK, G., DÖRR, W., TCHOUANKOUÉ, J.-P., ZULAUF, G., 2008. U–Pb zircon and microfabric data of 9meta) grranitoids of western Cameroon: Constraints on the timing of pluton emplacement and deformation in the Pan-African belt of central Africa. Lithos 102, 460–477.

NOYES, H.J., FREY, F.A., WONES, D.R., 1983. A Tale of Two Plutons: Geochemical Evidence Bearing on the Origin and Differentiation of the Red Lake and Eagle Peak Plutons, Central Sierra Nevada, California. Journal of Geology 91(5), 487–509.

OLIVEIRA, E.P., WINDLEY, B.F., ARAÚJO, M.N.C., 2010. The Neoproterozoic Sergipano orogenic belt, NE Brazil: A complete plate tectonic cycle in western Gondwana. Precambrian Research 181, 64–84.

OLIVEIRA, E.P., TOTEU, S.F., ARAÚJO M.N.C., CARVALHO, M.J., NASCIMENTO, R.S., BUENO, J.F., MCNAUGHTON, N., BASILICI, G., 2006. Geologic correlation between the Neoproterozoic Sergipano belt (NE Brazil) and the Yaoundé belt (Cameroon, Africa). Journal of African Earth Sciences 44, 470–478.

OLIVEIRA, E.P., BUENO, J.F., MCNAUGHTON, N., SILVA FILHO, A.F., NASCIMENTO, R.S., DONATTI-FILHO, J.P., 2015a. Age, composition, and source of continental arc- and syn-collision granites of the Neoproterozoic Sergipano Belt,

Southern Borborema Province, Brazil. Journal of South American Earth Sciences 58, 257–280.

OLIVEIRA, E.P., MCNAUGHTON, N.J., WINDLEY, B.F., CARVALHO, M.J., NASCIMENTO, RS., 2015b. Detrital zircon U–Pb geochronology and whole-rock Nd-isotope constraints on sediment provenance in the Neoproterozoic Sergipano orogen, Brazil: From early passive margins to late foreland basins. Tectonophysics 662, 183–194.

OLIVEIRA, E.P., WINDLEY, B.F., MCNAUGHTON, N.J., BUENO, J.F., NASCIMENTO, R.S., CARVALHO, M.J., ARAÚJO, M.N.C., 2017. The Sergipano Belt. In: HEILBRON, M., CORDANI, U.G., ALKMIM, F.F., (Eds.), São Francisco Craton, Eastern Brazil: Tectonic Genealogy of a Miniature Continent, Regional Geology Reviews, DOI 10.1007/978-3-319-01715-0_13, 241–254. Chapter XIII,.

O'NEIL, J., SHAW, S.F., FLOOD, R.H., 1977. Oxygen and hydrogen isotope compositions of granite genesis in the New England batholith, Australia. Contributions to Mineralogy and Petrology 62, 313–325.

OSAKO, L., 2005, Caracterização geológica da região entre as localidades de Paranatama e Curral Novo, PE, porção centro-norte do Complexo Pernambuco-Alagoas, Província Borborema. Unpublished PhD thesis, Federal University of Pernambuco, Recife, Brazil, 163 pp, (in Portuguese).

PAPOUTSA, A., PE-PIPER, G., 2014. Geochemical variation of amphiboles in A-type granites as an indicator of complex magmatic systems: Wentworth pluton, Nova Scotia, Canada. Chemical Geology 384, 120–134.

PATCHETT, P.J., VERVOORT, J.D., SÖDERLUND, U., SALTERS, V.J.M., 2004. Lu–Hf and Sm–Nd isotopic systematics in chondrites and their constraints on the Lu–Hf properties of the Earth. Earth and Planetary Science Letters 222(1), 29–41.

PATIÑO DOUCE, A.E., BEARD, J.S., 1995. Dehydration-melting of biotite gneiss and quartz amphibolite from 3 to 15 kbar. Journal of Petrology 36, 707–738.

PATIÑO DOUCE, A.E., JOHNSTON, A.D., 1991. Phase equilibria and melt productivity in the pelitic system: implications for the origin of peraluminous granitoids and aluminous granulites. Contributions to Mineralogy and Petrology 107(2), 202–218.

PEARCE, J., 1996. Sources and settings of granitic rocks. Episodes 19, 120–125.

PEARCE, J., HARRIS, N.B.W., TINDLE, A.D., 1984. Trace element discrimination diagrams for the tectonic interpretation of granitic rocks. Journal of Petrology 25, 956–983.

PECCERILLO, A., 1985. Roman comagmatic province (central Italy): Evidence for subduction-related magma genesis. Geology 13, 103–106

PENAYE, J., TOTEU, S.F., VAN SCHMUS, W.R., NZENTI, J.P., 1993. U–Pb and Sm–Nd preliminary geochronologic data on the Yaoundé Group, Cameroon: re-

interpretation of the granulitic rocks as the suture of a collision in the Centrafrican belt‘‘. Comptes Rendus de l‘Académie des Sciences, Paris 317, 789–794.

PERRY, F.V., BALDRIDGE, W.S., DEPAOLO, D.J., 1987. The role of asthenosphere and lithosphere in the genesis of Late Cenozoic basaltic rocks from the Rio Grande rift and adjacent regions of the southwestern United States: Journal of Geophysical Research 92, 9193–9213.

PETFORD, N., ATHERTON, M., 1993. Na-rich Partial Melts from Newly Underplated Basaltic Crust: the Cordillera Blanca Batholith, Peru. Journal of Petrology 37(6), 1491–1521.

PHILIPPIANS 3.14, Holy Bible: King James Version.

POLI, G.E., TOMMASINI, S., 1991. Model for the Origin and Significance of Microgranular Enclaves in Calc-alkaline Granitoids. Journal of Petrology 32(3), 657–666.

PUTIRKA., 2016. Amphibole thermometers and barometers for igneous systems and some implications for eruption mechanisms of felsic magmas at arc volcanoes. American Mineralogist 101, 841–858.

RAPP, R.P., WATSON, E.B., 1995. Dehydration melting of metabasalt at 8–32 kbar: Implications for continental growth and crust–mantle recycling. Journal of Petrology 36, 891–931.

RAPP, R.P., SHIMIZU, N., NORMAN, M.D., 2003. Growth of early continental crust by partial melting of eclogite. Nature 425, 605–609.

ROBERTS, M.P., CLEMENS, J.D., 1993. Origin of high-potassium, calc-alkaline, I-type granitoids. Geology 21(9), 825–828.

ROGERS, N.W., HAWKESWORTH, C.J., PARKER, R.J., MARSH, J.S., 1985. The geochemistry of potassic lavas from Vulsini, central Italy and implications for mantle enrichment processes beneath the Roman region. Contributions to Mineralogy and Petrology 90, 244–257.

ROLLINSON, H., 1993. Using Geochemical Data: Evaluation, Presentation, Interpretation. Longman Scientific and technical, London

ROTENBERG, E., DAVIS, D.W., AMELIN, Y., GHOSH, S., BERGQUIST, B.A., 2012. Determination of the decay-constant of ^{87}Rb by laboratory accumulation of ^{87}Sr. Geochimica et Cosmochimica Acta 85, 41–57.

RICHARD, P., SHIMIZU, N., ALLÈGRE, C.J., 1976. ^{143}Nd/^{146}Nd A Natural Tracer: An Application to Oceanic Basalts. Earth and Planetary Science Letters 31, 269–278.

RUDNICK, R.L., FOUNTAIN, D.M., 1995. Nature and composition of the continental crust: A lower crustal perspective. Reviews of Geophysics 33(3), 267–309.

RUTHERFORD, M.J., JOHNSON, M.C., 1992. Comment on Blundy and Holland's (1990) "Calcic amphibole equilibria and a new amphibole-plagioclase geothermometer. Contributions to Mineralogy and Petrology

SÁ, J.M., BERTRAND, J.M., LETERRIER, J., MACEDO, M.H.F. 2002. Geochemistry and geochronology of pre-brasiliano rocks from the transversal zone, Borborema Province, northeast Brazil. Journal of South American Earth Sciences 14, 851–866.

SANTOS, A.C.L., PADILHA, A.L., FUCK, R.A., PIRES, A.C.B., VITORELLO, I., PÁDUA, M.B., 2014. Deep structure of a stretched lithosphere: Magnetotelluric imaging of the southeastern Borborema province, NE Brazil. Tectonophysics 610, 39–50.

SANTOS, E.J., 1995. O complexo granítico de Lagoa das Pedras: acresção e colisão na região de Floresta (PE), Província Borborema. Unpublished PhD thesis, University of São Paulo, São Paulo, Brazil, 219 pp, (in Portuguese).

SATO, K., TASSINARI, C.C.G., BASEI, M.A.S., SIGA Jr, O., ONOE, A.T., SOUZA, M.D., 2014. Sensitive High Resolution Ion Microprobe (SHRIMP IIe/MC) of the Institute of Geosciences of the University of São Paulo, Brazil: analytical method and first results. Geologia USP: Série Cientifica 14(3), 3–18.

SATO, K., TASSINARI, C.C.G., KAWASHITA, K., PETRONILHO, L., 1995. O método Geocronológico Sm–Nd no IG/USP e suas aplicações. Anais da Academia Brasileira de Ciências 67(3), 313–336.

SANTOS, E.J., VAN SCHMUS, W.R., KOZUCH, M., BRITO NEVES, B.B., 2010. The Cariris Velhos tectonic event in Northeast Brazil. Journal of South American Earth Sciences 29, 61–76.

SANTOS, L.C.M.L., DANTAS, E.L., SANTOS, E.J., SANTOS, R.V., LIMA, H.M., 2015. Early to Late Paleoproterozoic magmatism in NE Brazil: The Alto Moxotó Terrane and its tectonic implications for the Pre-West Gondwana assembly. Journal of South American Earth Sciences 58, 188–209.

SANTOS, T.J.S., FETTER, A.H., HACKSPACHER, P.C., VAN SCHMUS, W.R., NOGUEIRA NETO, J.A., 2008. Neoproterozoic tectonic and magmatic episodes in the NW sector of Borborema Province, NE Brazil, during assembly of Western Gondwana. Journal of South American Earth Sciences 25, 271–284.

SAWYER, E.W., 2008. Atlas of Migmatites. The Canadian Mineralogist, Special Publication 9. NRC Research Press, Ottawa, Ontario, Canada 371 pp.

SCAILLET, B., HOLTZ, F., PICHAVANT, M., 2016. Experimental Constraints on the Formation of Silicic Magmas. Elements 12, 109–114.

SCHMIDT, M, W., 1992. Amphibole composition in tonalite as a function of pressure: an experimental calibration of the Al-in-hornblende barometer. Contributions to Mineralogy and Petrology 110, 304–310.

SCHMIDT, M.W., POLI, S., 2004. Magmatic Epidote. Reviews in Mineralogy and Geochemistry 56, 399–430.

SCHMIDT, M.W., THOMPSON, A.B., 1996. Epidote in calc-alkaline magmas: an experimental study of stability, phase relationships, and the role of epidote in magmatic evolution. American Mineralogist 81, 424–474.

SCHUBERT, M., DRIESNER, T., GERYA, T.V., ULMER, P., 2013. Mafic injection as a trigger for felsic magmatism: a numerical study. Geochemistry, Geophysics, Geosystems 14(6), 1910–1928.

SHABANI, A.A.T., LALONDE, A.E., 2003. Composition of biotite from granitic rocks of the Canadian Appalachian Orogen: a potential tectonomagmatic indicator? The Canadian Mineralogist 41, 1381–1396.

SHAND, S.J.,1947. Eruptive Rocks. Third edition, Hafner Publishing Company, New York, 488 pp.

SIAL, A.N., 1986. Granite-types in northeast Brazil: current knowledge. Revista Brasileira de Geociencias 16, 54–72.

SIAL, A.N., 1990. Epidote-bearing calc-alkaline granitoids in Northeast Brazil. Revista Brasileira de Geociências 20, 88–100.

SIAL, A.N., 1993. Contrasting metaluminous magmatic epidote-bearing granitic suites from two Precambrian Foldbelts in Northeast Brazil. Anais da Academia Brasileira de Ciencias 65 (supl. 1), 141–162.

SIAL, A.N., FERREIRA, V.P., 2016. Magma associations in Ediacaran granitoids of the Cachoeirinha–Salgueiro and Alto Pajeú terranes, northeastern Brazil: Forty years of studies. Journal of South American Earth Sciences 68, 113–133.

SIAL, A. N., FERREIRA, V.P., FALLICK, E.A., CRUZ, M.J., 1998. Amphibole-rich clots in calc-alkalic granitoids in the Borborema Province, Northeastern Brazil. Journal of South American Earth Sciences 11, 457–472.

SIAL, A.N., TOSELLI, A.J., SAAVEDRA, J., PARADA, M.A., FERREIRA, V.P., 1999. Emplacement, petrological and magnetic susceptibility characteristics of diverse magmatic epidote-bearing granitoid rocks in Brazil, Argentina and Chile. Lithos 46, 367–392.

SIAL, A.N., VASCONCELOS, P.M., FERREIRA, V.P., PESSOA, R.R., BRASILINO, R.G., MORAIS NETO, J.M., 2008. Geochronological and mineralogical constraints on depth of emplacement and ascension rates of epidote-bearing magmas from northeastern Brazil. Lithos 105, 225–238.

SILVA, L.C., ARMSTRONG, R., PIMENTEL, M.M., SCANDOLARA, J., RAMGRAB, G., WILDNER, W., ANGELIM, L.A.A., VASCONCELOS, A.M., RIZZOTO, G., QUADROS, M.L.E.S., SANDER, A., ROSA, A.L.Z., 2002. Reavaliação da evolução geológica em terrenos pré-cambrianos brasileiros com base em

novos dados U–Pb SHRIMP, Parte III: Províncias Borborema, Mantiqueira meridional e Rio Negro–Juruena. Revista Brasileira de Geociências 32, 529–544

SILVA, T.R., FERREIRA, V.P., LIMA, M.MC., SIAL, A.N., 2016. Two stage mantle-derived granitic rocks and the onset of the Brasiliano orogeny: Evidence from Sr, Nd, and O isotopes. Lithos 264, 189–200.

SILVA, T.R., FERREIRA, V.P., LIMA, M.M.C., SIAL, A.N., 2016. Cryogenian–Ediacaran magmatism record of the Pernambuco–Alagoas Domain, Borborema Province (NE Brazil): Implications for the early assembly of the West Gondwana. In: 48° Congresso Brasileiro de Geologia, Porto Alegre.

SILVA, T.R., FERREIRA, V.P., LIMA, M.M.C., SIAL, A.N., 2016. Two stage mantle-derived magma in a syn-tectonic ediacaran batholith and the onset of the Brasiliano orogeny: Evidence from Sr, Nd and O isotopes. In: 48° Congresso Brasileiro de Geologia, Porto Alegre.

SILVA, T.R., FERREIRA, V.P., LIMA, M.MC., SIAL, A.N., Isotope evidence for mantle-derived source rock of high-K calc-alkaline granites, Pernambuco-Alagoas Domain, northeastern Brazil. International Journal of Earth Sciences 2018, submitted.

SILVA, T.R., FERREIRA, V.P., LIMA, M.M.C., SIAL, A.N., PIMENTEL, M.M., 2015. Evidence for ediacaran juvenile crust in the Monteiropolis batholith, Pernambuco–Alagoas Domain, Northeastern Brazil: constraints from Sr, Nd and O isotopes. In: XXVI Simpósio de Geologia de Nordeste, Natal, boletim 24, p. 152–152.

SILVA, T.R., FERREIRA, V.P., LIMA, M.M.C., SIAL, A.N., SILVA, J.M.R., 2015 Synkinematic emplacement of the magmatic epidote bearing Major Isidoro tonalite-granite batholith: Relicts of an Ediacaran continental arc in the Pernambuco–Alagoas domain, Borborema Province, NE Brazil. Journal of South American Earth Sciences 64, 1–13.

SILVA FILHO, A.F., GUIMARAES, I.P., 2000. Sm/Nd isotopic data and U/Pb geochronology of collisional to post-collisional high-K shoshonitic granitoids from the Pernambuco-Alagoas terrane, Borborema Province, NE. Brazil. In: International Geological Congress, 31, Rio de Janeiro.

SILVA FILHO, A.F., GUIMARÃES, I.P., FERREIRA, V.P., ARMSTRONG, R., SIAL, A.N., 2010. Ediacaran Águas Belas pluton, Northeastern Brazil: Evidence on age, emplacement and magma sources during Gondwana amalgamation. Gondwana Research 17(4), 676–687

SILVA FILHO, A.F., GUIMARÃES, I.P., VAN SCHMUS, W.R., 2002. Crustal Evolution of the Pernambuco–Alagoas Complex, Borborema Province, NE Brazil: Nd Isotopic Data from Neoproterozoic Granitoids. Gondwana Research 5(2), 409–422.

SILVA FILHO, A. F., GUIMARÃES, I. P., VAN SCHMUS, W. R., DANTAS, E.L., ARMSTRONG R., COCENTINO, L.M., LIMA, D.R., 2013. Long–lived Neoproterozoic high-K magmatism in the Pernambuco–Alagoas Domain, Borborema Province, Northeast Brazil. International Geology Review 55, 1280–1299.

SILVA FILHO, A.F., GUIMARÃES, I.P., VAN SCHMUS, W. R., ARMSTRONG, R., SILVA, J.M.R., COCENTINO, L.M., OSAKO, L.S., 2014. SHRIMP U–Pb zircon geochronology and Nd signatures of supracrustal sequences and orthogneisses constrain the Neoproterozoic evolution of the Pernambuco–Alagoas Domain, southern part of Borborema Province, NE Brazil. International Journal of Earth Sciences (Geol Rundsch) 103, 2155–2190.

SILVA FILHO, A.F., GUIMARÃES, I.P., SANTOS, L., ARMSTRONG, R., VAN SCHMUS, W.R., 2016. Geochemistry, U–Pb geochronology, Sm–Nd and O isotopes of ca. 50 Ma long Ediacaran High-K Syn-Collisional Magmatism in the Pernambuco Alagoas Domain, Borborema Province, NE Brazil. Journal of South American Earth Sciences 68, 134–154.

SISSON, T.W., RATAJESKI, K., HANKINS, W.B., GLAZNER, A.F., 2005. Voluminous granitic magmas from common basaltic sources. Contributions to Mineralogy and Petrology 148, 635–661.

SPEER, J.A., 1984. Micas in igneous rocks. Reviews in Mineralogy 13, pp 299–356.

STRECKEISEN, A., 1976. To each plutonic rock its proper name. Earth-Science Reviews 12(1), 1–33.

SUN, S.-S., MCDONOUGH, W.F., 1989. Chemical and isotopic systematics of ocean basalts: implications for mantle composition and processes. In: Saunders, A.D. and Norry, M. J. (eds) Magmatism in the Ocean Basins. Geological Society, London, Special Publications 42, 313–345.

TAYLOR, S.R., MCLENNAN, S.M., 1985. The continental crust: Its composition and evolution. Blackwell Scientific Publications, Oxford

TEPPER, J.H., NELSON, B.K., BERGANTZ, G.W., IRVING, A.J., 1993. Petrology of the Chilliwack batholith, North Cascades, Washington: generation of calc-alkaline granitoids by melting of mafic lower crust with variable water fugacity. Contributions to Mineralogy and Petrology 113(3), 333–351.

TOLLARI, N., TOPLIS, M.J., BARNES, S.J., 2006. Predicting phosphate saturation in silicate magmas: An experimental study of the effects of melt composition and temperature. Geochimica et Cosmochimica Acta, 70, 1518–1536.

TOTEU, S.F., MACAUDIÉRE, J., BERTRAND, J.M., DAUTEL, D., 1990. Metamorphic zircons from northern Cameroon: implications for the Pan-African evolution of central Africa. Geologisch Rundschau 79, 777–786.

TOTEU, S.F., VAN SCHMUS, R.W., PENAYE, J., NYOBÉ, J.B., 1994. U–Pb and Sm–Nd evidence for Eburnian and Pan-African high-grade metamorphism in cratonic rocks of southern Cameroon. Precambrian Research 67, 321–347.

TOTEU, S.F., VAN SCHMUS, R.W., PENAYE, J., MICHARD, A., 2001. New U–Pb and Sm–Nd data from north-central Cameroon and its bearing on the pre-Pan-African history of central Africa. Precambrian Research 108, 45–73.

TOTEU, S.F., PENAYE, J., DELOULE, E., VAN SCHMUS, W.R., TCHAMENI, R., 2006. Diachronous evolution of volcano-sedimentary basins north of the Congo craton: insights from U–Pb ion microprobe dating of zircons from the Poli, Lom and Yaoundé Groups (Cameroon). Journal of African Earth Sciences 44, 428–442.

THOMPSON, R.N., 1982. Magmatism of the British Tertiary volcanic Province. Scottish Journal of Geology 18, 50–107.

TROMPETTE R., 1994. Geology of Western Gondwana (2000–500 Ma): Pan-African-Brasiliano Aggregation of South América and Africa. A.A. Balkema, Rotterdam, Brookfield, 350p.

TROMPETTE, R., 1997. Neoproterozoic (~600 Ma) aggregation of Western Gondwana: a tentative scenario. Precambrian Research 82(1–2), 101–112.

TROMPETTE, R., 2000. Gondwana evolution; its assembly at around 600 Ma. Acad Sci Paris, Sciences de la Terre et des planètes. Earth Planet. Sci. 330, 305–315.

TULLOCH, A.J., 1979. Secondary Ca–Al Silicates as Low-Grade Alteration Products of Granitoid Biotite. Contributions to Mineralogy and Petrology 69, 105–117.

TULLOCH, A.J., 1986. Comments and Reply on "Implications of magmatic epidote-bearing plutons on cirustal evolution in the accreted terranes of northwestern North America" and "Magmatic epidote and its petrologie significance". Geology 14, 186–187.

VALLEY, J. W. 2003. Oxygen isotopes in zircon. In: Hanchar, J. M. and Hoskin, P. W. O. (eds) Zircon. Mineralogical Society of America/ Geochemical Society, Reviews in Mineralogy and Geochemistry 53, 343–385.

VALLEY, J. W., BINDEMAN, I. N., PECK, W. H., 2003. Calibration of oxygen isotope fractionations in zircon. Geochimica et Cosmochimica Acta 67, 3257–3266.

VALLEY, J.W., CHIARENZELLI, J.R., MCLELLAND, J.M., 1994. Oxygen isotope geochemistry of zircon. Earth and Planetary Science Letters 126, 187–206.

VALLEY, J.W., KINNY, P.D., SCHULZE, D.J., SPICUZZA, M.J., 1998. Zircon megacrysts from kimberlite: oxygen isotope variability among mantle melts. Contributions to Mineralogy and Petrology 133, 1–11.

VALLEY, J.W., KITCHEN, N., KOHN, M.J., NIENDORF, C.R., SPICUZZA, M.J., 1995. UWG-2, a garnet standard for oxygen isotope ratios: Strategies for high precision and accuracy with laser heating. Geochimica et Cosmochimica Acta 59(24), 5223–5231.

VALLEY, J.W., LACKEY, J.S., CAVOSIE, A.J., CLECHENKO, C.C., SPICUZZA, M.J., BASEI, M.A.S., BINDEMAN, I.N., FERREIRA, V.P., SIAL, A.N., KING, E.M., PECK, W.H., SINHA, A.K., WEI, C.S., 2005. 4.4 billion years of crustal maturation: oxygen isotope ratios of magmatic zircon. Contributions to Mineralogy and Petrology 150, 561–580.

VAN SCHMUS, W.R., BRITO NEVES, B.B., HACKSPACHER, P.C., BABINSKY, M., 1995. U/Pb and Sm/Nd geochronologic studies of the eastern Borborema Province, NE Brazil. Journal of South American Earth Sciences 8(3–4), 267–288

VAN SCHMUS, W.R., KOZUCH, M., BRITO NEVES, B.B., 2011. Precambrian history of the Zone Transversal of the Borborema Province, NE Brazil: insights from Sm–Nd and U–Pb geochronology. Journal of South American Earth Sciences 31, 227–252.

VAN SCHMUS, W.R., OLIVEIRA, E.P., SILVA FILHO, A.F., TOTEU, S.F., PENAYE, J., GUIMARÃES, I.P., 2008. Proterozoic links between the Borborema Province, NE Brazil and the Central African Fold Belt. In: PANKHURST, R.J., TROUW, R.A.J., BRITO NEVES, B.B., DE WIT, M.J. (eds) West Gondwana: Pre-Cenozoic Correlations Across the South Atlantic Region. Geological Society, London, Special Publications 294, pp 69–99. doi:10.1144/SP294.5

VAUCHEZ, A., EGYDIO-SILVA, M., 1992. Termination of a continental-scale strike-slip fault in partially melted crust: The West Pernambuco shear zone, northeast Brazil. Geology 20(11), 1007–1010.

VAUCHEZ, A., NEVES, S.P., CABY, R., CORSINI, M., EGYDIO-SILVA, M., ARTHAUD, M., AMARO, V., 1995. The Borborema shear zone system, NE Brazil. Journal of South American Earth Sciences 8(3–4), 247–266.

VYHNAL, C.R., MCSWEEN JR., H.Y., SPEER, J.A., 1991. Hornblende chemistry in southern Appalachian granitoids: Implication for aluminum hornblende thermo barometry and magmatic epidote stability. American Mineralogist 76, 176–188.

WATSON, E.B., 1979. Apatite saturation in basic to intermediate magmas. Geophysical Research Letters 6, 937–940.

WATSON, E.B., HARRISON, T.M., 1983. Zircon saturation revisited: temperature and composition effects in a variety of crustal magma types. Earth and Planetary Science Letters 64, 295–304.

WEINBERG, R.F., SIAL, A.N., MARIANO, G., 2004. Close spatial relationship between plutons and shear zones. Geology 32, 377–380.

WEINBERG, R.F., SIAL, A.N., MARIANO, G., 2005. Close spatial relationship between plutons and shear zones: Comment and Reply: REPLY. Geology 33, e74, doi: 10.1130/0091-7613-33.1.e73

WEINBERG, R.F., VEVEAKIS, E., LIEB, R., 2015. Compaction-driven melt segregation in migmatites. Geology 43, 471–474.

WHITE, A.J.R., 1979. Sources of granite magmas. Geological Society of America. Abstract with Programs 11, p. 539.

WHITNEY, D.L., EVANS, B.W., 2010. Abbreviations for names of rock-forming minerals. American Mineralogist 95, 185–187.

WILLIAMS, I.S., 1998. U–Th–Pb geochronology by ion microprobe. In: McKibben MA, Shanks WC, Ridley WI (eds) Applications of Microanalytical Techniques to Understanding Mineralizing Processes. Reviews in Economic Geology 7, pp 1–35.

WILLIAMS, I.S., CLAESSON, S., 1987. Isotopic evidence for the Precambrian provenance and Caledonian metamorphism of high grade paragneisses from the Seve Nappes, Scandinavian Caledonides II. Ion microprobe zircon U–Pb–Th. Contribution to Mineralogy and Petrology 97, 205–217.

WILSON, M., 1989. Igneous Petrogenesis: A global tectonic approach. Unwin Hyman, London, 466 pp.

WOLF, M.B., WYLLIE, P.J., 1994. Dehydration-melting of amphibolite at 10 kbar: the effects of temperature and time. Contributions to Mineralogy and Petrology 115(4), 369–383.

WONES, D.R., 1989. Significance of the assemblage titanite+magnetite+quartz in granitic rocks. American Mineralogist 74, 744–749.

WONES, D.R., EUGSTER, H.P., 1965. Stability of biotite: experiment, theory and application. American Mineralogist 50, 1228–1272.

ZEN, E.-A., 1986. Aluminum Enrichment in Silicate Melts by Fractional Crystallization: Some Mineralogic and Petrographic Constraints. Journal of Petrology 27(5), 1095–1117.

ZEN, E-A, HAMMARSTROM, J.M., 1984. Magmatic epidote and its petrologic significance. Geology 12(9), 515–518.

ZINDLER, A., HART, S., 1986. Chemical geodynamics. Annual Reviews of Earth and Planetary Science 14, 493–571.

APÊNDICE A – Abstracts publicados no 46º Congresso Brasileiro de Geologia

CRYOGENIAN–EDIACARAN MAGMATISM RECORD OF THE PERNAMBUCO–ALAGOAS DOMAIN, BORBOREMA PROVINCE (NE BRAZIL): IMPLICATIONS FOR THE EARLY ASSEMBLY OF THE WEST GONDWANA

Thyego R. da Silva, Mariucha M. Correia de Lima, Valderez P. Ferreira, Alcides N. Sial
NEG–LABISE, Department of Geology, Federal University of Pernambuco, Recife, PE, Brazil

---

Abstract: A combined study of new whole-rock major-trace elements, mineral chemistry, Sr–Nd–O isotopes, and zircon U–Pb ages, was carried out for one biotite-hornblende granodiorite to granite orthogneiss (Jacaré dos Homens orthogneiss), emplaced along the Jacaré dos Homens transpressional shear zone, and one pluton (Santo Antonio granite) from the southern Águas Belas–Canindé composite batholith of the Pernambuco–Alagoas Domain, northeastern Brazil. SHRIMP zircon U–Pb dating of the Jacaré dos Homens orthogneiss and the Santo Antonio granite yields $^{206}Pb/^{238}U$ weighted apparent mean ages of 642.4 ± 3.4 Ma and 636.1 ± 3.6 Ma, respectively, which suggests that they were emplaced in the Criogenian–Ediacaran transition. These rocks were emplaced in a regional strain field combining transpressive deformation. The occurrence of a low-angle foliation, controlled by a transpressive deformation, suggests that thrusting has operated in the area. Concordant zircon U–Pb data from this study and from the literature date the beginning of the Brasiliano orogeny in the interval between 642 and 600 Ma. The studied granitic rocks show high-K calc-alkaline to shoshonitic composition, magnesian nature and metaluminous to slightly–moderately peraluminous signature, typical of I-type granitoids. They are enriched in the alkalis (7.69 to 11.79 wt.%), Rb, Ba, Th, K and light rare earth elements, depleted in Nb, Ta, Sr and Ti, consistent with a convergent tectonic setting. Nd isotopic data for the Jacaré dos Homens orthogneiss reveal t_{DM} age of 1.21 Ga with slightly negative $\varepsilon Nd_{(642\ Ma)}$ of −1.56, show initial $^{87}Sr/^{86}Sr$ ratios of 0.7067 with $\delta^{18}O_{(zircon= + 7.0‰)}$ value more high than mantle values. While the Santo Antonio pluton shows Nd- model age varying from 1.04 to 1.05 Ga, with $\varepsilon Nd_{(636\ Ma)}$ positive to slightly negative of +0.09 to −0.63 and back-

calculated (636 Ma) initial $^{87}Sr/^{86}Sr$ ratios from 0.7048 to 0.7049. The geochemistry indicates that the studied granitoids and the plutons from the literature that intruded the Águas Belas–Canindé composite batholith were either derived by partial melting of the Tonian mantle-derived magmas or by Tonian lower continental crust (evidenced from inherited zircon cores) triggered by uplift asthenosphere and underplating of lithospheric mantle.

Keywords: Syn-orogenic emplacement; Sr–Nd–O–Pb isotopes; Tectonic evolution

TWO STAGE MANTLE-DERIVED MAGMA IN A SYN-TECTONIC EDIACARAN BATHOLITH AND THE ONSET OF THE BRASILIANO OROGENY: EVIDENCE FROM SR, ND AND O ISOTOPES

T.R. Silva*, V.P. Ferreira, M.M.C. Lima, A.N. Sial

NEG–LABISE, Department of Geology, Federal University of Pernambuco, Recife, PE, Brazil

---

Abstract: The elongate Monteirópolis batholith (270 km^2) is composed of alkali feldspar granite to granodiorite, it is part of the Águas Belas–Canindé composite batholith and intruded rocks of the Pernambuco–Alagoas Domain, northeastern Brazil. This batholith is limited by the NNE-SSW-trending Jacaré dos Homens transpressional shear zone in its southwestern portion, and displays low-angle foliation, coeval to the development of a regional flat-lying foliation. Microgranular dioritic enclaves and amphibole-rich clots are abundant. Syn-plutonic dikes of diorite composition are also present. The mineralogy of this pluton comprises quartz, alkali feldspar and plagioclase as essential phases, biotite and amphibole as major accessory phases, besides titanite magmatic epidote. Major and trace element chemistry shows high SiO_2, total alkalis, Ba and Sr, low Fe# [(FeO_t / (FeO_t + MgO)] and Nb contents, attesting to high-K calc-alkaline and metaluminous to slightly peraluminous character, typical of I-type granites. The rocks are enriched in LREE and LILE and depleted in HFSE, and show fractionated chondrite-normalized REE patterns (LaN/LuN = 27.6 to 125) with Eu/Eu*= 0.67 to 1.25. Chondrite-normalized spidergrams show marked negative Nb, Ta, Sr and Ti anomalies, typical of subduction-related magmas. The Al_2O_3/TiO_2 ratios and P_2O_5 vs. SiO_2 contents suggest near-liquidus temperatures of 950–800°C. U–Pb SHRIMP zircon data yielded a crystallization age of 626 ± 4 Ma. Regional structures and U–Pb geochronological data for the Jacaré dos Homens transpressional shear zone suggest that shearing was installed at ca. 640 Ma. Movements along this shear zone may have contributed to provide space for magma emplacement. The rocks in this batholith are characterized by slightly negative to slightly positive εNd values (–0.78 to + 1.06), average Nd- model age of 1.0 Ga, low initial $^{87}Sr/^{86}Sr_{(626\ Ma)}$ values of 0.7050 to 0.7052, and low $\delta^{18}O$ values (zircon) of + 5.00 to 5.94‰ V-SMOW. The magma was likely formed by partial melting of Tonian mantle-derived rocks in the lower continental crust,

probably triggered by underplating of mantle-derived mafic magma during collision of the São Francisco Craton and the Pernambuco–Alagoas Domain during onset of the Brasiliano orogeny close to the Cryogenian–Ediacaran transition.

Keywords: Onset of the Brasiliano Orogeny; Sr–Nd–O isotopes; U–Pb SHRIMP zircon dating

APÊNDICE B – Abstract publicado no XXVII Simpósio de Geologia do Nordeste

ISOTOPE EVIDENCE FOR MANTLE CONNECTION IN THE SOURCE ROCK OF HIGH-K CALC-ALKALINE GRANITES, PERNAMBUCO–ALAGOAS DOMAIN, NORTHEASTERN BRAZIL

Thyego R. Silva*, Valderez P. Ferreira, Mariucha Maria C. Lima, Alcides N. Sial

NEG–LABISE, Department of Geology, Federal University of Pernambuco, Recife, PE, Brazil

We report whole-rock major, trace element, mineral and isotope chemistry study of the Jacaré dos Homens orthogneiss, emplaced along the Jacaré dos Homens transpressional shear zone, and of the Santo Antonio granite from the Águas Belas–Canindé batholith, Pernambuco–Alagoas Domain, northeastern Brazil. These rocks exhibit low-angle foliation, suggesting emplacement under a regional strain field, associated with transpressive deformation. Both plutons are dominantly made up of potassic feldspar, quartz and plagioclase with biotite as the main mafic phase and minor hornblende, attesting to metaluminous, calc-alkaline nature. The orthogneiss displays magnesian, slightly peraluminous and alkali-calcic character. The Santo Antonio granite is magnesian, metaluminous to slightly-moderately peraluminous. These two plutons are enriched in alkalis (up to 10.28 wt.%), Mg#, Rb, Ba, Sr, Th and LREE, and depleted in HFSE, with distinct Nb, Ta, and Ti depletion consistent with magmatism in a subduction-related setting. U–Pb zircon dating of these two plutons yielded $^{206}Pb/^{238}U$ weighted apparent mean ages of 642.4 ± 3 Ma and 636.1 ± 4 Ma, respectively. Nd isotopic data for the Jacaré dos Homens orthogneiss reveal t_{DM} age of 1.21 Ga with slightly negative $\varepsilon Nd_{(642\ Ma)}$ of −1.58, initial $^{87}Sr/^{86}Sr$ ratios of 0.7068, and $\delta^{18}O_{(zircon)}$ value of +7.0‰. The Santo Antonio pluton yielded Nd-model ages from 0.96 to 1.05 Ga, with $\varepsilon Nd_{(636\ Ma)}$ from +1.17 to −0.67, initial $^{87}Sr/^{86}Sr$ ratios from 0.7050 to 0.7052, and $\delta^{18}O_{(zircon)}$ value of + 5.0 to 5.9‰. The chemical features are typical of I-type granites. Altogether, the petrological, geochemical and isotopic data are consistent with the hypothesis that the studied granitoids were either derived by partial melting of a Tonian mantle-derived basalt or Tonian/Stenian lower continental crust, and we envisage that partial melting was triggered by the uplift of asthenosphere and underplating of lithospheric mantle.

Keywords: Continental growth; Sr–Nd–Pb–O isotopes; Northeastern Brazil